PALAEOZOIC PORPHYRY MOLYBDENUM-TUNGSTEN DEPOSIT IN THE MYSZKÓW AREA, SOUTHERN POLAND

Scientific Editor: Maciej Podemski

Polish Geological Institute Special Papers, 6

WARSZAWA 2001

CONTENTS

Polish Geological Institute Special Papers, 6 (2001): 1–88

Podemski M. Ed., 2001 — **Palaeozoic porphyry molybdenum–tungsten deposit in the Myszków area, southern Poland**. *Polish Geological Institute Special Papers*, 6: 1–88.

Maciej Podemski, Polish Geological Institute, Rakowiecka 4, PL-00-975 Warszawa, Poland. E-mail: podemski@pgi.waw.pl

Abstract. The Myszków porphyry molybdenum-tungsten deposit is one of several porphyry copper-type deposits that have been identified within a poorly defined belt of Precambrian to Palaeozoic rocks in south-central Poland. It is in a complex of Proterozoic (Vendian) to early Palaeozoic (Early Cambrian)-aged metasedimentary rocks that was intruded by a predominantly granodioritic pluton. The intrusive rocks and associated mineralisation phases are Late Carboniferous age, a time of porphyry-copper deposit formation not known to be present elsewhere in Europe.

The chemistry, mineralogy, and vein morphology of the Myszków mineralisation are similar to calc-alkaline-associated porphyry copper deposits. The deposit at Myszków consists mainly of stockwork veins; skarn minerals are uncommon. Several substages of mineral deposition have been identified in the Myszków area, five of which are closely related to formation of this porphyry deposit. The results of a factor analyses determined for analyses run on samples of drill core support the concept of multiple stages of mineralisation at Myszków.

The Myszków deposit is strongly enriched in Cu and Mo but contains very little gold. In comparison to other calc-alkaline-type porphyry Cu deposits, this deposit also contains an unusually high concentration of tungsten, particularly in the mineralised part of the stock. Therefore, the Myszków mineralisation can best be described as representing a rather unique, porphyry molybdenum-tungsten type of deposit.

Overall, the mineralisation at Myszków exhibits typical mineralogy for the deeper parts of a porphyry Cu system. Thus, it may be concluded that the upper (perhaps significant) part of this deposit was removed by rapid erosion that was followed by rapid burial of the erosion surface by a sequence of Triassic marine rocks. More complete deposits of this type which might also contain supergene enrichment zones, could be present in down-faulted blocks in other parts of the Kraków–Lubliniec region.

Key words: porphyry molybdenum-tungsten deposit, Palaeozoic porphyry copper-type deposit, magmatic and postmagmatic fluids, mineral zoning, geochemical zoning, factor analyses, mineralisation model, genesis of mineralisation.

Abstrakt. Porfirowe złoże molibdenowo-wolframowe w Myszkowie jest jednym z szeregu złóż miedziowo-porfirowych odkrytych w południowej Polsce, w słabo rozpoznanej strefie skał prekambryjsko-paleozoicznych obszaru Kraków–Lubliniec. Złoże myszkowskie występuje w kompleksie słabo zmetamorfizowanych skał proterozoiczno (wend)–dolnopaleozoicznych (dolny kambr), intrudowanych przez skały magmowe, głównie granodiorytowe. Wiek skał magmowych oraz mineralizacji kruszcowej określony został na górny karbon. Warto podkreślić, iż w Europie nie są znane inne złoża miedziowo-porfirowe tego wieku.

Zarówno skład chemiczny i mineralogiczny mineralizacji kruszcowej złoża w Myszkowie, jak i występujące w nim rodzaje użylenia, są charakterystyczne dla złóż miedziowo-porfirowych, związanych z wapniowo-alkalicznymi masywami magmowymi. Złoże myszkowskie zbudowane jest głównie z żył o charakterze sztokwerku. Rzadsze są minerały skarnowe. Wyróżniono w nim kilka stadiów mineralizacji kruszcowej. Pięć z nich związanych jest ściśle z powstaniem złoża porfirowego. Hipoteza wielostadialnej genezy mineralizacji myszkowskiej wsparta została wynikami analizy czynnikowej danych pochodzących z badań geochemicznych wybranych rdzeni wiertniczych.

Złoże w Myszkowie jest wzbogacone w Cu i Mo, natomiast jest bardzo ubogie w Au. W porównaniu z innymi złożami miedziowo-porfirowymi, związanymi z masywami wapniowo-alkalicznymi, złoże w Myszkowie jest niezwykle wzbogaco-

ne w wolfram. Dlatego uznano, że reprezentuje ono unikatowy typ złoża porfirowego: molibdenowo-wolframowy.

Ogólnie biorąc, skład mineralny oraz mineralizacja kruszcowa złoża myszkowskiego są charakterystyczne dla głębszych partii złóż miedziowo-porfirowych. Nie można więc wykluczyć, że górna część złoża myszkowskiego, być może najbogatsza w mineralizację kruszcową, została między górnym karbonem a triasem usunięta przez erozję. W obniżonych częściach obszaru Kraków–Lubliniec mogły jednak zachować się inne, pełniejsze złoża typu myszkowskiego, być może posiadające nawet wzbogaconą strefę wietrzeniową.

Słowa kluczowe: porfirowe złoże molibdenowo-wolframowe, paleozoiczne złoże typu miedziowo-porfirowego, fluidy magmowe i pomagmowe, strefowość mineralna, strefowość geochemiczna, analiza czynnikowa, model mineralizacji, geneza mineralizacji.

INTRODUCTION

Metallic ores have been mined for centuries along the north-eastern border of the Upper Silesian Coal Basin, also known as the Kraków–Lubliniec region. Until the late 1950's, prospecting for and mining of these ores were primarily done in shallow, Mesozoic-aged rocks. Deposits mined in these rocks included siderite ores in Jurassic host rocks and silver-rich, Pb-Zn sulphide ores in Triassic host rocks.

After the World War II, intensive prospecting for Triassic Pb-Zn ore deposits was conducted in Poland. In the mid 1950's, subeconomic mineralisation was discovered in locally metamorphosed, Precambrian to early Palaeozoic rocks below a thick sequence of flat-lying, Mesozoic rocks. In some areas, these metamorphosed, sedimentary rocks were intruded by felsic igneous magmatic rocks.

The increasing amount of geological information on these Precambrian to Palaeozoic mineralised rocks along the north-eastern border of the Upper Silesian Coal Basin has gradually encouraged an interest by both the Polish geological community and the State authorities in the mineral potential of that region, especially near areas intruded by magmatic rocks. In the second half of the 1970's, prospecting began in this region followed in the 1980's by intensive exploration.

Numerous geophysical and geological investigations were conducted, first by the Polish Geological Institute (Państwowy Instytut Geologiczny), which at that time was called the Geological Institute of the Central Geological Board (Instytut Geologiczny Centralnego Urzędu Geologii), and by the Geological Enterprise in Kraków (Przedsiębiorstwo Geologiczne w Krakowie), which in the 1970's was also monitored by the Central Geological Board. Those intensive investigations produced discoveries of polymetallic (copper, molybdenum, tungsten, lead and zinc) mineralisation in several areas (Myszków, Zawiercie, Pilica, Dolina Będkowska) along the north-eastern border of the Upper Silesian Coal Basin. These discoveries were regarded as being partly porphyry-copper-type mineralisation and partly skarn-type. In the course of the investigations, the possible sedimentary-remobilization origin of these deposits was also suggested.

The mineralisation found in the vicinity of Myszków was regarded as the most interesting discovery. The presence of a substantial amount of molybdenite suggested the occurrence of a Mo deposit at a time when molybdenum was in high demand and no deposits of this type were known to exist in Poland. Therefore, in the second half of the 1980's, exploration activities were concentrated in the Myszków area.

Those activities abruptly stopped at the end of eighties, caused both by a sharp drop in Mo, W, and Cu prices on the world market and by the dramatic change in 1989 of the political system in Poland. The geological data and economic aspects of the exploration work carried out in Myszków area were summarised in 1993 in a prefeasibility-type report that included a preliminary ore reserves estimate classed in the Polish C_2 category.

This publication summarises the results of investigations of the polymetallic mineralisation found in the Myszków area. Information to date has been contained only in numerous unpublished reports and/or in publications (mostly in Polish) that covered selected geological aspects only.

This publication also contains a discussion of the geology of the Kraków–Lubliniec region (the north-eastern border of the Upper Silesian Coal Basin), and, in particular, the geology of the contact zone between two Precambrian to Palaeozoic geotectonic blocks: the Upper Silesian Block and the Małopolska Block. Knowledge of the geology of this zone is essential for understanding the genesis and spatial distribution of the Myszków mineralisation.

This publication includes also results of new research on the geochemistry and age of the Myszków deposit, conducted in the mid 1990's by a team of scientists from the Polish Geological Institute and the United States Geological Survey, under a Polish-American, Maria Skłodowska-Curie Fund II project.

The Myszków deposit, classified as a porphyry molybdenum-tungsten type, is probably unique for European deposits both for its type of mineralisation and for its Late Carboniferous age.

The frequent occurrence in the Kraków–Lubliniec region, in the Precambrian (Vendian) to early Palaeozoic (Early Cambrian) sedimentary rocks, of intrusive rocks and associated polymetallic mineralisation, suggests the possibility of the existence of additional porphyry Myszków-type deposits in the contact zone between the Upper Silesian and Małopolska blocks.

GEOGRAPHIC LOCATION

The Myszków area is located in the Kraków–Lubliniec region (the north-eastern border of the Upper Silesian Coal Basin). This region extends from the vicinity of Lubliniec in the north-west, through the Żarki, Myszków, Zawiercie, Pilica, and Olkusz areas, to Kraków in the south-east (Fig. 1). The area is part of a geomorphologic unit known as the Silesian–Kraków Highlands.

The Myszków area is one with generally flat terrain, with elevations ranging from 297.1 m a.s.l. in the north-west to 305.8 m a.s.l. in the south-east. Localities in the western and south-western edges of the area, studied near Będusz and Mrzygłód, exhibit slightly greater relief, with about 30–40 m differences in elevation.

From an administrative point of view, the mineralised area near Myszków is part of the Silesian Voivodship. The area containing mineralisation is located near the south-western outskirts of Myszków. Accessibility for any future mining is available via both roads and trains. An important electric train line connects Myszków with such large cities as Katowice, Częstochowa, and Warszawa.

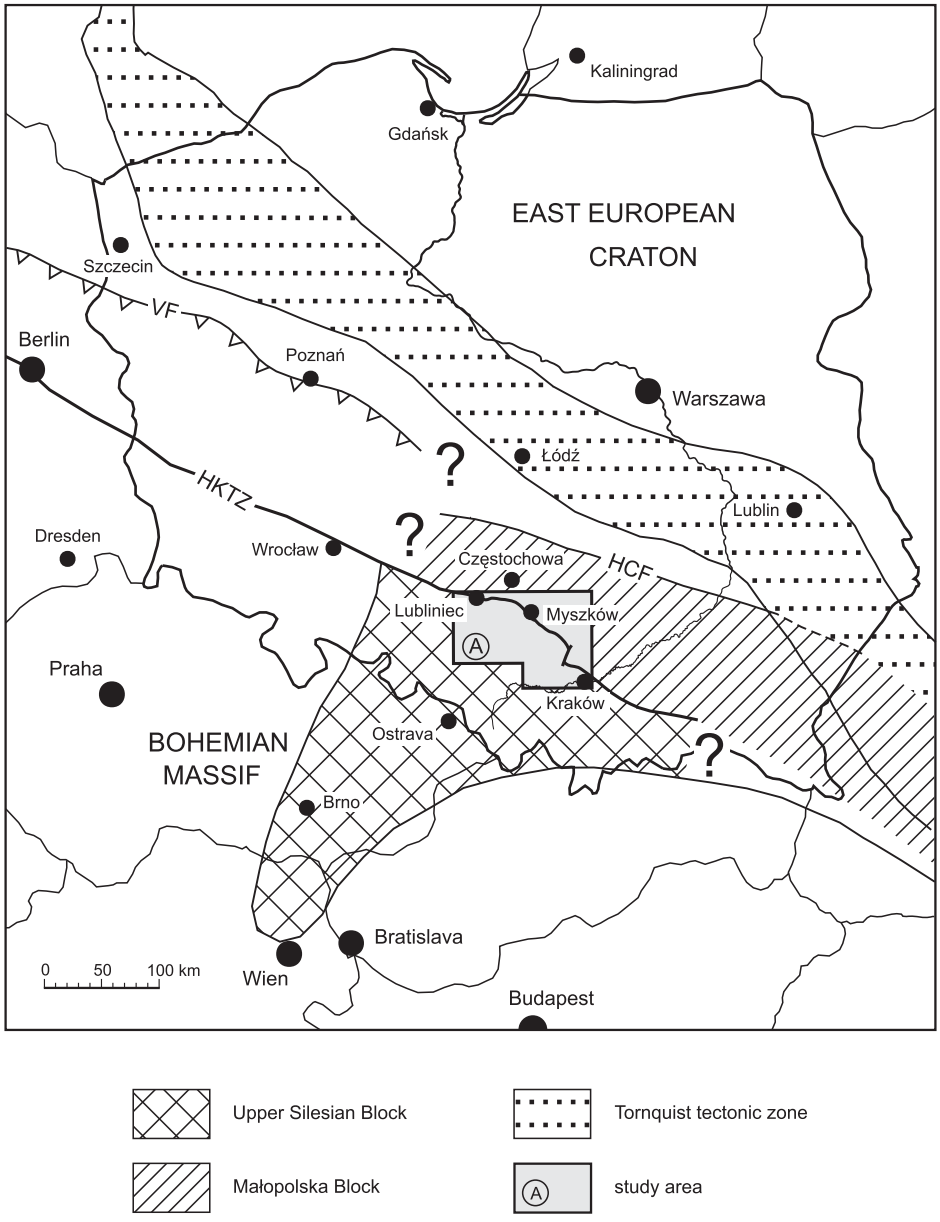

Fig. 1. Geographical position of the Myszków area, with the main geotectonic units of Poland at the background

HCF — Holy Cross Mts. Fault, HKTZ — Hamburg–Kraków tectonic zone, VF — Variscan Frontier

HISTORY OF INVESTIGATIONS

The first studies of the polymetallic mineralisation in the Palaeozoic rocks along the north-eastern border of the Upper Silesian Coal Basin (the Kraków–Lubliniec region) were conducted between 1954 and 1957 by the Polish Geological Institute (formerly the Geological Institute of the Central Geological Board). At that time, boreholes were drilled near Mrzygłód and Kotowice. The boreholes were drilled to investigate the regional geological structures, including the source of the Mrzygłód, Krzywopłoty, and Bębło magnetic anomalies that were discovered during a regional geophysical survey (Skorupa, 1953).

Several of these early boreholes penetrated below the Triassic sequence and found, for the first time, at depths of 288–500 m, a complex of dark, slightly metamorphosed schists that were cut by numerous apophyses and dikes of porphyries, diabases, and keratophyres, all of which contained weak pyritic mineralisation with traces of copper, lead and zinc minerals. The age of that complex was at that time considered to be Early Carboniferous (Ekiert, 1957), and the mineral showings were not considered to be of economic interest.

The discovery in borehole M-9 Mrzygłód of Silurian graptolite fauna within the metamorphic schists (Siedlecki, 1962) was very important because it demonstrated that the schists were, in fact, early Palaeozoic in age. Based on that discovery, Siedlecki confirmed that, in addition to already known the Devonian hypothetical Dębnik–Siewierz ridge, there existed another zone of the early Palaeozoic rocks. He named the zone: Kraków–Mrzygłód zone.

The differences of opinion about the geological structure of the Palaeozoic basement in the Kraków–Lubliniec region generally continue to this day. Several geologists (Bukowy, 1964a, b, 1984, 1994; Ekiert, 1971; Harańczyk, 1982a, b; Piekarski, 1982b; Znosko, 1965, 1983) regarded the Palaeozoic complex as a lateral extension of the Variscan orogen (Kraków branch of the Variscides) or as a part of the Caledonian orogen (so-called Krakovides). On the other hand, Pożaryski and Kotański (1979) considered the complex to be the Caledonian–Variscan Kraków aulacogen, and Harańczyk (1994a, b) considered it a part of the Lubliniec–Zawiercie–Wieluń terrane.

Other authors (Bogacz, 1980; Brochwicz-Lewiński *et al.*, 1983; Harańczyk, 1988; Kotas, 1982, 1985; Pożaryski, 1990; Pożaryski *et al*., 1992) suggested that a wide deep fracture zone might be present in the Kraków–Lubliniec region and that this zone forms a boundary between the Upper Silesian and Małopolska blocks (? massifs, terranes). This view has been confirmed by the latest lithostratigraphic and tectonic studies of the Precambrian to early Palaeozoic formations in the area, as well as by gravity and magnetic data (Buła, 1994, 2000; Buła and Jachowicz, 1996; Buła *et al*., 1997; Buła *et al*., unpubl. report, 1996; Żaba, 1995, 1996b, 1999). These authors have supported the hypothesis that there is a major structural contact that is present between the Upper Silesian and Małopolska blocks, along the Kraków–Lubliniec tectonic zone, and is about 0.5 km wide (Fig. 1).

Znosko (1964) was the first to report that subvolcanic rocks, encountered in the Mrzygłód area and their associated hydrothermal mineralisation, were the end products of magmatic processes resulted from a deep seated, hidden, granitoid batholith. This author also suggested that prospecting drilling in the apical part of the hypothetical batholith be done.

In 1965, borehole 1-P was drilled to a depth of 1003.4 m in order to test Znosko's hypothesis. This hole penetrated a thick series of Silurian (?) and probable Ordovician schists that were cut by numerous porphyritic and microgranitic dikes containing traces of pyrite and copper mineralisation that were generally similar to other mineral occurrences in the Mrzygłód area. Information from borehole 1-P and other deep holes, drilled at the same time in that area, generally confirmed the subeconomic mineral potential of the early Palaeozoic metamorphic rocks in the Silesian–Kraków region (Bukowy and Ślósarz, 1968). The mineral potential of the Devonian and Early Carboniferous carbonate rocks was regarded more optimistically.

Piekarski (Piekarski, 1971a; Banaś *et al*., 1972) described a different view of the mineral potential of the early Palaeozoic rocks in the Silesian–Kraków region. As a result of the discovery in 1968 and 1969, in a borehole near Lubliniec, of the syngenetic copper and siderite-manganese intercalations in the clayey Silurian sedimentary rocks (Piekarski, 1971b), and the additional discovery in 1969 of copper and molybdenum mineralisation in metamorphic schist and granitoid intrusions in the Myszków area, Piekarski concluded that a high economic potential might be present for deposits of these types. He further concluded that an older, syngenetic, disseminated form of mineralisation existed in the clayey sedimentary rocks, and that this mineralisation was remobilized during metamorphic processes, primarily by meteoric water, and redeposited in the neighbouring magmatic rocks. However, at the time Piekarski wrote this report, the limited available geological data was insufficient to solve the issue of the origin of all the types of observed mineralisation.

In 1972, the Central Geological Board approved a drilling program for the Myszków area that consisted of seven boreholes to test Piekarski's hypotheses (Piekarski, unpubl. report, 1970). These boreholes were drilled between 1972 and 1975. Several horizons of dark schists containing traces of pyrite and copper minerals, as well as polymetallic mineralisation, were identified within the early Palaeozoic sequence. Numerous porphyry and granitoid intrusions were encountered in borehole Pz-5, at a depth of 701 m. Several intervals at this depth contained copper, molybdenum, and tungsten minerals in mineralised zones that were as much as a few metres thick. Analyses for these mineralised zones yielded 0.15–3.5% Cu, 0.02–0.95% Mo, and 0.05–0.3% W. These results confirmed the value of systematic prospecting in the Myszków area.

Poor knowledge of the basement geology of the entire Kraków–Lubliniec region was at one point the main obstacle to any prospecting activity in that area. Therefore, to better delineate favourable mineralised formations and areas, a program

that included complementary basic research on early Palaeozoic lithology, stratigraphy and geologic structure was undertaken between 1975 and 1978. At the same time, some surface magnetic and gravity geophysical surveys were conducted in the Poraj–Mrzygłód area, and 12 shallow boreholes were also drilled (Piekarski *et al*., unpubl. report, 1979).

The results of those investigations produced a new geological model of the Mesozoic basement in the Myszków–Mrzygłód area. For the first time, Ordovician and earliest Silurian deposits in that region could be separated by using new palaeontologic and lithologic data (Piekarski and Siewniak-Witruk, 1978). That knowledge was crucial for more precisely determining the stratigraphic position of various mineral discoveries.

After 1978, several new mineralised areas, with different mineral suites and probably also with different sources, were discovered. A new Pb-Zn ore association was also identified (Piekarski *et al*., 1982). However, two different hypotheses concerning genesis of the Cu-Mo mineralisation still existed. The first one regarded the Myszków deposit as being a porphyry copper type because the hydrothermal alteration and zonal distribution seemed to be typical for this type of deposit (Ślósarz, 1982). The second one suggested that all of the mineralisation resulted from sedimentary-remobilization processes (Piekarski, 1982a).

In his 1982 paper, Piekarski (1982a) suggested that the hydrothermal solutions had a greater influence on the genesis of ore mineral concentrations than previously believed because his new investigations proved that ore elements did not show any signs of remobilization in the metamorphosed schists. Piekarski also thought that the hydrothermal solutions leached some metals (mainly Cu and Mo) from the schists, and concentrated them in the magmatic rocks and in the feldspathic vein metasomatites. That process helped to explain the concentrations of molybdenum veins in those parts of the granitoids and porphyries that had cut the early Palaeozoic schists, and the lack of molybdenum veins in the rhyodacite or microgranitic porphyries that do not occur in the schists.

In the 1980's, prospecting and exploration was conducted in the vicinity of Myszków for Pb-Zn mineralisation in Triassic strata. This work produced much new information about geological structure in the Precambrian to early Palaeozoic rocks in the area. Boreholes drilled for Triassic Pb-Zn deposits were also designed to provide information on the pre-Triassic basement. As a result, these holes penetrated basement for distances between several metres and a few hundred metres. Some of these holes encountered polymetallic mineralisation in the basement rocks (Wielgomas *et al*., unpubl. reports, 1986, 1988).

The ore-bearing granite and porphyry intrusions still remained the most important prospecting targets. Within the early Palaeozoic sedimentary rocks, the important ore-bearing formations include the Early Silurian (Llandoverian–Early Ludlovian) sequence of dark, clayey and clayey-carbonatic schists, which contain weak, Cu-pyrite and Cu-Mo mineralisation, and the Middle and Late Ordovician clayey and carbonatic sedimentary rocks, which contain Cu-pyrite and polymetallic skarn mineralisation.

By the end of the 1970's, the large, positive magnetic anomalies were thought to identify areas where the ore-bearing formations occurred at very shallow depth and, therefore, were considered to be promising targets for mineral prospecting. The Myszków, Bębło, and Krzywopłoty anomalies were regarded as the most favourable locations for potential mineral deposits. In addition, most of the ore-bearing granite and porphyry intrusions were found to be located within uplifted Caledonian structures.

In 1979, a new mineral prospecting program began. This program concentrated on the early Palaeozoic rocks in the Poraj–Mrzygłód area (Piekarski *et al*., unpubl. report, 1979) and included detailed exploration of the Mrzygłód geophysical anomaly, and reconnaissance work over the smaller Poraj and Kotowice magnetic anomalies. As part of this program, six boreholes were drilled to depths of 1200 m in the Myszków–Mrzygłód area.

Information derived from cores from those six boreholes, which were drilled between 1982 and 1987, proved to be very interesting. Several zones of polymetallic mineralisation were encountered. Five of the holes contained the thickest and the richest zones of ore minerals found to date along the north-eastern border of the Upper Silesian Coal Basin (Piekarski, 1988). Copper, molybdenum, and tungsten mineralisation was found in the metamorphic schists, metasomatites, porphyries, and granites. Boreholes Pz-17, Pz-28, Pz-29, and Pz-31 were especially interesting. The highest concentrations of metals (2.55% Cu, 0.89% Mo, and 1.12% W) were encountered in those boreholes. All these boreholes were stopped at depths of 1250 m, being still in the mineralised granitoid rocks.

Using the new data from the six boreholes, Piekarski (1988) was able to distinguish several different types of mineralisation. He recognised that the Cu-pyrite and Cu-Mo mineralisation that occurred in the dark, metamorphic schist complex, was probably syngenetic, sedimentary in origin. The weak, chalcopyrite-pyrite mineralisation that was disseminated in the porphyries and granitoids, was judged to be of magmatic origin, and classified as a porphyry copper-type deposit. The Cu-pyrite mineralisation, which is sometimes associated with molybdenite and magnetite and is located in the older quartz-chlorite veins that cut dark metamorphic schists and graywackes, he recognised as associated with regional and/or contact metamorphic events, as is the Cu-pyrite skarn mineralisation (Piekarski, 1988).

The Cu-Mo-W mineralisation associated with stockwork quartz or quartz-feldspar veins, Piekarski (1988) acknowledged as hydrothermal in origin, overprinting the older types of mineralisation. The Cu-Mo-W mineralisation was developed (1) in intensively, tectonically altered sedimentary rocks, (2) in granitoids and diabases, and (3) occasionally in the smaller porphyry apophyses. Piekarski (1988) concluded that Cu-pyrite and Cu-Mo-W stockwork deposits probably had the highest economic potential and that porphyry copper-type deposits had less potential.

However, Ślósarz (1988) suggested that the main Myszków mineralisation was really a porphyry Cu-Mo deposit that was produced by low fluorine magmatic complexes. Ślósarz considered this type of deposit as having a high potential for economic polymetallic mineralisation.

An extensive addition to the 1979 program was prepared in 1987 to follow on the results of previous programs (Piekarski

et al., unpubl. report, 1987). Twenty additional boreholes were planned to reach depths of 1200–1500 m, and a gravity survey of an area of about 150 km^2, was also approved. Those investigations were expected to complete the detailed exploration of the remaining part of the Mrzygłód anticline.

The boreholes were drilled between 1987 and 1990, and the laboratory analyses were completed in 1992. The geophysical survey was never executed, however, as a result of financing problems. A shortage of funds and, especially, political changes in Poland at that time, eventually brought all the mineral exploration activities within the Kraków–Lubliniec region to a standstill.

The final report, summing up all of the geological and analytical data on the Myszków deposit, was completed in 1993 (Piekarski *et al*., unpubl. report, 1993). A preliminary estimation of the Cu-Mo-W ore reserves for the Myszków deposit was calculated, using an area of about 0.5 km^2, depths to 1300 m, and average metal contents of 0.152% Cu, 0.049% Mo, and 0.041 % W. The minimum equivalent content (Mo_e) was taken from the equation: $Mo_e = (Mo\%) \times 1.5\,(W\%) \times 0.3\,(Cu\%)$. A deposit with 800 million t of ore, containing 700 000 t Cu, 350 000 t Mo, and 200 000 t W, was established.

During the 1990's, petrologic, geochemical, and ore genesis studies of the Precambrian to Palaeozoic mineralised complex in the Myszków area were continued in order to define further mineral exploration targets in the entire Kraków–Lubliniec region (Badera, 1992, 1999; Habryn *et al*., 1994; Heflik, 1992; Lasoń, 1992; Markiewicz, 1994; Markiewicz *et al*., 1993; Markowiak and Habryn, unpubl. report, 1994; Piekarski, 1995; Piekarski and Migaszewski, 1993; Szełęg, 1997; Ślósarz, 1993; Ślósarz *et al*., unpubl. report, 1995; Ślósarz and Truszel, unpubl. report, 1997; Truszel, 1994; Żaba, 1994).

Detailed geochemical investigations were conducted between 1992 and 1996 by the Polish Geological Institute (Państwowy Instytut Geologiczny) and the United States Geological Survey (USGS), under a Polish-American Maria Skłodowska-Curie Fund II project. These investigations have also provided important information about the Myszków deposit (Chaffee *et al*., 1994, 1997, 1999; Podemski and Chaffee, unpubl. report, 1996). The results of this co-operative Polish-American project constitute a significant part of the present monograph.

Transfer to the Polish area of American methods and techniques that could be used for prospecting and exploration for concealed metal ore deposits in Poland, was the main objective of this geochemical project. A major part of the geochemical investigations was to sample, describe, and analyse core samples collected along the length of boreholes drilled along two cross-sections, and core samples collected over two lateral surfaces at depths of 300 m and 700 m below the present surface. Those investigations have materially assisted in explaining the geochemistry, origin, and age of the Myszków deposit. They have also helped to identify where there may be extensions of the currently defined deposit.

RESULTS OF THE GRAVITY AND MAGNETIC SURVEYS

The Silesian–Kraków monocline has been used as the regional framework for constructing gravity and magnetic anomaly maps of the Myszków area (Fig. 2A and 3A). The initial data were collected during the semi-detailed gravity and magnetic surveys (gravity: 6 readings/km^2, magnetic: 21 readings /km^2) that were completed between 1975 and 1978.

REGIONAL GRAVITY FIELD

Strong, regional and local gravity changes characterise the regional gravity field associated with the Silesian–Kraków monocline. The total amplitude of those changes exceeds 300 m/sec^2.

Generally, two wide-spread anomalies can be distinguished on the gravity map (Fig. 2A). The south-western part of the area is dominated by gravity highs, and the north-eastern part by gravity lows. A broad zone with a strong gravity gradient separates the two areas. This zone is generally oriented in a NW–SE direction that extends from the Wolbrom area, through Zawiercie and Myszków, toward Częstochowa.

The central part of the zone exhibits the highest changes in gradient. North-west of Myszków, it visibly broadens. South-east of Wolbrom, some obvious gradient changes that are caused by perpendicular displacements can be seen. These changes in the areas of relatively high gravity values are in the shape of broad embayments impinging from the south-west into the broad gravity low. The gradient zone is less well defined there, and the intensity of the gravity values are visibly diminished.

The NW–SE direction is dominant in the overall gravity field (Fig. 2A). Several perpendicular disturbances can be seen within the complicated anomalous areas of the gravity highs and lows. A broad negative anomaly is evident within the area of gravity lows. This anomaly is centred near Kotowice (east of Myszków). It is adjacent to and parallel with the Myszków–Wolbrom gradient zone.

Another gravity low is present north-east of the Kotowice low. A broad gravity gradient zone there is parallel to the Myszków–Wolbrom zone, but is of a lower intensity.

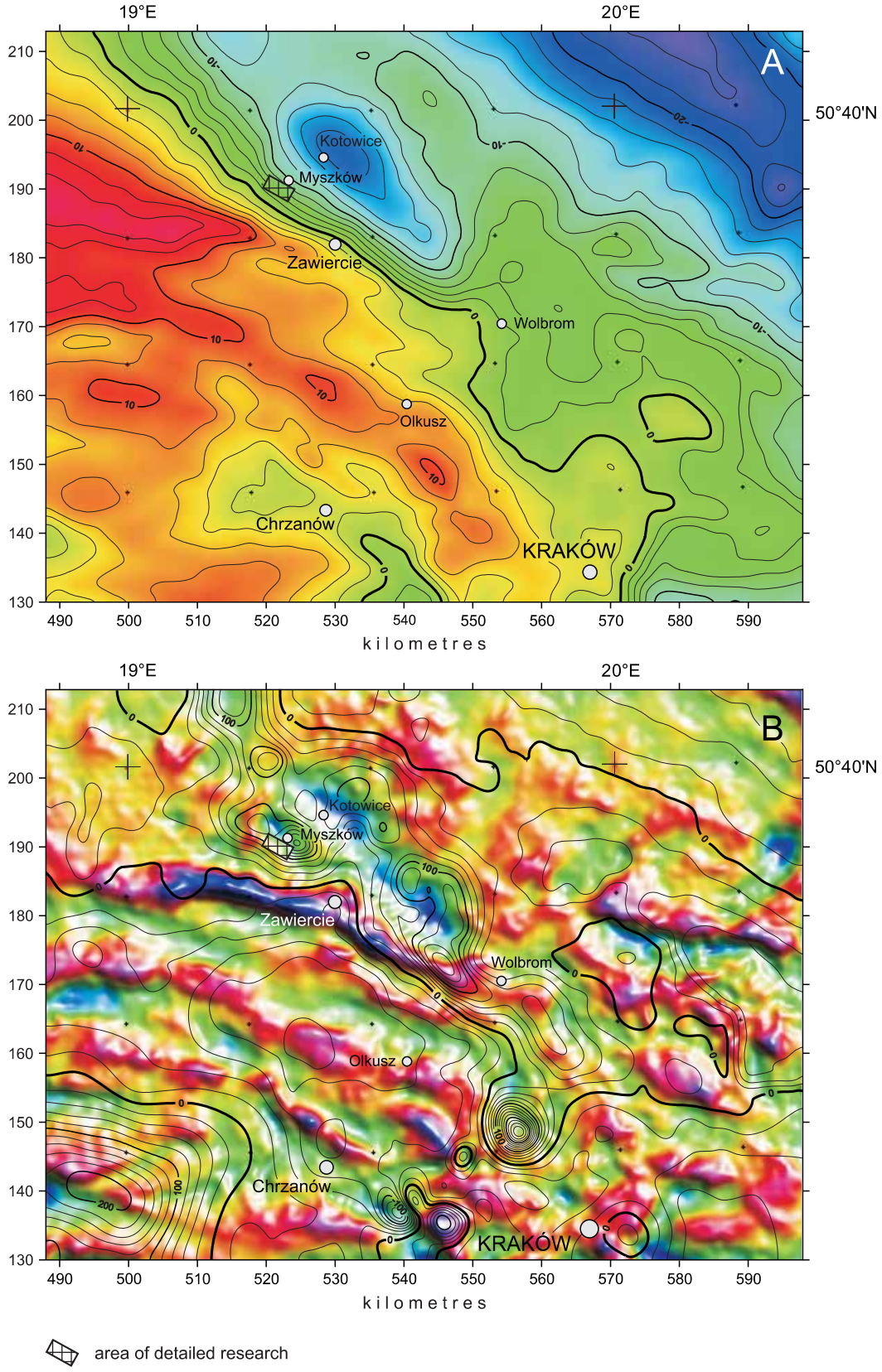

Fig. 2. Gravity anomalies of the Myszków–Kraków region

2A — map of the Bouguer anomalies; isolines every 1 miliGal; **2B** — shadowed map of the local anomalies (r = 4.5 km), with isolines of magnetic anomalies (referred to the pole) from Fig. 3A at the background; light from north-east

REGIONAL MAGNETIC FIELD

The regional magnetic patterns are roughly similar to the regional gravity field patterns. In detail, the area of the disturbed magnetic field is spatially a fairly close equivalent of gravity lows area, especially in the Kotowice gravity low. Elsewhere, weak magnetic field changes and low magnetic values can be seen in the areas of gravity highs (Fig. 3A).

A magnetic high that contains several local anomalies is the dominant regional feature (Fig. 3A). There are three significant local anomalies. The Myszków and Krzywopłoty anomalies, west of Wolbrom, are oriented NW–SE and have readings exceeding 260 nT. The Koziegłowy anomaly, north-west of Myszków, has a slightly lower amplitude (Fig. 3A, B).

Along the Myszków–Wolbrom gravity gradient zone (Fig. 2A), there is a zone composed of high magnetic gradients closing from the south-west a magnetic highs zone (Fig. 3A). The strong, local, Myszków and Krzywopłoty magnetic highs are located within that zone or on its north-eastern slope (Fig. 3B).

THE MYSZKÓW–WOLBROM ZONE

The Myszków–Wolbrom strong gravity gradient zone is the most important gravity unit in that area. Its importance has already been noted by authors of a geophysical interpretation (Cieśla *et al*., unpubl. report, 1984). This gravity gradient is thought to be caused by a considerable density contrast between various rock units present at the depths from 1.5 km to several km. The contact between these units is most probably strongly dipping toward the north-east; that is, toward the less dense rock masses, which may be a granitoid intrusion. The contact is probably tectonic in character and represents a tectonic zone that extends to a considerable depth. The strong magnetic anomalies near Myszków and Krzywopłoty are located within and are parallel to that strong gradient zone (Fig. 3B). That may prove inter-connection of their origin.

Measurements of magnetic properties in core samples from boreholes drilled in the Myszków area show that the porphyries and some of the Palaeozoic schists are the most magnetic rock types. The combined magnetic levels in the porphyries and "magnetic" schists, however, are small in comparison to the regional values (Cieśla *et al*., unpubl. report, 1984).

Modelling completed since 1984 suggests that the top of the rock mass, regarded as the source of the magnetic anomaly at Myszków must be at a depth greater than 1500 m. Modelling of the Krzywopłoty magnetic anomaly suggests a very similar depth. This depth is in agreement with the depth of the upper boundary of the Myszków–Wolbrom tectonic contact zone represented by the mentioned above Myszków–Wolbrom gravity gradient. This coincidence suggests a genetic connection between the two magnetic anomalies, and especially between the anomaly at Myszków and the Myszków–Wolbrom tectonic zone.

Most of the positive magnetic anomalies identified in the north-eastern part of the study area, north-east of the suggested Myszków–Wolbrom deep tectonic zone, are located within or near to the local gravity low found near Kotowice (Fig. 2B and 3B).

There are no clear equivalents on the gravity map for most the local magnetic anomalies. The only exception is the magnetic anomaly near Myszków, which overlaps a local gravity low (Fig. 2B). Generally, local dominant anomalies extend in two main directions: NW–SE and NE–SW (Fig. 3B). There is no privileged direction for local gravity anomalies (Fig. 2B).

South-west of the inferred Myszków–Wolbrom tectonic zone, in the south-eastern part of the study area, both geophysical methods exhibit different patterns than those north of the zone. Bands of strong local gravity anomalies, which are generally oriented WNW–ESE, can be seen on the gravity map (Fig. 2B). Those anomalies are associated with steeply dipping, Devonian and Early Carboniferous series, cropping out under the Mesozoic cover. The substantial differences in density of these units (the Middle Devonian rocks are especially dense) produced alternating bands of local gravity highs in the Devonian rocks and local gravity lows in the Carboniferous rocks. Faulting perpendicular to the orientation of these bands, is expressed as local breaks and displacements in the dominant bands.

The dominant magnetic pattern of the area south of the zone is, for the most part, only slightly disrupted (Fig. 3A, B). Disruptions in the intensive magnetic field can be seen south-east of the Olkusz–Chrzanów line (Fig. 3A, B). Several anomalies can be distinguished in that area, including an extensive anomaly at Bębło (south-east of Olkusz), which is complex but roughly circular; another positive anomaly at Dębnik (south-west of the anomaly at Bębło); and two additional anomalies that are south-west of the first two. The first is a positive anomaly at Regulice, and the second, just to south-west, is a very strong, complex, circular, positive anomaly at Zalas–Rybna.

The magnetic highs at Dębnik and Zalas–Rybna have counterparts on the gravity map. A local gravity low corresponds to the magnetic high at Dębnik. These coincident anomalies are caused by a porphyry intrusion that was intercepted in borehole Dębnik IG 1. The porphyry rocks are characterised by a high magnetic susceptibility (4×10^{-3}SI) and by a very low density (2.45 g/cm^3).

The magnetic anomaly at Zalas–Rybna correlates well with a strong gravity high. This coincidence of anomalies is undoubtedly caused by rocks of high magnetic susceptibility and high density, which may be diabase or another type of mafic intrusion. The high values of gravity anomalies suggest the existence of substantial thickness of rocks that disrupt the gravity field.

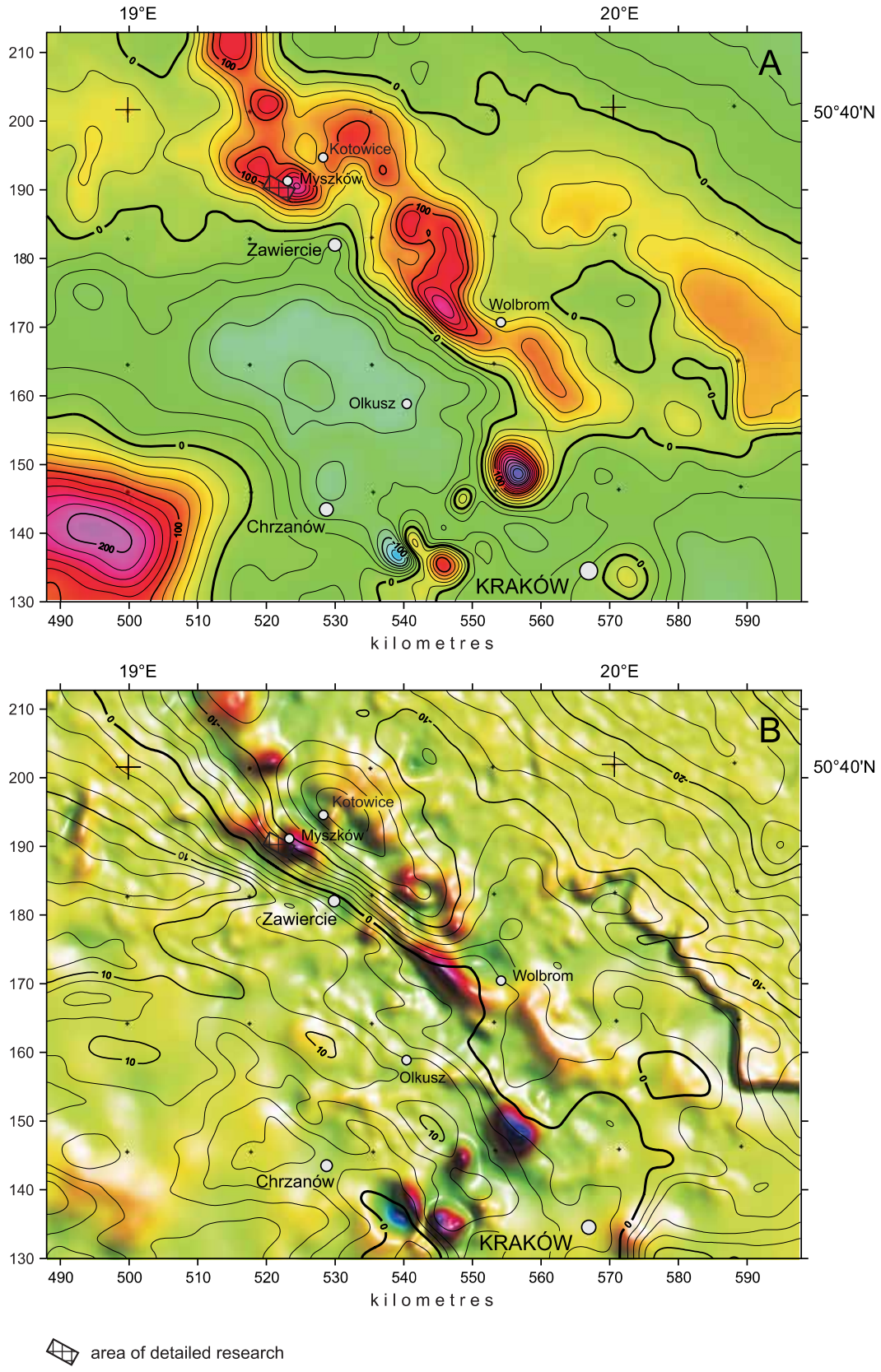

Fig. 3. Magnetic anomalies of the Myszków–Kraków region

3A — Map of the magnetic anomalies, referred to the pole; isolines every 20 nTesli; **3B** — shadowed map of the local anomalies (r = 4.5 km), with isolines of Bouguer anomalies from Fig. 2A; light from north-east

GEOLOGIC SETTING

The Myszków area is part of the Kraków–Lubliniec region (Bukowy, 1982, 1984), which is also known as the north-eastern border of the Upper Silesian Coal Basin (Fig. 4). Quaternary and Mesozoic formations, which are a part of the Silesian–Kraków monocline, crop out in the vicinity of Myszków. Palaeozoic rocks, including rocks of Devonian, Carboniferous, and Permian ages, crop out only locally near Myszków (Fig 6).

Intercepts of Palaeozoic (Cambrian through Permian) and possibly Precambrian (Vendian) rocks that vary in thickness from a few metres to several hundred metres have been observed in core samples from one or more of about 2500 boreholes, that were drilled in the Kraków–Lubliniec region. Most of the boreholes were drilled during exploration for Pb-Zn deposits in Triassic strata. Additional boreholes were drilled just to explore for polymetallic mineralisation known to be present in the Precambrian and Palaeozoic rocks, underlying the Myszków, Mrzygłód, Zawiercie, Pilica, and Dolina Będkowska areas. Several deeper (1700–3000 m) boreholes were drilled for general, geological purposes.

The Kraków–Lubliniec region is transected by the narrow (about 0.5 km wide) Kraków–Lubliniec tectonic zone (Fig. 5), which is probably part of the major, transcontinental, Kraków–Hamburg tectonic zone, that has been identified in the Carpathian Palaeozoic basement to the south-east of Kraków (Brochwicz-Lewiński *et al*., 1983). The Kraków–Lubliniec zone is thought to have originated in Precambrian and to have been re-activated several times after that, with the highest activity taking place between Cambrian and Permian periods

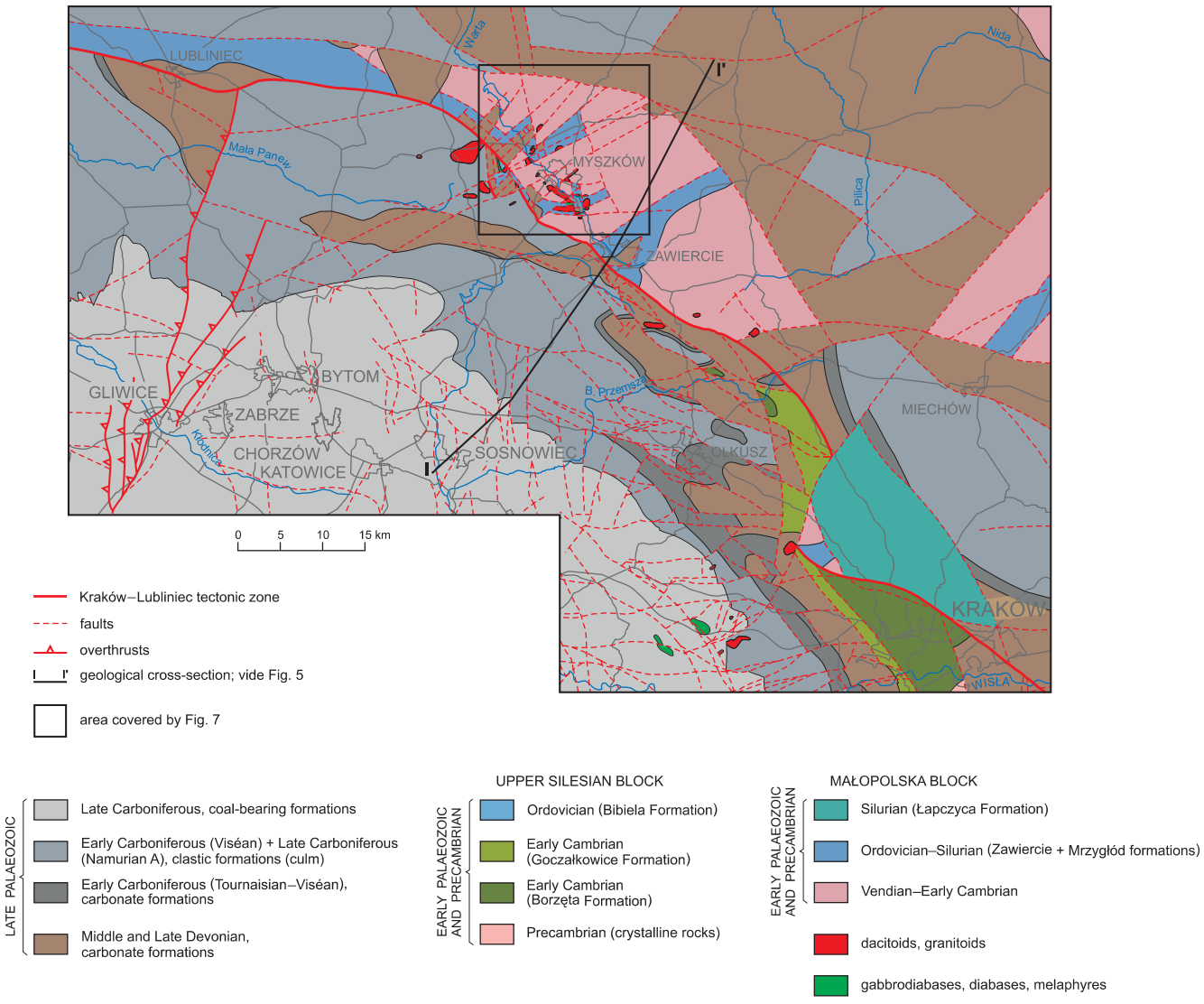

Fig. 4. Contact zone of the Upper Silesian and Małopolska blocks; geological map without Permian and younger formations (Buła, Habryn, Krieger, Kurek, Markowiak, Woźniak)

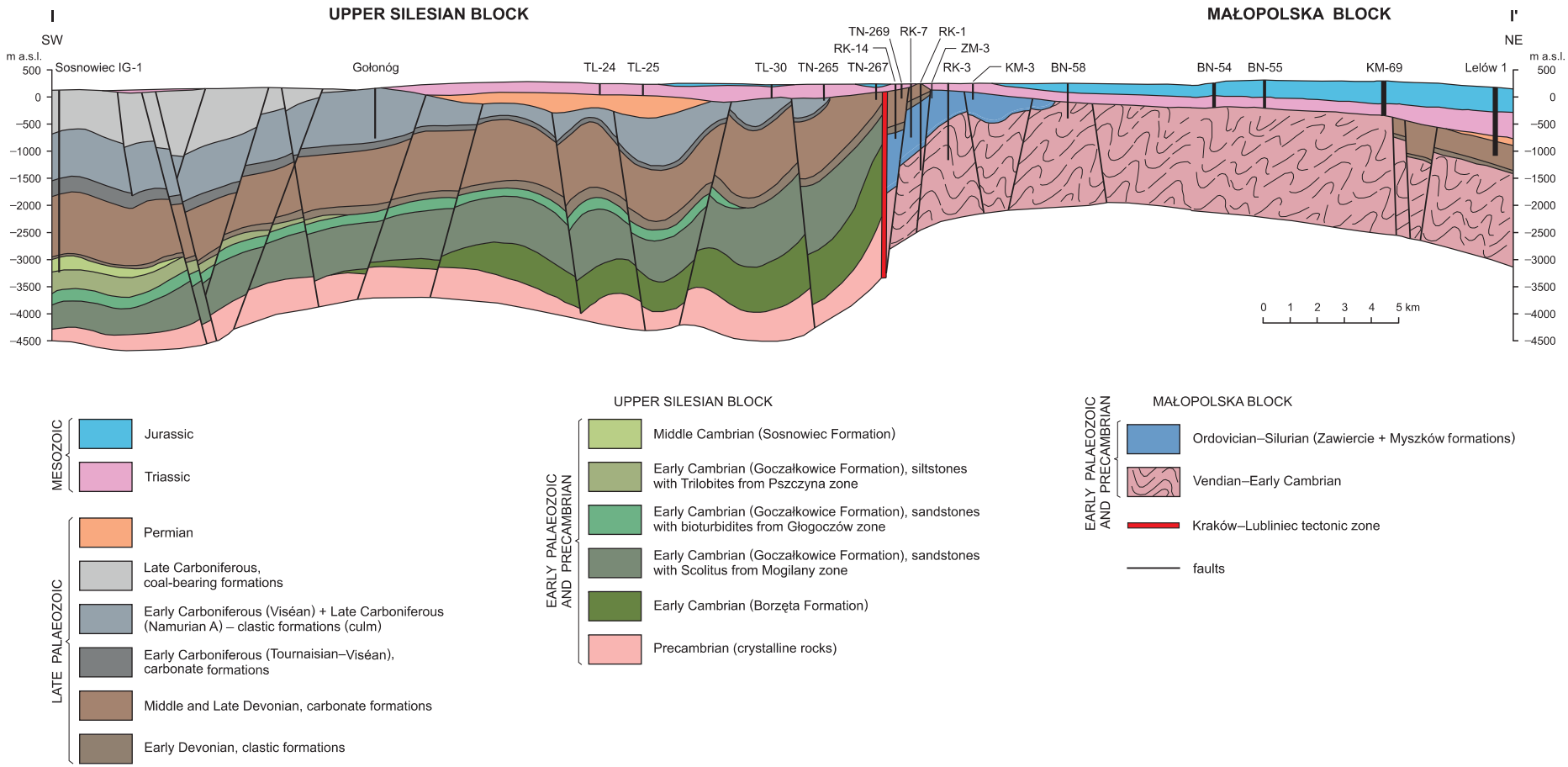

Fig. 5. Sosnowiec–Zawiercie–Lelów geological cross-section (after Buła, 2000)

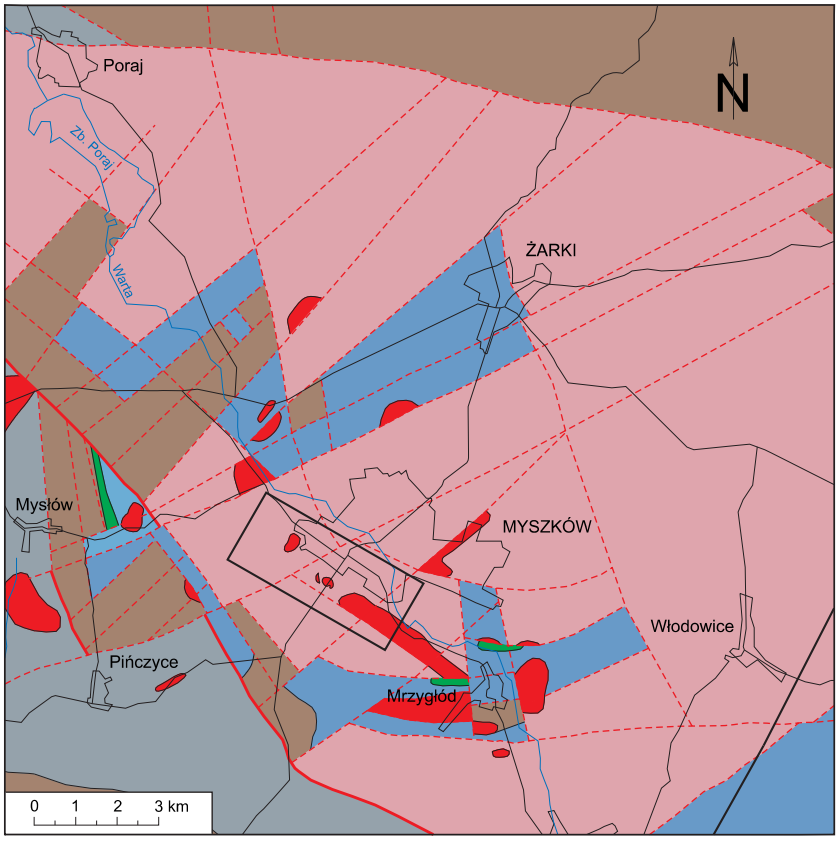

Fig. 6. Geological map of the Myszków area, without Permian and younger formations (Buła, Markowiak, Habryn)

For explanations see Figure 4. Rectangular form south-west of Myszków: area covered by Figure 7

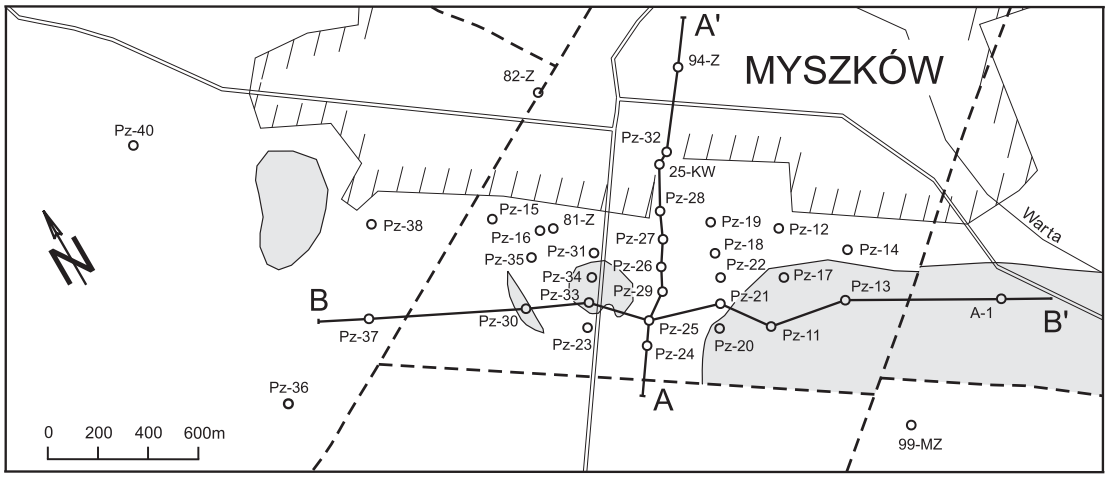

metamorphosed clastic rocks of Vendian–Early Cambrian

dacitoids, granitoids

faults

Pz-36 boreholes

A A' geological cross-section lines; see Figs. 8 and 9

Fig. 7. Location of boreholes in the Myszków area

(Buła, 2000; Buła *et al*., 1996, 1997; Żaba, 1996a, 1999). Wrench-faulting played an important role in the evolution of this tectonic structure (Żaba, 1995a, b, 1996a, 1999).

Two important tectonic units, the Upper Silesian and Małopolska blocks, are in contact along that zone (Figs. 4 and 5). The deposition of sediments forming the Precambrian and Palaeozoic (especially early Palaeozoic) rocks of these two blocks, and the structural evolution of the blocks, were influenced by repeated tectonic movement along the Kraków–Lubliniec zone (Buła, 1994, 2000; Buła *et al*., unpubl. report, 1996, Buła *et al*., 1997; Żaba, 1996, 1999). The tectonic activity of that zone is also associated with very intense magmatism along the common borders of both blocks.

During exploration for mineralisation in the Mesozoic and Precambrian to Palaeozoic rocks of the Myszków area, 35 boreholes were drilled. The boreholes were numbered: Pz-11 to Pz-38, Pz-40, A-1, 25-KW, 99-MZ, 81-Ż, 82-Ż, and 94-Ż (Fig. 7).

These holes encountered only rocks of the Vendian to Early Cambrian ages in the Precambrian–Palaeozoic formations (Fig. 6). These rocks are composed of metamorphosed, clayey to silty to sandy material (Buła, 2000; Buła *et al*., unpubl. report, 1996). These sedimentary rocks were intruded locally by a Late Carboniferous-aged granitoid body and its associated polymetallic mineralisation. Flat-lying, Triassic-age rocks and local Quaternary deposits cover the older formations to thickness of as much as 170 m.

The chapters that follow give a simplified description of the Precambrian and Palaeozoic sequences remaining in the Upper Silesian and Małopolska blocks, with special emphasis to the Myszków vicinity, and also describe their structural evolution within the contact zone of both blocks.

PRECAMBRIAN AND EARLY PALAEOZOIC

UPPER SILESIAN BLOCK

The Precambrian metamorphic rocks of the Upper Silesian Block have been found in the southern, sub-Carpathian part of the block, in the Puńców–Bielsk–Rzeszotary area (Heflik, 1982; Kotas, 1982, 1985; Moryc and Heflik, 1998; Ślączka, 1976, 1982).

The entire early Palaeozoic section in the Upper Silesian Block has not yet been found. Fragments of Early Cambrian clastic sedimentary rocks have only been recognised in cores from a few boreholes that were drilled along eastern margin of the block near Olkusz and Kraków (Buła, 1994, 2000; Buła and Jachowicz, 1996). Those sedimentary rocks have been assigned to the Borzęta and Goczałkowice formations, which have been defined in the southern part of the block.

An incomplete Middle Cambrian section, which is composed of about 200 m of silty to sandy clastic rocks, has been found in boreholes drilled near Sosnowiec, in the northern part of the Upper Silesian Block. This sequence has been assigned to the Sosnowiec Formation (Buła and Jachowicz, 1996).

Incomplete clastic to carbonate sections of Ordovician age that are as much as 80 m thick, were discovered in core from holes drilled farther north, outside of the Upper Silesian Coal Basin, in the Bibiela and Mysłów areas, between Siewierz and Kalety (Gładysz *et al*., 1990; Piekarski *et al*., 1985). These rocks have been named the Bibiela Formation (Buła, 2000).

The Early Cambrian rocks of the Borzęta and Goczałkowice formations, which in the Olkusz area may reach a thickness of 2500 m, the Middle Cambrian rocks of Sosnowiec Formation, and the Ordovician sedimentary rocks of the Bibiela Formation together constitute the Cambrian to Ordovician sequence found in the Upper Silesian Block (Buła, 2000). The problems of the stratigraphic continuity of the Cambrian formations and the structural relations between the Ordovician and Cambrian formations, are still unresolved.

In the eastern and northern margins of the Upper Silesian Block, the Early and Middle Cambrian rocks as well as the Ordovician rocks, are covered by Devonian rocks. Locally, however, the pre-Devonian rocks are covered directly by Mesozoic deposits. In the Olkusz area, a distinct unconformity (at an angle of as much as 30°) has been mapped between Early Cambrian and Early Devonian formations (Buła, 1994).

That unconformity is associated with tectonic events, which occurred between Early Cambrian and Early Devonian time and deformed existing rocks along the marginal, the eastern, and probably also along the northern, parts of the Upper Silesian Block. The extent and character of those deformations are unknown, as they were destroyed by later more intense disruptions related to deformations during the Variscan orogeny (Buła, 2000; Buła and Jachowicz, 1996).

MAŁOPOLSKA BLOCK

Precambrian and early Palaeozoic sedimentary rocks that are part of the western margin of the Małopolska Block have been mapped north-west of Kraków, between Lubliniec, Żarki, Zawiercie, Pilica, Wolbrom, and Dolina Będkowska. A carbonate sequence, which is found in vicinity of Żarki, Mrzygłód, and Zawiercie, and is as much as 100 m thick, constitutes the oldest known early Palaeozoic rocks and has been named the Zawiercie Formation (Buła, 2000). Conodont ages place these rocks in the Ordovician period (Arenigian age) through Early Silurian–Llandoverian and Wenlockian ages (Nehring-Lefeld *et al*., 1992; Nehring-Lefeld and Szymański, 1998; Siewniak-Madej, 1994; Szymański and Nehring-Lefeld, 1995).

Clayey to silty sedimentary rocks of the Mrzygłód Formation lie conformably above the carbonate sequence of the Zawiercie Formation. The Mrzygłód Formation has a maximum thickness of about 1500 m (Buła, 2000) and contains graptolites and acritarcha belonging to the Silurian period: Late Wenlockian and Ludlovian ages (Jachowicz, unpubl. report, 1995; Piekarski and Szymański, 1982; Szymański and

Nehring-Lefeld, 1995; Szymański and Teller, 1998; Tomczyk and Tomczykowa, 1983). The stratigraphy of the Mrzygłód Formation was compiled from incomplete sections mapped in the Lubliniec–Dolina Będkowska area.

The Łapczyca Formation, which consists of conglomeratic to sandy to silty rocks that are about 300 m thick (Buła, 2000), is regarded as the youngest Silurian unit found in the Małopolska Block. This formation has been recognised in several localities, including the areas near Zawiercie, Dolina Będkowska, Batowice, and Łapczyca.

The Ordovician to Silurian carbonate and clastic rocks of the Zawiercie, Mrzygłód, and Łapczyca formations unconformably overlie tectonically a sequence of clayey to silty to sandy rocks, containing intercalations of sandy gravels and small pebble-sized conglomerates. These sequence is characterised by various colours that range from green, through dark-grey with green or willow-green tint, to cherry-brown, ashen-grey, and violet-grey. These rocks are strongly indurated and, locally, exhibit steeply-dipping (40–80°) cleavage and varying degrees of metamorphism (greenschist facies) that has formed phyllites.

The stratigraphic position of these metamorphosed rocks is still not precisely known and can only be indirectly defined. Partial sections with this sequence have been encountered in more than 230 boreholes drilled between Żarki and Dolina Będkowska. Although these rocks have been found most commonly below Ordovician, Silurian or Devonian sequences, they are sometimes also found directly beneath Mesozoic-aged rocks.

These rocks have been tentatively assigned a Precambrian (Vendian) to Early Cambrian age (Buła, 1994, 2000; Buła *et al*., 1997) based on their comparison with rocks recognised in the Nida Depression, which are older than Ordovician, are lithologically similar, are metamorphosed to the same degree, and exhibit the same tectonic deformation.

At this time, reconstructing the complete Vendian to Early Cambrian stratigraphy is not possible because of an incomplete knowledge of those lithologically differentiated rocks, including a lack of information on the full thickness of each measured section and on the general absence of an identified lower contact for this sequence.

In conclusion, two structural complexes can be recognised in the Małopolska Block: the older, Vendian to Early Cambrian complex, which is present in the western part of the block, and the younger one of Ordovician to Silurian age, which consists of rocks belonging to the Zawiercie, Mrzygłód, and Łapczyca formations (Buła, 2000) that overlie the older complex.

In the Myszków area, which is located on the south-western margin of the Małopolska Block, the Vendian to Early Cambrian rocks are the only pre-Mesozoic sedimentary rocks present (Fig. 6). In this area, the lack of any correlatable horizons, as well as the partial metamorphism of the rocks, and intense tectonic deformation precludes any clear reconstruction of the complete stratigraphic profile. Piekarski (1985) regarded this sequence at Myszków as being metamorphosed Caledonian-aged rocks associated with early geosynclinal formation.

In the Myszków area, the Vendian to Early Cambrian complex is intruded by a Late Carboniferous, granitoid body. Near their contact with the intrusion, the Vendian to Early Cambrian rocks exhibit contact metamorphism and hydrothermal alteration (Karwowski, 1988; Ryka, 1978; Truszel, 1994).

LATE PALAEOZOIC

Lithologically similar Devonian and Carboniferous (early Namurian A included) rocks are present in the marginal parts of both structural blocks. These sequences consist of clastic or clastic-carbonate rocks of Early Devonian age, carbonate deposits of Middle to Late Devonian, and Early Carboniferous ages, and non-marine culm deposits of middle and late Viséan to early Namurian A ages (Bojkowski and Bukowy, 1966; Bukowy, 1984; Kotas, 1982, 1985; Narkiewicz, 1978; Narkiewicz and Racki, 1984; Pajchlowa *et al*., unpubl. report, 1983; Paszkowski, 1988; Siewniak-Madej, 1994). Toward the centre of the Upper Silesian Block, the late Palaeozoic is represented by a Late Carboniferous, coal-bearing sedimentary sequence (Fig. 4).

Although no real differences have been observed between the nature of the late Palaeozoic sedimentary rocks on either side of the Kraków–Lubliniec tectonic zone, one can see significantly different tectonic style. In the eastern and northern margins of the Upper Silesian Block, the thin, folded block structures dominate. On the other hand, in the western part of the Małopolska Block, the Devonian to Carboniferous rocks are only found in large, block-type structures (Fig. 4).

The Permian deposits of the eastern and northern margins of the Upper Silesian Block have been recognised in two elongated tectonic structures: the Sławków Graben and the Nieporaz-Brodło Trough (Kiersnowski, 1991). Their longer axes are parallel to the Kraków–Lubliniec tectonic zone. In the Małopolska Block, the predominantly clastic Permian rocks are located north and east of the Lubliniec–Żarki–Słomniki area and in the Miechów Depression (Jurkiewicz, 1975).

No late Palaeozoic-aged sedimentary rocks have been found in the Myszków area (Fig. 6). However, the granitoid rocks that intruded the Vendian to Early Cambrian-aged rocks have been assigned to the Late Carboniferous. The intrusion is elongated in a NW–SE direction (see the perpendicular cross-section A–A'; Fig. 8) and has been explored by a network of boreholes for a distance of about 7 km, from Mrzygłód area (Pz-10), through Myszków, to Nowa Wieś (60-Ż). Locally, the intrusion was exposed on the pre-Mesozoic erosion surface (Pz-30, Pz-33, Pz-34 and 60-Ż).

This granitoid intrusion formed in several stages that are characterised by complicated structure and varying mineral content. Numerous apophyses have been identified around the main mass of the intrusion. Faults have offset the main intrusion in many places (Fig. 9). It has been suggested that the uppermost part of the intrusion contains the strongest concentrations of Cu-Mo-W mineralisation and that later tectonic

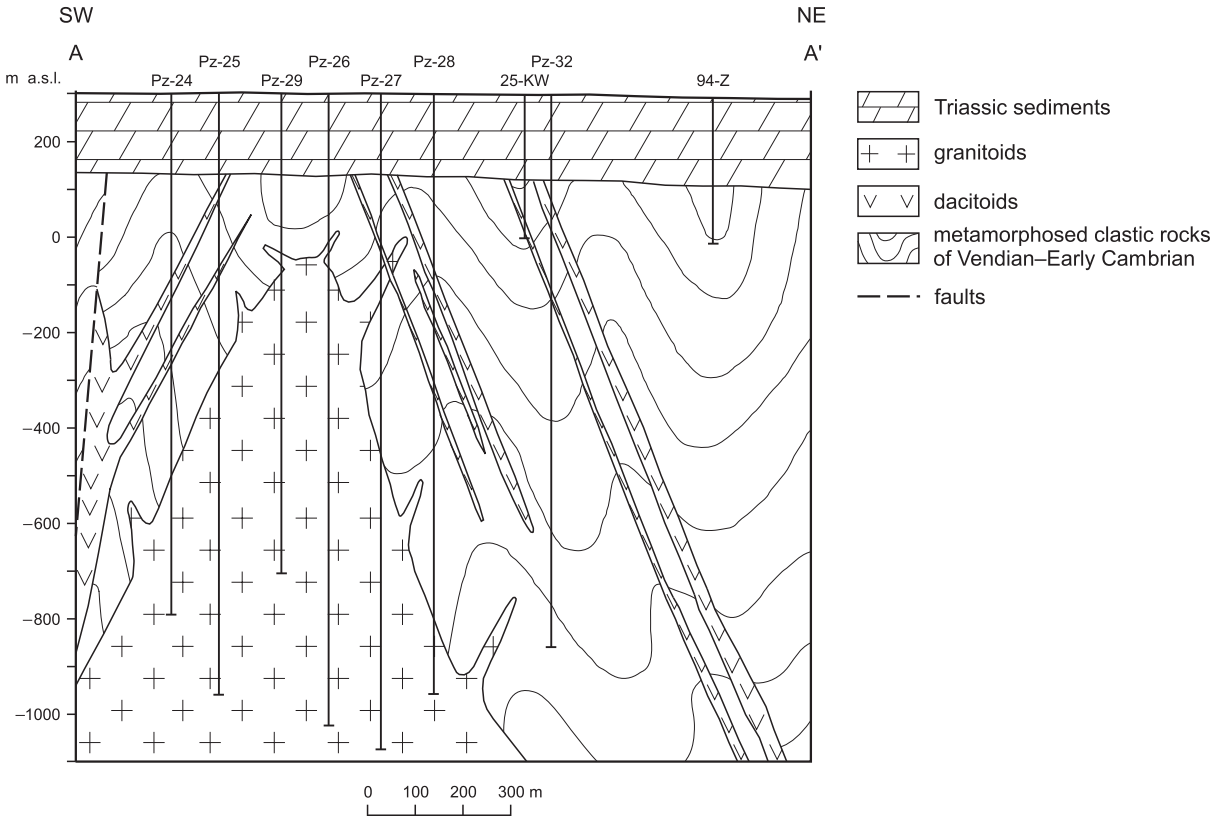

Fig. 8. Geological cross-section A–A'

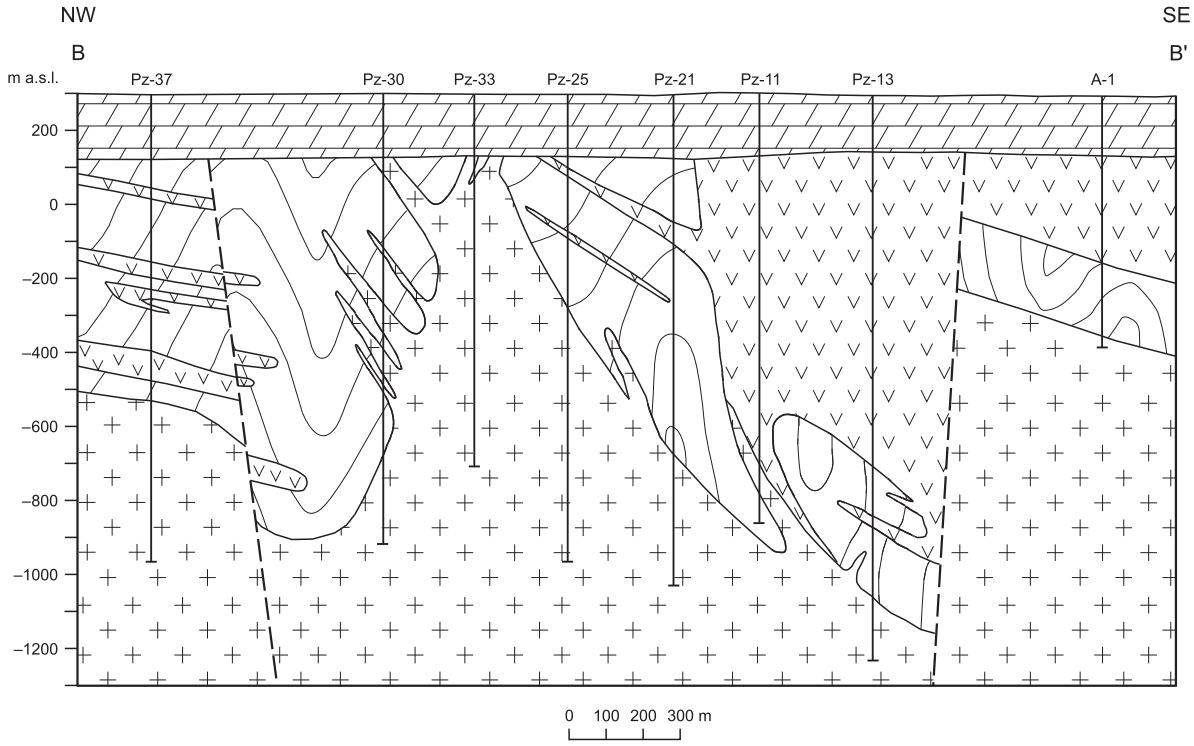

Fig. 9. Geological cross-section B–B'

For explanations see Figure 8

movements down-faulted that part of the intrusion into a tectonic depression.

Multistage porphyry intrusions are also important in the geological evolution of the Myszków area, as seen in core from borehole Pz-13 and the neighbouring boreholes (cross-section B–B', Fig. 9). These intrusions were probably associated with the faulting that offset the granitoid intrusion into blocks.

Two main types of porphyritic rocks have been identified: rhyolites and dacites. The quartz porphyry intrusion in Myszków area is shaped something like a lopolith and reaches a maximum thickness of 848 m in borehole Pz-13. In some localities, this intrusion is dike-like in form, with a true thickness of about 400 m. This porphyry intrusion is located above the granitoid intrusion and extends for as much as 3.5 km as seen in borehole A-3 near Mrzygłód.

Dacite porphyries are very common in the area and form thin dikes that are usually steeply inclined (around 70°) and very rarely exceed 20 m in thickness. The dacites are probably older than the rhyolites; however, their age relation with the granitoids has not yet been defined.

The contact between the pre-Mesozoic rocks (the Vendian to Early Cambrian sedimentary rocks and the Late Carboniferous granitoid massif), and the overlying Mesozoic–Cainozoic rocks is an erosional surface of varying relief. The overall surface is gently inclined, generally toward the north-east, and varies from 144.3 m a.s.l. (hole 99-MZ) in south-east, to 107.9 m a.s.l. (hole 82-Ż), and 108.8 m a.s.l. (hole Pz-40) in the north and north-west. The surface is higher locally (155.2 m a.s.l.; hole Pz-13) near pre-Mesozoic exposures of the rhyolites.

STRUCTURAL EVOLUTION OF THE PRECAMBRIAN–PALAEOZOIC ALONG THE CONTACT ZONE BETWEEN UPPER SILESIAN AND MAŁOPOLSKA BLOCKS

TECTONIC DEFORMATION EVENTS

In the Palaeozoic (and Vendian) stratigraphic sections along the contact between the Upper Silesian and Małopolska blocks (Fig. 4), the effects of four distinct deformations (D_1 to D_4) that produced fold macrostructures have been recognised. Each of the events ended with a distinct extensional episode.

The oldest **deformation event**, **D_1**, affected only the metasedimentary rocks of the Vendian to Early Cambrian sequence found in the Małopolska Block. This sequence was folded and regionally metamorphosed, probably after Early Cambrian time (Żaba, 1995), but possibly as late as the transition time between the Cambrian and Ordovician periods (Jurkiewicz, 1975; Pożaryski and Tomczyk, 1968; Znosko, 1996). This deformation event has not been observed in the sedimentary rocks of the Early Cambrian and Ordovician sections near the contact within the Upper Silesian Block.

Deformation event D_2 affected both the Cambrian and Ordovician sedimentary rocks found near the contact zone of the Upper Silesian Block, and the Vendian to Early Cambrian, and Ordovician to Silurian rocks found near the contact zone in the Małopolska Block.

The D_2 deformation occurred in several phases during the Late Silurian, as much as the Silurian/Devonian transition time (Żaba, 1994). During the Devonian to Carboniferous period of subhorizontal extension (locally, until the early Namurian A), which terminated the D_2 events, intense vertical movements were active in the contact zone between the Upper Silesian and Małopolska blocks. These movements most probably occurred at the end of the Devonian period and/or during the transition between Devonian and Early Carboniferous times (Żaba, 1996b, 1997a, b), and were accompanied by intrusions of diabases and older porphyries.

Deformation event D_3 occurred after Namurian A time (Żaba, 1996a) and affected diabases and certain porphyries, the Devonian to Carboniferous sedimentary rocks as well as all older rock complexes. Faulting styles included first thrusting, then, transpression and locally, strike-slip.

The D_3 deformation event had the greatest influence on the structure of the Palaeozoic rocks along the contact between both blocks and dominates the present-day tectonic style of this zone. After Westphalian B time, vertical displacements took place and granitoid intrusions, together with accompanying porphyries, were emplaced near the contact zone but only in the Małopolska Block.

Deformation event D_4 affected the contact zones of both the Upper Silesian and Małopolska blocks, as well as the granitoid bodies and related porphyries. This event took place during the transition between Westphalian and Stephanian ages and possibly, also during early Stephanian time (Żaba, 1996a), before deposition of the overlying Permo-Mesozoic rocks.

STRUCTURAL EVOLUTION

Several stages of structural development of the Palaeozoic rocks were identified in the contact zone between the Upper Silesian and Małopolska blocks.

Stage 1. Along the south-western margin of the Małopolska Block, sedimentation and diagenesis of flysch-type clastic rocks of Vendian to Early Cambrian age occurred (Fig. 10). This sedimentation may have continued into Middle Cambrian time, because the rocks of that age, which have been identified in other regions of the Małopolska Block, may have been entirely eroded in the study area. Sedimentation and diagenesis processes were accompanied by development of various synsedimentary deformational structures.

Stage 2. It is related to the oldest deformation event D_1, which occurred exclusively in the contact zone in the Małopolska Block, within the Vendian to Early Cambrian sequence. Folding of these rocks created recumbent, or — less frequently

— inclined, open to tight flexural macrofolds that are often transitional to shear folds.

The D_1 deformation produced disjunctive (fracture) cleavage and, in many areas, a penetrative, continuous S_1 slaty cleavage. The folding processes were accompanied by epizonal, regional alteration that produced either zeolite or lower to middle-greenschist facies metamorphism. The D_1 deformations probably occurred between the Cambrian and Ordovician periods (the Sandomierz orogeny?) but did not affect the Early Cambrian clastic sedimentary rocks near the contact zone of the Upper Silesian Block (Fig. 10).

The folded Vendian to Early Cambrian metasedimentary rocks underwent later denudation processes, probably during the earliest Ordovician and possibly also during Late Cambrian time. These processes led to the formation of an erosional-denudation-abrasional palaeosurface (Fig. 10).

Stage 3. In this stage, sedimentation of the clastic rocks (Cambrian) and of the clastic carbonates rocks (Ordovician) may have continued until Silurian time along the contact zone of the Upper Silesian Block (Fig. 10). This sedimentation was accompanied by numerous depositional and deformational structures. Some of these processes occurred synchronously with the events of Stages 1 and 2, which have taken place in the contact zone of the Małopolska Block, only.

Following deformation D_1, metamorphism and partial denudation of the Vendian to Early Cambrian sequence (and possibly, also rocks of Middle Cambrian age) occurred in the contact zone of the Małopolska Block. Following the denudation phase, sedimentation and diagenesis of the Ordovician to Silurian rocks occurred (Fig. 10). These rocks consist of carbonate deposits of the Zawiercie Formation and clastic deposits of the Mrzygłód Formation (Buła, 2000).

Stage 4. This stage includes all the processes associated with deformations of the D_2 event in the contact zones of both the Upper Silesian and Małopolska blocks. The deformations most likely occurred under recurrent sinistral transpression conditions from Late Silurian time until its transition into the Devonian period (the late Caledonian orogeny). The D_2 folding was not accompanied by metamorphism.

At the beginning of Stage 4, the deformations occurred under thrusting (compressional) conditions that led to folding of all of the rock sequences formed to that time. The limbs of the flexural macrofolds that formed at that time exhibit dip angles of as much as 15–20°. The folding was accompanied by the formation of fracture cleavage.

In close proximity to the Kraków–Lubliniec fault zone (in the region of Mysłów), the "fold" deformation was much more intense, and created asymmetrical, inclined, flexural macrofolds that show well developed, continuous slaty cleavage.

The Ordovician to Silurian sedimentary sequence and the Vendian to Early Cambrian metasedimentary sequence were folded in the contact zone of the Małopolska Block. In the Ordovician to Silurian rocks, open to tight, asymmetrical flexural folds formed. These folds were usually inclined, occasionally recumbent, and showed well developed, often penetrative, continuous cleavage.

The D_2 deformations also affected the rocks of the Vendian to Early Cambrian sequence that had already been folded during the D_1 event and created non-penetrative S_2 foliation. Those processes were terminated by short-term, subhorizontal extension that is weakly expressed in the marginal zones of both blocks.

The later deformations of D_2 event were solely related to the transpressional activity of the Kraków–Lubliniec fault. In the structural border zone between the Upper Silesian and Małopolska blocks, positive flower structures developed (Fig. 11A). These structures were accompanied by numerous minor deformational structures that contained both strike-slip and dip-slip displacement components. Following the cessation of tectonic compression, various extensional structures formed, including tension gashes, open fractures, and normal faults.

The D_2 deformations were terminated by subhorizontal compression that produced structural compressional wedges, pop-up structures, "tectonic" stylolites, reverse faults, and other features in the contact zone of the Małopolska Block only, and mainly in the Ordovician to Silurian rocks. The folded early Palaeozoic rocks subsequently underwent denudation, which led to the formation of erosional-denudation-abrasional palaeosurface (Fig. 10).

Stage 5. During this stage, sedimentation and diagenesis of the Devonian rocks occurred, along the contact zone between the Upper Silesian and Małopolska blocks (Fig. 10). In the contact zone of both blocks, distinct vertical movements took place at the end of Devonian and/or at the transition from Devonian to Early Carboniferous time (the Bretonic orogeny). The displacements, which usually show a normal fault style (subhorizontal extension), took place under ductile or brittle-ductile conditions.

At the end of Stage 5, diabase bodies and certain porphyries intruded the sedimentary wall rocks and produced weak, mostly thermal, contact metamorphic changes. The intrusions followed fault-related zones of mylonites, cataclasites, and tectonic breccias.

Stage 6. During this stage, sedimentation and diagenesis of Early Carboniferous carbonate and clastic rocks occurred along the contact zone between the Upper Silesian and Małopolska blocks. This events continued locally until early Namurian time (Fig. 10), during which various sedimentary structures were formed.

Stage 7. During this pre-intrusive stage (Żaba, 1996a), which post-dated Namurian A time, the deformations of phase D_3 took place. They occurred under dextral transpressional conditions during which the maximum compressional axis changed from north-east–south-west to north–south, and produced intense folding and faulting of the Palaeozoic sequences. These processes were not accompanied by metamorphic alteration.

During the Stage 7, regional anticlinal macrostructures formed, including flexural folds and cleavage-type structures, particularly in slates. Brittle-ductile to brittle shear zones of reverse-slip kinetics and medium dip angles were commonly formed in sedimentary and metasedimentary rocks as well as in diabases and porphyries. Those structures are often penetrative in nature.

During the Stage 7, some rather insignificant thrusting also occurred that was mostly oriented north or north-east but

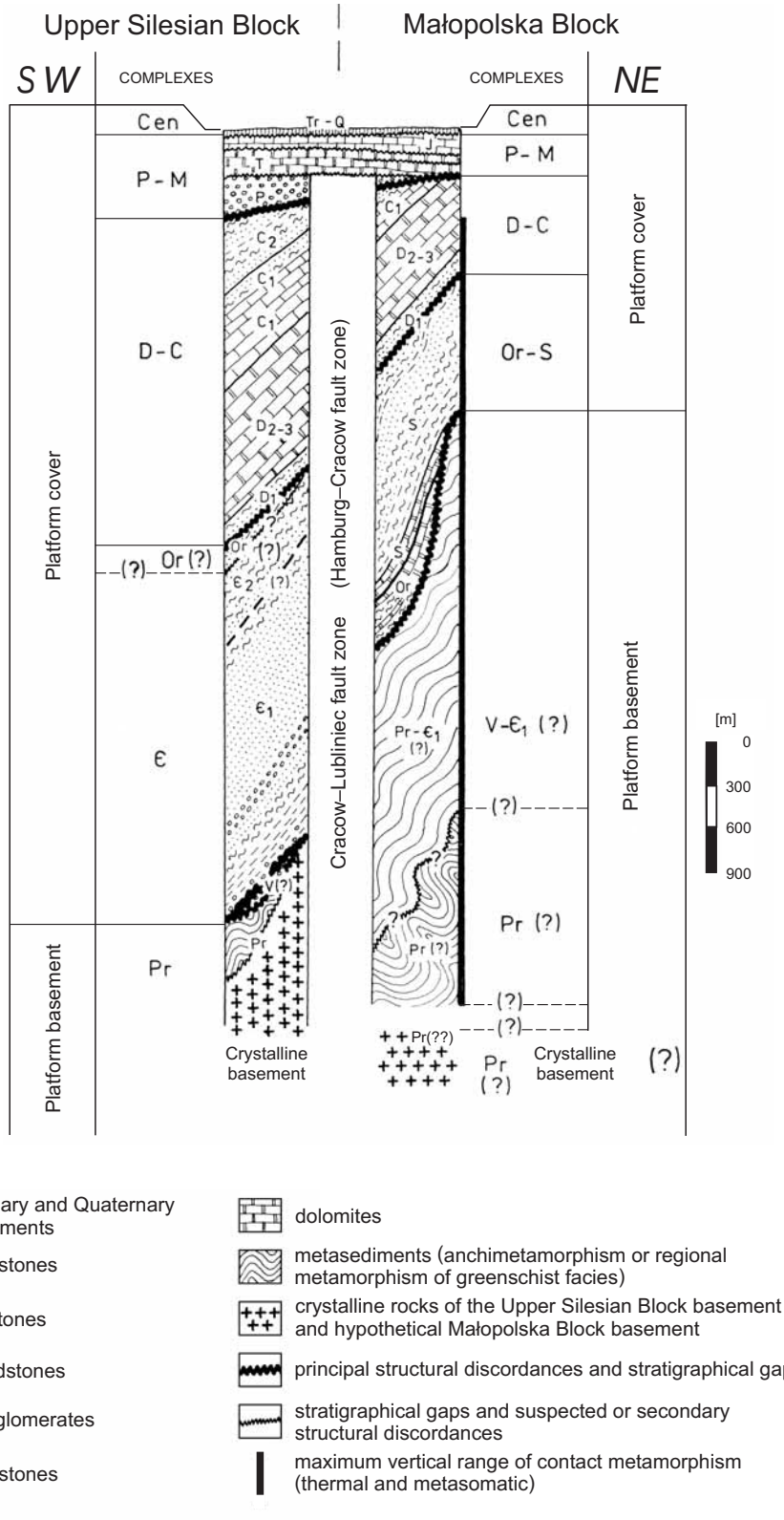

Tertiary and Quaternary sediments
claystones
siltstones
sandstones
conglomerates
limestones
dolomites
metasediments (anchimetamorphism or regional metamorphism of greenschist facies)
crystalline rocks of the Upper Silesian Block basement and hypothetical Małopolska Block basement
principal structural discordances and stratigraphical gaps
stratigraphical gaps and suspected or secondary structural discordances
maximum vertical range of contact metamorphism (thermal and metasomatic)

Fig. 10. Lithostratigraphic-structural complexes in contact zone of the Upper Silesian and Małopolska blocks — without magmatic phenomena (after Żaba, 1999)

Stratigraphy: Pr — Precambrian, V — Vendian, ϵ_1 — Early Cambrian, ϵ_2 — Middle Cambrian, Or — Ordovician, S — Silurian, D_1 — Early Devonian, D_2 — Middle Devonian, D_3 — Late Devonian, C_1 — Early Carboniferous, C_2 — Late Carboniferous, P — Permian, T — Triassic, J — Jurassic, Tr — Tertiary, Q — Quaternary

Lithostratigraphic-structural complexes: Pr — Precambrian complex, V_1 — Vendian-Early Cambrian complex, ϵ — Cambrian complex, Or — Ordovician complex, Or-S — Ordovician-Silurian complex, D-C — Devonian-Carboniferous complex, P-M — Permian-Mesozoic complex, Cen — Cainozoic complex

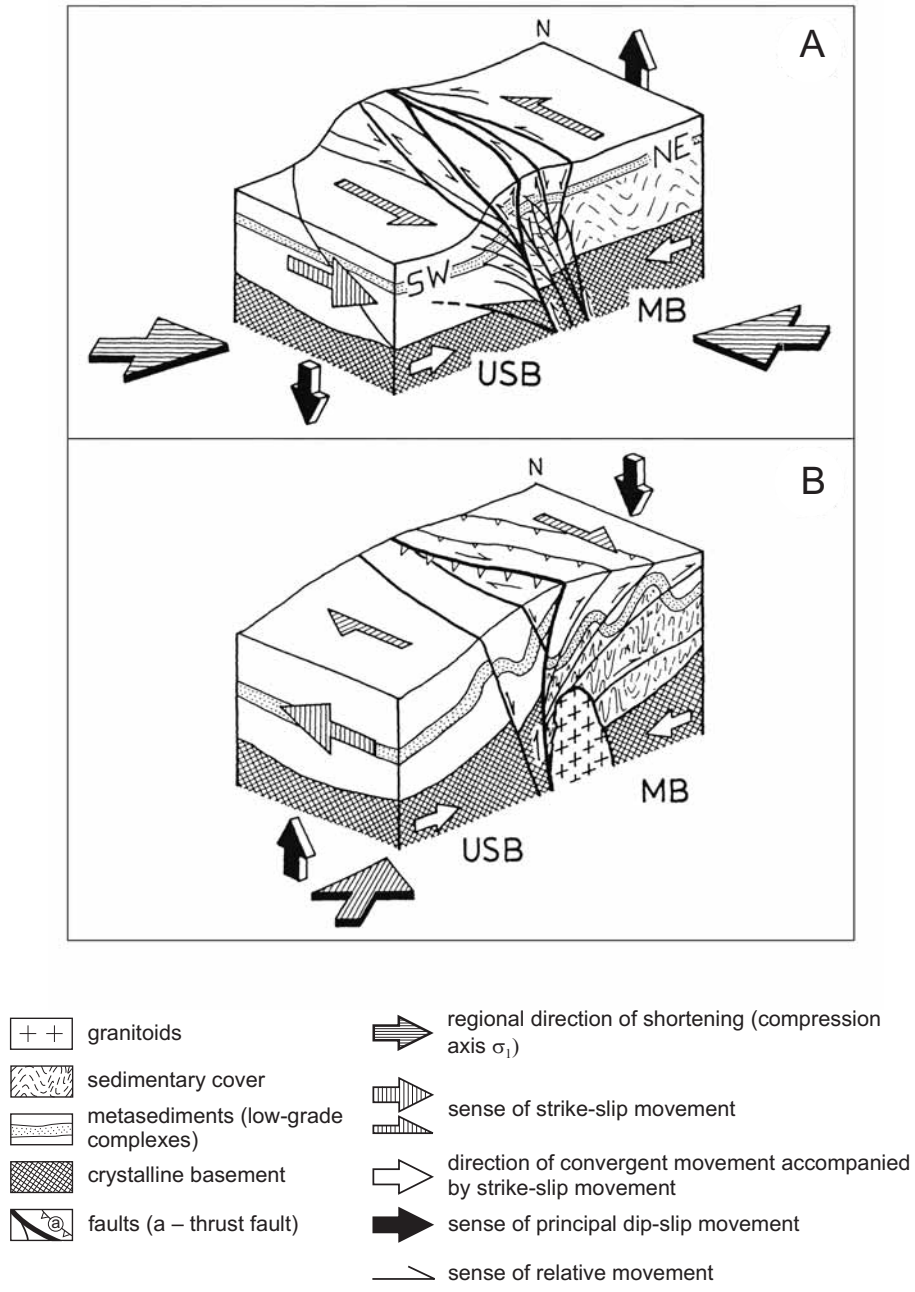

Fig. 11. Principal tectonic periods of strike-slip activity in the contact zone between the Upper Silesian (USB) and Małopolska (MB) blocks

After Żaba, 1994, 1996b; Buła *et al*., 1997; schematic model, not to scale.

11A — sinistral transpression (approximately west-east shortening direction) at or near the end of the Silurian; **11B** — dextral transpression (NNE–SSW directed compression) during the Late Carboniferous (post-Namurian A).

much less frequently south to south-west. These faults took advantage of existing structural and sedimentary contacts (Fig. 11B). During the D_3 deformations, granitoid magma was presumably generated. At the end of this stage, intense erosion began, leading to the formation of another erosional--denudation-abrasional palaeosurface (Fig. 10).

Stage 8. During this stage (the intrusive stage; Żaba, 1996a), which post-dates Westphalian B time (the Leonian orogeny), the dextral transpression gradually diminished and was replaced, as a result of a further sinistral rotation of the principal stress axis σ_1 (assuming NNW–SSE or, even, NW–SE orientation), by dextral and, locally, sinistral transtension.

During the initial phase of Stage 8, granitoid bodies began to rise within the lower levels of the contact zone of the Małopolska Block (Fig. 11B). At depth, stockwork-type quartz veins were formed. Formation of these veins was accompanied by numerous phases of ore mineralisation.

During the final phase of Stage 8, granitoids intruded into active, extensional shear zones and reached higher levels, including those presently accessible to drilling. These processes

created widespread contact metasomatic and thermal alteration zones. The granitoids, sedimentary wall rocks, and the diabase bodies were subsequently cut by veins, which were formed in several stages.

Stage 9. Stage 9 (the post-intrusive stage; Żaba, 1996a) occurred during the transition between Westphalian and Stephanian times and, also possibly during early Stephanian time (the Asturian orogeny). During this stage, the deformations recurred under dextral transpression conditions. As a result of dextral rotation, the compression axis, which initially had a nearly north-south orientation, changed to a NNE–SSW or NE–SW orientation.

All of the rock sequences formed by the time of Stage 9 along the contact zone between the Upper Silesian and Małopolska blocks were affected by deformations of phase D_4. In the granitoids found near the Małopolska Block contact zone, a number of structural features associated with this stage have been observed. In the entire area, folds, reverse faults, and minor thrusts formed but generally on a more restricted scale. These structures formed parallel to similar structures developed during phase D_3.

Stage 10. This stage has been dated as occurring at the end of the Late Carboniferous, and during Permian and Early Triassic times. During this stage, sedimentation and diagenesis of Permian and Lower Triassic deposits took place under extensional conditions that were characterised by a vertically positioned axis that had the least principal stress and, partly, under sinistral transtension conditions (σ_1 oriented approximately NW–SE).

The structures formed during the Stage 10 time are associated with normal-slip or normal-oblique faulting that occurred under brittle and, locally, brittle-ductile conditions. The deformations were, to a high degree, related to an intense vertical movement of the entire area. Numerous normal faults were newly formed or were reactivated, as were pre-existing grabens, horsts and fault blocks. Fault zones were accompanied by tectonic breccias, kakirites, lenticular structures and en échelon extensional joints that are sometimes transitional to sigmoidal fractures. This stage was also accompanied by numerous magmatic phases that produced quartz porphyries, lamprophyres, diabases, and ore mineralisation.

PERIODS OF INCREASED STRIKE-SLIP ACTIVITY

Strike-slip faulting plays a dominant part in the multistage structural evolution of the contact zone between the Upper Silesian and Małopolska blocks that constitutes the Kraków–Lubliniec fault zone. This faulting was particularly active during two main periods.

Period I was associated with the sinistral transpression that occurred at the end of the Silurian period or at the transition between the Silurian and Devonian periods (Fig. 11A). During period I, the early Palaeozoic sequences along the contact zone between the Upper Silesia and Małopolska blocks were folded. This process was accompanied by minor magmatic activity that produced discordant mafic and felsic dikes.

As a result of east-west compression, sinistral strike-slip faulting occurred along the Kraków–Lubliniec fault zone. This faulting was accompanied by a synchronous, relative uplifting of the Małopolska Block along that zone and a relative subsidence of the Upper Silesian Block (Żaba, 1994). In these areas, positive flower structures formed. These features were, presumably, related to an oblique collision of two distinct, rigid crustal blocks.

The left-lateral displacements along the Kraków–Lubliniec zone probably took place between Early Ordovician and Early Devonian times (Brochwicz-Lewiński *et al*., 1983). These displacements are partly consistent with the sinistral movements along the Teisseyre-Tornquist Line (Pożaryski *et al*., 1982) that occurred between Middle Ordovician and Late Silurian time. However, according to Paszkowski (1988), the left-lateral displacements must have occurred in the Kraków–Lubliniec zone somewhat later, probably during Devonian period, between Geddinian and Frasnian ages.

Period II was related to Late Carboniferous dextral transpression, which was repeated twice and led to the second folding of the early Palaeozoic rocks and the first folding of the Late Palaeozoic rocks that existed at the time of Period II. These processes were accompanied by intense magmatism, that continued until Early Permian times.

Late Carboniferous transpression (compression in a north--south direction that subsequently changed to a NE–SW orientation) took place after Namurian A time. This transpression caused the north-eastern margin of the Upper Silesian Block to be thrust over the Małopolska Block along a high-angle reverse fault (Żaba, 1996a). This movement produced numerous reverse faults and minor thrust faults, mostly along the contact zone in the Małopolska Block (Fig. 11B).

During Period II, granitoid magma was formed and accumulated at depth. Subsequently, after Westphalian B time, magma intruded into the more disrupted, marginal zone of the Małopolska Block (Fig. 11B). The granitoid intrusions were emplaced under conditions of a dextral (locally also sinistral) transtension that was associated with sinistral rotation of the principal stress axes. During the transition from Westphalian to Stephanian time, the granitoids of the marginal part of the Małopolska Block underwent a series of deformations that were related to the recurrence of dextral transpressional conditions (Żaba, 1996a).

EFFECTS OF TECTONICS ON ROCKS IN THE MYSZKÓW AREA

Rocks from the Myszków area were subjected to regional, multistage stresses of varying types and orientations. The most commonly observed tectonic structures include (Badera, unpubl. report, 1999):

- fractures — open or closed (barren or mineralised);
- veins — fissure infilling, metasomatic, and breccia types. These include veins (*sensu stricto*) that are greater than 10 cm, veinlets that are 1 mm to 10 cm thick, and microveinlets that are less than 1 mm thick;

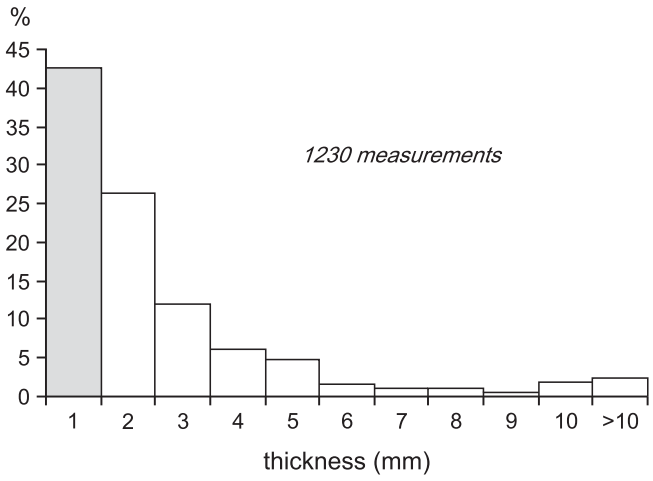

Fig. 12. Histogram of quartz and quartz-feldspar veins cumulative thickness, from boreholes Pz-12, Pz-17, Pz-18, Pz-19, and Pz-22 cores (Badera, unpubl. report, 1999)

Unqualified number of measurements: uncorrected, partitions dextrally closed; grey — modal partition

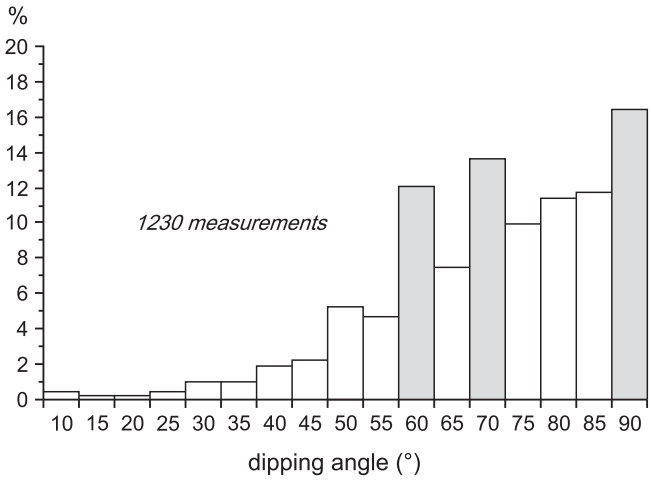

Fig. 13. Histogram of quartz and quartz-feldspar veins dipping, from boreholes Pz-12, Pz-17, Pz-18, Pz-19, and Pz-22 cores (Badera, unpubl. report, 1999)

Unqualified number of measurements: uncorrected, partitions dextrally closed; grey — modal partition

- breccias and kakirites: tectonic, hydraulic, and magmatic;
- crushed material, sometimes associated with tectonic clays;
- slip structures: slickensides, tectonic splinters, and tectonic striations.

The main mineralised system is a stockwork type and is composed of a network of cross-cutting veins, veinlets, and microveinlets that are oriented in several different directions. These vein structures are present both in magmatic rocks (mainly in granitoids) and in wall rocks. These structures are most commonly filled with quartz but may also contain feldspars, and, more rarely, chlorite, sericite, carbonates, and ore minerals.

Statistical analyses based on observations of veins in core from five selected boreholes (Pz-12, Pz-17, Pz-18, Pz-19, and Pz-22) proved that microveinlets and veinlets that are as much as 2 mm thick dominate over thicker quartz and quartz-feldspar veins (stockwork) and constitute greater than 70% of all vein structures (Badera, unpubl. report, 1999; Fig. 12).

Most of the veins dip 60 to 90° (Fig. 13). There are two independent vein systems. The first contains dips between 50 and 75°, and the second, between 75 and 90°. Relatively flat-lying secondary veins that have dips between 0 and 50° are less important.

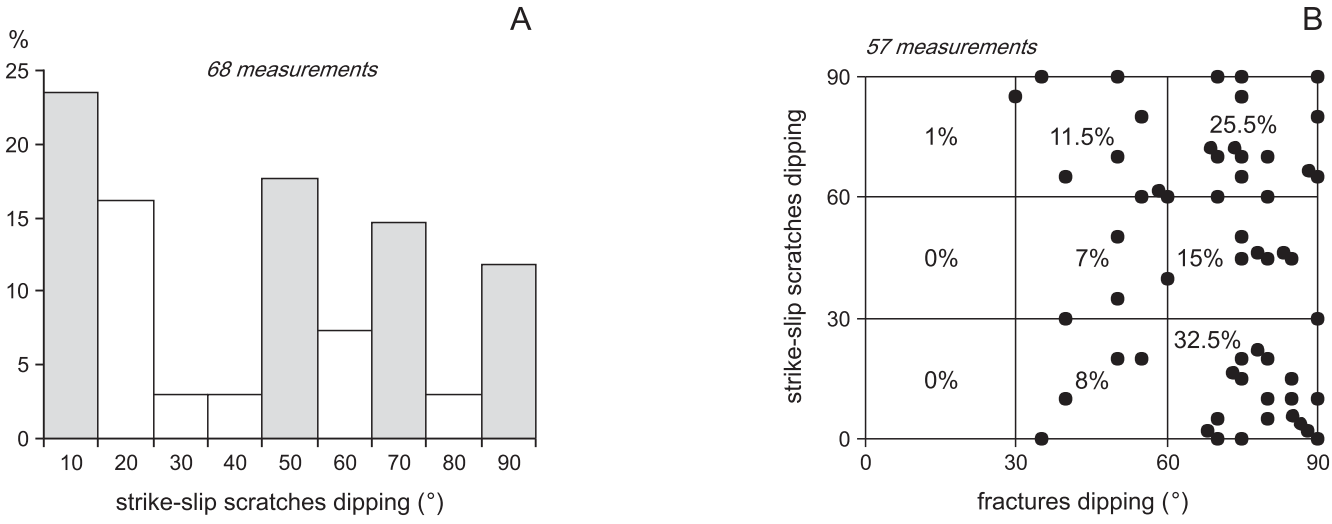

Fig. 14. Orientation of strike-slip scratches on postintrusive fractures (Badera, unpubl. report, 1999)

14A — Unqualified number of measurements: uncorrected, partitions dextrally closed; grey — modal partition; **14B** — Particular measurements and their participation (%) in angle groups (every 30°)

Vein density is variable but averages about 10–50/m. In the wall rocks, their density increases as one approaches contacts with the granitoid intrusion. The entire granitoid massif, but especially its endo- and exocontact zones, exhibits the highest density of veins.

The least mineralised or completely barren structures formed during the youngest (post-orogenic) stage. These structures include cataclasites (unconsolidated sand to clay-sized material in fault zones), tectonic breccias, cleavage, and fault and joint fractures.

The cumulative thickness of the deformed zones in cores is somewhat greater than 5%. The cumulative thickness of tectonic breccias approaches several tens of metres (Badera, unpubl. report, 1999).

Cleavage and joint structures that appear in the youngest fracture system occur in subparallel zones, which range from a few to more than a dozen metres thick, are also important. The distance between individual cleavage planes varies from 1 mm to a few centimetres, and, between the joint planes, from a few centimetres to more than 10 centimetres. These structures are generally horizontally oriented, and are found every 1 to 5 cm at the depth exceeding 900 m, particularly in the granitoids.

The fault and joint fractures, which are locally mineralised with carbonates or chlorite, are less common and dip at 45 to 90°, with most dipping 60 to 80°. Distances between fractures varies from about 10 centimetres to several metres.

As observed in the boreholes, all of the deformation structures, with the exception of cleavage, are found in zones that are as much as 50 to 60 m thick. The actual thickness probably does not exceed 20 m. Deformation intensity increases toward the middle of each zone, changing from single-fault fractures at the fringes, to breccias with tectonically pulverised material in the middle. The tectonic features present on fracture surfaces, indicate the strike- and dip-slip character of faults (Fig. 14; Badera, unpubl. report, 1992, 1999; Wojnar, unpubl. report, 1985, 1989).

Because of the substantial number, steep dip angle (60–80°), and variable mineral content of the fault zones observed in drill cores, their correlation between boreholes was not possible. The generally great distance between boreholes also made correlation difficult. Geophysical logging, especially the measurement of borehole diameters, was often very helpful in locating fault zones that were over 1 metre thick.

METAMORPHIC ROCKS

Metamorphic rocks were discovered in the Myszków area under a flat-lying Triassic sedimentary section at depths of about 150 m to 1200 m. Prior to metamorphism, the pre-Triassic rocks consisted of clayey to silty to fine-grained, sandy sequences that were locally carbonate-rich. Claystones occurring as layers or interbeddings within mudstones and sandstones, were the dominant rock type. Mudstones formed thin interbeddings in claystones and sandstones. Sandstones commonly occurred in several tens of metres thick sequences or as interbeds in other sedimentary rocks.

As a result of regional metamorphism, various types of phyllites, crystalline schists, and quartzites were formed. Minerals developed in these rocks are typical of the chloritic and biotitic zones of greenschist facies metamorphism (Truszel, 1994).

Contact metamorphism is younger than regional metamorphism. Where wall rocks are in contact with magmatic rocks, this later event has produced actinolite-pyroxene hornfelses (Heflik, 1992) and skarns. Sharp boundaries between the different rock types are quite common.

In a relatively short time after magmatic intrusions were emplaced, the metamorphic rocks were also subjected to several metasomatic events that occurred during both the pre-mineralisation and mineralisation processes. During these events, metasomatites with accompanying mineralisation were formed (Ślósarz and Truszel, unpubl. report, 1997; Truszel, 1994).

EFFECTS OF REGIONAL METAMORPHISM

PHYLLITES AND SCHISTS

Rocks described in this chapter were classified according to grain size, using the scheme of Pettijohn *et al*. (1972). Rocks with grains less than 0.12 mm in diameter were primarily classed as clayey-mudstones. These rocks commonly contained a small amount of carbonate-rich material. As a result of regional metamorphism, these rocks were transformed into metapelites (metamorphosed mudstones) and meta-aleurites (metasiltstones) (Ryka, 1971, 1973).

These rock types are very common in examined cores, with the relative thickness of the metamorphosed sequence varying between 100 m and 800 m. The metamorphosed rocks are generally massive, dark-grey to green-grey, locally silky in appearance, with fine and medium crystalline textures, and with more or less parallel structures. These rocks contain, in decreasing

Table 1

Average modal composition of phyllites

Minerals	Content in volume %	
	Range	Average
Quartz	0.0–44.6	18.1
Albite	1.0–51.6	16.3
Muscovite	3.1–54.5	22.3
Sericite	0.1–69.2	3.6
Biotite	4.8–54.0	33.4
Chlorite	0.1–33.7	3.6
Epidote + amphibole	0.1–0.8	<0.1
Opaque minerals	0.5–18.8	1.9

order: quartz, feldspar, sericite, muscovite, biotite, chlorite, epidote, and amphibole (Table 1).

The results of point counts for phyllites were plotted on a Winkler (1967) classification triangle, with its apexes representing percentages of quartz-albite-muscovite, biotite, and chlorite, respectively (Fig. 15). The phyllites are located in the albite phyllite, albite gneiss, sericite-chlorite gneiss, and sericitite fields.

The Winkler classification, however, does not fully take into consideration the mineral variations in the rocks examined, especially the variations in albite, sericite, muscovite, biotite, and chlorite. When those variations are considered, the examined rocks are best classified as being sericite, sericite-chlorite, muscovite-chlorite-albite, and muscovite-chlorite--epidote phyllites and schists.

Sericite phyllites represent the least altered rocks and are characterised by finely crystalline textures and parallel structures. Sericite, their main mineral component, usually forms aggregates of thin plates that decrease in abundance in a dominant direction. Single plates of sericite size do not exceed 0.02 mm. Locally, sericite has recrystallised to muscovite plates that may be as much as 0.05 mm in diameter.

Small amounts of chlorite, quartz, and plagioclase may be present in sericite phyllites. In cases where larger amounts of chlorite are present, sericite-chlorite phyllites can be distinguished. In the most strongly altered phyllites, sericite has been replaced by muscovite and the amount of albite has increased. Muscovite sometimes forms either synkinetic clusters that are as much as 0.4 mm thick, or postkinetic porphyroblasts.

A relatively high biotite content is present in rocks classified as schists. These are generally albite-muscovite-biotite schists, which may also contain chlorite, epidote, and (or) actinolite. Schists textures are finely- to medium-crystalline, and structures are usually parallel to each other or may be massive, as in the case of rocks containing epidote or actinolite.

The quantitative chemical content of biotite and epidote, from the albite-muscovite-biotite schists (with epidote), have been determined using an X-ray energy microprobe. Analysed biotite contain: SiO_2: 36.46–37.81%, Al_2O_3: 17.82–19.60%, FeO: 18.00–20.37%, MgO: 9.79–12.49%, TiO_2: 1.70–3.10%, and MnO: 0.11–0.49%. In contrast, the content of K_2O varies only slightly (K_2O: 10.19–10.45%). The Mg/(Mg+Fe) ratio ranges between 0.48 and 0.59.

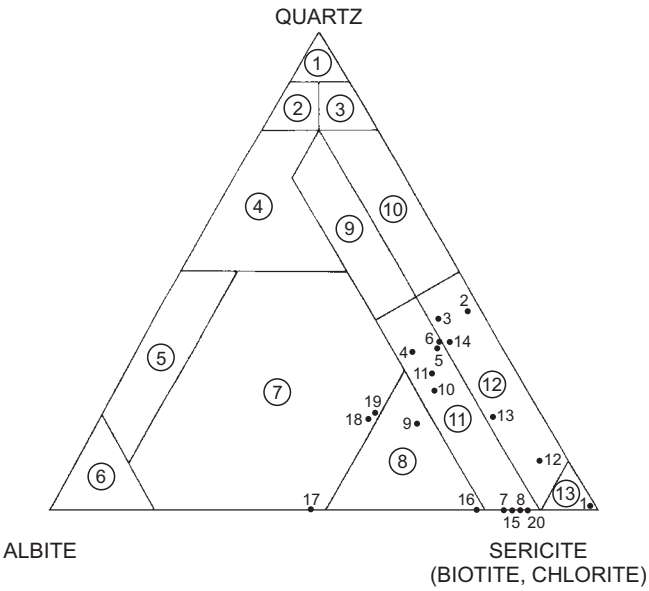

Fig. 15. Lithological classification of phyllites (after Winkler, 1967)

Fields (in circles): *1* — quartzite, *2* — albite-(microcline)-quartzite, *3* — mica quartzite, *4* — quartzitic gneiss, *5* — quartz-albite-(microcline) fels, *6* — albite fels, *7* — sericite-chlorite gneiss, *8* — albite-(microcline) gneiss, *9* — albite-(chlorite)-quartz phyllite, *10* — quartz phyllite, *11* — albite-(chlorite) phyllite, *12* — phyllite, chlorite schist, *13* — sericite phyllite; samples — black points with numbers

Chemical formulas for biotites are as follows:

Pz-17/ 775,7 m: $K_{0.88}\ Na_{0.07}\ Mg_{1.13}\ Fe^{2+}_{1.05}\ Al_{0.10}\ (OH)_2\ [Al_{1.43}\ Ti_{0.10}\ Si_{2.41}\ O_{10}]$

Pz-29/ 218,0 m: $K_{0.91}\ Na_{0.04}\ Mg_{1.30}\ Fe^{2+}_{0.90}\ Mn_{0.04}\ (OH)_2\ [Fe^{3+}_{0.17}\ Al_{1.21}\ Ti_{0.15}\ Si_{2.64}\ O_{10}]$

Pz-32/ 721,0 m: $K_{0.86}\ Na_{0.06}\ Mg_{0.97}\ Fe^{2+}_{1.13}\ Al_{0.03}\ (OH)_2\ [Al_{1.46}\ Ti_{0.08}\ Si_{2.46}\ O_{10}]$

The chemical formula for epidote is as follows:

$Ca_{1.68}\ (Fe^{2t+}_{0.79}\ Mn_{0.02})\ Al_{1.48}\ [(O, OH)\ (Si_{3,11}O_{11})]$

Epidote contains 22.55% CaO, 18.08% Al_2O_3, and 13.65 FeO. That chemical composition is typical for most epidotes (Deer *et al.*, 1962), as is the FeO/(Al_2O_3+FeO, ratio of 0.43 (Miyashiro, 1973).

Characteristic patchy structures that vary in size between 0.06 and 0.5 mm but are sometimes found in sizes between 3 and 5 mm, are present both in phyllites and in polymineralic schists. The irregular patchy habit, which is clearly visible in core samples, occurs in zones that vary from a few cm wide to several tens of centimetres wide. The distribution of these structures suggests a spatial relationship with zones that have been strongly affected tectonically.

Groups of these patchy structures can be differentiated according to their shape, size, and mineral composition. Most commonly, the patchy structures are composed of aggregates of thin plates of sericite or muscovite present in a biotite-chlorite matrix, or of aggregates of biotite plates containing chlorite and opaque minerals that are surrounded by sericite. The variable mineral content of the patches may have resulted from mylonitisation of laminated rocks, with the laminae having different mineral contents (Spry, 1969).

METAPSAMMITES

The metamorphosed sandstones (metapsammites) are found in phyllites and exhibit sharp contacts with surrounding foliated rocks. The metapsammites occur most commonly as layers interbedded in the phyllites (Pz-17, Pz-24, Pz-28, and Pz-31) and, more rarely, as thick groups of layers (Pz-32). The metapsammites are greenish-grey, massive, contain random or indistinct parallel structures, and have macroscopically visible grains. They contain characteristic sandstone relicts. Both textural/structural and mineral differentiation can be seen under a microscope. Irregular development of secondary alteration minerals is also evident.

Textures in metapsammites vary from those of well preserved primary sandstones (Pz-32), to those of almost completely metamorphosed rocks containing mostly recrystallised and porphyroblastic textures. The structures also vary from random, indistinctly parallel ones to mylonites with distinct orientations.

The metapsammites from boreholes Pz-17, Pz-28, and Pz-29 have fine grained (0.12–0.25 mm) and medium grained (0.25–0.5 mm) textures. These medium grained rocks are poorly sorted and contain some coarse-grained material. Metapsammites from boreholes Pz-31 and Pz-32 are more poorly sorted, with fine to coarse sand grains ranging in size between 0.08 and 1.0 mm, and sporadically as much as 1.2 mm.

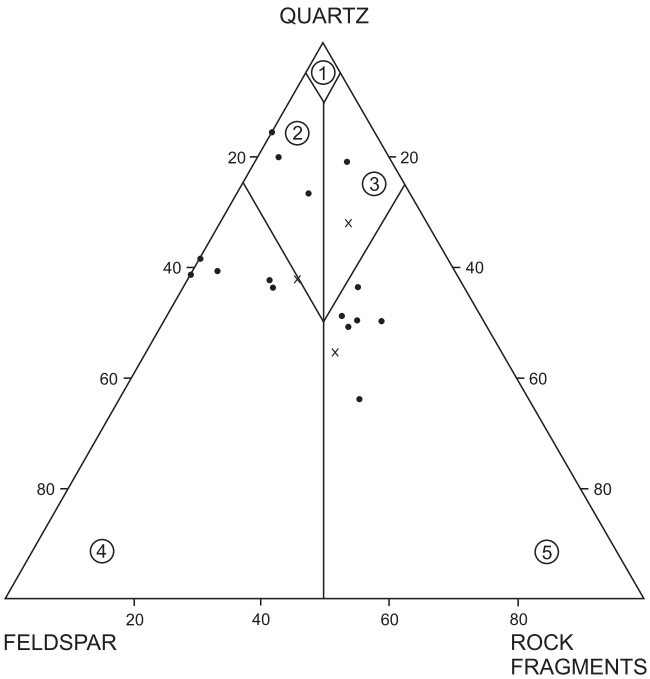

Fig. 16. Lithological classification of metapsammites (after Pettijohn *et al*., 1972)

Fields (in circles): *1* — quartzwacke, *2* — arcosic wacke, *3* — sublithic arenite, *4* — feldspar graywacke, *5* — lithic graywacke; samples: black points — wackes, x — arenites

The high degree of recrystallisation and secondary alteration of feldspars, rock fragments, and matrix in the metapsammites tends to conceal grain boundaries locally and make point counting difficult. However, most of the analysed samples in boreholes Pz-17, Pz-28, Pz-29, Pz-31, and Pz-32 contain greater than 15% of matrix material. According to Pettijohn *et al*. (1972), that percentage classifies these rocks as subarkoses and lithic graywackes. The few samples containing less than 15% of matrix material (Pz-17 and Pz-32) are classified as sublithic and lithic arenites (Fig. 16).

Quartz, feldspars, micas, and lithic fragments have been recognised as being the major mineral components. The primarily clayey to siliceous matrix, which is locally carbonate-rich, underwent strong recrystallisation.

Lithic fragments are more common in the coarser grained rocks. Fragments of metamorphic rocks composed of quartzite, gneiss, and quartz-chlorite schist constitute the most common lithic material. Less common are grains of plutonic (granite) and subvolcanic (microgranite, and diabase) rocks. Rutile, tourmaline, zircon (zoned), and apatite are the most common accessory minerals in the metapsammites.

Intra-granular space in the metapsammites is filled with recrystallised matrix, which very often exhibits overgrowths on some grains. The matrix is composed of biotite, albite, chlorite, muscovite, and sericite, with sporadic amounts of actinolite, chloritoid, and epidote.

The dominant mineral in most of the analysed rocks is secondary crystallised biotite, which has grown at the expense of matrix material, of some plutonic rock fragments, and of feldspars (Pz-24, 723.1 m). The secondary biotite is a neogenic, pre-kinematic, deformed, and distorted mineral (Spry, 1969; Vernon, 1976). Recrystallised, syn-kinematic biotite is present in small, parallel flakes. Post-kinematic biotite, which recrystallised following tectonic activity, is characterised by larger crystal sizes. This latter type of biotite forms flaky, irregular aggregates or plates that are overgrowths on other minerals. Small grains of primary, detrital biotite with grey-brown pleochroism, have been seen in a few samples.

In some samples, albite is more common than biotite (Pz-28 and Pz-31). This albite is poikiloblastic, forms overgrowths on surrounding minerals, and contains inclusions of these minerals. The contents of albite and biotite increase with depth.

Flaky and platy muscovite is generally less common than biotite. This muscovite is fine grained and has parallel structure and synkinematic features. Larger muscovite aggregates contain random structures that suggest they are related to post-kinematic recrystallisation.

Chlorite found in the metapsammites is pale green, exhibits very low interference colours, is fine grained, and shows overgrowths of muscovite and sericite.

Both epidote aggregates and fine, flaky sericite are found in metapsammites in trace amounts. Chloritoid with grey-green pleochroism was sporadically noted.

CHEMICAL CONTENT OF THE REGIONALLY METAMORPHOSED ROCKS

The analytical results for samples of regionally metamorphosed rocks are presented in Table 2. These samples are characterised by a high SiO_2 and Al_2O_3 content. Metapsammites contain the highest concentrations of SiO_2. Their overall chemical composition clearly differs with that of epidote-bearing rocks which contain lower Al_2O_3 and higher concentrations of CaO than do the metapsammites. Concentrations of Na_2O and K_2O vary. The epidote-bearing rocks are also characterised by a low alkali metal content. On the other hand, the albite-muscovite-biotite schists are high in alkali metals.

The Niggli (1954) triangular plot of minerals from this study recalculated as percentages of Q, L, and M (Figs. 17–19) suggests that the rocks are over saturated with silica because most of the plotted points are located above the PF (pyroxene — foids) line. Below that line the only points are for three samples of epidote-bearing rocks. The main concentration of plotted points is found within the Q = 40–60%; L = 25–40%, and M = 4–30% field.

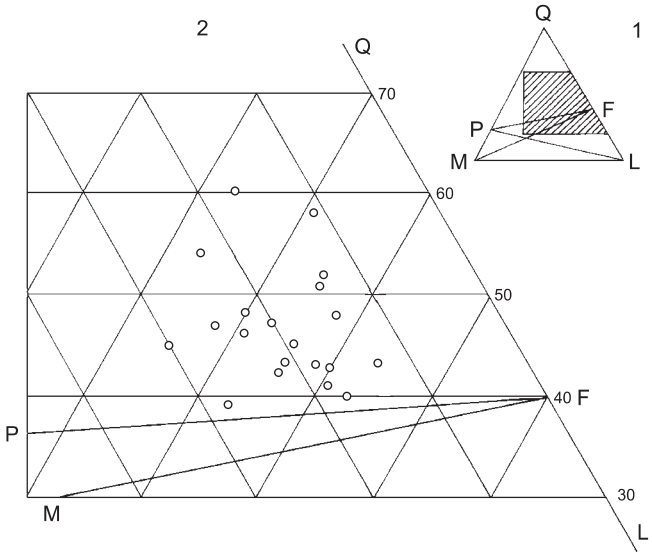

Fig. 17. QLM projection for phyllites (after Niggli, 1954)

1 — whole QLM projection triangle; dashed field: phyllites appearance; *2* — fragment of the phyllites appearance field; circles: projection points of the analysed samples

Table 2

Chemical composition of metamorphic rocks

Component	Phyllites		Crystalline schist		Metapsammites		Hornfelses	
	Range	Average	Range	Average	Range	Average	Range	Average
	wt %		wt %		wt %		wt %	
SiO_2	53.45–69.61	59.89	59.55–72.79	62.77	52.83–69.95	64.09	48.58–66.57	56.46
TiO_2	0.69–1.30	0.90	0.52–1.11	0.83	0.47–1.60	0.96	0.60–1.34	1.02
Al_2O_3	11.80–22.32	18.08	7.43–18.81	16.57	12.96–18.88	15.56	10.04–21.31	16.92
Fe_2O_3	1.55–6.26	3.39	0.82–6.71	2.77	0.73–7.60	3.58	4.00–10.55	7.82
FeO	0.39–5.67	3.12	1.06–5.10	3.21	1.74–4.72	3.32	–	–
MnO	0.01–0.38	0.08	0.04–0.26	0.12	0.06–0.21	0.10	0.07–0.25	0.16
MgO	1.89–4.20	2.80	1.12–3.71	2.58	2.23–5.12	3.09	2.09–12.10	4.82
CaO	0.30–9.56	1.55	0.37–3.21	1.27	0.82–3.30	1.71	0.92–14.02	2.58
Na_2O	1.07–5.18	2.72	0.69–6.76	3.06	0.26–3.57	2.66	1.29–4.33	3.11
K_2O	2.29–8.59	4.93	1.26–7.73	6.14	1.93–5.50	3.40	0.46–7.42	5.08
P_2O_5	0.05–1.24	0.20	0.07–0.80	0.14	0.08–0.11	0.09	–	–
H_2O^+	1.49–3.88	2.07	1.39–3.55	2.46	1.30–4.11	2.37	–	–
H_2O^-	0.08–0.49	2.53	0.11–0.33	0.22	0.15–0.33	0.20	–	–
CO_2	0.10–0.44	0.25	0.15–1.34	0.37	0.10–1.19	0.38	0.24–1.28	0.53
S	0.02–2.65	0.73	0.14–2.21	0.76	0.02–0.55	0.18	–	–

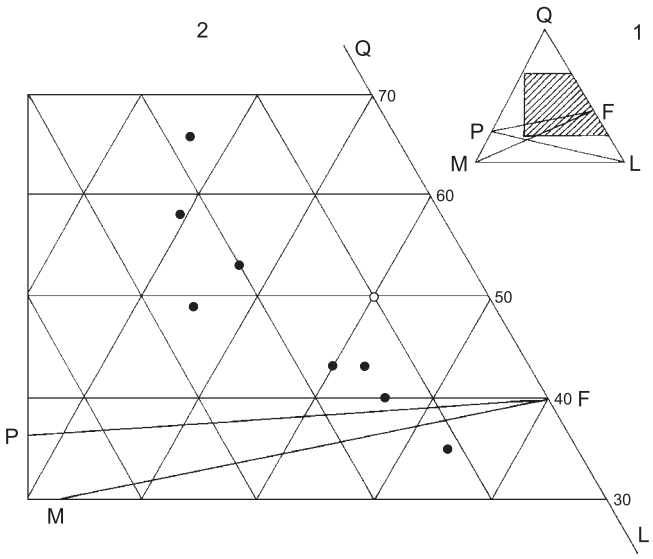

Fig. 18. QLM projection for crystalline schists (after Niggli, 1954)

1 — whole QLM projection triangle; dashed field: schists appearance; *2* — fragment of the crystalline schists appearance field; circles: projection points of the analysed samples

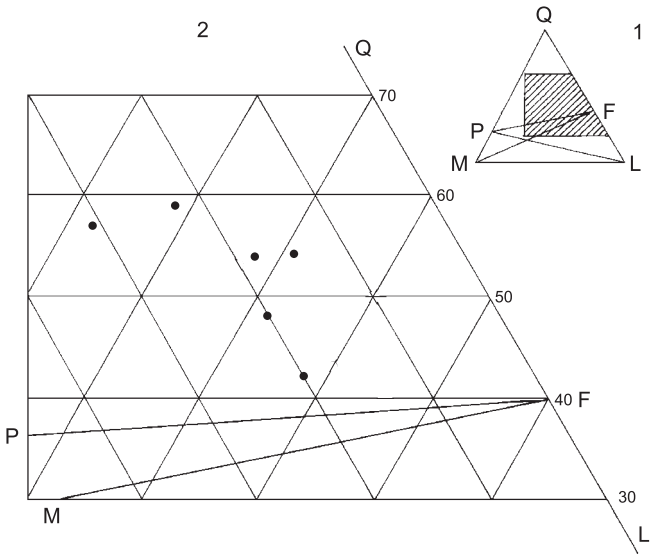

Fig. 19. QLM projection for metapsammites (after Niggli, 1954)

1 — whole QLM projection triangle; dashed field: metapsammites appearance; *2* — fragment of the metapsammites-schists appearance field; circles: projection points of the analysed samples

EFFECTS OF THERMAL AND THERMAL-METASOMATIC METAMORPHISM

HORNFELSES

The effects of granitoid magma on the wall rocks extend from a few tens of centimetres to as much as several metres from their common contact. The effects are mainly a darkening and hardening of the wall rocks. The thermal alterations are primarily associated with blasto-aleurite (blastosiltstone) and blasto-porphyry textures. The common, stockwork-like hornfelse textures are indicative of contact alterations (Spry, 1969; Vernon, 1976). The hornfelses have random structures. Quartz, plagioclase (albite), potassium feldspar, chlorite, biotite, and occasionally epidote are the most common minerals.

Chemical analyses of hornfelses are presented in Table 2. This rock type is characterised by a varying content of silica, domination of K_2O over Na_2O, and high concentration levels of Fe_2O_3 and TiO_2. The increase in the amount of biotite in the contact zones may explain the increase of K_2O, TiO_2, and Fe_2O_3 in hornfelses. Concentrations of the trace elements Sr, Ba, and Mn in hornfelses (Tables 3, 4) may also document the effects of granitoid magma on the wall rocks. The wall rocks show higher Ba and Sr contents near intrusive contacts compared to points farther from the contact. The distribution of Mn relative to contacts is not as obvious.

SKARNS

Skarns are the products of contact thermal-metasomatism on carbonate rocks. Skarns have been found only locally in the Myszków area, as carbonate rocks are rather uncommon within the Vendian to Early Cambrian formations.

Pyroxene-amphibole skarns were observed only in borehole Pz-33 in a 30 cm-thick zone. These skarns have a heterogranular texture and random structure, and are com-

Table 3

Mn, Ba, and Sr contents in hornfelses near granitoides (after Lasoń, 1990)

Range in ppm	Pz-17 borehole	Pz-28 borehole	Pz-29 borehole	Pz-31 borehole
Mn	220–440	600–1170	160–170	99–873
Ba	1000–1170	10–1490	400–560	630–1050
Sr	360	80–245	220–305	195–420

Table 4

Mn, Ba, and Sr contents in hornfelses (after Lasoń, 1990)

Range in ppm	Pz-17 borehole	Pz-28 borehole	Pz-29 borehole	Pz-31 borehole
Mn	640–3000	270–400	340–660	251–648
Ba	440–950	180–470	130–570	500–770
Sr	110–215	80–470	125–175	70–200

posed of pyroxenes, amphiboles, epidote, quartz, and albite. Pyroxene, represented by augite and diopside, is the dominant mineral. These two minerals appear both in unevenly granular aggregates and columnar forms that are 0.2 mm high.

The amphibole actinolite occurs as greenish rods that are arranged in fans or bunches. Xenoblastic calcite, together with epidote, quartz, and albite constitutes the matrix.

METASOMATITES

The distribution of pre-mineralisation metasomatic alterations minerals is very localised. The maximum width of altered zones generally ranges from a few tens of centimetres to several metres. The resulting metasomatites appear in phyllites and metapsammites in forms that vary from tiny inclusions, to clot-like or irregular agglomerations, to massive impregnations (Pz-32).

The metasomatites are characterised by finely crystalline (0.05–0.1 mm diameter) and xenoblastic textures, and random structures. Mineral associations in the metasomatites include:

- epidote + quartz ± chlorite ± plagioclase ± pyroxene,
- amphibole + quartz ± plagioclase ± sericite,
- pyroxene + chlorites ± biotite ± plagioclase ± calcite.

Pyroxenes (mainly diopside) and amphiboles (tremolite-actinolite group) are the dominant minerals in the metasomatites. Quartz, biotite, plagioclase, epidote, and other minerals are less common. Locally, the pre-ore metasomatites contain moderately rich and diversified ore minerals assemblages that include chalcopyrite, pyrite, scheelite, and magnetite, and more rarely, rutile, sphalerite, galena, molybdenite, and chalcocite.

Compared to unaltered rocks, the metasomatites contain higher concentrations of Al_2O_3, CaO, and Na_2O, and lower concentrations of total Fe, SiO_2 and K_2O.

MAGMATIC ROCKS

Granitoids have been encountered in almost all deep boreholes drilled in the Myszków area. The deepest samples were collected from borehole Pz-13 at about 1520 m. Following the terminology of IUGS Committee for Magmatic Rocks Systematics, which uses grain size and mineral and chemical contents to classify rock types (Ryka, 1987; Ryka and Maliszewska, 1991), the granitoids have been classified mostly as granodiorites and more rarely as granites (Fig. 20).

The granitoids exhibit intrusive contacts with their wall rocks. The contact alteration zones are not very wide, and are characteristic of temperatures in the 500–600°C range (Łydka, 1973). Numerous, thin microgranitic apophyses penetrate the metamorphic wall rocks.

Dacites and rhyolites are associated with granitoids in the Myszków area and are generally in the form of dikes. The contacts of these units with wall rocks are rarely distinct. Trachyandesites and lamprophyres have also been observed in a few boreholes.

Numerous intervals of magmatic rocks are commonly found in a single borehole. Their thickness varies from 0.2 m to as much as several hundred metres. The cumulative length of magmatic rocks intervals intersected in boreholes from the Myszków area is about 16 000 m.

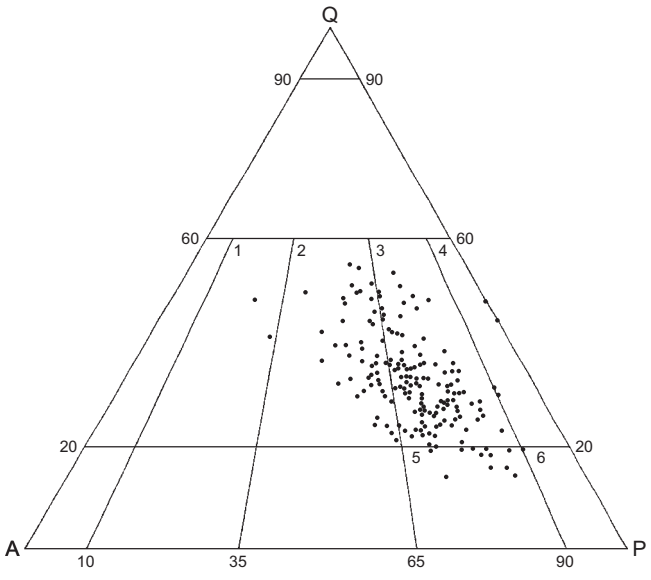

Fig. 20. QAP projection for granitoids, based on mineral content

Q — quartz, A — alkali feldspars ($An_{0–5}$), P — plagioclases ($An_{>5}$); 1–2 — granite, 3 — granodiorite, 4 — tonalite, 5 — monzodiorite, 6 — diorite

Numerous xenoliths of wall rock material are present in the exocontact zones of the granitoids and their subvolcanic equivalents. Intrusive breccias were also encountered in a few boreholes.

A high density network of ore-related veins has cut both the magmatic rocks and the wall rocks. Ore minerals are found in most of these veins. Many of the veins have also been intensely altered by overlapping autometasomatic and hydrothermal processes (Karwowski, 1988; Ślósarz, 1982).

Petrologic investigations presented here are based on samples from boreholes Pz-11, Pz-13, Pz-14, Pz-17, Pz-18, Pz-25, Pz-26, Pz-27, Pz-29, Pz-33, Pz-34, Pz-35, and Pz-38 (Fig. 7). About 1300 thin sections were analysed under a microscope, mostly by J. Markiewicz (Markiewicz, unpubl. report, 1989; Markiewicz and Markowiak, unpubl. report, 1998; Piekarski *et al*., unpubl. report, 1993). However, several other petrologists also contributed to this study. W. Heflik investigated rocks from boreholes Pz-25 and Pz-26; Z. Migaszewski, from boreholes Pz-13, Pz-23, Pz-30, and Pz-33, and O. Jeleński, from borehole Pz-27 (Piekarski *et al*., unpubl. report, 1993). Additional petrographic studies were also undertaken as a part of the Polish-American Maria Skłodowska-Curie Fund II project: *Geochemical Prospecting in Areas of Covered and Concealed Mineral Deposits in Poland* (Podemski and Chaffee, unpubl. report, 1996).

GRANITOIDS AND DACITOIDS

Megascopically, granitoid rocks have widely varying colours and textures related to the effects of varying crystallisation conditions as well as differences in the effects of autometasomatic and hydrothermal processes. Slightly altered granitoids are light grey or greyish-rose. With increasing effects of hydrothermal and metasomatic alteration, the colours change to rose, red rose, yellow green, or brown.

Granitoid textures are medium grained, semi-automorphic, and usually porphyritic, with feldspar, quartz, and biotite being the most common macroscopically visible phenocrysts. Granitoids from near contact zones are finer grained and more porphyritic. On average, the fine grained matrix constitutes 10–30% by volume of a typical rock. In some specimens, the matrix makes up a higher percentage of the rock, and in others it is completely absent, producing eugranitic texture.

Plagioclases, quartz, and biotite are the main mineral components of the granitoids. The variability of the mineral content of the granitoids is presented on graphs (Fig. 21) for samples of core from selected boreholes. For the selected samples, feldspars and quartz are the most common minerals, with their total amount varying between 81.7% and 97.6% by volume and averaging 92.1%.

The dominance of feldspars and quartz in the selected rocks is also apparent on a Niggli QLM plot (Niggli, 1954; Fig. 22). Plagioclase, which is dominant feldspar, constitutes 9.7 to 67.5% by volume in the selected samples and averages 44.5%. The plagioclase phenocrysts appear in the form of prisms that are usually 1.2–2.4 mm in diameter, with a maximum of about 5 mm. The plagioclase exhibits well developed, recurrent zoning with a large andesine-oligoclase core (An_{46-26}) and several rims. The outermost rim is very often albitic. The cores have irregular shapes. The rim boundaries are also irregular and indistinct. Histograms (Fig. 23) show the content of plagioclase cores and rims.

The plagioclases are commonly polysynthetically twinned in accordance with albite, pericline, and more rarely, Carlsbad laws. The quantitative chemical composition of three plagioclases was determined with an electron microprobe, and recalculated into the following chemical formulas:

$Na_{0.634}\ K_{0.021}\ Ca_{0.252}\ Al_{1.195}\ Si_{2.799}\ O_{8.000}$

$Na_{0.564}\ K_{0.021}\ Ca_{0.328}\ Al_{1.252}\ Si_{2.737}\ O_{8.000}$

$Na_{0.691}\ K_{0.031}\ Ca_{0.141}\ Al_{1.079}\ Si_{2.925}\ O_{8.000}$

Postmagmatic processes, mainly sericitisation and, more rarely, carbonatisation and saussuritisation, have usually obscured the internal structure of primary plagioclases. Sericite pseudomorphs have commonly replaced entire plagioclase crystals. However, the albitic rims were not affected by those alteration phases.

Plagioclase grains very often appear fractured and crushed, and their edges are uneven and regenerated. Fractures are usually filled with chlorite or potassium feldspar. The twinning is sometimes deformed. When disturbed, single lamellae are often thickened, broken, and displaced. Inclusions of biotite, zircon, and apatite are found in plagioclases.

Potassium feldspar (orthoclase, orthoclase microperthite) is less common in the granitoids than plagioclase and averages 18.2% by volume. It usually forms fine xenomorphic grains that are commonly 0.2–0.5 mm in diameter but sometimes may be as much as about 1.6 mm in diameter. Potassium feldspar crystals have a low birefringence and show wavy light extinction. Larger plagioclase grains contain relicts that have been resorbed to varying degrees. The perthites can be subdivided into primary (magmatic) and secondary (metasomatic) types.

The chemical formulas for two potassium feldspars, determined by microprobe point counts are as follows:

$Na_{0.033}\ K_{0.989}\ Ca_{0.000}\ Mg_{0.036}\ Al_{1.011}\ Ti_{0.008}\ Si_{2.959}\ O_{8.000}$

$Na_{0.072}\ K_{0.973}\ Ca_{0.000}\ Al_{1.017}\ Ti_{0.019}\ Si_{2.946}\ O_{8.000}$

Quartz in granitoids generally averages from 5.9 to 51.0% by volume of the rock. It is xenomorphic, with grains being as much as about 1 mm in diameter. Quartz crystals that are 2-10 mm in diameter are less common. The quartz grains are usually rounded, with traces of corrosion. Large grains are very often fractured. Quartz exhibits wavy light extinction.

Biotite is the most common mafic mineral. Its content varies between 2.0 and 16.0% by volume, and averages 7.0%. Biotite forms single plates that are about 2 mm in diameter. More rarely seen are fine flakes or their aggregates that have a maximum diameter of 0.4 cm. Biotite is characterised by the following pleochroism: α – yellowish-green; $\beta = \gamma$

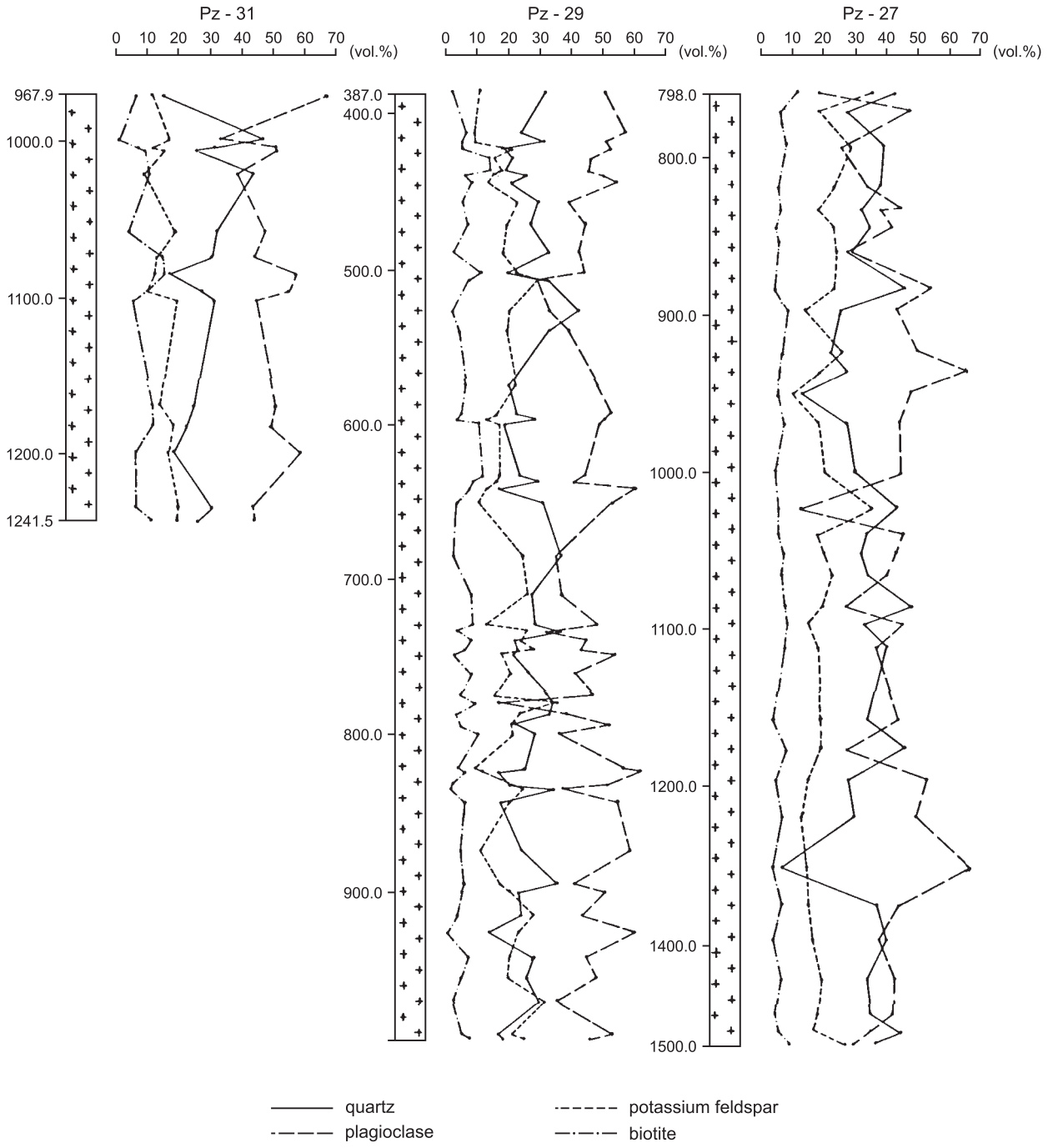

Fig. 21. Variability of mineral content in granitoids from the selected boreholes

– reddish-brown. Chemical formulas for three biotites, determined by microprobe point counts are as follows:

$(K_{1.22}\ Na_{0.04})\ (Fe^{+2}_{1.43}\ Mg_{1.25}\ Al_{0.35}\ Ti_{0.34}\ Mn_{0.06})\ (OH)_2\ O_{10}\ (Al_{1.22}\ Si_{2.78})$

$(K_{1.20}\ Na_{0.06})\ (Fe^{+2}_{1.35}\ Mg_{1.46}\ Al_{0.30}\ Ti_{0.29}\ Mn_{0.01})\ (OH)_2\ O_{10}\ (Al_{1.06}\ Si_{2.94})$

$(K_{1.23}\ Na_{0.02})\ (Fe^{+2}_{0.76}\ Mg_{2.15}\ Al_{0.35}\ Ti_{0.17}\ Mn_{0.02})\ (OH)_2\ O_{10}\ (Al_{0.80}\ Si_{3.20})$

Biotite is commonly chloritised. Products of various stages of that process, from its initial development along fissures to entire chlorite pseudomorphs, are recognisable under the microscope. Chlorite from pseudomorphs is characterised by light yellow to green pleochroism, a negative optic sign, and bright blue interference colours. In pseudomorphs after biotite, one commonly sees iron oxides and sometimes also titanium oxides, leucoxene, and epidote. Calcite and hydromuscovite are found in smaller amounts. Very rarely, amphibole relicts, consisting of pale coloured common hornblende with α = pale yellow and γ = pale green, have been observed (Pz-24, Pz-26, and Pz-27).

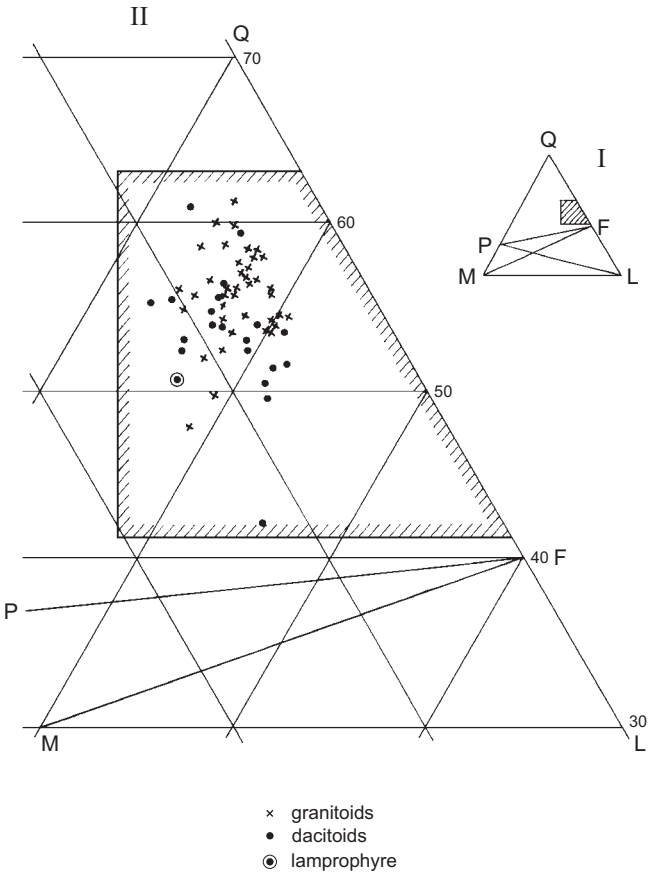

Fig. 22. QLM projection for magmatic rocks (after Niggli, 1954)

I — whole QLM projection triangle; dashed field: magmatic rocks appearance; II — enlarged fragment of the area I

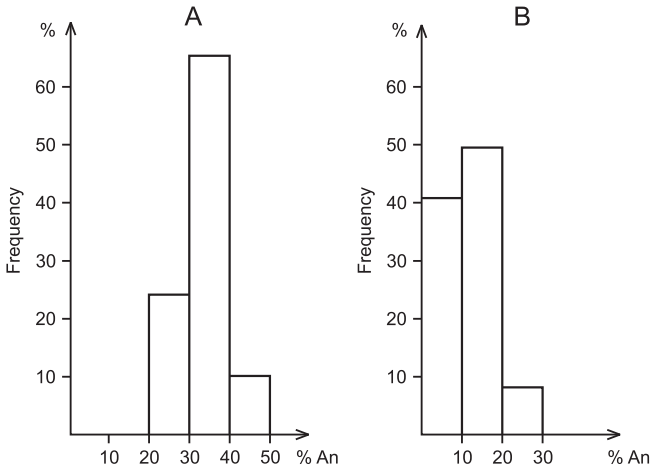

Fig. 23. Composition of plagioclases in granitoids

A — central parts, n = 178; **B** — rims, n = 212

A finely crystalline matrix constitutes about 20% by volume of a typical granitoid rock. The matrix is similar in content to a microdiorite with automorphic and hipautomorphic oligoclase and biotite crystals, and xenomorphic quartz, and potassium feldspar crystals. The larger grains range from 0.08 mm to 0.24 mm in diameter. Locally, especially near feldspar and quartz-feldspar-rich veins, the matrix is more recrystallised. Potassium feldspar and quartz are more common in the matrix. Apatite, zircon, magnetite, rutile, and titanite are common accessory minerals found in the granitoid.

Textures, mineral contents, and types of inclusions can be used to classify dacitoids into subvolcanic microgranites or microgranodiorites (Karwowski, 1988). Macroscopically, dacitoids exhibit a variety of colours, including brown, rose, and grey, and more rarely, black or greyish-green, depending on the character and extent of later alteration phases. Feldspar, quartz, and biotite phenocrysts are found in an aphanitic matrix.

Many times, different rock types can be observed within a single dike. These differences are the result of variations in the matrix to phenocrysts ratio, matrix textures, and mineral ratios in both the phenocrysts and the matrix (Fig. 24). The dacitoids exhibit a porphyritic texture under the microscope and are composed of a holocrystalline matrix and plagioclase, quartz, biotite, and potassium feldspar phenocrysts.

Plagioclase is the most common type of phenocrysts and ranges between 0.8 and 62.0% by volume, and averages about 30%. It forms hipautomorphic prisms that are between 0.8mm and 2.0 mm in diameter, with a maximum diameter of 5.0 mm. Less common second generation plagioclases range between 0.2 mm and 0.4 mm in diameter. Fresh grains show albite twinning and more rarely twinning after pericline or Carlsbad laws. The outer rims of plagioclases are composed of albite and the cores of oligoclase-andesine. Crystal zoning is indistinct. Sometimes recurrent zones are visible.

The plagioclases are strongly altered as a result of sericitisation, carbonatisation, chloritisation, silicification, kaolinitisation, and saussuritisation processes. Plagioclase grains are very often fractured, crushed, and impregnated with a dust of opaque minerals. Antiperthites has been observed occasionally. Inclusions of biotite, zircon, and apatite are common.

Potassium feldspar phenocrysts are present in small quantities and average about 4% by volume. Larger amounts of potassium feldspar are often found in the matrix.

Quartz phenocrysts are present in highly variable quantities (0.0 to 36.0% by volume). These phenocrysts are usually rounded but may also occur as euhedral crystals that often show traces of magmatically related corrosion. In contrast to nearby, smaller grains, the larger quartz grains are usually euhedral and strongly fractured. Quartz grains vary in size between 0.3 and 10 mm in diameter, with most grains being between 1.0 and 2.4 mm in diameter. Inclusions in quartz crystals include biotite, zircon, apatite, rutile, opaque minerals, and matrix material.

Biotite in dacitoids is present in small quantities that average 6% by volume. It is generally strongly chloritised. Pennine, with its characteristic violet, subdued interference colours, completely replaced altered biotite. Biotites are accompanied by titanium minerals, including rutile, titanite, and leucoxene. Iron oxides, carbonates, hydromicas, and epidote are additional alteration products. Carbonate pseudomorphs after a columnar-like mineral, which is probably an amphibole, have been observed but are very uncommon.

The holocrystalline matrix of dacitoids is mainly composed of quartz and potassium feldspar and contains subordinate

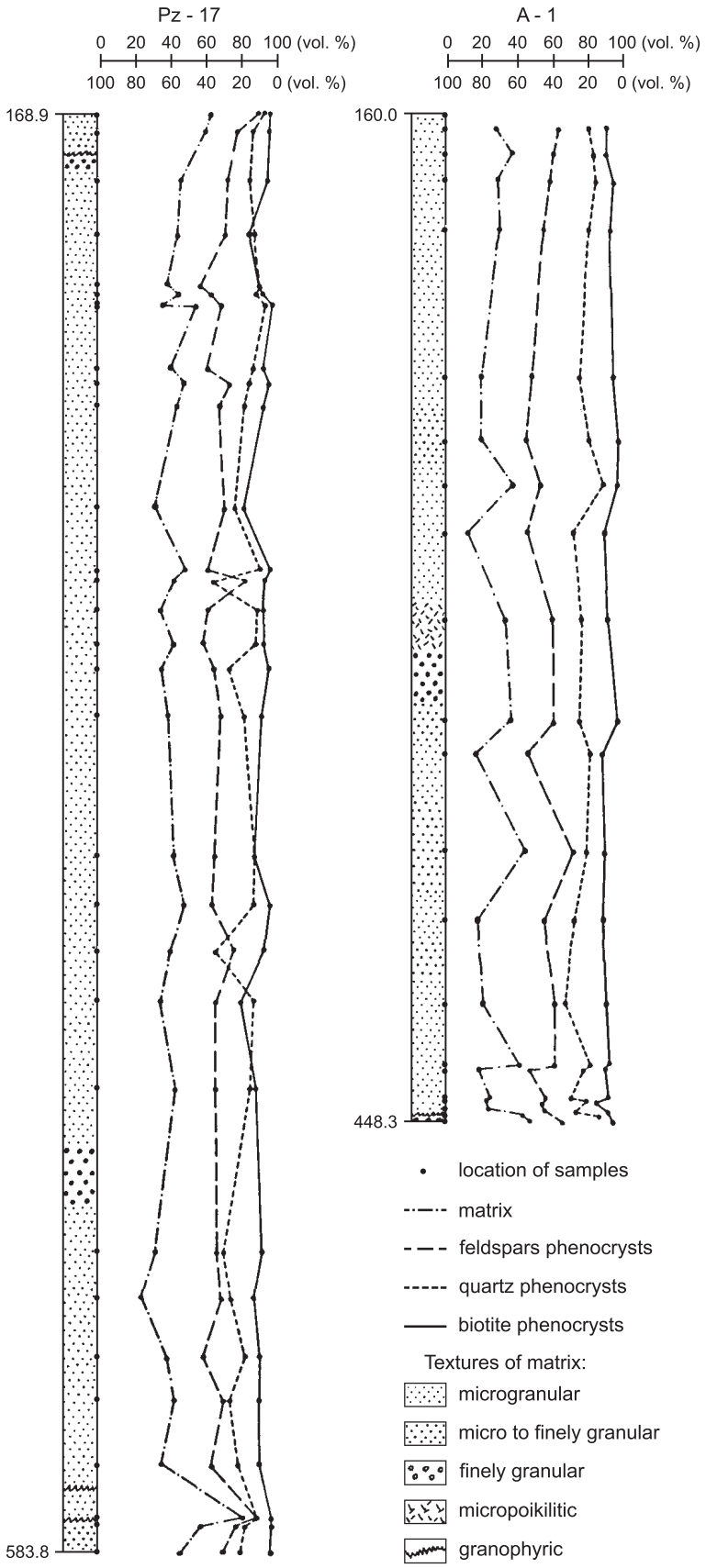

Fig. 24. Variability of matrix and phenocrysts in dacitoids (after Markiewicz, 1998)

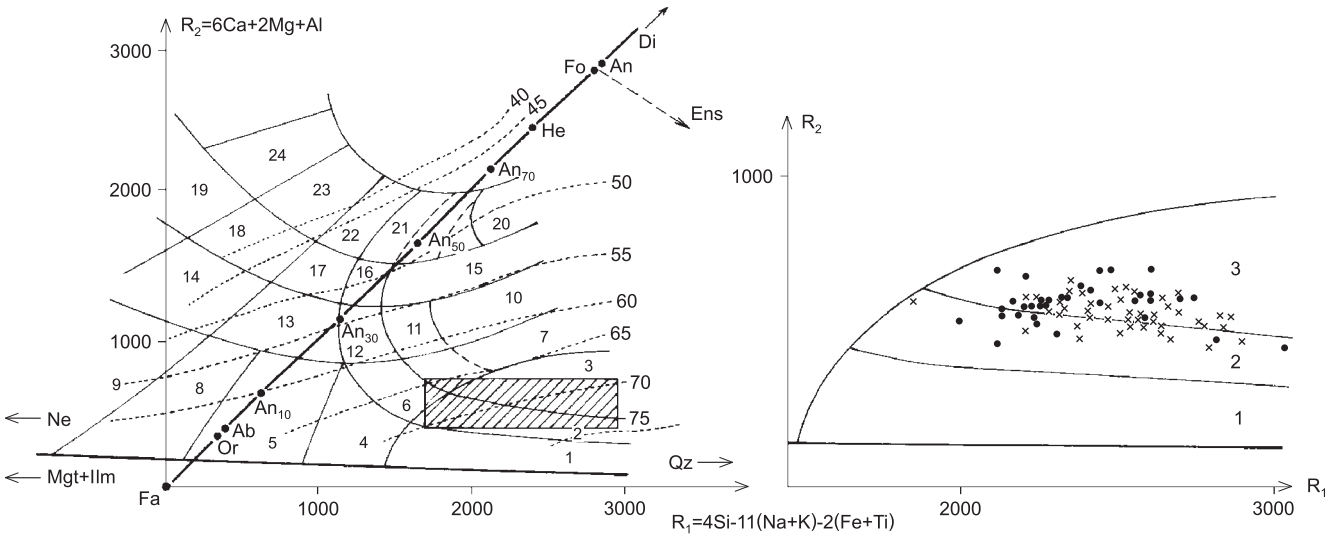

Fig. 25. Classificatory position of magmatic rocks (dashed field) on the R_1 — R_2 diagram (de La Roche *et al.*, 1980, after Markiewicz, 1998, supplemented)

On the right side: enlarged fragment of the diagram: *1* — alkali granite (alkali rhyolite), *2* — granite (rhyolite), *3* — granodiorite (rhyodacite); symbols: cross — granitoid; point — dacitoid

amounts of biotite, chlorite, albite, hydromicas, carbonates, and opaque minerals. The matrix texture is mostly micro-crystalline to finely crystalline. In contact alteration zones, this matrix was originally granophyric, micropoikilitic, or spherulitic. The contact zones sometimes exhibit a stream-like arrangement of fine lamellae of feldspars that gives the rocks a fluidal appearance. The same effect is visible in chlorite flakes that have crystallised after biotite.

The ratio of phenocrysts to matrix is quite variable. The mineral composition of the matrix is also variable in a given core intercept and may range from feldspar-rich to quartz-feldspar, to quartz-rich. The matrix, like the phenocrysts, has been altered by sericitisation, chloritisation, carbonatisation, silicification, and pyritisation processes.

Most of the phenocrysts found in the inner parts of the dacitoid dikes are often clearly second generation (plagioclase and quartz) and have grains that range between 0.08 and 0.4 mm in diameter. In such cases, an increased amount of flaky biotite is visible in matrix.

The granitoids and dacitoids are altered to varying degree as a result of overlapping autometasomatic and hydrothermal processes. The spatial relationship between potassium metasomatism (feldspathisation, biotitisation, and sericitisation) and ore mineralisation is visible in both hand specimens and thin sections.

Feldspar metasomatism is present in zones that are as much as several tens of centimetres thick. This zoning does not show any spatial relationship with fracturing. The contacts between altered and unaltered rocks are sharp. Potassium feldspar is the most common mineral in these zones and is the main component of the fine grained matrix. Locally, potassium feldspar forms large (to a few millimetres in diameter), xenomorphic grains that are often associated with plagioclase relicts. Less common minerals associated with potassium feldspar metasomatism include sericitised plagioclase, micas, and quartz. Opaque ore minerals, including molybdenite and chalcopyrite, are very common.

Granitoids are generally less altered than dacitoids. However, zones of strong alteration are present locally in granitoids and are characterised by sericitised and carbonatised plagioclases and intensely chloritised biotite. The pseudomorphs after biotite are composed of chlorite, hydromuscovite, calcite, epidote, and Fe and Ti oxides.

Sericitisation is commonly observed in quartz veins associated with polymetallic mineralisation. The main components (plagioclase and biotite) are present in the form of sericite-hydromuscovite pseudomorphs that are accompanied by nu-

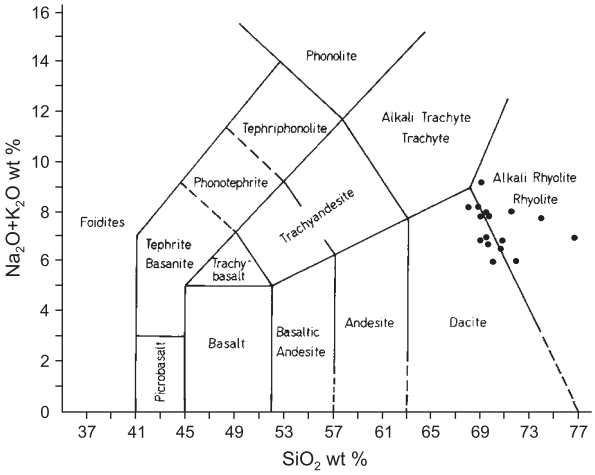

Fig. 26. TAS diagram (total alkali–silica) for dacitoids

Black points: projection of analysed rock samples

Table 5

Average chemical content of granitoids and dacitoids

Component	Granitoids		Dacitoids		Trachyandesites		Lamprophyres	
	Range	Average	Range	Average	Range	Average	Range	Average
	wt %		wt %		wt %		wt %	
SiO_2	65.18–73.89	70.79	66.48–75.28	69.02	57.30–60.21	58.56	62.96–63.19	63.08
TiO_2	0.25–0.57	0.37	0.26–0.63	0.41	0.98–1.17	1.09	1.25–1.30	1.28
Al_2O_3	11.81–16.90	14.46	12.20–16.34	15.09	15.30–18.70	16.57	14.42–15.80	15.11
Fe_2O_3	0.18–1.89	0.84	0.32–2.41	1.03	0.77–4.35	2.73	1.95–5.20	3.58
FeO	0.25–2.61	1.16	0.14–2.37	1.44	3.36–6.88	4.61	1.71–2.39	2.06
MnO	0.01–0.06	0.03	0.02–0.07	0.03	0.11–0.17	0.14	0.04–0.05	0.05
MgO	0.25–2.15	0.87	0.67–1.37	1.00	2.01–3.15	2.44	2.87–2.89	2.88
CaO	1.08–3.23	1.99	1.03–3.29	2.20	2.75–3.95	3.36	2.80–4.15	3.48
Na_2O	1.46–4.84	3.13	2.20–4.40	3.63	2.98–4.65	3.63	2.91–3.24	3.08
K_2O	1.47–7.23	4.47	1.68–6.12	3.61	2.36–2.65	2.47	2.63–4.04	3.34
P_2O_5	0.05–0.13	0.09	0.07–0.16	0.12	0.22–0.46	0.34	0.68–0.08	0.38
H_2O^+	0.00–0.95	0.63	0.00–1.45	0.55	–	–	–	–
H_2O^-	0.00–1.10	0.13	0.00–1.96	0.37	–	–	–	–
CO_2	0.00–0.95	0.24	0.00–1.45	0.39	–	–	–	–
S_T	0.00–0.62	0.15	0.00–1.23	0.12	–	–	0.37–0.61	0.49

merous microliths and by fine grained opaque minerals (pyrite, chalcopyrite, and molybdenite). The matrix components are better preserved than are the phenocrysts, especially in boreholes Pz-24, Pz-27, Pz-28, Pz-29, and 33.

The chemistry of 51 granitoid and 37 dacitoid samples were determined in the Central Chemical Laboratory of the Polish Geological Institute in Warsaw. The average concentration and ranges of values for these samples are presented in Table 5. The results of these chemical analyses have been recalculated using the formula of de La Roche *et al.* (1980), in order to define the relationship between the chemistry of these two rock types. A plot of points for the granitoids on a R_1–R_2 diagram classifies them mostly as granodiorites, and more rarely as granites (Fig. 25).

In hand specimens the dacitoids are mainly rhyodacites and rhyolites. A plot of their chemistry on a Le Maitre (1984) TAS diagram classifies them as dacites, rhyolites, and alkali rhyolites (Fig. 26). They represent magmatism of the Pacific province type, which produces a calc-alkaline type magma (Juskowiak, 1971; Karwowski, 1988; Markiewicz, 1998). Analyses plotted on a (Na_2O+K_2O)–$(FeO+0{,}9Fe_2O_3)$–MgO diagram are shown on Figure 27.

The chemical content of granitoids and dacitoids (Table 5) show similar concentrations of the SiO_2, Al_2O_3, and CaO. Generally, all of these rocks are saturated with silica, contain a high amount of alumina, and have a variable alkali metal content.

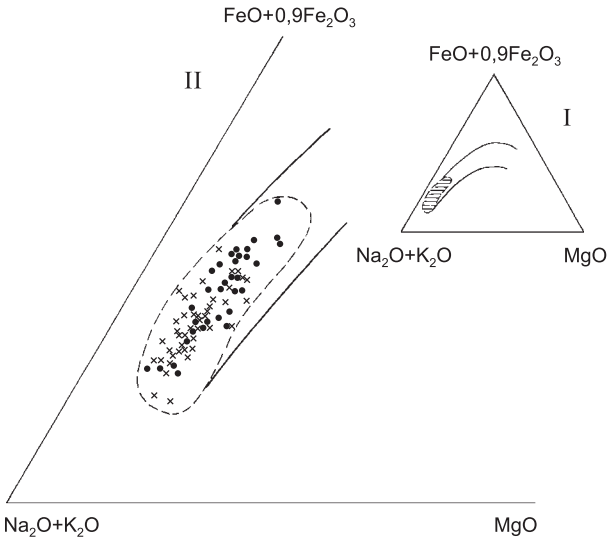

Fig. 27. Diagram (Na_2O+K_2O)–MgO–$(FeO+0{,}9\ Fe_2O_3)$ for magmatic rocks; after Masao *et al.*, 1965, supplemented by Markiewicz, 1998

Magmatic formations: TH — tholeitic, CA — calcium-alkali, A – alkali. Dashed area: field of rocks projection. Projection points: cross — granitoids, point — dacitoids.

The concentrations of Na_2O and K_2O yield much wider ranges than do the other major elements.

The chemical analyses of the selected granitoids and dacitoids have been compared with the chemical composition of rocks from other localities that host porphyry-copper deposits. Generally, the analysed rocks from the Myszków area are close to the composition of rocks from porphyry-copper deposits in the north-western part of the United States and in the Andeans Cordillera that were studied by Titley and Beane (1984).

Similar conclusions were reached by Karwowski (1988), who investigated the physico-chemical conditions of ore mineralisation connected with magmatic processes in the Myszków area. However, interpreting the origin of the granitoids, based solely on chemical analyses must be done very carefully because data for most Myszków samples plotted on a SiO_2-Al_2O_3/(CaO+Na_2O+K_2O) diagram plot close to the line that divide granitoids into the type I and type S field, and into the granite I field.

TRACHYANDESITES AND LAMPROPHYRES

Trachyandesites were encountered in borehole Pz-31 (Heflik and Piekarski, 1989), and in holes Pz-16, Pz-27, Pz-30, Pz-35, Pz-36, Pz-38, and Pz-40 (Markiewicz, unpubl. report, 1989), where they are found as dikes cutting granitoids. The trachyandesites have porphyritic textures and random structure. Their phenocrysts are most commonly variably altered oligoclase and pseudomorphs after mafic minerals. The matrix texture is finely crystalline, and locally trachytic. The mineral content of the matrix is composed of potassium feldspar (orthoclase; Heflik and Piekarski, 1989), plagioclase, chlorite, quartz, and calcite. Apatite, magnetite, and hematite are the accessory minerals.

In borehole Pz-31, the most common minerals in the trachyandesites are feldspars (Heflik and Piekarski, 1989). These include plagioclase (44.5% by volume) and potassium feldspar (20.0%). Also present are numerous iron oxides (15.0% by volume) and calcite (10.0%). Less common are quartz (4.0% by volume), chlorite (5.0%), epidote (1.0%), and apatite (0.5%). Irregular, clot-like forms that are a few mm in diameter and mainly composed of epidote with lesser amounts of quartz and calcite, were encountered in a dike in the bottom part of borehole Pz-31.

The investigated lamprophyres are equivalent to calc-alkaline lamprophyres (lamprophyres *sensu stricto*, after Wimmenauer, 1973), and are classified as minettes. They have been intersected in boreholes Pz-12, Pz-16, Pz-31, and Pz-36, in rocks of Silurian age.

These lamprophyres are brown-grey or brown-green in colour and have porphyritic textures. Under the microscope, they exhibit hipautomorphic, holocrystalline to porphyritic textures and consist of a holocrystalline matrix and of phenocrysts that are mainly composed of biotite (9.6 to 22.0% by volume). Apatite (3.4–3.5% by volume), oligoclase (0.0–8.1%), orthoclase and quartz (1.0–2.4%) are present in smaller amounts.

Biotite in the lamprophyres is well preserved and occurs as euhedral plates that are as much as 1.2 mm in diameter. Euhedral apatite crystals are very common, and are similar in size to biotite crystals. Less common are feldspars, which usually have a low birefringence, are carbonatised, and contain a dusting of Fe oxides.

The lamprophyres contain much more matrix material than phenocrysts (about a 3:1 ratio). The matrix material is composed of strongly altered feldspars, biotite, chlorite, sericite, calcite, kaolinite, and opaque minerals (magnetite and hematite). The diameter of grains in the matrix normally varies from 0.01 to 0.04 mm but occasionally are as much as 0,1 mm. Some matrix feldspars have dendritic or spherulitic habits.

The chemistry of the lamprophyres shows a wide range of values for many elements, partly because of their primary variability and partly because of alteration processes (Heflik *et al*., 1985, 1992; Ryka, 1978). Except for lamprophyres from borehole Pz-8, these rocks are depleted in silica, (Heflik *et al*., 1985; Ryka, 1974). All of the lamprophyres are characterised by a strong predominance of K_2O over Na_2O.

MAGMATIC AND POSTMAGMATIC FLUIDS

Samples for this study were collected from cores from boreholes Pz-1, Pz-2, Pz-3, Pz-5, Pz-6, Pz-7, Pz-9, Pz-10, Pz-17, Pz-18, Pz-20, Pz-21, Pz-22, Pz-24, Pz-25, Pz-26, Pz-29, Pz-31, Pz-35, and Pz-40. Samples were taken from the felsic magmatic rocks with various types of alteration and from veins, fissures, and other structures that cut the metamorphic and (or) magmatic rocks.

Temperature data on fluid inclusions were determined in ovens constructed by the author and R. Włodyka. The Naumov and Malinin (1968) methods was used to determine the crystallisation pressures of minerals. The homogenisation temperatures of the fluid inclusions were controlled using an alloy cooling technique (Roedder, 1971) and a pipe furnace constructed similarly to the one described by Kozłowski (1981).

Most of the crystalline phases were identified in polarised, reflected, and transmitted light, based on their optical and morphological properties. Electron microprobe and spectral laser analyses were used to identify crystalline phases in the inclusions. The water extraction technique of Kaljużnyj (1960) was used to determine the chemical composition of the postmagmatic inclusions. Electron probe analyses was used to establish the concentrations of the fluids in individual inclusions. The resulting data were recalculated to equivalent NaCl values (Kozłowski and Karwowski, 1972).

MAGMATIC FLUIDS

Relicts of the magmatic fluids are found in fluid inclusions, which have been preserved in the porphyry and granitoid rocks, mostly in magmatic quartz grains. During postmagmatic time these quartz grains underwent erosion and recrystallisation. Numerous solid inclusions of zircon, apatite, biotite, pyrrhotite, and rutile are present in quartz grains. Fluid inclusions have also been observed microscopically in apatite and zircon crystals.

Homogenisation temperatures for inclusions were determined for about 20 samples (Table 6). Irrespective of rock type, the homogenisation temperatures ranged from 1325 to 1260°C for apatites and 1360 to 1300°C for zircons. A temperature of 1360°C was, therefore, the initial crystallisation temperature of these two minerals in the magmatic fluid (Karwowski, 1988, 1989).

Several tens of inclusions in magmatic quartz grains from porphyry and granitoid rocks have been investigated thermometrically. At room temperature, all of these inclusions are filled with recrystallised silica-rich fluid. Most of these inclusions also contain a few gas bubbles.

Several generations of fluid inclusions, associated with crystallisation stages, could be distinguished. The highest homogenisation temperatures measured in the inclusions (1260–1220°C) were found in the centres of the quartz crystals. Lower homogenisation temperatures characterise inclusions formed during the final stages of crystallisation of the quartz phenocrysts. Inclusions in quartz grains from microgranodiorites yield lower homogenisation temperatures (1160–860°C) than do those in quartz grains from porphyries.

Minerals began to crystallise from the magma at 1360°C. Zircon, apatite, rutile, biotite, and pyrrhotite crystallised first. At 1260°C, quartz and feldspars began to crystallise. Crystallisation of these minerals terminated at about 870°C. The entire crystallisation in dacites was relatively rapid but was much slower in the microgranodiorites and granodioritic porphyries. It is estimated that crystallisation of the matrix in the dacitic porphyries occurred at the temperatures between 900 and 800°C.

Fluid inclusions that contained two unmixed phases were found to be inhomogeneous below a temperature of 1250°C. In addition to inclusions with a silica-rich phase, a second type with a chloride-rich phase was identified. These latter inclusions may indicate the separation of a chloride-rich fluid from the silica-rich fluid. However, it is also possible that those inclusions could have been partly filled at a later time with highly saturated, chloride-rich brines.

Saline inclusions were also encountered in magmatic quartz crystals (Plate I, Fig. 2). The fluid phase is present there at about 800°C. At 1200 to 1250°C, the solid and liquid phases homogenise. Gas bubbles reappear with the slightest temperature reduction, and at about 830°C, the crystalline phase also reappears. Inclusions of this type could not be homogenised by the fluid cooling technique.

All of the just described inclusions represent salt and silicate/salt fluids inclusions types. These observations suggest the possible separation of a saline-rich fluid from a silica-rich one. However, this possibility is not regarded as very likely because of the low chlorine content in the magmas (Jacobs and Parry, 1976; Parry, 1972; Wilson *et al*., 1980). The high salt content in the fluid at Myszków is, therefore, of secondary origin and caused by the boiling of fluids and associated water loss.

It is likely that in the primary magma, both chloride and water concentrations were relatively high. With the upward movement of magma pressure decreased and allowed some water to escape so that the chloride and silica fluid mix was no longer in equilibrium. At this point, the saline-rich and silica-rich phases could have separated.

Saline-rich inclusions are characterised by the existence of the crystalline infilling and by the absence of euhedral crystals. The infilling is usually isotropic. No changes in the infilling were seen below about 750 to 800°C. The infilling darkens at about 800°C, and a liquid phase appears. A very rapid transformation to a homogeneous fluid phase takes place with temperature changes of 10 to 30°C. Above 1200°C, complete homogenisation occurs. The homogenisation temperatures for the saline-rich inclusions are higher than those of the neighbouring silica-rich inclusions. The saline-rich fluid phase could have, therefore, existed in equilibrium with the gaseous phase.

Table 6

Homogenisation temperatures of fluid inclusions in magmatic quartz

Depth of borehole (m)	Number of determinations	Range of homogenisation temperatures (°C)
Pz-1; 161.0	4	1225–1140
Pz-1; 237. 5	6	1240–1130
Pz-2; 375.3	2	1115–1050
Pz-2; 615.0	5	1090–1025
Pz-10; 515.1; q	3	990–930
Pz-10; 542.0; q	4	1000–880
Pz-10; 692.4; q	3	1035–900
Pz-10; 764.4 ;q	5	1080–945
Pz-10; 770;6; q	3	1020–930
Pz-10; 785.0 ;q	2	1100–875
Pz-10; 931.0; q	4	1040–860
Pz-10; 956.7; q	3	1130–885
Pz-10; 1151.8; q	6	1160–895
Pz-17; 189.65		
a	6	1260–1230
b	5	1010–930
c	9	960–870
Pz-17; 471.3		
a	4	1120–1030
b	8	1050–930
c	7	920–900

a — inclusions of central part of crystals; b — inclusions of peripheral part of crystals; c — secondary inclusions; q — quartz of microgranodiorites

POSTMAGMATIC FLUIDS

In addition to inclusions in quartz, those found in albite, epidote, scheelite, fluorite, calcite, celestite, and gypsum were investigated. The postmagmatic fluid relicts were usually very small, with grain diameters ranging from several tens to a few μ, or, more rarely, to 0.0n mm.

Relicts of highly saturated, supercritical brines, comprise the first generation of postmagmatic inclusions. Within those inclusions, clear halide crystals form and gas bubbles are nearly spherical (Plate I, Fig. 1). The saturated-water phase is almost non-existent. These inclusions homogenise into a liquid phase at temperatures between 1150 and 950°C and appear only in magmatic quartz phenocrysts. Therefore, they represent the initial postmagmatic fluid composition.

The inclusions with highly saturated brines are found in both magmatic and postmagmatic quartzes and represent typical postmagmatic fluids. These inclusions contain crystalline salt phases, with halite being the most common mineral (Plate I, Figs. 3–7). Halite is accompanied by smaller, rounded crystals of sylvite. In addition to carbonates (Plate I, Fig. 5), anhydrite (?), chalcopyrite (Plate I, Figs. 3 and 5), bornite, pyrite (Plate I, Fig. 6), sphalerite, and specularite (Plate I, Fig. 4) also appear in these inclusions. Additional, unidentified mineral phases are marked X on the presented microphotographs.

Specularite was commonly noted both in inclusions that contain highly saturated brines and in inclusions with more diluted fluids. However, all experiments attempting to dissolve specularite at homogenisation temperatures failed. Therefore, that mineral has been recognised as a captured phase. All the other minor mineral phases (chalcopyrite, pyrite, sphalerite, etc.) are soluble in the saline solutions. Only large pyrite and chalcopyrite crystals behave similarly to specularite (Plate I, Fig. 6).

The salinity of postmagmatic inclusions and the temperatures of homogenisation decrease with increased distance from the central, mineralised part of the Myszków area. Inclusions of highly saturated brines are often found in the mineralised quartzes and occur as veins selvages. In the centres of veins, the fluids are more dilute. These inclusions with diluted fluids have partly replaced the fluid in formerly highly saturated inclusions. This observation was noted in both magmatic and postmagmatic quartz grains. Inclusions with more dilute fluids homogenise at lower temperatures (300–280°C).

Saline inclusions are often filled after their original formation with gaseous fluids. Crystals of halite and other later or captured phases are the only phases left from the original brine fluids (Plate I, Figs. 8 and 10) Sometimes, brine fills gaseous inclusions (Karwowski, 1988). This process is associated with sudden pressure changes that probably cause very rapid boiling of fluid. Liquid-gaseous inclusions were also encountered, with varying gas compositions and water solution ratios, and with varying homogenisation temperatures (Plate I, Fig. 9).

All generations of inclusions described above were again exposed to highly saturated brine-rich fluids. These fluids formed the subsequent generations of inclusions in filled fissures. The phase content of this later type of inclusions is similar to that of the earlier type (Plate I, Figs. 11–13).

The main differences between the early and late types of inclusions were identified as a result of homogenisation determination. Sylvite is always the first phase dissolved in the latter type of brine-rich inclusions. The dissolution temperature of sylvite does not exceed 80°C and usually varies between 50 and 70°C. The gaseous phase or halite is the next phase to be dissolved. Sulphide phases dissolve only after the inclusions have been subjected for a relatively long period of time to temperature close to that needed to homogenise halite and gas bubbles, which is about 250 to 600°C. The temperature of homogenisation decreases with a decrease in salinity. A further evolution of the phase relationships in inclusions results in halite and water solution being the only phases remaining.

Salinity decreases with the evolution of the early and late types of fluids. The sylvite phase disappears, and halite becomes less and less common (Plate I, Figs. 14, 15) until it also finally disappears. The concentrations in the saline fluids eventually fall below 26.4 wt % NaCl. The existence of more dilute fluids is the only manifestation of the further postmagmatic activity.

Locally, inclusions containing fluid rich in a liquid CO_2 phase have been identified. Such inclusions have been encountered in a zone surrounding the saline inclusions. Apparently, the fluid rich in liquid CO_2 was separated from the saline fluid at some point, as the salt solubility in the fluid rich in liquid CO_2 is very low.

The dilute hydrothermal fluids are represented by several generations of gaseous-liquid inclusions. Phases added after formation of the inclusions or captured sulphide phases, and unidentified minor phases, have been identified in those inclusions. Molybdenite (Plate I, Fig. 16), pyrite, chalcopyrite, and sphalerite are the sulphides found. Liquid-gaseous fluid appeared during the time that dilute fluids were active. The homogenisation temperatures of these inclusions vary from 360 to below 90°C. The deposition of the last ore mineral assemblages was associated with the activity of these fluids, which reacted with all the earlier types of fluids.

The ratio of phases fund in fluid inclusions in other minerals are very similar to those described above. Highly concentrated saline inclusions containing greater than 26.4 wt % NaCl were not encountered in albite, scheelite, fluorite, or epidote. In those minerals, gaseous-liquid type inclusions are common and sometimes contain captured phases or sulphide phases added after formation of the inclusion.

The highest homogenisation temperatures found in inclusions from the Myszków area were in scheelites (360–240°C; Szełęg, 1997) and in epidotes (360–200°C). In albites, the temperatures ranged from 340 to 270°C, and in high temperature calcites from 320 to 280°C. In low temperature calcites, the inclusions homogenised between 160 and 110°C. In fluorites, where the inclusions are of the gaseous-liquid type, homogenisation temperatures vary between 160 and 110°C.

The last manifestations of the activity of hydrothermal solutions are documented in numerous, single-phase (liquid) inclusions. These are the only type of inclusions found in celestite and gypsum. They are also present in most of the other mineral assemblages, but mostly in quartz. These single-phase inclusions are completely absent only in scheelite, epidote, albite, and fluorite.

PLATE I

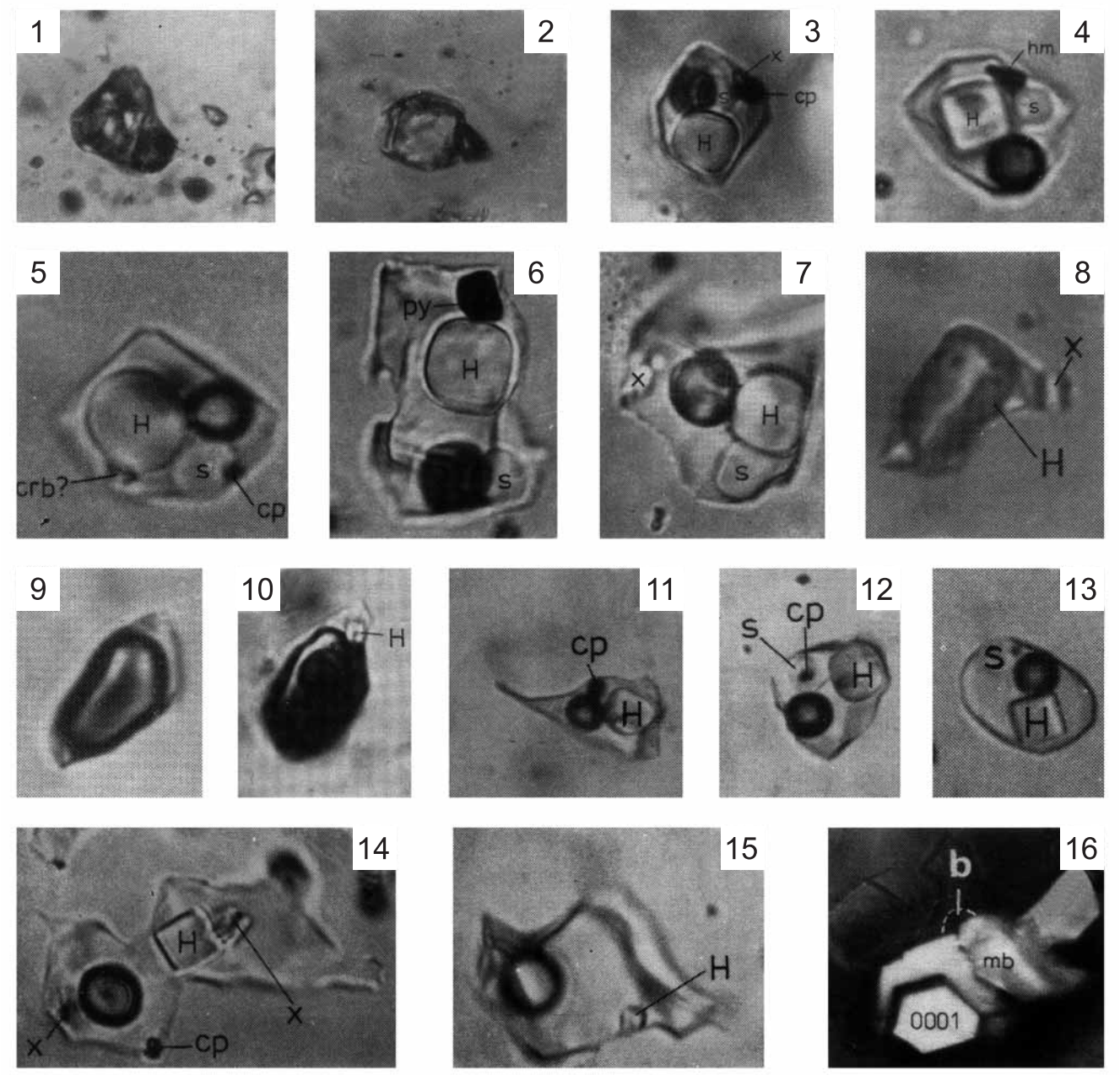

Fig. 1. Highly concentrated brine inclusion (non homogenous below 1 250°C) in magmatic quartz. Pz-17/471.3 m/x1 900. **Fig. 2.** Salt-melt inclusion; homogenisation temperature 1 224°C. Magmatic quartz. Pz-17/471.3 m/x2 200. **Fig. 3.** Highly concentrated brine inclusion; H — halite, s — sylvite, cp – chalcopyrite; unidentified anisotropic phase (T_h — 768°C) from quartz vein cutting porphyry. Pz–5/599.8 m/x 2 000. **Fig. 4.** Multi-phase brine inclusion; H — halite, s — sylvite, hm — specularite (T_h — 456°C). A–9/404.8 m/x 3 000. **Fig. 5.** Brine inclusion with crystals of halite (H), sylvite (s), chalcopyrite (cp), and probably of carbonate (carb). Magmatic quartz. Pz–3/262.0 m/x 2 200. **Fig. 6.** Inclusion of low-concentrated brine with halite (H), sylvite (s), and pyrite (py). Magmatic quartz. Pz-2/375.3 m/x 1 700. **Fig. 7**. Inclusion similar to the one above (Fig. 6) without pyrite, and with unidentified anisotropic phase (x), H — halite, s — sylvite. Pz-2/375.3 m/x 1 800. **Fig. 8.** Brine inclusion subsequently filled with gaseous fluid; in gas bubble poorly visible halite crystal (H), unidentifiable anisotropic mineral (x) also present. Magmatic quartz. Pz-17/189.6 m/x 2 100. **Fig. 9.** Liquid-gaseous inclusion in magmatic quartz. T_h about 400°C. Pz-10/764.4 m/x 1600. **Fig. 10.** Three-phase liquid-gaseous inclusion with halite (H). Magmatic quartz. T_h — about 760°C. Pz-1/237.5 m/x 1 700. **Fig. 11.** Brine inclusion with halite (H) and chalcopyrite (cp). Quartz vein. T_h — 343°C. (chalcopyrite non solvable). Pz-1/237.5 m/x 1 900. **Fig. 12.** IInd type brine inclusion with halite (H), sylvite (s), and chalcopyrite (cp). Magmatic quartz. T_h — 384°C. Pz-1/237.5 m/x 2 000. **Fig. 13.** IInd type fluid brine inclusion with lower halite (H) and sylvite (s) content. In sylvite — small grain of iron sulphide. Magmatic quartz. T_h — 361°C. Pz-1/237.5 m/x 1900. **Fig. 14.** Low-concentrated brine fluid inclusion with halite (H), chalcopyrite (cp), and unidentifiable anisotropic phase (x). Magmatic quartz. T_h — 321°C. Chalcopyrite non-solvable. Pz-7/615.0 m/x 2 100. **Fig. 15.** Inclusion of diluted brine with a small halite crystal (H). Magmatic quartz. T_h — 290°C. Pz-1/158.0 m/x 1 800. **Fig. 16.** Molybdenite crystals aggregate (mb) in gaseous-liquid inclusion. Gas bubble (b) and inclusion outline poorly visible. T_h of a gas bubble — 294°C. Quartz vein. Pz-10/525.5 m/x 1 100, reflected and transmitted light, one nicol.

Inclusion from Figures 1–15 taken by transmitted light, with one nicol.

In some mineral assemblages, the temperatures of formation of fluid inclusions are difficult to define. Two mineral associations: magnetite-chalcopyrite and quartz-feldspar, are though to have formed at higher temperatures than any other minerals and are associated with the time when the most highly concentrated fluids were active. The quartz-molybdenite-scheelite association and the black quartz-molybdenite association formed from more dilute solutions. Investigations of scheelite inclusions indicated that liquid concentrations contained less than 26.4 wt % NaCl and had homogenisation temperatures of 360 to 240°C. The rest of the mineral paragenetic assemblages are clearly connected with activity of the dilute, lower temperature fluids.

A marked decrease in the salinity and temperature of mineral forming fluids occurred during the genesis of the porphyry Cu-Mo-W mineralisation at Myszków. However, that general trend was modified by gas-rich fluids.

The general chemistry of the mineral forming fluids can be defined by analyses. Halite dominates over sylvite in the inclusions richest in crystalline phases. In inclusions with more dilute fluids, halite is the single phase. The chloride content of inclusions associated with the most highly concentrated brines is very high. In these inclusions, which were formed in magmatic and postmagmatic transition conditions, the equivalent NaCl content may run as high as 85 wt % and commonly ranges between 50 and 70 wt %. The very strongly concentrated solutions are, therefore, qualitatively close to that of the water-saline fluid. The density of this type of fluid is also very high and may run as high as 2.0 g/cm^3.

NaCl and KCl concentrations in the inclusions, which were defined using ratios of halite to sylvite crystalline phases and the Na/K ratios in the water extracts, exhibit a clear domination of sodium chloride over potassium chloride. The NaCl/KCl ratios are shown on a NaCl-KCl-H_2O triangle (Fig. 28). Most of the plotted points form an elongated field along the NaCl-H_2O side. The very highly concentrated inclusions are represented by single, isolated, randomly located points. The distribution of such points, which clearly trends toward the NaCl apex, is called “the halite trend” (Cloke and Kesler, 1979).

In more dilute saline solutions, decreases in KCl concentration clearly follow the very distinct decreases in NaCl concentration. This decrease in potassium may have been caused by the “consumption” of potassium during metasomatism that is related to its incorporation into newly formed minerals such as potassium feldspars, micas, hydromicas, and clay minerals.

The highest concentrations of the Na^+, K^+, Ca^{2+}, and Mg^{2+} cations have been found in water extracts of magmatic quartz crystals (phenocrysts). Chlorine is the main anion found. The water extracts from quartz inclusions that were heated to temperatures of 300 and 600°C were also investigated. At 300°C sodium and potassium are the dominant ions, and a high Na/K ratio is present in extracts from inclusions. At 600°C the extracts show distinctly lower Na/K ratios and higher concentrations of calcium and magnesium.

The mineral forming fluids were, therefore, very differentiated, but sodium and chloride ions were always dominant (Karwowski, 1988). Lithium and fluorine concentrations are small in all the investigated extracts. Thus, the general type of fluid found at Myszków is one enriched in Na, K, Ca, Mg, and Cl.

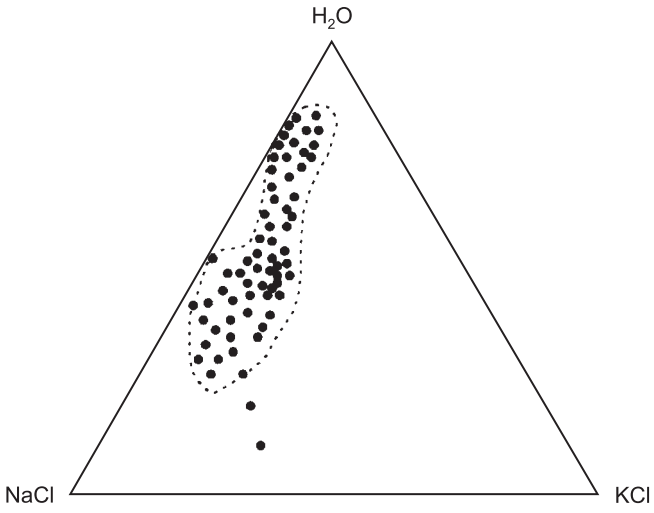

Fig. 28. Triangular projection (NaCl-KCl-H_2O) of 65 brine inclusions contents

The relatively small sulphide phases are homogenised in both the brine-rich and the more dilute inclusions. The metal and sulphur concentrations were calculated in the mineral forming fluids using sulphide solubilities, and yield metal (Cu, Fe, Zn) and sulphur concentrations that range from 0.06 to 0.4 wt %. Such high concentrations have also been observed in fluids from other porphyry copper deposits (Eastoe, 1978; Roedder, 1971; Reynolds and Beane, 1979; Bodnar and Beane, 1980).

At Myszków, mineral phases recognised in fluid inclusions, based on the element contents defined in micro areas include albite (in vesicles), potassium-feldspar or mica, calcium sulphate (gypsum or anhydrite), calcite, dolomite, ankerite, and calcium and magnesium chlorides.

Minerals found in inclusions from other porphyry copper deposits include, in addition to halite, sylvite, and sulphide phases, alkali feldspars, micas, anhydrite, gypsum, ankerite, magnetite, specularite, and chloride-hydroxide salts of potassium, iron, and manganese (Beane and Titley, 1984; Eastoe, 1978; Nash and Theodore, 1971; Wilson *et al*., 1980; Roedder, 1971).

PRESSURE CONDITIONS

Most probably, magma in Myszków area intruded under a pressure close to lithostatic. Unfortunately, the depth of emplacement of the cooling intrusions has not been established. By analogy to other micro granodioritic intrusions, one may assume, however, that rocks of that type at Myszków cooled at a depth of 1–2 km.

The depth of erosion in the Myszków area is also unknown. The locations of hypabyssal intrusions suggest that the thickness of overburden was in the range of 600–800 m. Pressures existing at the time of intrusive emplacement may thus be assumed to be 100–150 Mpa (1–1.5 Kbar) or slightly higher, based on the homogenisation temperature of fluid inclusions

that were determined in high temperature, magmatic, hexagonal quartz crystals.

Pressure conditions were determined using the Naumov and Malinin (1968) method, which is accurate within 5 Mpa. Postmagmatic fluid pressures determined by that method show a line of decreasing pressures that is parallel to the trend of fluid evolution. The greatest pressures (105 Mpa = 1.05 Kbar) correlate with the most highly concentrated brines. When the temperature decreases to about 300°C, the pressures associated with the brine-rich fluids decrease to 75 Mpa. In the dilute fluids (below 26.4 wt % NaCl), the pressures vary between 95 and 35 Mpa, and the temperatures vary between 450 and 120°C. The highest pressures, which are around 110 Mpa (1.1 Kbar), characterise the later type of brine-rich fluid. As the fluid evolves, these pressures decrease to 85 Mpa, within a temperature range of 300 to 250°C. The most dilute fluids are still present at pressures of 15–2 Mpa.

During evolution of the brine-rich fluids, pressures very frequently fell abruptly by as much as 70 Mpa. This drop caused an intense boiling of the saturated fluids and a loss of volatile-rich fluid. Generation of late brine-rich fluids, which contained higher concentration of brine than did the primary fluid, was another effect of the pressure drop.

During the evolution of both secondary brine-rich fluids and primary dilute fluids, such pressure changes occurred frequently. Pressure variations of such magnitude were caused by abrupt fracturing of both the intrusive rocks and wall rocks.

The pressures determined in liquid-gaseous fluids, which were generated during the boiling of the hydrothermal solutions, were small and in the range of 20 to 4 Mpa. On the other hand, temperatures changed over a large range, from 800 to 350°C. During evolution of the magmatic fluids, over a dozen different generations of liquid-gaseous fluids were developed.

MINERALOGICAL CHARACTERISTICS OF THE MINERALISATION

Mineralogical studies of the mineralisation in Myszków included macrostructure studies, microscopic analyses in reflected and transmitted light, diffraction analyses, and spectral X-ray analyses using a microprobe. Geochemical studies of trace elements in the principal ore minerals and sulphur isotope analyses were also conducted to establish the genesis of minerals.

Pyrite, chalcopyrite, molybdenite, magnetite, sphalerite, and scheelite are the main components of the mineralisation. Chalcocite, covellite, and malachite are sporadically encountered but only in the uppermost parts of the granitoid intrusion. The mineralisation is almost entirely hypogene.

Veins and associated disseminations are the main forms of mineralisation. The close spatial relationship of the mineralisation with the Variscan-aged Myszków–Mrzygłód granitoid intrusion has been described elsewhere (Ślósarz, 1982, 1985). The mineralisation is also closely related to post-intrusive tectonics, the earliest stages of which were associated with the cooling of the granitoid body. The mineralisation is characterised, first of all, by a locally developed, dense vein network that forms a stockwork. Later mineralisation stages were developed under subsurface conditions.

The ore mineralisation at Myszków occurred in a series of pulses. Most of the principal ore minerals (pyrite, chalcopyrite, and molybdenite) were deposited during several different stages. These stages occurred at different times, were controlled by different fissure systems, and were characterised by different paragenetic sequences (Table 7).

Table 7

Periods and stages of the molybdenum mineralisation at Myszków

Period	Mineral associations	Form of mineralisation	Alteration of wall rocks	Isotope composition δ^{34} S‰	Temperature conditions (after Karwowski, 1988)
Period I (Early, skarn forming)	Magnetite–chalcopyrite	Impregnation, nests	Hornfelses, skarns, metasomatites	+1.71 to +3.47	Nd
Period II (Main, hydrothermal)	Feldspar–molybdenite–biotite	Impregnation, voids infilling	K-rich metasomatism (feldspathisation)	+3.39	Nd
	Quartz–feldspar	Impregnation in pegmatite veins	Silicification	Nd	800–400°C (L)
	Quartz–molybdenite–scheelite	Stockwork veins, impregnation	Silicification, feldspathisation	+3.35 to +3.56	360–240°C (G)
	Black quartz–molybdenite	Banded veins, pseudobreccia	Phyllic metasomatism (sericitisation, silicification, pyritisation)	Nd	400–160°C (L)

Nd — not determined, L — inclusions homogenising in liquid phase, G — inclusions homogenising in gaseous phase

The mineralisation process was complex and long-term (Ślósarz and Karwowski, 1981, 1982, 1983). Veins from different stages overlap or cross-cut. Metasomatic replacements of one mineral by another are commonly observed. Mineral parageneses indicate a relatively large range of depositional temperatures (Table 7).

The complete mineral association consists of, from most common to least common, pyrite, chalcopyrite, magnetite, sphalerite, galena, scheelite, and rutile, all of which are encountered in all of the mineralisation stages. Bornite, hematite, pyrrhotite, marcasite, ilmenite, wolframite, and ferberite are found more rarely. Traces of bismuthinite, native Bi, chalcopyrrhotite, cubanite, emplectite, aikinite, hessite, tetradymite, cosalite, wittichenite, tetrahedrite, tennantite, valleriite, and chalcocite have also been identified. Chalcocite, covellite, malachite, and goethite are found in the weathering zone.

Gangue minerals at Myszków include quartz, feldspars (orthoclase, microcline, adularia, albite), chlorides, epidote, sericite, muscovite, biotite, calcite, ankerite, dolomite, barite, fluorite, and gypsum.

The ore mineralisation was generated by two main processes (Table 7):

- contact metamorphism (Period I – early, skarn forming),
- postmagmatic hydrothermal activity, represented by the finely disseminated and veinlet types of Cu mineralisation (porphyry copper *sensu stricto*), by multistage, vein type, Cu-Mo mineralisation (Period II — main, hydrothermal), and by low temperature, slightly mineralised veins (Period III — late, post-mineralisation).

PERIOD I — EARLY, SKARN FORMING

This period is represented by a magnetite-chalcopyrite paragenetic assemblage that is present in hornfelses, skarns, and metasomatites. These types of altered rocks are encountered both near intrusive contacts and in more distant areas (Pz-32; Fig. 7), where the thickness of metasomatites may be as much as 60 m.

In andradite and pyroxene-amphibole skarns, the thickness of the mineralised zones varies between a few cm and several tens of centimetres. Sometimes, massive aggregates of magnetite constitute as much as 30 wt % (Pz-10), and those of chalcopyrite, as much as 10 wt % (Pz-33).

Molybdenite is found in skarns only sporadically and is in the form of fine flakes. Scheelite, which is present in the form of large aggregates that are a few mm in diameter, is more common than molybdenite, especially in pyroxene-amphibole skarns. Chalcopyrite and pyrite are found filling the space between magnetite grains. Chalcopyrite also occurs independently and replaces platy minerals of the amphibole group (Plate II, Fig. 1).

Weak magnetite-chalcopyrite mineralisation is also commonly found in the hornfelses. It appears as disseminated grains or short, a few mm long, metasomatically growing chloride-epidote-quartz veins that may contain magnetite, pyrite, and chalcopyrite, as well as chalcopyrite intergrowths with sphalerite, galena, and bornite. Locally, small aggregates of wolframite, together with various sulphides, have been observed.

Metasomatites in the Myszków area are widespread. They are encountered in nearly all of the boreholes drilled in the area containing intrusive rocks. The most common are feldspar-epidote metasomatites, which are found in zones a few metres to several tens of metres thick. They occurred either as completely altered rock masses or as generally symmetrical aureoles around quartz veins that are usually about 10 centimetres thick and composed of mineral assemblages that are similar to the more massive metasomatites (Plate II, Fig. 2).

Magnetite, pyrite, hematite, and sphalerite were the principal ore minerals found in both metasomatites and veins. More rarely, scheelite, pyrrhotite, galena, ilmenite, marcasite, cubanite, bismuthinite, native Bi, and Bi sulphosalts were identified.

The order of mineral deposition is similar in all types of altered rocks. Sulphides (chalcopyrite and pyrite) formed after magnetite. Oxide mineralisation probably originated in the final, skarn-type alteration stage and was deposited within a similar temperature range. Sulphides younger than oxides were generated later, in the effect of the normal evolution of the hydrothermal solution: from alkali to acidic ones (Zharikov, 1970).

Temperatures of 550 to 500°C are assumed during formation of the pyroxene-garnet facies, and of 350 to 400°C during formation of the pyroxene-epidote facies (Zharikov, 1970). The paragenetic sequence in altered contact rocks also suggests a high temperature for oxide-sulphide mineral deposition. For example, magnetite and chalcopyrite locally contain inclusions of sphalerite and occasionally cubanite or pyrrhotite. The presence of wolframite and scheelite alongside sulphides emphasises the significant variation in the physico-chemical conditions of this stage of mineralisation. The mineralising solutions were obviously enriched in Fe, Cu, SiO_2, and CO_2.

PERIOD II — MAIN, HYDROTHERMAL

This period produced the significant Cu-Mo-W mineralisation of the Myszków area. It consists primarily of porphyry-type mineralisation that includes disseminated mineralisation and several stockwork-type vein systems.

The hypogene, disseminated copper mineralisation is found in all of the boreholes drilled in the Myszków area both in porphyries and granitoids. The sulphide content in the disseminated phase commonly varies between 0.5 and 3% and very

Table 8

Chemical content of altered rocks (wt %)

Component	K-rich metasomatism			Phyllic metasomatism				Argillisation
	Samples (m)							
	P-33 981.6	Pz-33 945.5	Pz-33 843.9	Pz-33 681.7	Pz-29 681.7	Pz-29 674.1	Pz-17 1216.0	Pz-33 304.8
SiO_2	60.43	62.75	65.19	73.55	74.36	70.61	71.94	65.49
Al_2O_3	18.98	17.66	16.61	11.25	12.62	16.09	15.19	17.82
CaO	1.4z8	1.57	2.20	1.35	0.81	1.39	0.76	2.38
MgO	0.88	0.20	0.65	0.36	0.26	0.43	0.37	0.60
Na_2O	2.32	1.46	3.60	0.19	0.27	0.24	0.19	0.72
K_2O	12.50	13.60	7.00	3.70	8.45	7.44	6.85	5.58
Fe_2O ((total Fe)	2.19	0.87	3.02	5.39	1.04	1.55	1.37	1.61
MnO	0.03	0.03	0.02	0.02	0.03	0.08	0.02	0.04
TiO_2	0.49	0.27	0.35	0.35	0.30	0.40	0.36	0.54
LOI	1.17	2.05	1.70	3.86	1.49	2.20	2.65	5.17
Total	100.47	100.46	100.34	100.02	99.63	100.43	99.70	99.95

rarely may be as much as 10% by volume. Pyrite and chalcopyrite are the main minerals. Sometimes pyrrhotite may be present instead of pyrite (Pz-40). Magnetite, bornite, sphalerite, and galena are also encountered locally.

Pyrite forms individual, euhedral grains that are very often recrystallised. Corroded grains are also observed. Numerous inclusions of gangue minerals as well as magnetite, chalcopyrite, cubanite, and galena are present in pyrite grains. Very often, chalcopyrite with bornite inclusions is seen replacing (corroding) pyrite.

Pyrrhotite forms single grains, that may be as much as 0.X mm in diameter and contain inclusions of gangue minerals. Granular aggregates of pyrrhotite with marcasite and chalcopyrite, have also been observed. Isolated veins of marcasite are also present.

Chalcopyrite forms individual, anhedral grains or monomineralic aggregates that are as much as 0.X mm in diameter but more rarely may be as much as a few mm in diameter. In addition, chalcopyrite fills fissures in pyrite aggregates, and is also present in magnetite aggregates. Chalcopyrite contains quartz, sphalerite, and bornite inclusions. It also forms intergrowths with sphalerite, bornite, and galena, and sometimes with chalcocite.

Finely disseminated sulphides in small “feather-like” chloride veins are the characteristic ore structures found in this period of mineralisation. Disseminated sulphide grains that are mainly chalcopyrite and pyrite are present both in matrix material and in phenocrysts in biotite grains.

The copper-molybdenum and associated tungsten mineralisation phase is the most widespread and contains the largest overall amounts of sulphide minerals. This phase is found in both porphyries and granitoids, as well as in hornfelses. Various types of hydrothermal alterations and varying intensities of alteration are associated with this type of mineralisation (Table 8).

The Cu-Mo-W mineralisation was formed in several stages that were clearly separated in time, and each stage was generally associated with different fissures systems (Table 7), and characterised by a different suite of minerals. The order of individual stages was defined on the basis of the cross-cutting sequence of veins (Plate II, Fig. 3). The stages differ in paragenesis from one another because they occurred at different temperatures and under different physico-chemical conditions. The two main ore minerals, pyrite and chalcopyrite, are present in veins from all stages, molybdenite is found in four stages, and scheelite in only three.

The following five mineral paragenetic assemblages (stages) have been distinguished:

1. Feldspar-molybdenite veins, with biotite.
2. Quartz-feldspathic, pegmatitic veins.
3. Quartz veins, with molybdenite and scheelite.
4. Black quartz veins, with molybdenite.
5. Quartz-polymetallic veins.

FELDSPAR-MOLYBDENITE VEINS, WITH BIOTITE

Veins in this stage are found in granitoids, in the central part of the intrusion (Pz-24, Pz-25, Pz-26, Pz-29, and Pz-33). They are associated with K-rich metasomatic zones (feldspathisation and biotitisation), but do not demonstrate any direct association with any fracture systems. The metasomatic alteration process has affected the entire rock mass (Plate II, Fig. 4).

Rocks altered during the feldspathisation process are composed mainly (as much as 90% by volume) of K-feldspars (Markiewicz, 1995, 1998). Sericitised plagioclases, quartz, and micas are present in smaller amounts. The replacement of plagioclase feldspars with K-feldspar is also very common. The thickness of the metasomatic zones was found to vary between 5 and 60 cm (in borehole Pz-33).

Hydrothermal biotite is commonly found as disseminated grains (Plate II, Fig. 5) or as aggregates oriented like schlieren veins. The aggregates, which are commonly a few mm in diameter and occasionally as much as 15 mm in diameter, are composed of biotite flakes with quartz and sulphides (chalcopyrite and molybdenite). Molybdenite, chalcopyrite, pyrite, and scheelite aggregates also exist in separate concentrations.

A characteristic feature of the altered rocks in this stage is a porous texture that results from a partial leaching of their phenocrysts. The pores are open or filled with sulphides or occasionally with epidote and scheelite. Disseminated ore minerals deposited in this stage compose 2 to 10% of the volume of the altered rock. Molybdenite sometimes forms veinlets a few mm thick. In addition to those mentioned above, the ore minerals include also a martite-rich magnetite, sphalerite, galena, rutile, ilmenite, and titanite.

Chemical analyses of the rocks altered by feldspathic metasomatism contain a K_2O content of as much as 13 wt % and a distinct depletion in SiO_2, Ca, and Mg (Table 8).

QUARTZ-FELDSPATHIC, PEGMATITIC VEINS

This stage of mineralisation is characterised by veins that are fairly thick (10 to 100 centimetres) and are mostly present in granitoid rocks. These veins are usually found along sharp contacts between the intrusive rocks and the host rocks, and very rarely contain fragments of the host rocks. Stage 2 veins consist of massive, milky quartz, feldspathic bands a few mm thick, chlorites, and ore minerals. Calcite is found between the quartz crystals.

These veins are sometimes banded parallel to the orientation of a given vein, with some bands containing finely crystalline sulphides, which are most commonly molybdenite and pyrite. Scheelite and chalcopyrite are randomly disseminated in the vein matrix. Coarsely crystalline sulphide aggregates with massive textures are very rarely encountered. Sphalerite, galena, bismuthinite, native Bi, wittichenite, emplectite, aikinite, rutile, and bornite have also been reported in Stage 2 veins.

QUARTZ VEINS, WITH MOLYBDENITE AND SCHEELITE

Stage 3 veins exhibit the most common paragenetic association and contain the highest molybdenum and tungsten concentrations. Stage 3 veins are found in granitoids and porphyries and in the metamorphic host rocks. These veins are steep and very often vertical in relation to core axes and are usually branched.

Along with associated disseminated sulphides, these veins consist of a classic stockwork (Plate III, Fig. 6). The average thickness of veins varies between 1 and 20 mm.

Stage 3 veins are accompanied by metasomatic alteration, including feldspathisation and silicification, that are most common where the veins widen and cross-cut other veins. The density of stockwork veins is high. Locally, the density may range from ten to several tens of veins in a given metre of core. These stockwork veins are often tectonically deformed by younger quartz-sulphide veins that may be associated with sericitisation processes (Plate III, Fig. 1).

These stockwork-associated ore minerals usually occur in finely crystalline aggregates in vein quartz. These veins may also contain feldspars and chlorite and, more rarely, epidote and calcite as gangue minerals. Ore minerals include molybdenite, scheelite, chalcopyrite, pyrite, sphalerite, galena, hematite, magnetite, rutile, and ferberite.

Two generations of molybdenite are associated with Stage 3. Molybdenite occurs as disseminated, submicroscopic flakes, which sometimes colour the associated quartz blue, and as fine to coarse rosette-like, nest-like (Plate III, Fig. 2), or bunch-like aggregates. It is also present in streaks that are a few mm long and are oriented parallel to veins. Inclusions of other phases are not found in this mineral. Molybdenites are most commonly intergrown with chalcopyrite, less commonly with scheelite (Plate III, Fig. 3), and rarely with pyrite.

Scheelite usually forms separate grains or monomineralic concentrations that are a few mm in diameter and mostly associated with quartz. Sometimes scheelite contains inclusions of titanium oxides or, rarely, ferberite. Locally, scheelite has been sulphidised and has been replaced by molybdenite and chalcopyrite. Molybdenum-rich scheelite was also found. This variety is characterised by a molybdenum content of 0.7 to 2.0 wt %.

Chalcopyrite exists in the form of individual grains that may contain inclusions of galena or sphalerite. Chalcopyrite grains and aggregates are less than a few mm in diameter.

BLACK QUARTZ VEINS, WITH MOLYBDENITE

The paragenetic assemblage in stage 4 veins is very characteristic for the Myszków area and is quite common. These veins represent the final stage of molybdenite mineralisation and do not contain any scheelite. This stage can be easily distinguished from earlier stage (Plate III, Fig. 4). Stage 4 veins contain a greater number of minerals and are associated with ore-re-

lated alteration phases, especially with sericitisation where it locally overprints feldspathisation.

Magmatic rocks altered by sericitisation of feldspars commonly exhibit sericite pseudomorphs after plagioclases and contain less common pseudomorphs of hydromuscovite, opaque minerals, and occasionally epidote. The matrix contains hydromicas and carbonates, as well as quartz and feldspars.

Chemical analyses of magmatic rocks altered during this stage confirm that these rocks are relatively enriched in K_2O (3.7% to 8.45% by wt; Table 8), silica, and carbonates.

The black quartz veins range in thickness from a few mm to as much as 10 cm. Where present in the host rocks, these veins are commonly found in breccia zones.

The main gangue mineral in these vein, black quartz, contains disseminated, microcrystalline sulphides that consist mostly of pyrite, chalcopyrite, and molybdenite. Pyrite is the principal ore mineral. It forms single euhedral grains, and polycrystalline aggregates, all with a cataclastic texture. The cataclastic fractures are filled with chalcopyrite, sphalerite, and galena, all of which have replaced pyrite.

Molybdenite flakes are finely crystalline with grains sizes varying from submicroscopic dust, to thousandth and hundredth parts of a millimetre. In this vein assemblage, more often than in any others, molybdenite is found intergrown with chalcopyrite, sphalerite, and galena.

Chalcopyrite is present in this stage in two forms: (1) in individual grains as well as large aggregates that are a few mm in diameter, and (2) in inclusions in sphalerite. Chalcopyrite is often intergrown with bismuth minerals. Bismuthinite, native Bi, wittichenite, and hessite have also been reported. Inclusions of bornite, cubanite, galena, tennantite, and tetrahedrite in chalcopyrite and of magnetite in pyrite are also present.

Sphalerite commonly contains chalcopyrite inclusions, and galena contains inclusions of bismuth minerals.

QUARTZ-POLYMETALLIC VEINS

Stage 5 is the final one for Period II ore mineralisation. Veins in this stage do not contain molybdenite. Chalcopyrite, pyrite, sphalerite, and galena are the most characteristic minerals. Sericitisation and muscovitisation accompany veins (Plate II, Fig. 5), mainly in symmetric aureoles. These veins are only found in the magmatic rocks.

Massive sulphides and quartz textures are another important feature of this stage (Plate III, Fig. 6). The quartz is commonly milky white but is sometimes transparent (especially in druses). In the central parts of veins, calcite may be present. The thickness of the veins varies between 2 and 10 cm. The sulphide content of these veins, which is mostly pyrite and chalcopyrite normally does not exceed about 10 volume %. Bornite, magnetite, rutile, and Bi minerals may also be present there.

*
* *

Two more types of molybdenite mineralisation have been distinguished in the main hydrothermal period. They only appear sporadically and do not cross-cut other assemblages. Their relative age within the general mineralisation scheme has thus not been defined.

The first type includes monomineralic molybdenite veins that are a few mm thick and composed of fine crystals. These veins were encountered in cores from boreholes Pz-17 and Pz-28, and may be present in cores from other holes as well. In some intervals in holes Pz-26 and Pz-27, they have replaced stylolitic structures.

The second molybdenite type was discovered in borehole Pz-28, in a granitoid pseudobreccia. The breccia matrix is composed of quartz, finely crystalline molybdenite, chlorite, calcite, and locally chalcopyrite.

PERIOD III — LATE, POST-MINERALISATION

In the Myszków area, this period is the last one in the mineralisation associated with of the Vendian–Early Carboniferous rocks. Two vein systems have been distinguished in Period III. One is ankerite-bearing and the other is barite-fluorite-bearing. Both are mineralised with pyrite, chalcopyrite, sphalerite, and galena. In addition, the barite-fluorite-bearing veins may also contain marcasite.

Ankerite occurs where the veins are densely branched. Ankerite metasomatism extends outward from the veins for several tens of centimetres. The fissures are completely filled with massive, milky ankerite. Locally, quartz, and fine aggregates of crystalline pyrite, sphalerite, galena, and, more rarely, chalcopyrite, are also present. Veins of this latter type have a rather limited extent and are most commonly found in cores from boreholes Pz-24, Pz-25, and Pz-26.

Barite-fluorite-bearing veins are much more widespread in extent and have been found in the area outside of any porphyry-related mineralisation. These veins show no spatial correlation with different types of hydrothermal alteration in the host rocks. The veins are characterised by crustification structures. Locally, barite and other minerals form a tectonic breccia matrix in these late-stage veins.

In the barite-fluorite veins, barite is the principal mineral. Quartz and calcite bands or druses coat barite crystals. Celestite appears sporadically. Earthy or colourless bands of fluorite are thought to be older than the barite. Ore minerals are found mostly in barite. Fine grains of chalcopyrite, semi-transparent sphalerite, galena, and marcasite, and lesser amounts of pyrite, have been identified locally.

PLATE II

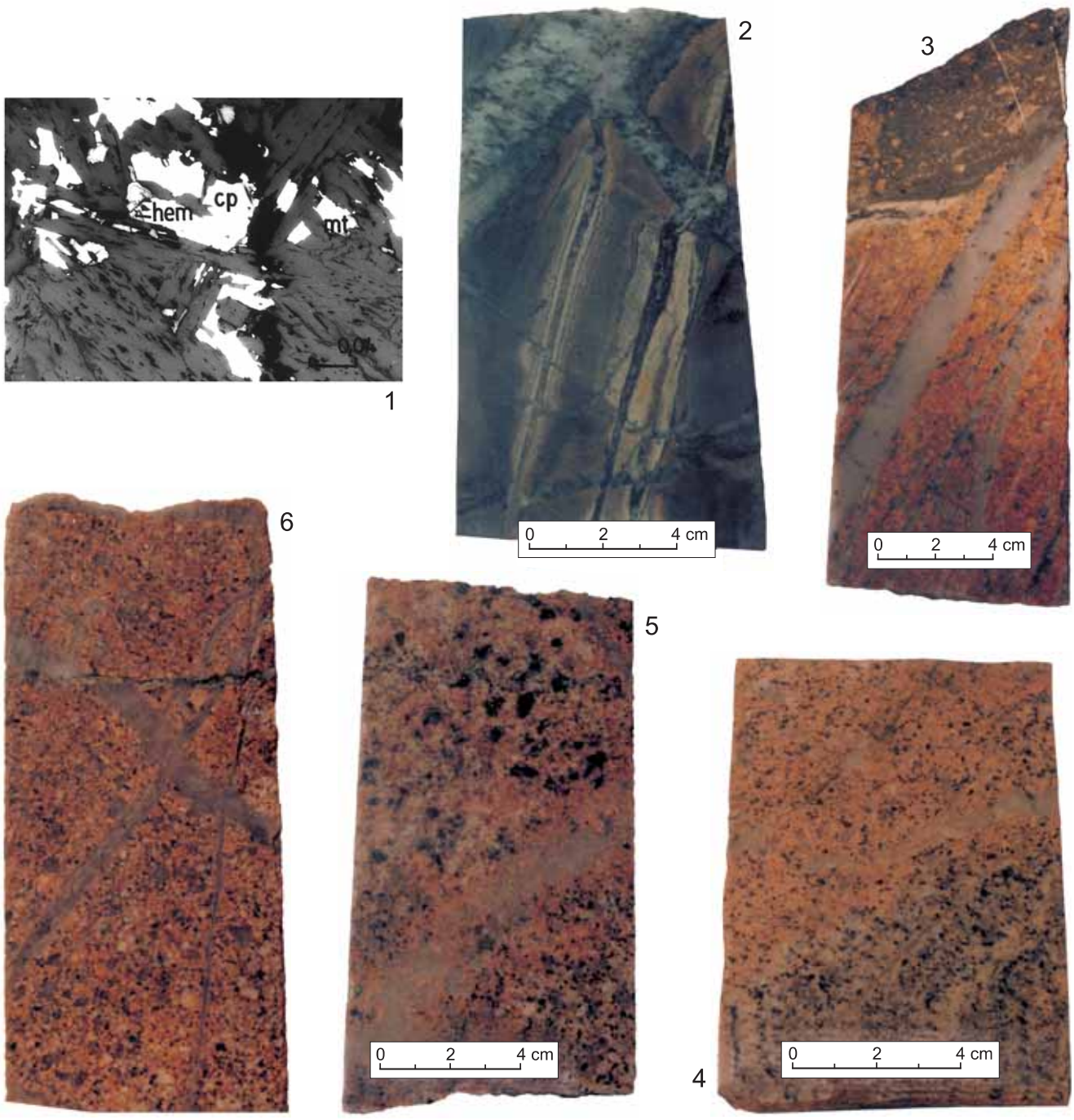

Fig. 1. Metasomatic replacement of amphiboles by chalcopyrite (cp), magnetite (mt), and hematite (hem). Pz-33/218.2 m/1N.

Fig. 2. Feldspar-epidote metasomatite with quartz-feldspar-chalcopyrite veins. Pz-32/673.7 m.

Fig. 3. Quartz stockwork cut by a vein composed of black quartz pseudobreccia with disseminated sulphides. Pz-29/747.1 m.

Fig. 4. Feldspar metasomatite. Unaltered parts of granodiorite — dark grey. Pz-33/986.2 m.

Fig. 5. Impregnation of secondary biotite in metasomatic feldspar mass. Pz-33/847.1 m.

Fig. 6. Two generations of quartz veins: (1) stockwork type — older, (2) black quartz with sericite and sulphides — younger. Pz-33/512.4 m.

PLATE III

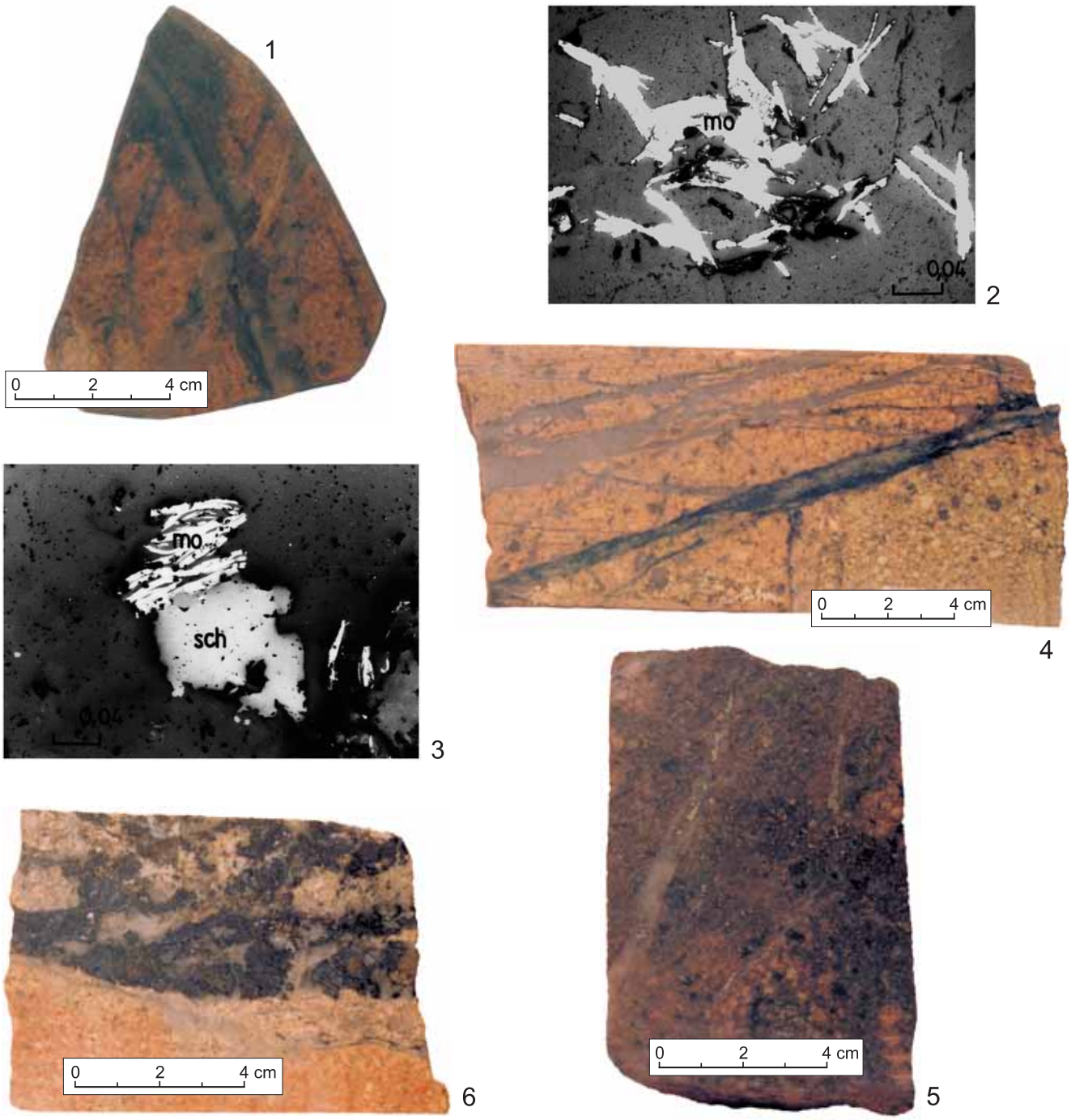

Fig. 1. Dark grey sericitised zone overlapping a deformed quartz vein. Pz-29/640.0 m.

Fig. 2. Monomineralic concentration of molybdenite (mo). Reflected light. Pz-17/1000.3 m/XN.

Fig. 3. Aggregate of molybdenite (mo) and scheelite (sch) in quartz. Reflected light. Pz-29/667.0 m/1N.

Fig. 4. Black quartz veins with sulphides overlapping a stockwork system of quartz veins with molybdenite. Pz-33/470.2 m.

Fig. 5. Granodiorite altered in phyllic metasomatism, impregnated by pyrite and chalcopyrite. Pz-26/526.6 m.

Fig. 6. Massive concentration of sphalerite, galena, chalcopyrite, and pyrite in quartz. Pz-10/756.5.

GEOCHEMICAL CHARACTERISTICS OF THE PRINCIPAL ORE MINERALS

Geochemical studies of the principal ore minerals included identifying various stages of ore mineral deposition, paragenesis, and paragenetic associations of the Cu-Mo-W mineralisation in the Vendian to Early Carboniferous rocks in the Myszków area. Investigation objectives included recognising the chemical content of selected minerals as well as identifying their most characteristic isomorphic mineral species. Emphasis was on identifying (1) the mineralogical forms of the main chemical components (Fe, Cu, Mo, W, Zn, Pb, Ti, and Bi) as well as (2) the mineral residence of associated trace elements, including Ag, Te, Se, Re, V, Cd, Sn, As, Co, Ni, and Ta.

The quantitative chemical content of selected minerals were conducted by Salamon (1989) at the Technical University of Mining and Metallurgy (Akademia Górniczo-Hutnicza) in Kraków, with an ARL SEMQ X-ray electron probe micro analyser (20 kV accelerating voltage and 150μA probe current). The following spectral lines and standards were used: Mg K_α (MgO), Ca K_α ($CaCO_3$), Al K_α, Si K_α (SiO_2), Ti K_α, Mn K_α, Fe K_α (FeS_2), Co K_α, Ni K_α, Cu K_α, Zn K_α, As L_α, Sb L_α, Se L_α, Te L_α, Sr L_α, Mo L_α, Ag L_α, Au L_α, Sn L_α, Cd L_α, W L_α, Ta L_α, Re L_α, Pb L_α (PbS), Bi L_α, V $K_{\beta 1}$, and S K_α.

A total of 229 point analyses were determined on the most typical minerals in samples of skarn, disseminated, and vein (including various stages) types of mineralisation. The average concentrations of selected elements are presented in Tables 9–14.

Pyrite from skarn pyrite mineralisation (Table 9) contains a constant range of Ni (0.03–0.32%) and Co (0.02–0.17%) concentrations. Except for Pb (0.19 average wt %, 1.79 maximum wt %), the smallest amounts of the isomorphic admixtures were detected in porphyry mineralisation-related pyrites. Pyrite from the barite-fluorite-bearing veins is characterised by very low concentrations of Ni, Co, Cu, and As, especially in comparison to concentrations in stockwork and polymetallic veins. The concentrations of Au, Ag, Mo, Sb, Te, and Zn were all below their respective lower limits of determination.

A constant but substantial amount of Zn is present in chalcopyrites (Table 10). This Zn is probably associated with solid solutions of $CuFeS_2$ – ZnS. A similar Ni and Co content was detected in chalcopyrites from various other mineral paragenesis. The As content varies more widely and is exceptionally high in skarn chalcopyrites. Substantial amounts of Se (0.18–0.40 wt %), which probably replace sulphur, have been recognised in a few chalcopyrite samples that co-exist with molybdenite.

In molybdenite, the concentrations of Se, Ag, and Re were analysed (Table 11). A substantial amount of Se was detected (0.15–0.23 wt %) in all generations of molybdenite as well as in molybdenite-bearing rocks. Although Re was commonly detected in molybdenite, the average concentration of Re never exceeded 1%, suggesting that high to moderate temperatures were associated with deposition of this mineral. The average Ag concentration is generally near the detection

Table 9

Average content of trace elements in pyrites (wt %)

Type of mineralisation	Ni	Co	Cu	Pb	As	Number of samples
Skarn	0.04	0.08	0.04	0.10	0.11	12
Impregnation	0.03	0.03	0.08	0.19	0.04	13
Quartz-molybdenite stockwork	0.11	0.09	0.05	0.06	0.05	5
Quartz-polymetallic	0.14	0.05	0.13	0.06	0.08	9
Barite-fluorite	0.03	0.02	0.04	0.06	0.05	2

Table 10

Average content of trace elements in chalcopyrites (wt %)

Type of mineralisation	Ni	Co	As	Zn	Number of samples
Skarn	0.03	0.02	0.16	0.09	3
Impregnation	0.03	0.02	0.09	0.12	7
Quartz-molybdenite stockwork	003	0.02	0.05	0.10	2
Quartz-polymetallic	0.04	0.02	0.05	0.08	3

Table 11

Average content of trace elements in molybdenites (wt %)

Type of mineralisation	Se	Ag	Re	Number of samples
Impregnation in metasomatites	0.15	0.12	0.15	4
Quartz-feldspar veins	0.20	0.12	0.07	3
Quartz-molybdenite stockwork	0.21	0.12	0.17	6
Quartz-polymetallic	0.23	0.12	0.17	10
Molybdenite veins	0.23	0.12	0.13	5

level (0.12 wt %). Some higher Ag concentrations (0.22 and 0.16 wt %) were found but only in skarn molybdenite and in monomineralic vein molybdenite (Pz-13).

Sphalerites all contained Fe, Cu, and Cd but no detectable Ag, Pb, or Mo. Iron is present in variable amounts (Table 12). Skarn sphalerites have the highest concentrations of Fe (4.84 average wt %, 11.39 maximum wt %). High Fe concentrations have been detected in sphalerites from quartz-polymetallic veins. This observation is in agreement with microscopic observations in reflected light that identified marmatite, a Fe-rich sphalerite, in barite-fluorite-bearing veins.

Copper admixtures are also very common in sphalerites, with the highest concentrations in sphalerites from quartz-rich polymetallic veins. The presence of Cu and Fe in sphalerites suggests that solid solutions of sphalerite-chalcopyrite-pyrrhotite may exist. The presence of such solid solution minerals has been microscopically confirmed in several mineral associations. These solid solution minerals may help to define the temperatures of mineral depositions.

Cadmium, the third characteristic element in sphalerite, is also present in variable amounts. The most common concentration levels are 0.17–1.86 wt %. Cadmium probably substitutes for Zn in sphalerites. The specific feature of the sphalerites from the Myszków area is that they lack detectable amounts of Mn and Pb.

Galena from various mineral associations generally contains Ag in small but constant amounts (Table 13). The highest Ag concentration (7 wt %) was detected in skarn galena. Silver correlates positively in galenas with Bi. High Ag concentrations in galenas may result from microscopically undetectable

Table 12

Average content of trace elements in sphalerites (wt %)

Type of mineralisation	Fe	Cu	Cd	Number of samples
Skarn	4.84	0.72	0.76	6
Impregnation	0.12	0.14	1.86	1
Quartz-polymetallic	3.66	2.49	0.32	8
Impregnation in sericitisation zones	1.71	0.81	0.27	4
Barite-fluorite	0.77	0.24	0.17	4

Table 13

Average content of trace elements in galenas (wt %)

Type of mineralisation	Ag	Bi	Se	Number of samples
Skarn	7.00	8.47	1.16	1
Impregnation	0.23	0.27	1.20	1
Quartz-polymetallic	0.28	1.05	1.37	5
Barite-fluorite	0.23	1.06	1.41	3

submicroinclusions containing Ag and Bi. However, the Bi content in galenas is rather low. Selenium is commonly present in galenas from all mineralised rocks. No Au and Te was detected in galenas.

Magnetite, which is associated with all types of mineralisation, contains generally constant concentrations of such elements as Mg, Al, V, and Ti (Table 14), and also contains traces of Cu and S.

The concentrations of Ca and W were determined in scheelites. In some scheelites, substantial Mo (as much as 2.04 wt %) and Fe admixtures were found (Table 15). These high Mo concentrations suggest the existence of molybdenum-rich scheelites. The presence of Mg (as much as 1.12 wt %) and Ti (as much as 0.17 wt %) has also been detected in some scheelites.

Table 14

Average content of trace elements in magnetites (wt %)

Type of mineralisation	Mg	Al.	V	Ti	S	Cu	Number of samples
Skarn	0.10	0.30	0.04	0.66	0.03	0.03	6
Impregnation in K-metasomatites	0.02	0.13	0.08	0.10	0.04	0.06	2
Quartz-molybdenite stockwork	0.06	0.09	0.36	0.22	0.90	0.05	3

Table 15

Chemical content of scheelite (wt %)

Borehole	Depth in m	Mg	Ca	Ti	Mo	Sn	W	Fe
Pz-28	624.4	≤0.03	12.87	≤0.03	1.48	0.10	61.61	≤0.04
Pz-28	663.5	≤0.03	13.92	≤0.03	≤0.06	≤0.09	63.33	≤0.04
Pz-28	663.5	≤0.03	13.71	≤0.03	≤0.06	≤0.09	63.12	≤0.04
Pz-28	614.5	≤0.03	13.99	≤0.03	≤0.06	≤0.09	63.88	≤0.04
Pz-28	1035.2	≤0.03	8.84	≤0.03	≤0.06	≤0.09	64.50	7.06
Pz-28	1106.3	0.6	14.43	0.17	0.37	≤0.09	64.01	≤0.04
Pz-28	1184.7	≤0.03	12.66	≤0.03	0.71	0.11	62.12	≤0.04
Pz-28	1205.7	≤0.03	14.27	≤0.03	≤0.06	≤0.09	64.12	≤0.04
Pz-29	527.3	≤0.03	13.97	≤0.03	0.47	≤0.09	63.22	≤0.04
Pz-29	862.0	0.07	14.05	0.14	2.04	≤0.09	61.96	≤0.04
Pz-33	218.8	1.12	12.61	≤0.03	0.15	≤0.09	62.37	0.17

Unusual amounts of W have also been detected in Ti oxides that are associated with sulphides in copper-molybdenum veins and scheelite veins. Tungsten concentrations in Ti oxides vary from barely detectable traces to 5.10 wt % (Table 16).

High W concentrations in rutile from veins is probably associated with submicroinclusions of W that are not visible microscopically. The opposite situation — inclusions of Ti oxides in scheelite — is very common in many mineralised veins. In addition, Ti oxides contain substantial concentrations of Fe (0.27–0.86 wt %), Al, Si, and sporadically Ta (0.38%).

Over a dozen samples of bismuth minerals collected from skarn and quartz-polymetallic veins were also analysed. These minerals, especially bismuthinite (0.18–0.58% Ag), tetradymite, emplectite, and aikinite (0.57–1.84%), are enriched in Ag, Substantial admixtures of Cu (0.31–0.38%) were also found in native Bi.

Table 16

Trace elements contents in Ti oxides (wt %)

Borehole	Depth in m	Al	Si	W	Fe	Ta
Pz-17	603.6	0.92	3.13	0.96	0.68	–
Pz-17	603.6	–	–	0.55	–	–
Pz-17	603.6	–	–	5.10	–	–
Pz-17	603.6	–	–	0.37	–	–
Pz-17	603.6	≤0.02	0.11	0.34	0.27	–
Pz-17	603.6	–	–	3.59	–	–
Pz-17	603.6	–	–	0.95	–	–
Pz-17	603.6	–	–	0.92	–	–
Pz-28	1106.3	–	–	0.46	0.33	0.38
Pz-32	851.7	–	–	0.70	0.77	–
Pz-33	219.5	–	–	0.10	0.56	–
Pz-33	219.5	–	–	1.06	0.86	–

Table 17

Content of δ^{34} S‰ isotope in ore minerals at Myszków

Location of sample		Host rock	Mineral	δ^{34} S ‰
Borehole	Depth			
Pz-7	234.0	Skarn	Pyrite	+6.89
Pz-10	374.6	Skarn	Chalcopyrite	+1.71
Pz-10	388.65	Skarn	Pyrite	+2.06
Pz-33	219.10	Skarn	Chalcopyrite	+3.47
Pz-10	1149.5	Feldspar metasomatite	Pyrite	+3.99
Pz-10	921.0	Sericitised granodiorite	Sphalerite	+0.16
Pz-10	975.7	Sericitised granodiorite	Pyrite	+4.46
Pz-10	975.7	Sericitised granodiorite	Chalcopyrite	+3.10
Pz-29	673.9	Sericitised granodiorite	Sphalerite	+2.11
Pz-2	430.7	Propylite porphyre	Pyrite	+2.73
Pz-17	896.0	Stockwork quartz vein	Molybdenite	+3.56
Pz-29	592.6	Stockwork quartz vein	Molybdenite	+3.35
Pz-31	431.9	Quartz-polymetallic vein	Sphalerite	+1.27
Pz-29	673.9	Quartz-carbonate vein	Sphalerite	+2.16
Pz-5	672.7	Molybdenite vein	Molybdenite	+3.07
Pz-14	1377.0	Porphyry with impregnation	Molybdenite	+3.76

The concentrations of sulphur isotopes were also analysed in selected ore minerals. The investigations were conducted by S. Hałas from the Physics Institute of the Maria Skłodowska-Curie University in Lublin, on a mass spectrometer. Chalcopyrite, molybdenite, and sphalerite, from various mineral associations of the skarn and disseminated mineralisation types, were investigated. The results are presented in the Table 17. Most of the detected d^{34} S‰ values are similar. They are generally positive values that are close to 0‰ and are typical of porphyry-type mineralisation.

GEOCHEMICAL CHARACTERISTICS OF THE MINERALISED AREA

COLLECTION, PREPARATION, AND ANALYSES OF GEOCHEMICAL SAMPLES

As part of a Polish-American Maria Skłodowska-Curie Fund II project, conducted between 1992 and 1996 (Podemski and Chaffee, unpubl. report, 1996), 572 samples were collected from drill cores stored in the Polish Geological Institute archives. These samples were selected from boreholes located along the two sections crossing the Myszków mineralised area (Figs. 8–9). All these samples were collected at intervals of about 30 metres, from lithologically homogeneous, five--metre-long sections of core along the entire length of each hole. For each sample, the rock type as well as the alteration type and ore-related minerals were identified.

Of these 572 samples, 466 were collected from Vendian to Early Carboniferous-aged rocks from 7 boreholes (Pz-24, Pz-25, Pz-26, Pz-27, Pz-28, Pz-29, and Pz-32) located along line A–A' (Fig. 8), which is aligned across the axis of the Myszków deposit, and from the 6 boreholes (Pz-11, Pz-13, Pz-21, Pz-30, Pz-33, and Pz-37), located along line B–B' (Fig. 9), which is nearly perpendicular to A–A'. An additional

64 samples were collected from Triassic and Quaternary (post-mineralisation-aged) rocks.

Samples were also collected from Vendian to Early Carboniferous rocks from other boreholes (Pz-10, Pz-12, Pz-14, Pz-15, Pz-16, Pz-17, Pz-18, Pz-19, Pz-20, Pz-22, Pz-23, Pz-31, Pz-34, Pz-35, Pz-36, Pz-38, and Pz-40) located throughout the Myszków area (Fig. 7, except for hole Pz-10, which is located about 2 km south-east of holes Pz-13 and Pz-14, outside of the map area) at depths of about 300 and 700 m, respectively. These samples were collected to provide, on two levels, a more regional geochemical setting for the Myszków mineralisation in order to identify any lateral chemical zoning that might be related to previously reported mineralogical zoning (Ślósarz, 1985). Altogether 45 samples were collected for that purpose.

The samples were crushed to grains less than about 3 mm and then milled to produce material <0.06 mm in diameter. Chemical analyses were carried out in the Central Chemical Laboratory of the PGI in Warsaw and in the US Geological Survey Laboratory in Denver, Colorado, USA.

In the PGI Laboratory, samples were analysed for 37 variables. The content of 17 variables (Ag, Al, Au, Ca, Cu, Fe, K, Li, Mg, Mn, Mo, Na, Pb, Si, Ti, V, and Zn) were determined by atomic-absorption spectrometry; 16 variables (Be, Ce, Co, Cr, Cd, Ga, La, Nb, Nd, Ni, P, S, Sc, Th, Y, and Yb) by inductively-coupled plasma atomic-emission (ICP-AES) spectroscopy, after a total digestion; 3 variables (Ba, Sr, and W) by X-ray fluorescence; and F — using an ion-selective electrode (ISE).

In Denver, Colorado, the samples were analysed for 67 variables, including 50 elements analysed by ICP-AES, 11 by X-ray fluorescence, 4 (Au, Hg, Te, and Tl) by atomic-absorption spectrometry, and 2 by other techniques (W by photospectrometry and S by an ignition technique).

After removing data for variables with no reported values above the lower limit of determination for the variable, a total of 43 variables (Ag, Al, As, Au, Ba, Be, Bi, Ca, Cd, Ce, Co, Cr, Cu, Fe, Ga, Hg, K, La, Li, Mg, Mn, Mo, Na, Nb, Nd, Ni, P, Pb, S, Sb, Sc, Si, Sr, Te, Th, Ti, Tl, V, W, Y, Yb, Zn, and loss on ignition at 925°C) remained for further evaluation (Chaffee *et al*., 1999).

As, Bi, Sb, Te, Tl, and the loss on ignition (LOI) concentrations were determined only in the US Geological Survey Laboratory, whereas F was determined only in the PGI Laboratory. In general, the results obtained in both laboratories for most other variables were closely comparable.

Samples of the Triassic and Quaternary rocks were analysed to determine whether they contained the same suite of elements present in the Vendian to Early Carboniferous rocks. The results show that the suite of mineralisation-related elements in the Triassic rocks are distinctly different from the suite in the mineralised Vendian to Early Carboniferous rocks, indicating that the ore-related elements present in the Vendian to Early Carboniferous rocks did not migrate upward into the Triassic rocks. Therefore, the distributions of ore-related elements in the Triassic rocks are not related in any way to the mineralisation in the Myszków system.

However, anomalous concentrations of Cu (380 ppm) and Ag (1.2 ppm) were found in clastic fragments from basal conglomerates and sandstones of the Lower Buntsandstein (the lowest Triassic strata) that unconformably overlie the Vendian to Early Carboniferous basement. This locally anomalous Cu and Ag is probably derived from weathering of originally exposed, mineralised basement rocks.

Anomalous Pb (maximum 560 ppm), Zn (860 ppm), and Cd (6.50 ppm), were found in a few samples of Triassic dolomite and are thought to be associated with a Mississippi Valley Pb-Zn type mineralisation, which is very common in the Triassic carbonate formations of the Silesia–Kraków region.

STATISTICAL EVALUATION OF THE ANALYSES

Tables 18 and 19 summarise statistical information for the chemistry of 292 samples of felsic intrusive rocks and 174 samples of Vendian to Early Cambrian metasedimentary rocks, respectively. For each variable, the tables list the maximum and minimum values, the number and percentage of unqualified (uncensored) values, as well as geometric mean values and estimates of crustal abundances for Ca-rich granites (Table 18) and shale (Table 19). Abundance values for high-Ca granite were selected for comparison because these values best represent what is thought to be the pre-mineral deposit lithology for most of the intrusive rocks sampled. Abundance values for shale were selected as the closest sedimentary rock analogue to meta-siltstones.

The geometric mean values are based on unqualified values only. They provide typical values for the abundance for each element in each of the two main lithologies found in the Myszków area. For the elements As, Au, and Sb, the data were too highly censored (too few unqualified analyses) and, therefore, values were estimated after examining distributions of each element in the Myszków analytical data set.

The column of maximum values for the elements in each table indicates that, when compared with mean or abundance values, 29 elements (Ag, Al, As, Au, Ba, Be, Bi, Cd, Ce, Co, Cr, Cu, Fe, Hg, K, La, Li, Mn, Mo, Na, Ni, Pb, S, Sb, Sr, Te, Tl, W, and Zn) are clearly enriched in one or more samples, indicating that these elements may be associated in some way with formation of the Myszków mineralisation, if only very locally.

FACTOR ANALYSES

Factor analyses was performed on a data set with 466 samples and 43 variables that included both felsic igneous and metasedimentary rocks. For the 43 selected variables, values were substituted for all qualified determinations as follows: for

Table 18

Summary statistics for 292 samples of felsic intrusive rocks

Variable	Range of values		No. Unqual.	Percent Unqual.	Geometric mean	Ca-granite Abundance[4]
	Minimum	Maximum				
Ag[1]	N(0.067)	14	280	96	0.68	0.051
Al%	4.7	9.1	292	100	7.14	8.20
As[1]	N(0.67)	36	41	14	<1.0	1.9
Au[1]	N(0.002)	0.25	57	202	0.002	0.004
Ba	44	2100	292	100	580	420
Be	1.0	6.0	292	100	2.6	2
Bi[1]	N(0.67)	99	137	47	3.3	0.033
Ca%	0.42	2.9	292	100	1.30	2.53
Cd[1]	N(0.050)	16	255	87	0.28	0.13
Ce	19	140	292	100	40	47
Co	L(1.0)	91	291	99	4.9	7
Cr	3.0	800	292	100	8.3	22
Cu	18	9100	292	100	630	30
Fe%	0.71	4.80	292	100	1.58	2.96
Ga	11	21	292	100	17	17
Hg	N(0.02)	0.43	125	432	0.037	0.08
K%	1.40	5.20	292	100	3.52	2.52
La	11	89	292	100	24	45
Li	5.0	110	292	100	22	24
LOI 925	0.36	5.08	292	100	1.16	–
Mg%	0.23	2.10	292	100	0.50	0.94
Mn	88	1900	292	100	280	540
Mo	L(2.0)	2900	287	98	140	1.0
Na%	0.86	5.3	292	100	2.25	2.84
Nb	L(4.0)	21	275	94	9.3	20
Nd	8.0	58	292	100	17	33
Ni	L(2.0)	370	263	90	5.5	15
P%	0.03	0.16	292	100	0.052	0.092
Pb	L(4.0)	2600	291	99	33	15
S%	L(0.05)	2.5	287	98[3]	0.35	0.03
Sb[1]	N(0.67)	150	89	30	<1.0	0.2
Sc	2.0	18	292	100	4.5	14
Si%	26.6	36.7	292	100	32.9	31.4
Sr	130	9600	292	100	320	440
Te[1]	N(0.05)	5.0	177	612	0.18	0.02
Th	L(4.0)	13	291	99	8.4	8.5
Ti%	0.13	0.61	292	100	0.21	0.34
Tl	0.30	60	289	99[2]	0.72	0.72
V	20	130	292	100	34	88
W	N(10)	1500	288	99[2]	90	1.3
Y	7.0	20	292	100	10	35
Yb	L(1.0)	2.0	167	57	1.1	3.5
Zn	9.0	1100	292	100	53	60

[1] Element has more than one lower limit of determination. Lowest value shown.
[2] Only 289 samples analysed for Au, Hg, Te, Tl, and W.
[3] Only 290 samples analysed for S.
[4] Values for Bi (Santoliquido and Ehmann, 1972), Ce (Taylor, 1969), and Te (Beaty and Manuel, 1973) are for granodiorite. All other values are from Turekian and Wedepohl (1961) for high calcium granites.

All values in parts per million (ppm) unless '%' is shown after variable symbol. For qualified analyses, 'L' = element detected but in a concentration less than the lower limit of determination shown, and 'N' = element not detected at the lower limit of determination shown. Except for As and Sb, mean values based on unqualified values only. '–'= no meaningful value. Bolded variable symbol indicates probable enrichment of variable in study area.

Table 19

Summary statistics for 174 samples of metasedimentary rocks

Variable	Range of values		No. Unqual.	Percent Unqual.	Geometric mean	Shale Abundance[2]
	Minimum	Maximum				
Ag[1]	N(0.067)	7.8	162	93	0.47	0.07
Al%	4.9	10	174	100	8.13	8.00
As[1]	N(0.67)	69	48	28	<1.0	0.5
Au[1]	N(0.002)	0.01	22	13	0.002	0.004
Ba	38	1200	174	100	460	580
Be	1.0	13	174	100	3.1	3
Bi[1]	N(0.67)	290	83	48	3.9	0.5
Ca%	0.28	3.7	174	100	0.81	2.21
Cd[1]	N(0.050)	7.1	147	84	0.26	0.3
Ce	40	100	174	100	64	59
Co	8.0	60	174	100	16	19
Cr	8.0	140	174	100	59	90
Cu	14	8000	174	100	330	45
Fe%	2.10	6.40	174	100	4.00	4.72
Ga	12	26	174	100	20	19
Hg	N(0.02)	0.24	72	42	0.052	0.4
K%	2.20	6.80	174	100	3.65	2.66
La	22	54	174	100	34	39
Li	22	120	174	100	50	66
LOI925	0.39	6.69	174	100	1.67	–
Mg%	0.91	3.00	174	100	1.54	1.50
Mn	200	2100	174	100	720	850
Mo	L(2.0)	1500	148	85	110	2.6
Na%	0.12	3.00	174	100	1.82	0.96
Nb	L(4.0)	24	170	98	14	11
Nd	20	48	174	100	31	24
Ni	13	190	174	100	32	68
P%	0.03	0.25	174	100	0.070	0.07
Pb	L(4.0)	760	173	99	25	20
S%	L(0.05)	3.5	171	98	0.32	0.24
Sb[1]	N(0.67)	12	38	22	<1.0	1.5
Sc	8.0	22	174	100	17	13
Si%	26.2	33.5	174	100	29.5	–
Sr	57	2100	174	100	130	300
Te[1]	N(0.05)	70	113	65	0.31	0.05
Th	6.0	24	174	100	9.9	12
Ti%	0.30	0.70	174	100	0.49	0.46
Tl	0.35	2	174	100	1.0	0.3
V	53	150	174	100	100	130
W	N(10)	460	169	97	35	1.8
Y	9.0	27	174	100	16	26
Yb	L(1.0)	3.0	165	95	1.8	2.6
Zn	24	980	174	100	91	95

[1] Element has more than one lower limit of determination. Lowest value shown.

[2] Values for As, Bi, and Te are estimates based on analyses of unaltered samples of meta-siltstone from the study area. Correct values are probably lower than estimates shown. Value for La is average of four shale values listed in Wedepohl (1978). All other values are from Turekian and Wedepohl (1961).

All values in parts per million (ppm) unless '%' is shown after variable symbol. For qualified analyses, 'L' = element detected but in a concentration less than the lower limit of determination shown, and 'N' = element not detected at the lower limit of determination shown. Except for As and Sb, mean values based on unqualified values only. '–' = no meaningful value. Bolded variable symbol indicates probable enrichment of variable in study area.

samples qualified with the letter "N" (Tables 18 and 19), a value equal to half the lower limit of determination shown in parentheses was substituted for each variable; for values qualified with the letter "L", a value equal to 0.7 times the lower limit of determination shown in parentheses was substituted. Because most of the variables displayed log-normal distributions, the data were log-transformed prior to running the factor analyses. Fluorine concentrations were not included in the factor analyses.

A 6-factor model with varimax rotation was selected as best fitting observed geologic conditions. This model accounts for 72 percent of the variance in the data. Table 20 summarises the factor loadings obtained for this model.

Factor 1 is the main lithologic factor and shows positive loadings for 21 of the 43 variables evaluated. The elements listed for factor 1 are most closely associated with chemical differences associated with contrasting rock types. The highest concentrations for these elements are associated closely with the distributions of metasedimentary rocks and the lowest concentrations are closely associated with the distributions of the granitoid and porphyries.

The negative loadings for Si and Sr on this factor indicate a reversal of the overall concentration levels by rock type, with these two elements having relatively lower overall concentrations in the metasedimentary rocks and relatively higher overall concentrations in the granitoids and porphyries.

Factor 2 is a major sulphide mineralisation factor that includes variables associated with at least one stage of chalcopyrite deposition. Variables in this factor are associated with high temperature stages of mineralisation. Loss on ignition (LOI) generally measures the percent of volatile materials that are lost from the sample when heated to 925° C.

At Myszków, a high value for LOI generally indicates a loss of CO_2 from carbonate-rich rocks or a loss of S from one or more sulphide minerals. A positive loading value for LOI thus suggests that carbonate minerals are locally associated with the Cu sulphide-rich veins. Petrographic studies confirm this relationship for stage 4 veins (Chaffee *et al*., 1994, 1999; Ślósarz, 1993). The negative loading for Ba suggests a loss (redistribution) of this element during formation of this stage (or of several stages) of mineralisation.

Factor 3 includes variables related to potassic metasomatism associated with hydrothermal alteration of the intrusive and wall rocks. The positive loading of K and negative loadings for Sr, Ca, and Na indicate the loss of these last three elements at the expense of added K. This exchange generally occurs when plagioclase feldspar is altered to orthoclase feldspar, sericite (white mica), and(or) biotite.

Table 20

Factor loading values for 43 variables in samples from the Myszków area.
Six-factor model, varimax loading. Elements in parentheses ( ) indicate secondary loading values.

Factor 1	*Factor 2*	*Factor 3*	*Factor 4*	*Factor 5*	*Factor 6*
Nd 0.94 Ti 0.92 Sc 0.92 Ce 0.91 V 0.90 Mg 0.90 Fe 0.89 La 0.86 Cr 0.81 Co 0.81 Al 0.81 Ga 0.80 Y 0.79 Ni 0.77 Li 0.73 P 0.70 Yb 0.66 Th 0.65 Mn 0.64 Nb 0.59 Tl 0.40 ——— Sr –0.60 Si –0.90	S 0.80 Bi 0.75 Te 0.69 Ag 0.69 Cu 0.60 As 0.52 (LOI 0.48) ——— Ba –0.61	K 0.46 ——— Sr –0.54 Ca –0.66 Na –0.70	Pb 0.85 Cd 0.79 Zn 0.69 Sb 0.62 (As 0.47) (Hg 0.47) (Mn 0.42)	LOI 0.58 ——— Cu –0.47 Mo –0.63 Be –0.66 W –0.67	Hg 0.51 Au 0.46 ——— K –0.61
Percent variability explained					
39%	11%	8%	7%	4%	3%

Factor 4 includes base metal-sulphide-associated elements common to a stage of mineralisation associated with skarn-type, peripheral sulphide minerals (mainly sphalerite and galena). Although mainly associated with the stage 3 veins of Ślósarz (1993), the elements included in Factor 4 are not closely associated, spatially, with the stage of mineralisation represented by the Cu sulphide suite in Factor 2. They may represent relatively low-temperature stages of mineralisation.

Factor 5 is another major mineral deposit-related suite that includes LOI, Cu, W, Mo, and Be. The variables are closely associated with the distribution of the felsic igneous rocks. Factor 5 may represent another high temperature stage of mineralisation. The negative loadings of Cu, W, Mo, and Be on a factor with positive loadings for LOI suggest that carbonate minerals are not a significant component of this stage of mineral deposition. The Stage 3 veins described by Ślósarz (1993), which are also not closely associated with carbonate minerals, may correspond to the mineralisation represented by Factor 5.

This classification of Cu-related variables into at least two factors suggests that each suite may have been deposited during a different mineralising event. This observation corroborates the petrographic and visual studies of the core at Myszków (Chaffee *et al*., 1994; Ślósarz, 1993).

Factor 6 includes elements of largely undefined affinity and consists of positive loadings for Au and Hg and a negative loading for K. The isolation of these first two elements into a separate factor emphasises (1) that they may not be significantly associated with any of the four possible stages of mineralisation related to Factors 2 through 5 and (2) the generally low values and limited range of values for these two elements and the high percentage of qualified samples for each (Tables 18 and 19). The loadings on this factor suggest that Au and Hg concentrations are highest where K-metasomatism is weak or non-existent. Gold and Hg may also be associated with one of the relatively low-temperature stages of mineralisation.

DISCUSSION OF VARIABLES RELATED TO THE MYSZKÓW MINERALISATION

Table 21 summarises data for the variables that are positively loaded on Factors 2 to 6, factors that are all related to mineralisation. Enrichment factor values, which are a ratio of the geometric mean value for each variable (column A) to its crustal abundance (column B), are also shown. By examining

Table 21

Summary statistics for mineralisation-related variables in 466 samples of core

Variable	Range of values		No. Unqual.	Percent Unqual.	**A** geometr. mean	**B** Crustal Abund.	**A/B** Enrich. factor
	Minimum	Maximum					
Ag[1]	N(0.067)	14	442	95	0.59	0.05	12
As[1]	N(0.67)	69	89	19	<1.0[4]	1.5	<0.67[4]
Au[1]	N(0.002)	0.248	79	17[2]	<0.002[4]	0.0018	<1.0[4]
Be	1.0	13	466	100	2.7	3.0	0.9
Bi[1]	N(0.67)	290	220	47	3.5	0.13	27
Cd[1]	N(0.50)	16	402	86	0.27	0.098	2.8
Cu	14	9100	466	100	500	25	20
Hg	N(0.02)	0.43	197	43[2]	0.04	0.08	0.5
K%	1.40	6.80	466	100	3.57	2.80	1.3
LOI 925	0.36	6.69	466	100	1.33	–	–
Mn	88	2100	466	100	400	600	0.67
Mo	L(2.0)	2900	435	93	130	1.5	87
Pb	L(4.0)	2600	464	99	29	20	1.5
S	L(0.05)	3.52	458	99[3]	0.34	0.026	13
Sb[1]	N(0.67)	150	127	27	<1.0[4]	0.2	<5[4]
Te[1]	N(0.05)	70	290	63[2]	0.22	0.002	110
W	N(10)	1500	457	99[2]	64	2.0	32
Zn	9.0	1100	466	100	65	71	0.92

[1] Element has more than one lower limit of determination. Lowest value shown.
[2] Only 463 samples analysed for Au, Hg, Te, and W.
[3] Only 464 samples analysed for S.
[4] Value estimated because of low percentage of unqualified values.
[5] Hg and S values from Taylor (1964). Te value from Coakley (1975). All other values from Taylor and McLennan (1995) for the upper continental crust.
All values in parts per million (ppm) unless '%' is shown after variable symbol. For qualified analyses, 'L '= element detected but in a concentration less than the lower limit of determination shown, and 'N' = element not detected at the lower limit of determination shown. Except for As and Sb, mean values based on unqualified values only. '–'= no meaningful value. Bolded variable symbol indicates probable enrichment of variable in study area.

these ratios, one can determine the relative degree to which the variables have been added to the overall Myszków area during formation of the Myszków mineralisation.

Variables with enrichment factors >1 include, in order of enrichment value, Te, Mo, W, Bi, Cu, S, Ag, Cd, Pb, K, and probably Sb. The first seven of these variables (Te through Ag) have been added to the system in significant amounts. The last four (Cd through Sb) have been added but in much less significant amounts, suggesting that most of these last four elements have been only locally enriched as a result of remobilization during alteration of the host rocks and deposition of the Myszków mineralisation.

With the exception of Te, all of the variables with enrichment factor values >1 have values in Table 21 that fall between similar values calculated (but not shown) for these same variables segregated by rock type in Tables 18 and 19. For Te the value is 9 for Ca-rich granite and about 6 for shale. In the case of Te, the crustal abundance estimate of 0.002 is probably too low, perhaps by about an order of magnitude.

The remaining variables in Table 21 (As, Au, Be, Hg, Mn, and Zn), although shown by factor analyses to be associated with the Myszków mineralisation, have enrichment factors <1, and thus have not been significantly added to the mineralised area. Their association with the mineralisation is, therefore, probably a result of remobilization within the system to form local concentrations.

DISTRIBUTIONS OF SELECTED VARIABLES ON CROSS-SECTIONS

The figures that follow show the distributions of variables related to lithologies, hydrothermal alteration, and(or) the mineral deposits at Myszków. The variables are grouped according to their associations in the six factors determined in the factor analyses.

Many of the mineralisation-related variables are anomalous relative to estimated regional background values for distances greater than the outer limits of the study area. Queries (?) on the sections indicate areas where anomalies are not adequately defined.

FACTOR 1 — ELEMENTS RELATED TO LITHOLOGY

Neodymium and titanium. Figures 29 and 30 outline the distributions on the two geologic cross-sections of relatively low concentrations of Nd, the most strongly loaded element on Factor 1. The distribution of low Nd concentrations (<23 ppm) correlates very closely with the distribution of intrusive rocks. The distributions of Ti are almost identical to those of Nd. The consistently low concentrations of these two elements in virtually all samples of intrusive rocks strongly suggests a common magmatic parentage. High concentrations of both elements generally identify metasedimentary rocks.

Titanium is most highly enriched locally in many of the wall rock samples collected in the immediate vicinity of intrusive-wall rock contacts. These high concentrations probably indicate enrichment of Ti in skarn zones. The same local enrichment is not apparent for Nd.

Silicon and strontium, both negatively loaded on Factor 1, are additional elements whose distributions are predominantly related to lithology. However, in contrast to Nd and Ti, the highest concentrations of Si (Figs. 29, 30) and Sr are found in the intrusive rocks.

The distribution of anomalous Si shows a distinct zoning within the main intrusion. This zoning is thought to represent a combination of (1) Si in various rock-forming and alteration-associated silicate minerals and (2) Si added as quartz in veins and as amorphous silica flooding into the matrix adjacent to these veins. This zoning may also be a result of an increasing amount of non- or low-Si mineral impurities in the intrusion as its contact with the adjacent wall rocks is approached.

This Si zoning is not well developed in the intrusive unit in the upper right part of section B–B', suggesting that Si added during alteration and mineralisation (category 2, above) was not a strong factor in this intrusive unit.

Strontium is loaded on two factors and is discussed in detail with Ca, under Factor 3, below.

FACTOR 2 — ELEMENTS RELATED TO MAJOR SULPHIDE MINERALISATION

Total sulphur is strongly loaded on Factor 2. Some secondary sulphate minerals (mainly barite) have been identified in the Myszków mineralisation. However, most of S represents sulphide minerals. Anomalous S (>0.39%) is widely distributed throughout the two sections. The areas of highest S concentrations (>0.80% S) are found mostly in the contact zones associated with the intrusive porphyries and mostly in the upper levels of the Myszków system.

Neither the distribution of pyrite observed in core samples (a major source of the S at Myszków) nor the distribution of total S reveals the presence of a pyrite-related halo spatially associated with anomalous Cu or Mo.

Bismuth, primarily a chalcophyllic element, is strongly loaded on Factor 2, suggesting that it is mostly tied up in sulphide minerals, probably pyrite and chalcopyrite, but also in bismuthinite (Chaffee *et al*., 1999). Bismuth data in Ahrens and Erlank (1978) suggest that Bi is somewhat more abundant in chalcopyrite than in pyrite.

In many mineral deposits trace Bi may also be found in galena or in one of several other, relatively rare Bi minerals, such as native Bi, which was identified in thin sections of core from the Myszków area (Chaffee *et al*., 1999). However, galena is not an abundant mineral at Myszków. Note also that Bi and Pb are not loaded on the same factor (Table 20). The distribution of anomalous Bi (10 ppm; Figs. 31, 32) is similar to that of S, especially on section A–A'.

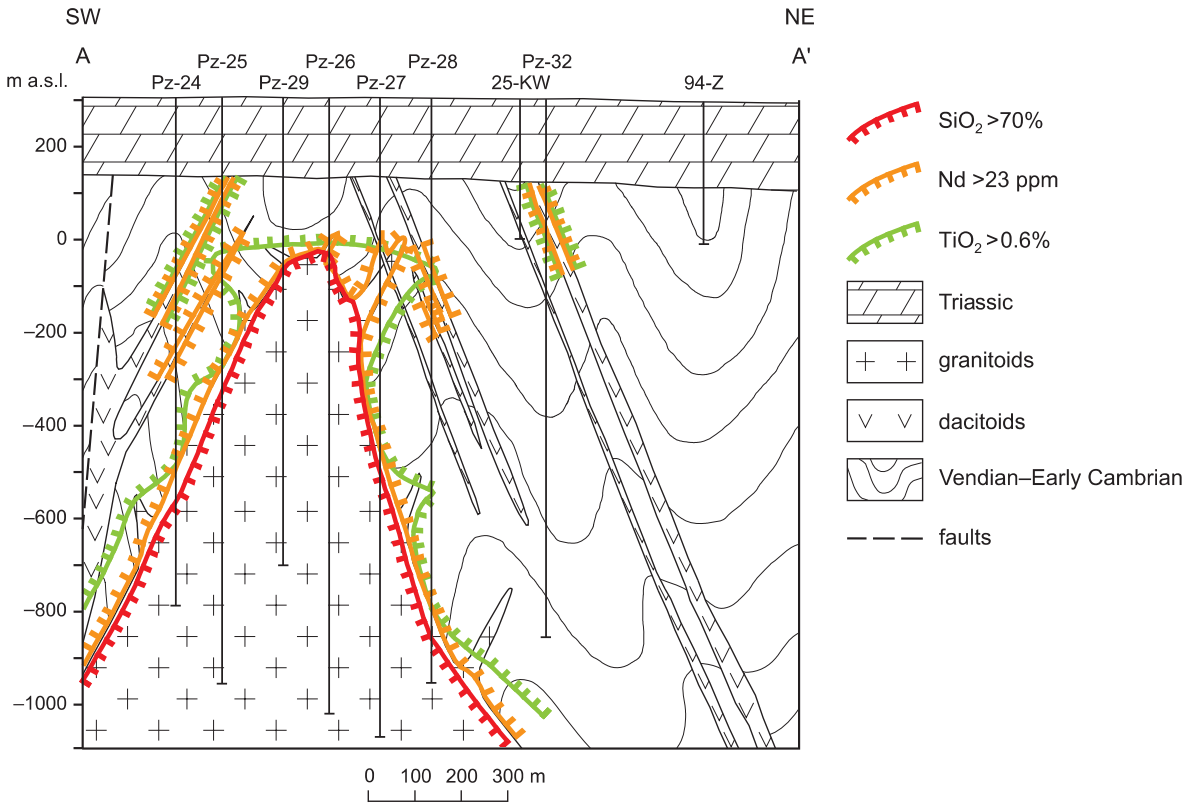

Fig. 29. Geochemical cross-section A–A': elements related to lithology

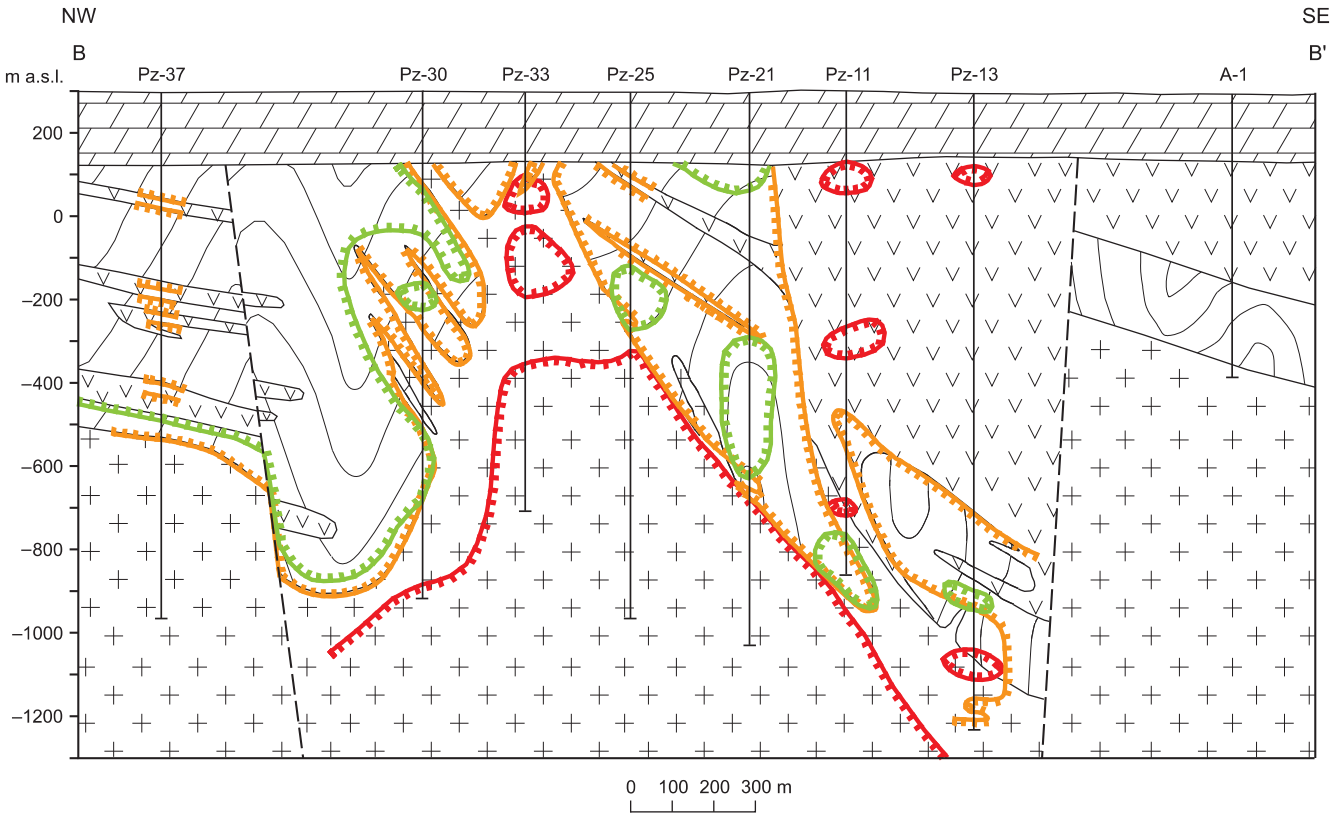

Fig. 30. Geochemical cross-section B–B': elements related to lithology

For explanations see Figure 29

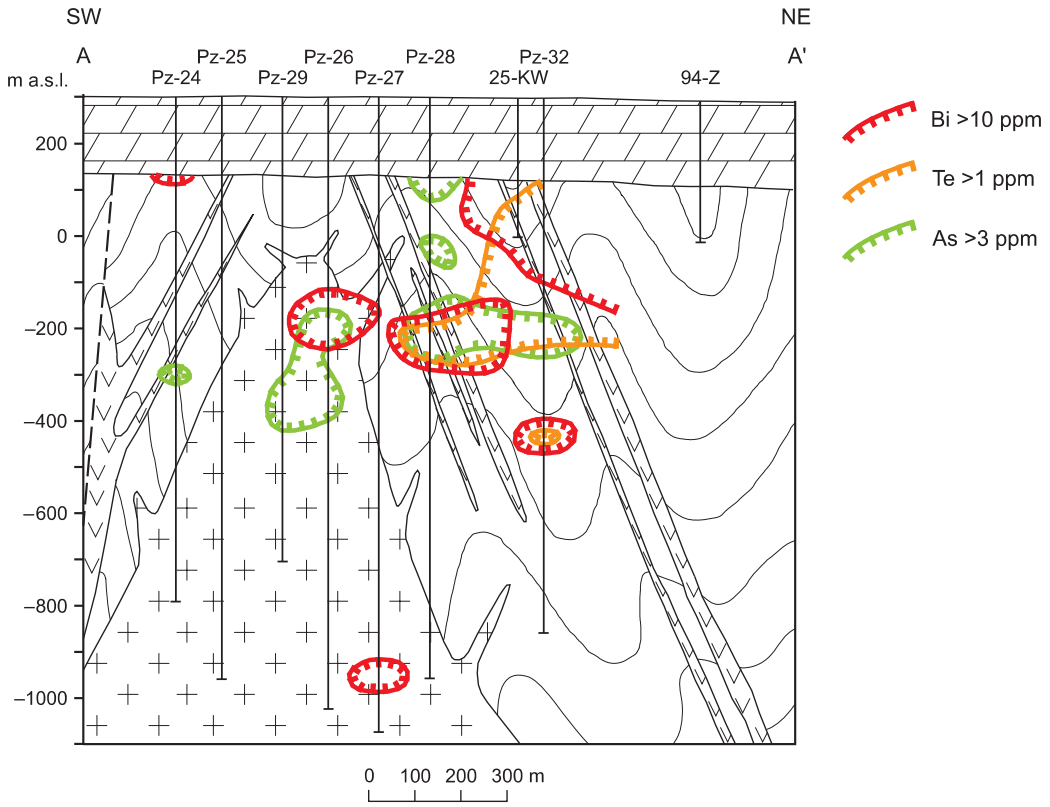

Fig. 31. Geochemical cross-section A–A`: elements related to major sulphide mineralisation

For explanations of geology see Figure 29

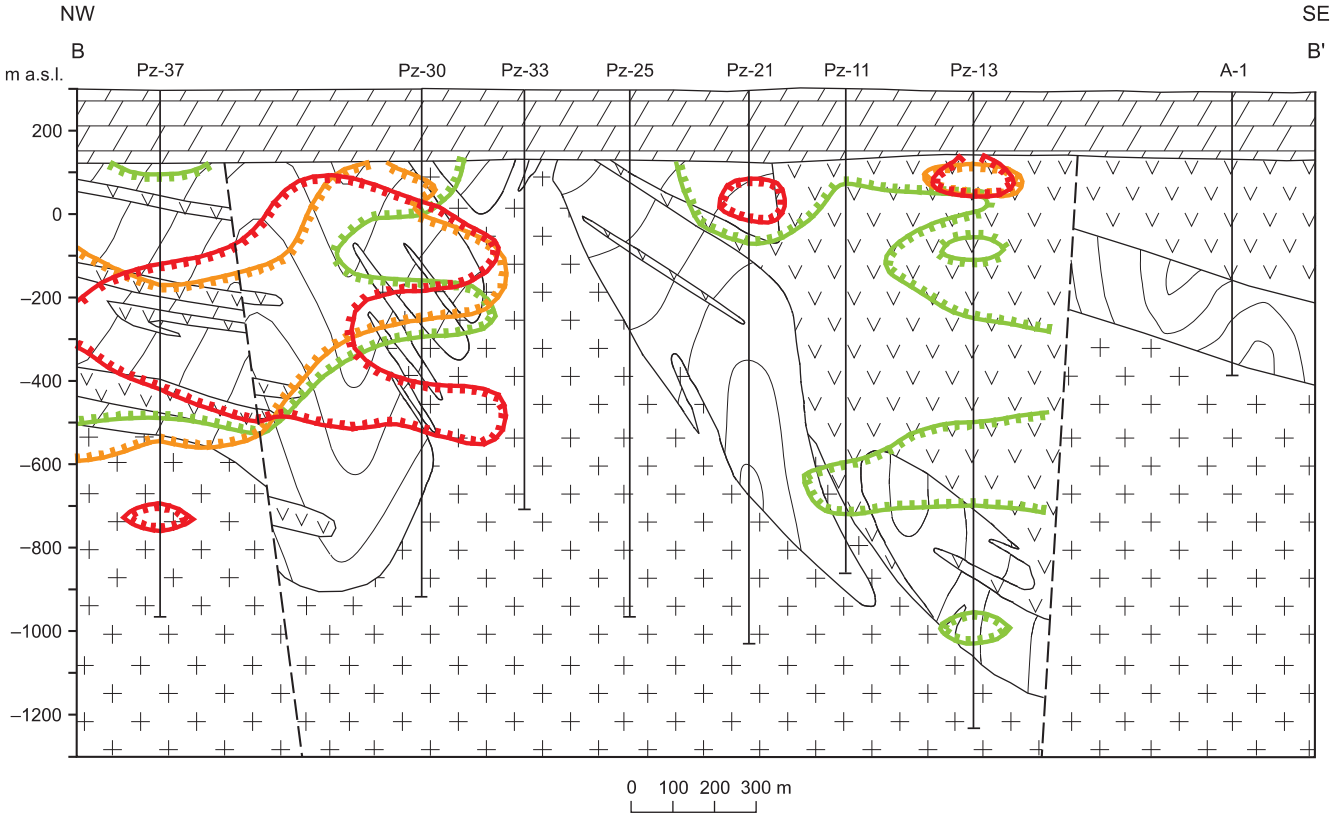

Fig. 32. Geochemical cross-section B–B`: elements related to major sulphide mineralisation

For explanations see Figure 31

Copper is primarily loaded on Factor 2 and is secondarily loaded on Factor 5, suggesting at least two stages of Cu mineralisation. A major Cu (primarily chalcopyrite) anomaly constitutes the Myszków mineralisation. Nearly all of the areas represented by the two sections are anomalous (>100 ppm) for Cu. Copper anomalies (>1500 ppm Cu) are generally spatially associated with the upper parts of the intrusive rocks (Figs. 33, 34). These anomalies locally extend into the metasedimentary host rocks as well. The highest Cu concentrations are mostly found in the upper parts of the areas of both sections.

Silver is another element loaded on Factor 2. The distribution of anomalous Ag (0.80 ppm) is similar to that of Cu, indicating a close association of the two elements. Most Ag is probably hosted in chalcopyrite.

Tellurium, which is also strongly loaded on Factor 2, tends to substitute for S in sulphide minerals. The distributions of anomalous Te (>1 ppm; Figs. 31, 32) are roughly similar to those of S. Like S, Te is mostly concentrated in the upper levels of the Myszków system.

Data in Leutwein (1978) suggest that chalcopyrite and pyrite are the most common hosts for Te. Because it is spatially closer to the distribution of anomalous S than to that of Cu, anomalous Te is probably hosted in tellurides and sulphide minerals other than just chalcopyrite — most likely pyrite, as observed elsewhere.

Barium is strongly negatively loaded on Factor 2. Barite ($BaSO_4$), a common Ba mineral, has been identified at Myszków elsewhere. Barium is also commonly found in trace to minor amounts in K-rich feldspars and less commonly in Ca-rich plagioclase feldspars and in micas (Puchelt, 1978). However, the mean and crustal values for Ba in Tables 18 and 19 indicate that this element has not been significantly added to, or removed from, the Myszków system. At Myszków, anomalous Ba (>650 ppm) is not spatially associated with either K or Ca alone, but may be associated with a combination of the two. The negative loading of Ba on factor 2 and the distributions of Ba on the sections suggest that the introduction of sulphide minerals has resulted in depletion of Ba in areas of significant sulphide deposition.

FACTOR 3 — ELEMENTS RELATED TO POTASSIC METASOMATISM

Potassium is the only element with a significant positive loading value on Factor 3. It also exhibits a strong negative loading on Factor 6. Like Si, K concentrations are a combination from at least two different time periods (Chaffee *et al*., 1994; Ślósarz, 1993). Primary (early) K was present in rock-forming silicate minerals such as orthoclase and biotite. Secondary (later) K was then added during various stages of mineral deposit formation as orthoclase or white mica (sericite) in quartz veins and in zones flooding outward from the veins.

These veins cut both the intrusive rocks and the metasedimentary wall rocks. Late-stage, K-rich, mineralisation-related biotite and white mica are present locally in the intrusive rocks. These observations are reflected in the distribution of anomalous K, which is found in both major units (Figs. 35, 36).

Overall, K concentrations tend to decrease in the intrusion with depth. This observation corroborates the change in intrusive-rock type with depth. Potassium concentrations are relatively high in the uppermost parts of both sections, suggesting a much wider aureole of potassium may have existed in the area in pre-Triassic-aged rocks that were subsequently eroded before deposition of the Triassic sedimentary rocks.

Sodium, which is negatively loaded on the K-metasomatism factor, is present at Myszków mostly in feldspar minerals. Overall, this element is more concentrated in the intrusive rocks than in the metasedimentary rocks (Tables 18, 19). The factor loadings and the distributions of anomalous sodium (Figs. 35, 36) indicate that the overall concentration of Na is commonly lower where K is enriched. This distribution pattern would result from K replacing Na in feldspars during hydrothermal alteration of the Myszków area.

Calcium and strontium are also negatively loaded on Factor 3. In addition, Sr is negatively loaded on Factor 1. Sr commonly substitutes for Ca in its minerals. At Myszków, these two elements are present mostly in feldspar minerals but may also occur locally in carbonate minerals, such as calcite and ankerite.

The distributions of anomalous Ca (>2% CaO; Figs. 35, 36) and Sr are similar to each other but quite different from those of K and Na. Their negative loadings on the K factor suggest that these two elements have been somewhat depleted at the expense of K additions.

FACTOR 4 — ELEMENTS RELATED TO BASE-METAL MINERALISATION

Lead is the most strongly loaded element on Factor 4. Total Pb concentrations consist of Pb present in feldspars (minor) and Pb in the sulphide mineral, galena (major). Pb concentrations greater than about 50 ppm are associated with galena and not with feldspars. The distribution of anomalous Pb (>50 ppm; Figs. 37, 38) shows a distinct difference in overall concentration levels between the two sections, with Pb exhibiting much higher concentrations in section B–B'. This difference can also be seen in the distributions of Pb in the 300 and 700-m levels described later.

Most of the high Pb concentrations occur near the contact zone between the central intrusion and the metasedimentary wall rocks. However, Pb is also anomalous in the intrusion found in the upper right part of section B–B', in an area also anomalous for the sulphide mineralisation-related element suite in Factor 2. Thus, the overall distribution of Pb (and the rest of the variables loaded on this factor) would suggest enrichment in the contact metasomatic zones as well as in some fracture controlled zones in intrusive rocks.

Zinc is also strongly loaded on Factor 4. Total Zn concentrations are composed of a minor rock-forming mineral compo-

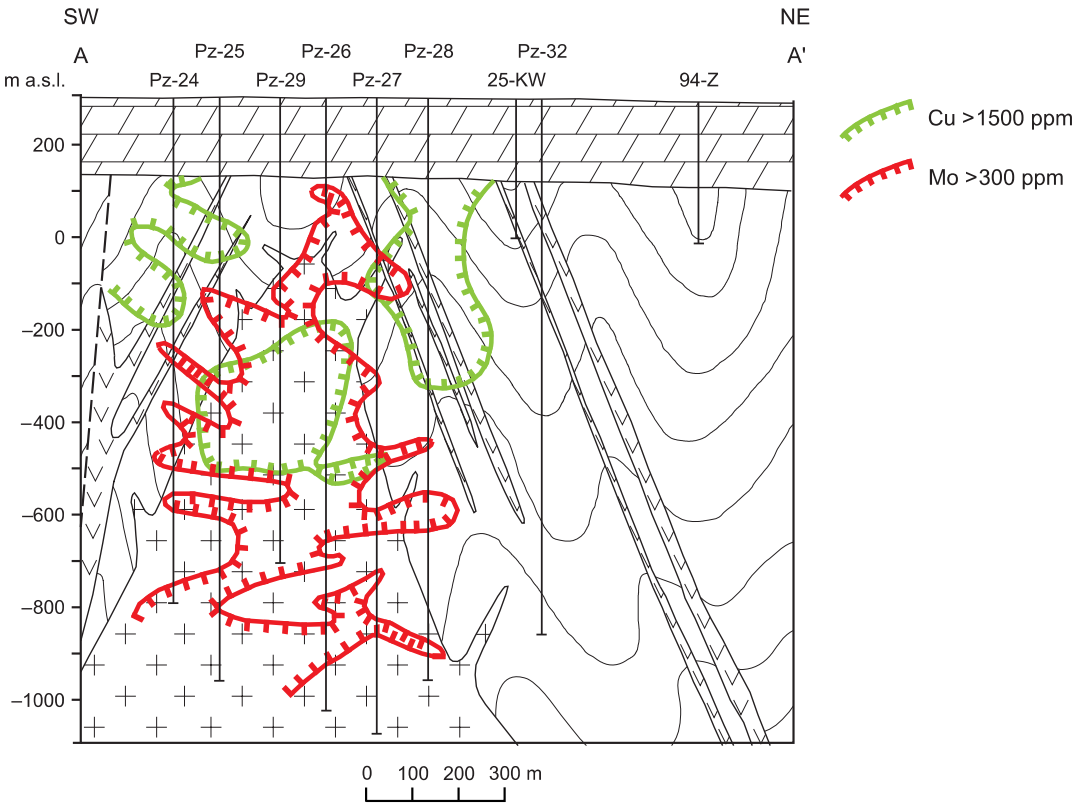

Fig. 33. Geochemical cross-section A–A`: elements related to major sulphide mineralisation

For explanations of geology see Figure 29

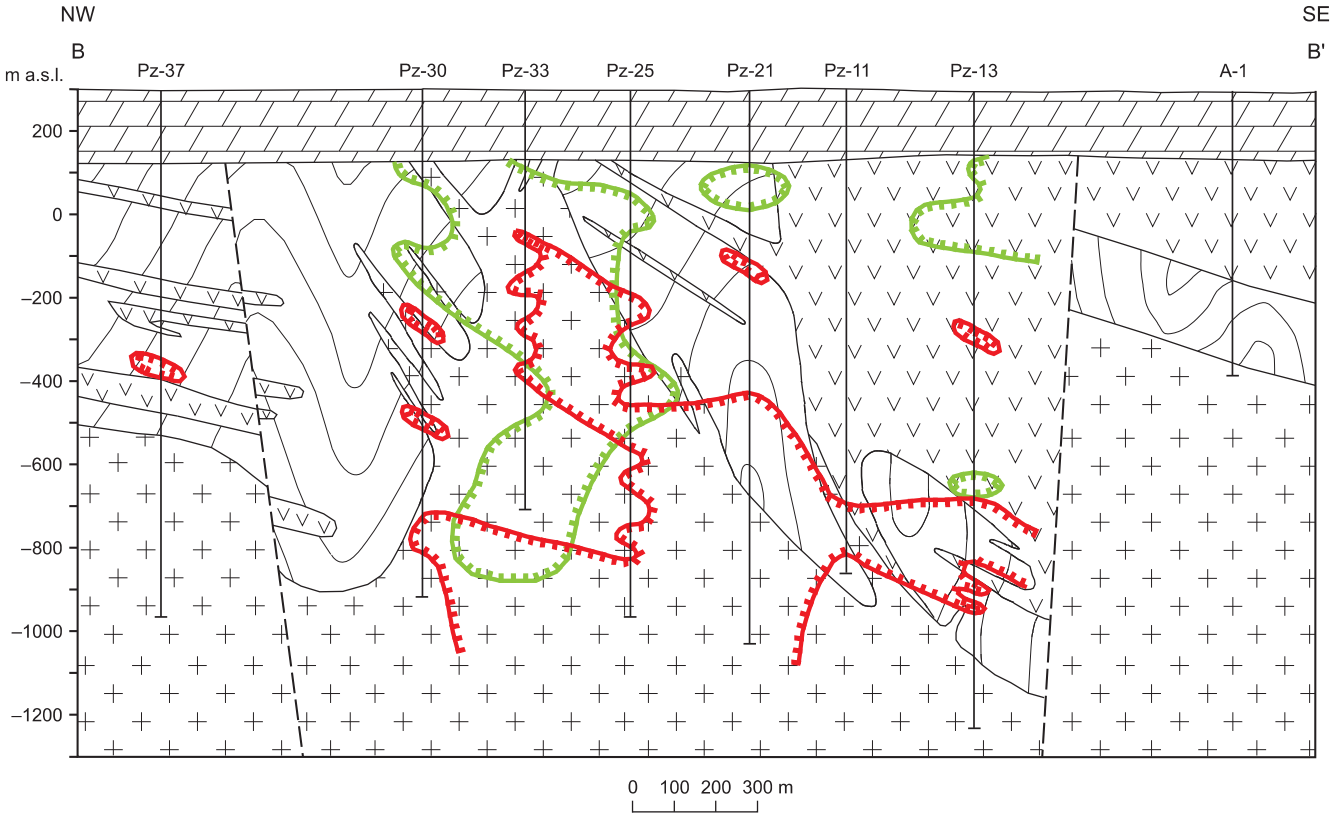

Fig. 34. Geochemical cross-section B–B`: elements related to major sulphide mineralisation

For explanations see Figure 33

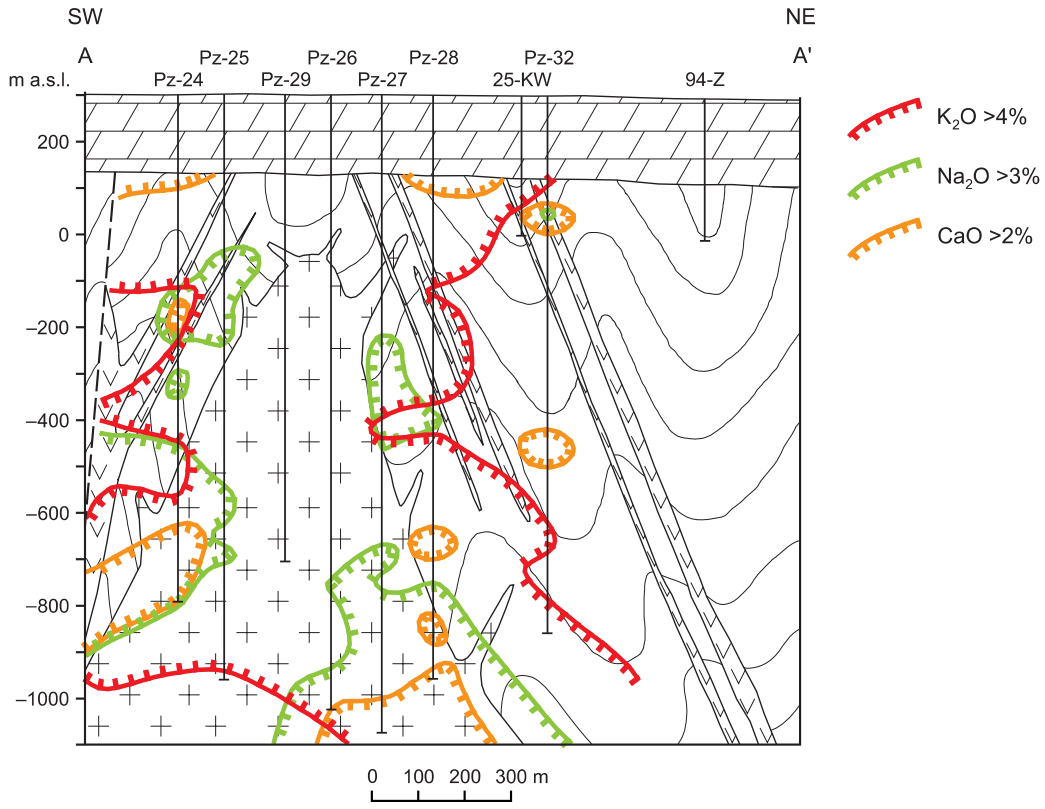

Fig. 35. Geochemical cross-section A–A`: elements related to rock alteration processes

For explanations of geology see Figure 29

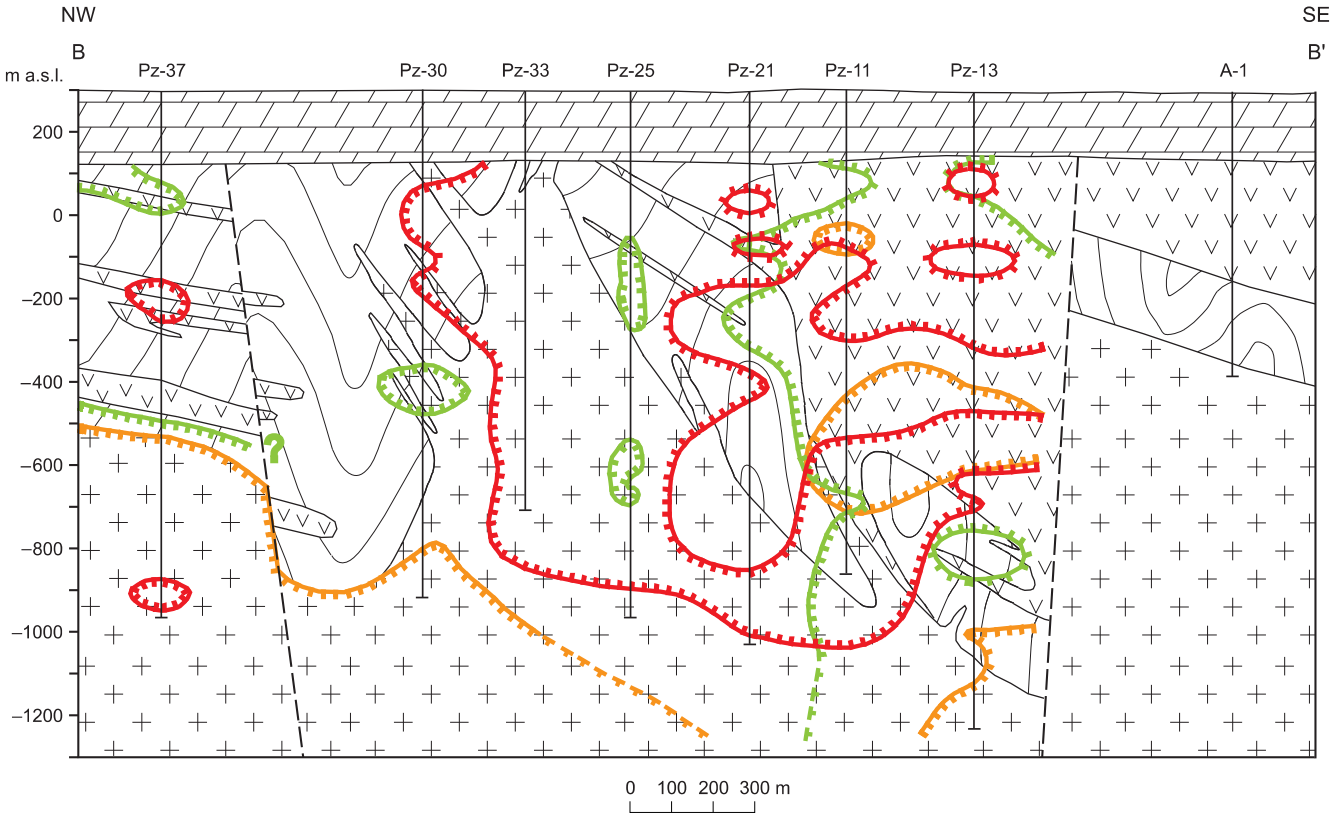

Fig. 36. Geochemical cross-section B–B`: elements related to rock alteration processes

For explanations see Figure 35

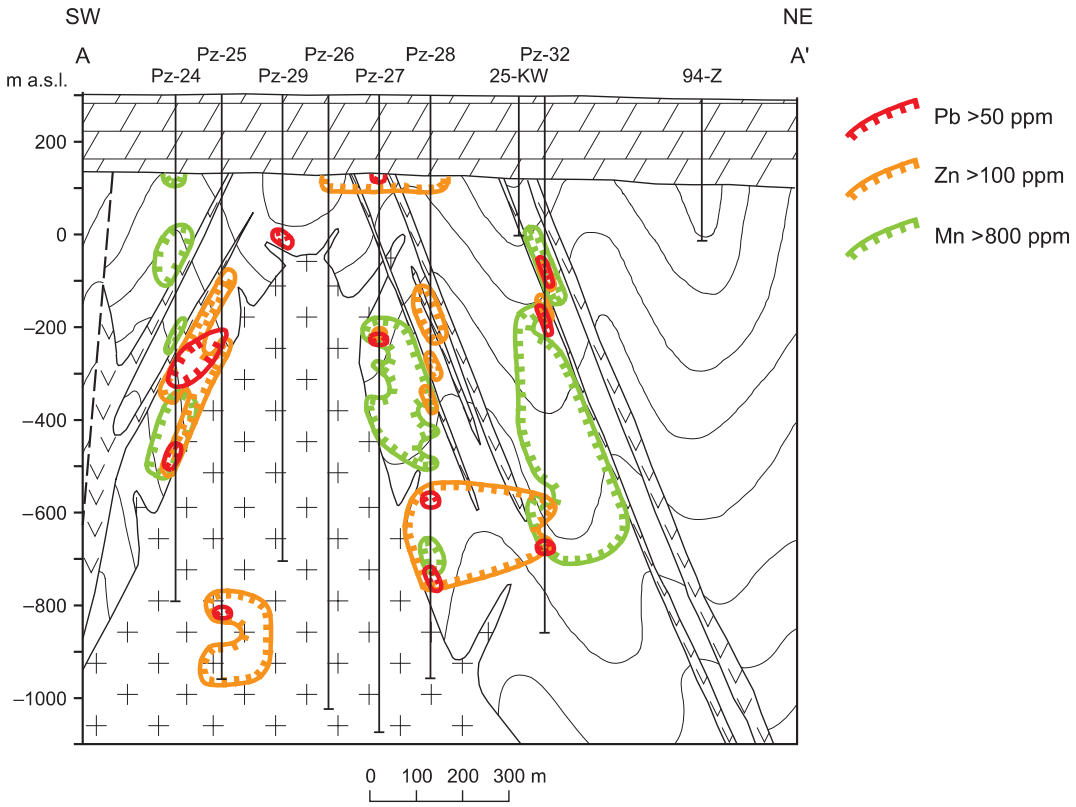

Fig. 37. Geochemical cross-section A–A`: elements related to base-metal mineralisation

For explanations of geology see Figure 29

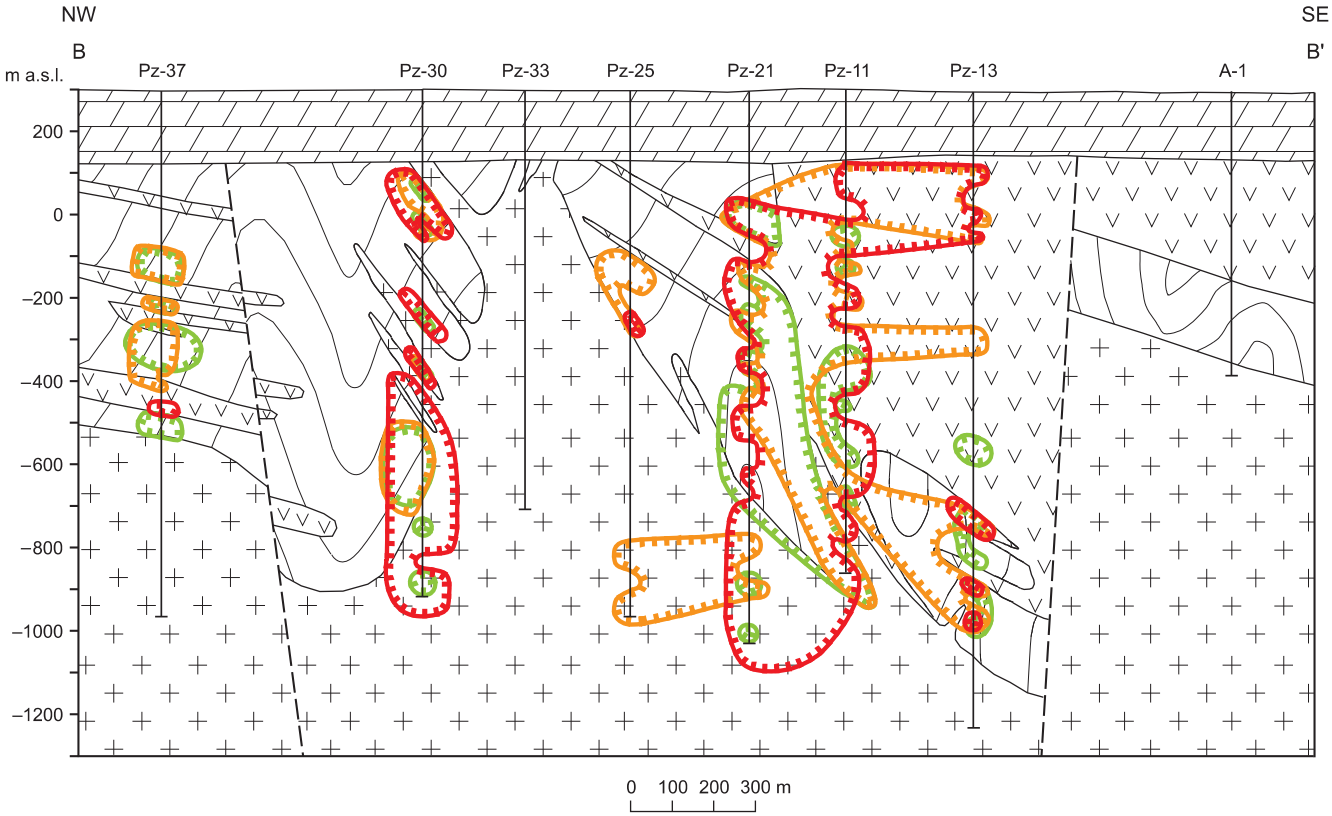

Fig. 38. Geochemical cross-section B–B`: elements related to base-metal mineralisation

For explanations see Figure 37

nent (mainly magnetite and other accessory minerals) and a major, sulphide-mineral component (mainly sphalerite). Zinc concentrations greater than about 100 ppm are related to a mineralisation stage. The distribution of anomalous Zn (>100 ppm; Figs. 37, 38) is roughly similar to the distribution of anomalous Pb. Zinc is most anomalous in the contact zones between the central granitoid intrusion and the wall rocks, as well as in the intrusion in the upper right part of section B–B', emphasising the close association of these two elements in a sulphide-mineral stage of deposition at Myszków.

Cadmium is another element loaded on Factor 4. This element is associated with Zn and substitutes in Zn minerals rather than forming its own minerals. The distributions of Cd at Myszków are similar to those of Zn.

Manganese is primarily loaded on Factor 1 (Table 20) but has a secondary loading on Factor 4, indicating a strong lithology component but also a mineralisation-related component. The relatively low concentration range of Mn (Table 21) indicates that it is not present in discrete Mn minerals but instead occurs as a trace constituent, either in rock-forming minerals (major source), such as feldspars, magnetite, ilmenite, hornblende, and biotite, or in mineral deposit-associated minerals (minor source), such as sphalerite (mainly), but also possibly in Ca- and Mg-rich carbonate minerals and(or) garnet family minerals (less important; Wedepohl, 1978).

The enrichment value (0.67) indicates that Mn has not been added to the system during mineralisation in the district. Spatial distributions, however, indicate that it has been locally remobilized during one or more stages of sulphide-mineral deposition. Anomalous Mn (>800 ppm) concentrations are generally found in the metasedimentary wall rocks near the contact zone between the intrusion and the wall rocks (Figs. 37, 38) and are probably related to contact metasomatic processes.

Arsenic and antimony. These two generally chalcophyllic elements are loaded on mineral deposit-related Factor 2 (As only) and(or) Factor 4 (both As and Sb; Table 20), suggesting that these two elements are associated with more than one stage of sulphide-mineral deposition. Arsenic, and antimony (which is not shown on the cross-sections) occur only in very low concentrations in the Myszków system (Figs. 31, 32). The few high concentrations are generally found in contact zones between the intrusive rocks and their wall rocks and are somewhat higher in the zone in section B–B'.

FACTOR 5 — ELEMENTS RELATED TO FELSIC INTRUSIVE ROCK-ASSOCIATED MINERALISATION

Loss on ignition (LOI) reflects the volatilisation or remobilization of carbonate minerals but also possibly of sulphide minerals. LOI is positively loaded on Factor 5 (Table 20), along with strong negative loadings for Cu, Be, Mo, and W. This observation is corroborated by the spatial associations of felsic intrusive rocks with positive anomalies of Cu, Mo, W, and Be and negative anomalies of LOI. LOI also has a secondary loading on Factor 2, indicating that high LOI values (high carbonate and(or) sulphide concentrations) are also associated with that stage of mineralisation.

Low LOI values (<1.3%) are generally concentrated in the igneous rocks, which commonly contain fewer carbonate minerals than do the metasedimentary wall rocks.

Tungsten, strongly negatively loaded on Factor 5, is present at Myszków mainly as scheelite ($CaWO_4$) but also locally as powellite [$Ca(Mo,W)O_4$]. The distribution of strongly anomalous W (Figs. 39, 40) is spatially similar to the distribution of the intrusion shown in section A–A' and in the centre of section B–B', but not to the intrusion shown in the upper right of section B–B'. This distribution pattern suggests that the deposition of W is closely associated with the emplacement of the one intrusive phase but perhaps not with the second one. The distribution of weakly anomalous W (>5 ppm) is also widespread and, like Cu, extends well outside of the area of deep drilling at Myszków. Tungsten tends to have concentrations that increase with depth.

Beryllium is also strongly negatively loaded on Factor 5, indicating that its distribution is related to this Cu-Mo-W stage of mineralisation. The enrichment value for Be (Table 21) indicates that this element has not been added to the system to any significant degree, suggesting that its correlation with the other three elements is a result of remobilization during one or more stages of mineralisation.

Areas of anomalous Be (>3 ppm) are found mostly in the metasedimentary wall rocks near the intrusive contacts. These concentrations are related to contact metasomatism during emplacement of the central intrusion, in particular. Anomalous Be thus occurs in an aureole around the associated Mo-W mineralisation.

Molybdenum is also negatively loaded on Factor 5. The mineral residence for Mo at Myszków is mostly molybdenite, although powellite and scheelite may also be minor mineral residences of Mo locally. Like Cu, anomalous Mo (2 ppm) extends well beyond the limits of the two sections. Strongly anomalous Mo (300 ppm) is largely, but not entirely, confined to the intrusive rocks. Like that of W, this distribution is different from that of Cu (Figs. 33, 34), emphasising the overlapping of multiple stages of mineralisation at Myszków.

On both sections, the distribution of anomalous Mo is more restricted than that of anomalous Cu, especially in the upper parts of the sections. Conversely, the centres of maximum Mo enrichment generally tend to be deeper than those of Cu. As was the case for W, anomalous Mo is largely absent from the intrusion in the upper right part of section B–B'.

FACTOR 6 — ELEMENTS OF LARGELY UNDEFINED AFFINITY

Gold, mercury, and potassium. Factor 6 (Table 20) is mathematically reserved for those elements that do not fit well into any other factor. This lack of fit for Au and Hg is due largely to the fact that the analyses for these two elements are generally highly censored and also exhibit relatively narrow ranges of concentration (Tables 18, 19, and 21). Like As and Sb, Au, and Hg occur only in very low con-

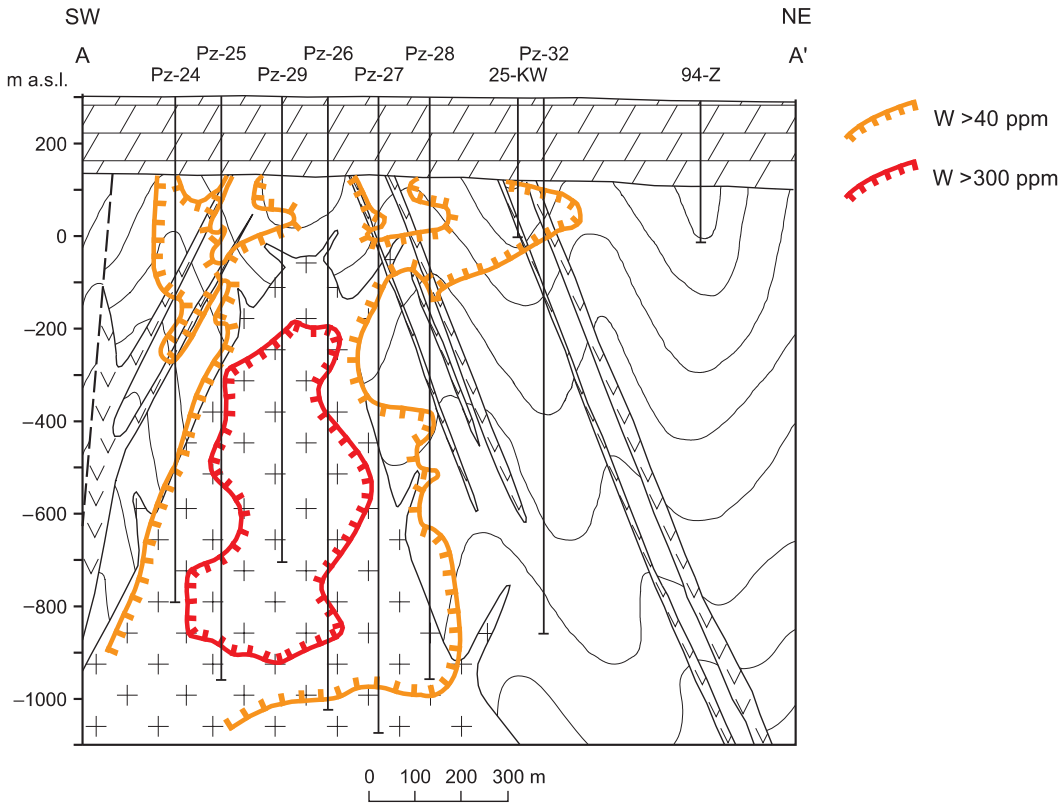

Fig. 39. Geochemical cross-section A–A`: element related to felsic intrusive rock-associated mineralisation

For explanations of geology see Figure 29

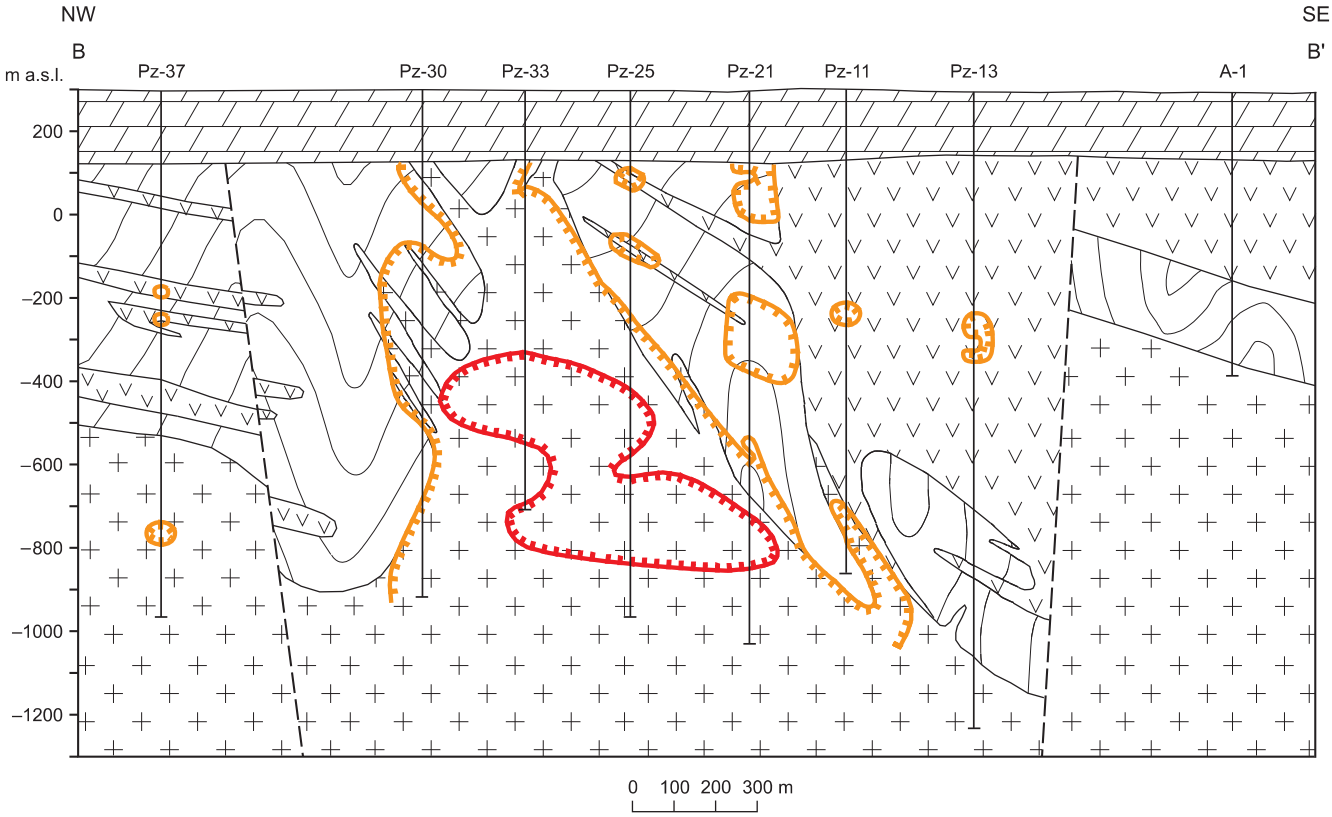

Fig. 40. Geochemical cross-section B–B`: element related to felsic intrusive rock-associated mineralisation

For explanations see Figure 39

centrations in the Myszków system. The few high concentrations are generally found scattered in contact zones between the intrusive rocks and their wall rocks and are relatively higher in section B–B'.

The assignment of K (previously discussed above under Factor 3) to this factor is not well understood, but suggests that anomalous Au and Hg are most likely to occur where K is least enriched.

DISTRIBUTION OF SELECTED VARIABLES ON THE 300-M AND 700-M LEVELS

A previous study of the Myszków area (Ślósarz, 1985) suggested that the Myszków mineralisation, in plan view, shows a Mo-rich core surrounded by a Cu- and Mo-rich zone, with Pb and Zn locally concentrated in the periphery. Because this zoning was described as occurring mostly outside of the area shown on the two sections, the distributions of selected elements were examined over a wider area and on two levels — at depths below the surface of 300 and 700 m.

Neodymium and titanium. The distributions of relatively low concentrations of Nd (<0.23 ppm) have a close spatial correlation with the intrusive rocks. The distributions of Ti show similar patterns to those of Nd.

Silicon. On both levels, anomalous Si (>32.3%) displays a strong NW–SE linear anomaly that is not entirely controlled by lithology. This anomaly represents the addition of quartz and other silicate minerals to the system as a result of hydrothermal alteration and sulphide mineralisation. Zoning of Si concentrations can be seen on both levels, with the highest concentrations centred near the intersection of the two cross-sections at the 700-m level (Pz-25) and centred a few hundred meters farther to the north-west on the 300-m level.

Copper. On both levels anomalous Cu (>200 ppm) is widespread, not well defined, and probably extends well outside of the area of drilling. Copper anomalies are not spatially related to lithology.

Molybdenum shows widespread anomalies (>40 ppm), especially at the 700-m level. Overall levels of Mo are higher at the 700-m level than at the 300-m level, emphasising its increase in concentration with depth. A NE–SW linear anomaly pattern is evident, particularly on the 300-m level. Areas of weakly anomalous Mo (>2 ppm) probably extend well beyond the area of drilling, particularly at depth.

Tungsten. Unlike the distributions of W seen on the sections (Figs. 42, 43), the distributions of strongly anomalous W (>20 ppm) on the two levels do not seem to be spatially related to intrusive rock. Like Mo, the W anomaly on the 300-m level seems to be linear. The main anomaly on the 700-m level is more circular in pattern, with the highest concentrations in boreholes Pz-26, Pz-27, and Pz-29. Like Mo, the overall levels of W concentrations are also relatively higher at 700 m, emphasising a general increase of this element with depth. Like Cu and Mo, weak W anomalies (>5 ppm) extend beyond the area of drilling.

Sulphur at Myszków is largely the sum of S in pyrite, chalcopyrite and molybdenite. Sulphur anomalies (>0.40% S) are widespread on both levels and extend beyond the limits of deep drilling, particularly on the 300-m level. Anomalies extend more to the north-west on the 700-m level. On the 300-m level the distribution suggests a possible halo around a central linear low.

Silver. Anomalous Ag (>0.80 ppm) shows distributions similar to those of Cu and S, but the anomalies are not as pronounced. The linear low seen for S on the 300-m level is also present for Ag. The spatial correlation of Ag with both Cu and S on the plans and sections emphasises that Ag is present at Myszków in trace amounts in sulphide minerals, principally in chalcopyrite but probably also in pyrite and sulphosalts.

Tellurium. Anomalous Te (>0.15 ppm) shows distributions similar to those of S, Cu, and Ag. A well-defined linear low is present at 300 m surrounded by a large, undefined area of enrichment. A more restricted Te anomaly is present at the 700-m level. Weak Te anomalies (>0.05 ppm) probably extend well beyond the area of drilling, particularly in the upper levels of the Myszków mineralisation.

Lead concentrations >50 ppm are related to mineralisation processes and not to lithology. On both levels, Pb anomalies are very restricted and do not closely match those of the other, major sulphide-related elements, such as Cu and Mo. Lead values are generally higher at the 300-m level than at the 700-m level, emphasising that this element is more concentrated in the upper levels of the system.

Zinc and cadmium. Anomalous Zn (>100 ppm) and Cd (>0.2 ppm), like Pb, are generally more concentrated at the 300-m level and exhibit only scattered anomalies related to mineralisation. Concentrations of Zn and Cd are somewhat higher to the south-east on both levels, a pattern similar to that seen for lead.

Potassium. The distribution of anomalous K (>3.5%) on the two levels is not strongly controlled by lithology. Anomalous concentrations are more widespread on the 300-m level than on the 700-m level, indicating a greater addition of this element to the upper levels of the system. The overall relative difference in concentration levels of K with depth in the Myszków system reflects the presence of granodiorite as the dominant pre-mineralisation rock type at depth and granite as the dominant post-K-metasomatism rock type higher in the system. The K anomalies are open-ended to the south-west, particularly on the 300-m level, and may represent an extension of K-metasomatism and possibly Cu-Mo mineralisation.

Loss on ignition. Low values for this variable (<1.2%) are found in both rock units and indicate sites with samples low in volatiles. This variable also shows a good NW–SE linear anomaly on both levels.

GEOCHEMICAL PATTERNS AND PATH-FINDERS OF THE MYSZKÓW MINERALISATION

For the purpose of economic evaluation, three geochemical zones have been distinguished in the mineralised Myszków area: (1) a central (core) ore deposit zone, (2) an intermediate ore deposit zone (intermediate zone), and (3) a peripheral zone (Fig. 41). The core zone is defined by the presence of mineralised rocks with minimum thicknesses of 10 m and by minimum concentrations of Mo and W of 500 ppm. This zone extends outward for 300 m from the location of borehole Pz-29. The intermediate zone extends between 300 m and 700 m from the centre of mineralisation, and the peripheral zone is located beyond 700 m from the centre of mineralisation.

Most of the significant ore related elements are found in all three zones but in varying amounts. The most important ore elements: Cu, Mo, and W, are found in all three zones as are S and K. These 5 elements form widespread, distinct geochemical anomalies over most, or all, of the entire area studied. Areas showing strong anomalies of these elements are shown on Fig. 41 in order to emphasise the differences between the three mineralised zones.

Copper concentrations are everywhere greater than the Clarke value for Cu, which means that the copper anomaly probably extends well beyond the drilled area. Molybdenum anomalies (>10 ppm) are also observed over the entire area studied, except near the area of borehole Pz-32. The continuous W anomaly is very closely associated spatially with the granitoid body and the intermediately surrounding area. However, anomalous zones and isolated sample points with concentrations of W >10 ppm are present in all of the boreholes that were sampled for this study.

Potassium and Ag that co-exists with copper are also characteristic of the core zone. However, anomalous Ag is found in all three zones. Small amounts of Bi and As have also been detected in the core zone. These traces are probably in inclusions in chalcopyrite. Silica, which is a good indicator of stockwork veining, is also anomalous in this zone.

Four main alteration zones: potassic, propylitic, argillic, and phyllic, are described in the classic model of hydrothermal alterations zoning in the rocks of porphyry deposits (Lowell and Guilbert, 1970). These four zones are also present at Myszków.

In the mineralised area of Myszków, propylitic, argillic, and phyllic alteration zones are only present locally in cores from boreholes drilled outside the core zone. Potassic alteration, characterised by presence of orthoclase, and more rarely, biotite, predominate in the core zone and parts of the intermediate zone at Myszków. Minerals associated with the potassic alteration zone are found mainly in quartz veins and along their selvages. Locally, potassium minerals flood the matrix around veins systems. Potassic alterations is found in the upper part of the granitoid intrusive, in a substantial part of the dacitoids, and locally, also in the metasedimentary host rocks.

The highest K concentrations (>4% K_2O) decrease with depth below 1300 m. This decrease reflects the gradual lithological change of the intrusion, which is a granodiorite at depth that is altered to granitoid at higher elevations. The highest K concentrations are found within a 480 m radius from the centre of mineralisation. It may continue in a southerly direction beyond the area of drilling.

Anomalous concentrations of Cu, Mo, and W, are closely related to the core zone. The lack of any significant spatial correlation between K and these three elements suggests, however, that K-metasomatism and the main mineralisation stage may have occurred at different times. A significant Tl anomaly identified in the core zone, is also associated with K, though, this element characteristic for the core zone is also associated with K; however, Tl is most characteristic of the intermediate zone, at the outer margin of the K-alteration zone.

The maximum content of silica is also found in the core zone. The distribution of this element partly reflects changes in lithology. The highest concentrations of silica (>68% SiO_2) are found in the granitoid intrusion in areas where there is a high density of quartz veins. The strong statistical correlation of silica with elements associated with altered rocks (mainly Sr and Ca, but to lesser degree, Ba and Na) suggests that silica was remobilized during the period of K-metasomatism.

The core zone is also characterised by negative anomalies of Ca, Na, and to some extent, Ba and Mn, all elements closely associated with rock alteration. Strontium is distributed differently. Negative anomalies for Sr are found at the contacts of the metasedimentary rocks with the granitoid intrusion. In the central part of the intrusion, Sr is found in Clarke concentrations.

These five elements were leached from the core zone during feldspar metasomatism, which resulted in plagioclase being replaced by orthoclase. Weak, positive Ca, Na, Ba, and Sr anomalies are found in the intermediate and peripheral zones. Weak Mn anomalies are also found in the transition areas between the core zone and the intermediate zone.

The outer fringes of the anomalies for Mo and W, and partly that of Cu, also contain anomalies of Be and F. Isolated anomalous Be concentrations of as much as 16.5 ppm can be observed in the metasedimentary rocks near where they are in contact with the intrusion. The F anomaly (>0.1%) is much larger than that of Be and extends outward to the middle of the intermediate zone. In contrast, the central part of the granitoid intrusion contains only Clarke amounts of Be and F. The central parts of the intermediate zone contain anomalies of Au, Hg, and Sb, and locally also Cu, and Ag, Ca, Na, and Sr.

Gold anomalies in the intermediate zone are weak. Isolated sites with higher Au concentrations (10–40 ppb, maximum 248 ppb) are found along contacts between the granitoid and porphyry dikes, to a distance of about 300–550 m from centre of the Mo-W mineralisation.

Most of the samples analysed for Hg also contain only background levels. Anomalous Hg (100–300 ppb, maximum 430 ppb) is found along contacts of the magmatic rocks with the wall rocks, mostly about 300–700 m from the centre of

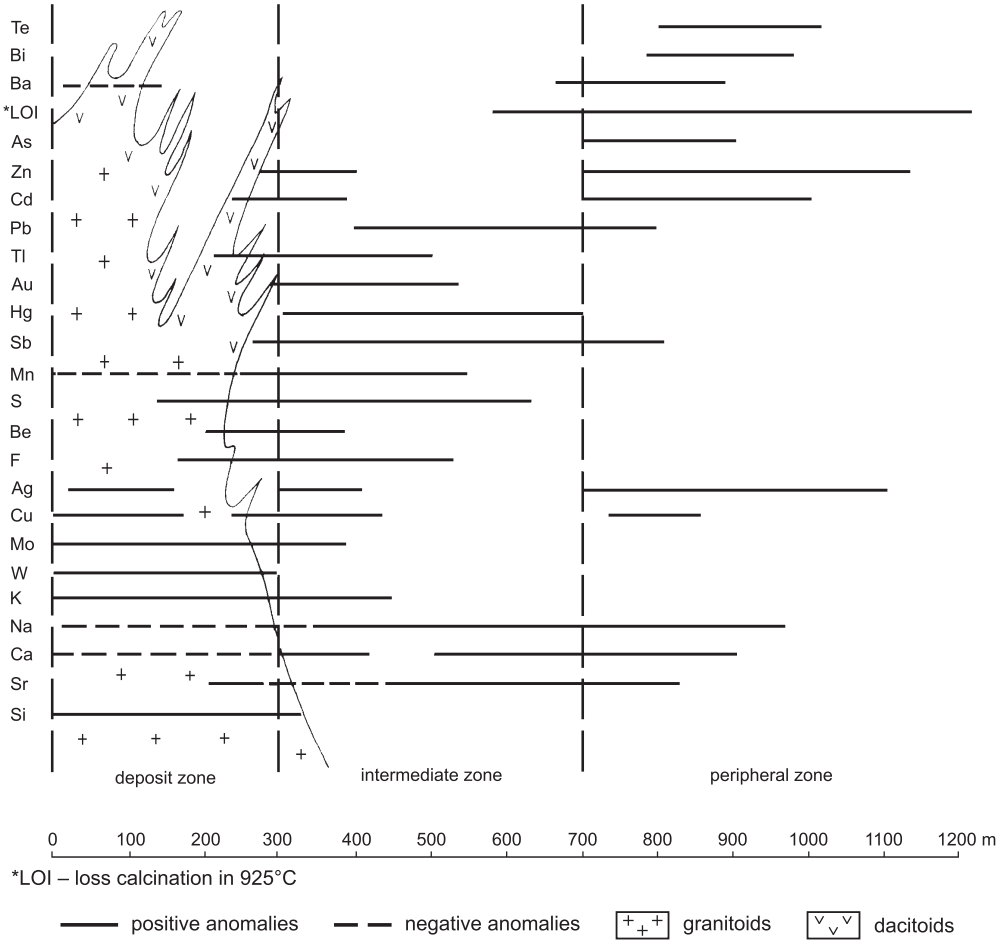

Fig. 41. Schematic zoning of the main elements in the Myszków deposit

Mo-W mineralisation. In the intermediate zone, Hg coexists with Au. The area of anomalous Hg is wider than that of Au, and encompasses the entire intermediate zone. The area with isolated points containing anomalous Sb (>4 ppm) extends even farther than that of Hg and includes part of the neighbouring peripheral zone.

Anomalous Pb is found in the transition area between the intermediate and peripheral zones (400–900 m from the centre of Mo-W mineralisation). Average lead concentrations are generally much higher in the intermediate zone (92 ppm) than in the peripheral zone (31 ppm). The highest Pb concentrations (0.1–0.3%) were detected in all types of magmatic rocks where they are in contact with adjacent wall rocks.

Anomalous LOI values (>1.5%) are present over a large area that extends from the outer part of intermediate zone (600 m from the centre of mineralisation) to the farthest parts of the peripheral zone investigated to date (about 1200 m from the centre of mineralisation).

The characteristic elements for the areas located farthest from the mineralisation centre (700–1200 m) include: Ba, Zn, Cd, As, Bi, and Te, and locally Ag and Cu. The average Ba content increases gradually with distance from the centre of mineralisation. Barium concentrations >800 ppm are characteristic for areas located between 650 and 850 m from the centre of mineralisation.

There are no distinct Zn and Cd anomalies in the Myszków deposit. However, single anomalous points are scattered over all of the intermediate and peripheral zones. The average concentrations of Zn and Cd increase from the core zone outward toward the peripheral zone (to as much as 84 ppm Zn and 0.61 ppm Cd). The highest individual anomalous samples for these two elements are found in the areas near the core zone in the host rocks where they are in contact with dacitoids dikes.

The highest As concentrations (over 10 ppm) are also found in the peripheral zone. This element shows a very strong spatial correlation with Cu and Sb in that zone, suggesting that minerals of the tetrahedrite-tennantite group may be present.

Average Bi concentrations also increase with distance outward from the core zone and reach a maximum of 6.68 ppm in the peripheral zone. There are no large distinct Bi anomalies. Single samples with anomalous Bi have been identified in the uppermost parts of the Vendian to Early Carboniferous complex, where the magmatic rocks are in contact with the wall

rocks. The highest Bi concentrations (as much as 290 ppm) were found in an area about 750 to 950 m from the centre of Mo-W mineralisation.

Tellurium is another characteristic element of the peripheral zone. Like Bi, average concentrations of Te increase outward and reach their maximum in the peripheral zone. The highest Te concentrations are found in the uppermost parts of the Vendian to Early Carboniferous rocks in the dacitoid dikes where they are in contact with the metasedimentary rocks. The common distributions of Te and Bi suggests that minerals such as tetradymite or tellurobismuthite may be present. The coincidence of Te and Ag suggests the presence of hessite. The highest Te concentrations (as much as 700 ppm) are found in the peripheral parts of the area investigated, about 800–1050 m from the centre of Mo-W mineralisation.

Strong Cu and Ag anomalies are present in all three zones. In the peripheral zone, which has the lowest average Cu content, Ag concentrations are at their highest (1 ppm). In this zone, both elements behave differently than they do in the other two zones where they show a positive spatial correlation with elements of the low-temperature mineralisation stage, especially with As and Sb, a phenomenon not seen in other zones. These observations suggest that some of these elements may also be associated with the low temperature mineralisation process, and that they may occur in minerals such as tennantite-tetrahedrite and hessite, as well as in Ag sulphotellurides. These minerals are typical of the peripheral zones of the porphyry mineralisation.

Geochemical investigations of mineralisation in the Myszków area suggest that the path-finder elements, listed in decreasing order of importance, may be used in the search for concealed porphyry mineralisation: W, Mo, Cu (Ag), K, Be, F, Sb, Hg, Au, Pb, Ba, As, Ag, Zn ± Cd, Bi, and Te. This is a very generalised order, as many of these elements may have been deposited in several mineralisation stages.

Other variables, such as Na, Ca, Sr, Si, Mn, Tl, and LOI, which are associated with alteration processes, are less important for prospecting because they do not form obvious geochemical anomalies. However, several types of relationships may be of interest. For instance, the gradual increases in K to Na and K to Ca ratios toward the centre of mineralisation may have a prospecting value, as some weak, negative Na and Ca anomalies are associated with strong, positive K anomaly in the core zone.

The K_2O/Na_2O ratio increases from 1.40 in the peripheral zone, to 1.75 in the intermediate zone, to 2.10 in the core zone. Similarly, the K_2O/CaO ratio increases from 2.62 in the peripheral zone, to 3.28 in the intermediate zone, to 4.01 in the core zone.

Sulphur forms a strong, widespread anomaly over the entire area investigated. Concentrations lower than the Clarke values are rare. Areas with the highest S concentrations correlate closely spatially with areas containing high Cu concentrations. However, S anomalies are not very good indicators of the ore deposits at Myszków because pyrite, the most common source of S, is abundant in all parts of the mineralised area.

THE SPATIAL DISTRIBUTION OF THE MINERALISATION

SAMPLING AND CHEMICAL ANALYSES OF CORES FROM BOREHOLES

During the exploration phase of drilling for polymetallic mineralisation in the Myszków area, a special emphasis was given to representative sampling, and to selecting adequate methods of investigations. The boreholes were completely cored and were drilled at a spacing of about 100–120 m along lines spaced about 200 m apart. The sampled holes were located along six parallel lines that were oriented NE–SW, perpendicular to the longest dimension of the granitoid intrusion (Fig. 7). Over 43 000 samples were collected from 24 boreholes.

The cores were geologically logged and next cut into two halves along the core axis. One half was stored in the Central Geological Archives of the Polish Geological Institute and the second half was used for laboratory analyses. Standard investigations included chemical, geochemical and petrographic analyses of rocks and ore minerals.

Taking the stockwork and disseminated character of the mineralisation into consideration, the following methods were used to collect samples for standard chemical analyses:

- channel sampling: samples 0,5 m in length for intervals with macroscopically visible mineralisation and 1,0 m in length for intervals with relatively weak mineralisation (98% of the total number of samples),
- point sampling, for intervals containing macroscopically invisible mineralisation (2% of the total number of samples).

The Vendian to Late Carboniferous rocks were sampled in detail in most of the investigated boreholes. Cores from four boreholes (Pz-11, Pz-13, Pz-14, and Pz-17) were generally point sampled and only sporadically channel sampled because most of the cores were of only weakly mineralised porphyry rocks.

Standard chemical analyses, for prefeasibility study purpose, were determined in the laboratories of the following institutions: the Polish Geological Institute in Warsaw (Central Chemical Laboratory), the Polish Geological Institute Regional Branches in Sosnowiec, Kielce, and Wrocław; the Geological Enterprises in Warsaw, Kraków, and Katowice; the Mining and Metallurgical Works "Orzeł Biały" in Pie-

kary Śląskie; the Institute of Iron Metallurgy in Gliwice; and the KGHM Polish Copper S.A. in Lubin. X-ray fluorescence spectrometry, atomic absorption spectrophotometry, emission spectrography, and ICP techniques were used to determine six elements (Cu, Mo, W, Zn, Pb, and Bi).

For quality control, splits of samples were analysed for Cu, Mo, and W in three different laboratories, including those of the Polish Geological Institute in Warszawa, the Institute of Base Metals in Gliwice, and the Technical University in Wrocław.

VERTICAL ZONING OF THE MINERALISATION

The vertical distribution of Mo-W-Cu mineralisation in the Myszków area is shown on the two vertical geological cross-sections (A–A' and B–B'). Analyses for Cu, Mo, and W from almost twenty thousand samples were used to produce the geochemical cross-sections.

The krieging procedure (Environmental Protection Agency "GeoEAS" program, Las Vegas, 1988) was used to produce the contour maps for Cu, Mo, and W. The analysed samples were grouped over 5 m intervals, and the average Cu, Mo, and W concentrations for each interval was calculated. The distribution of the three metals was selected by using histograms. Then, the analytical functions approximated the variability. These functions were afterwards used as the geostatistical variability models. The model type is presented in the Table 22.

Concentration levels for Cu, Mo, and W are shown on cross-sections A–A' and B–B' which were constructed using krieging and contouring techniques in Golden Software's "Surfer" programme. A grid with 25 m length squares was used to calculate a random variability parameter.

Molybdenum mineralisation. On cross-section A–A' (Fig. 42), Mo is concentrated in the granitoid. It is also present in lower concentrations in the wall rocks within about 50–150 m of the contact with the intrusion. The 500 ppm Mo contour line is almost completely within the intrusion boundary.

On cross-section B–B' (Fig. 43), the centre of Mo mineralisation extends beyond the granitoid intrusion, toward borehole Pz-21. Anomalous Mo occurs at a greater depth on this section than on section A–A'. The maximum Mo concentrations on both cross-sections is about 1250–1300 ppm.

The distribution of the ***tungsten mineralisation*** is similar to that of Mo. However, W is more closely associated spatially with granitoid rocks than is Mo (Figs. 44–45). The distribution of tungsten based on the 500 ppm W contour line is more restricted than is the anomaly for 500 ppm Mo. The W anomaly is confined to the granitoid intrusion on both cross-sections. The maximum W concentration is less than that of Mo, with maximum values reaching 1000–1250 ppm W.

Copper mineralisation has the most complex distribution of the three elements. There are three positive Cu anomalies on cross-section A–A'(Fig. 46). One of them is connected with the upper part of the granitoid intrusion. The other two are located closer to the surface, in metamorphosed host rocks and in the dacitoid veins that cut the host rocks on the both sides of the intrusion. The highest Cu concentrations are 0.4–0.5% Cu.

The distribution of anomalous Cu mineralisation on cross-section B–B' (Fig. 47) is more irregular that that on section A–A' (Fig. 46). The highest Cu concentrations are located both in the intrusion and in its apophyses (Pz-30).

Table 22

Geostatistical variation models of the Cu, Mo and W mineralisation (cross-sections Figs. 42–47)

Cross-section	Element	Model	Parameters		
			c_0 (ppm^2)	c (ppm^2)	a (m)
A–A'	Cu	spherical	400 000	900 000	240
	Mo	spherical	40 000	120 000	700
	W	spherical	70 000	80 000	600
B–B'	Cu	spherical	400 000	500 000	500
	Mo	spherical	50 000	90 000	700
	W	spherical	30 000	50 000	600

c_0 — random variability; c — range of random variability; a — extend of autocorrelation

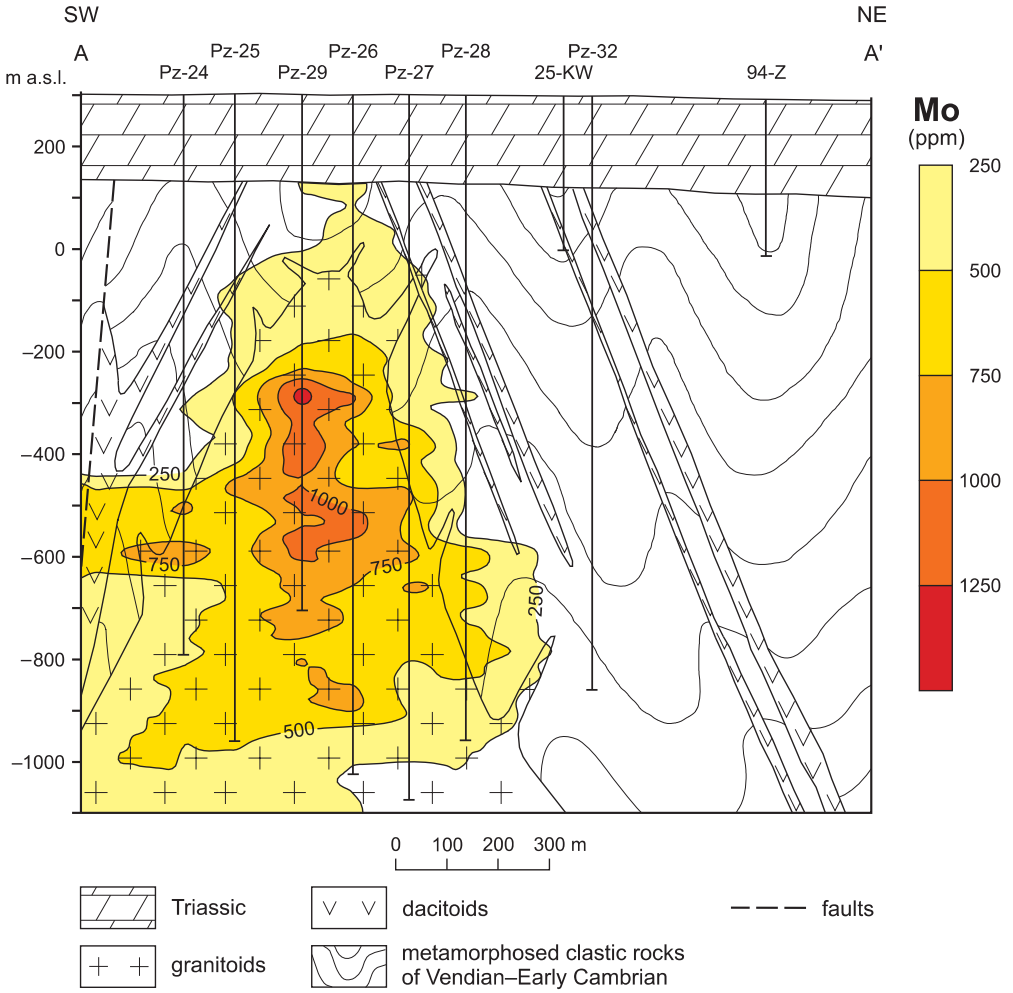

Fig. 42. Molybdenum content on the cross-section A–A'

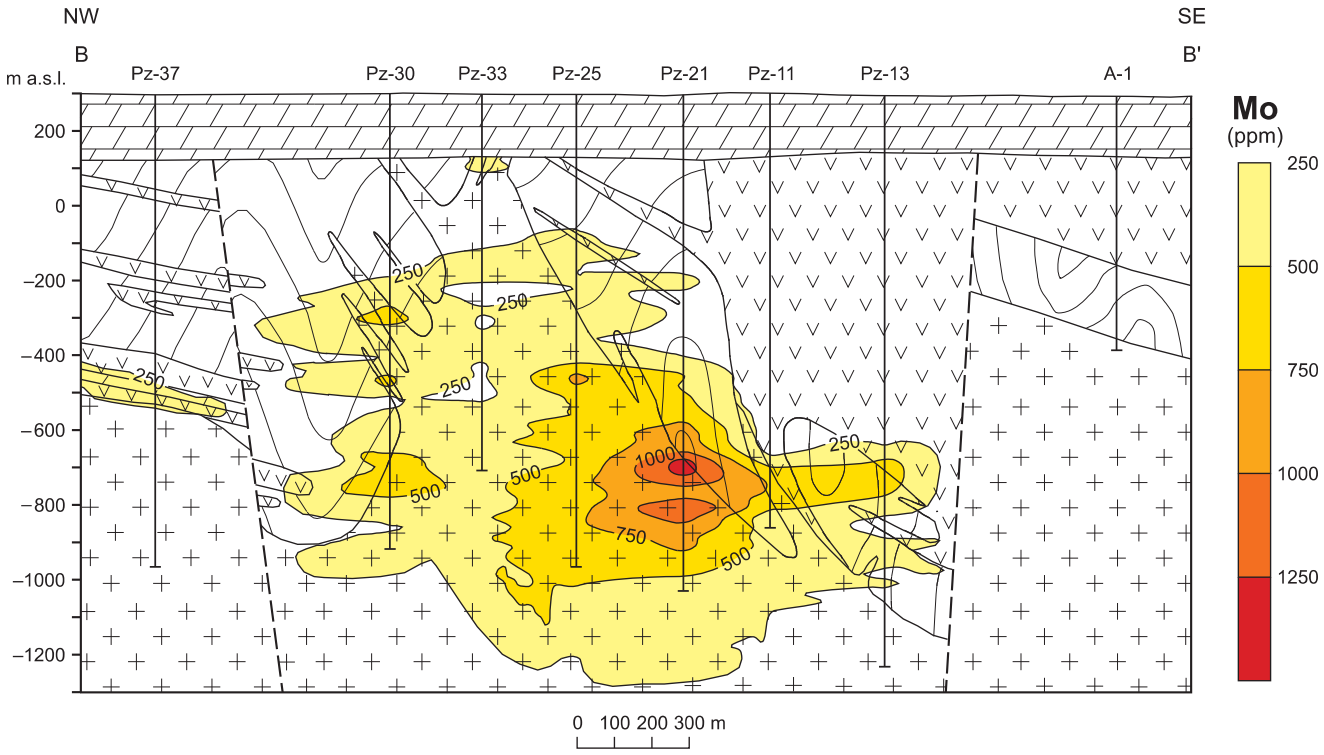

Fig. 43. Molybdenum content on the cross-section B–B'
For explanations of geology see Figure 42

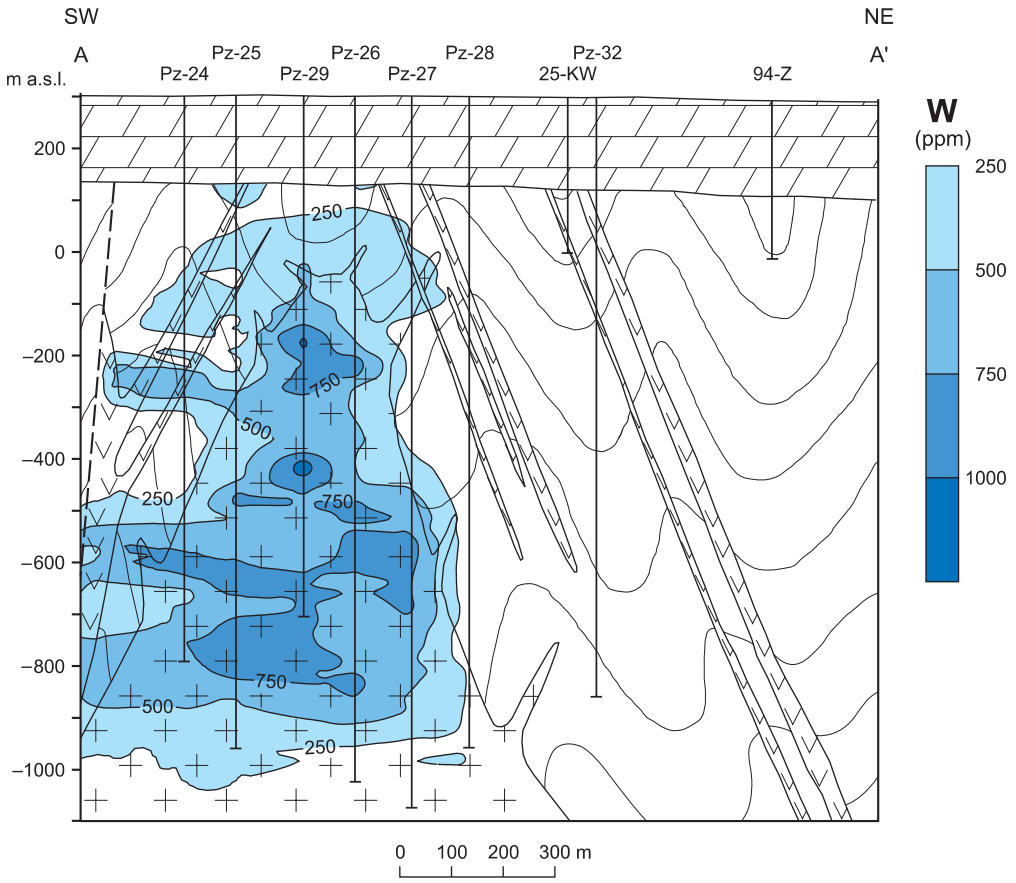

Fig. 44. Tungsten content on the cross-section A–A'

For explanations of geology see Figure 42

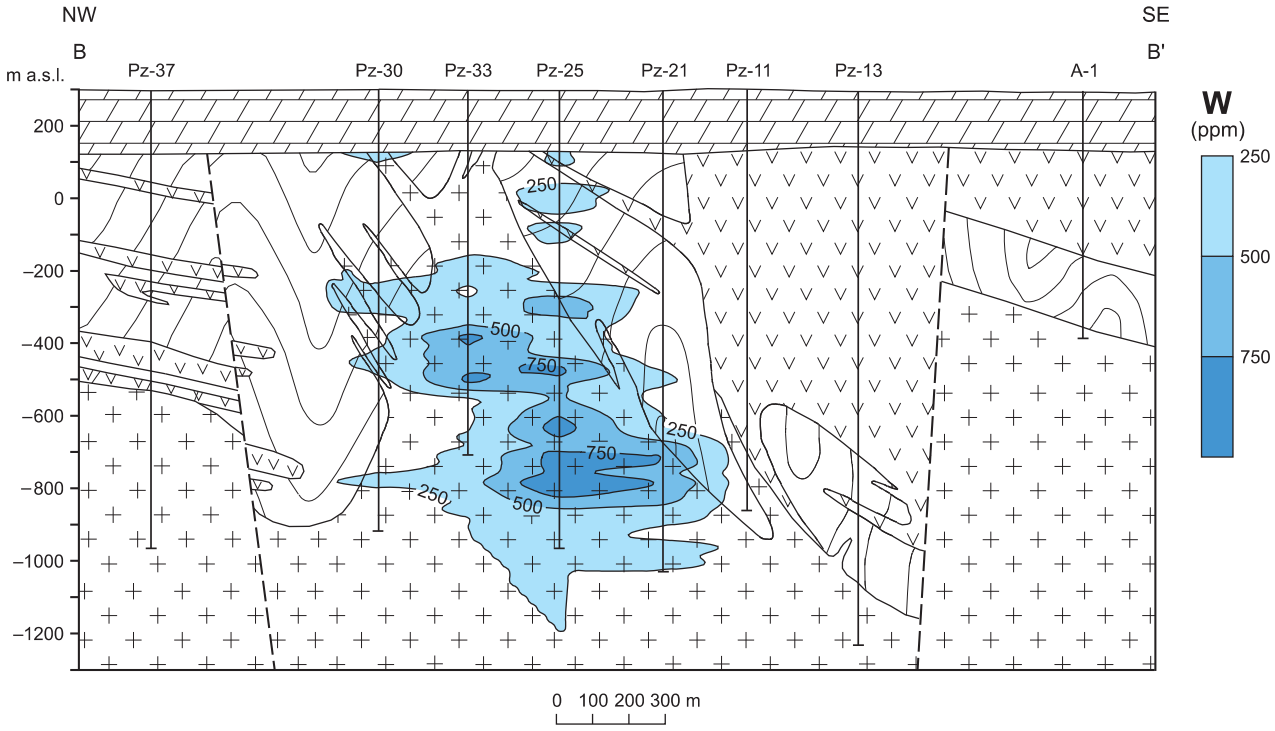

Fig. 45. Tungsten content on the cross-section B–B'

For explanations of geology see Figure 42

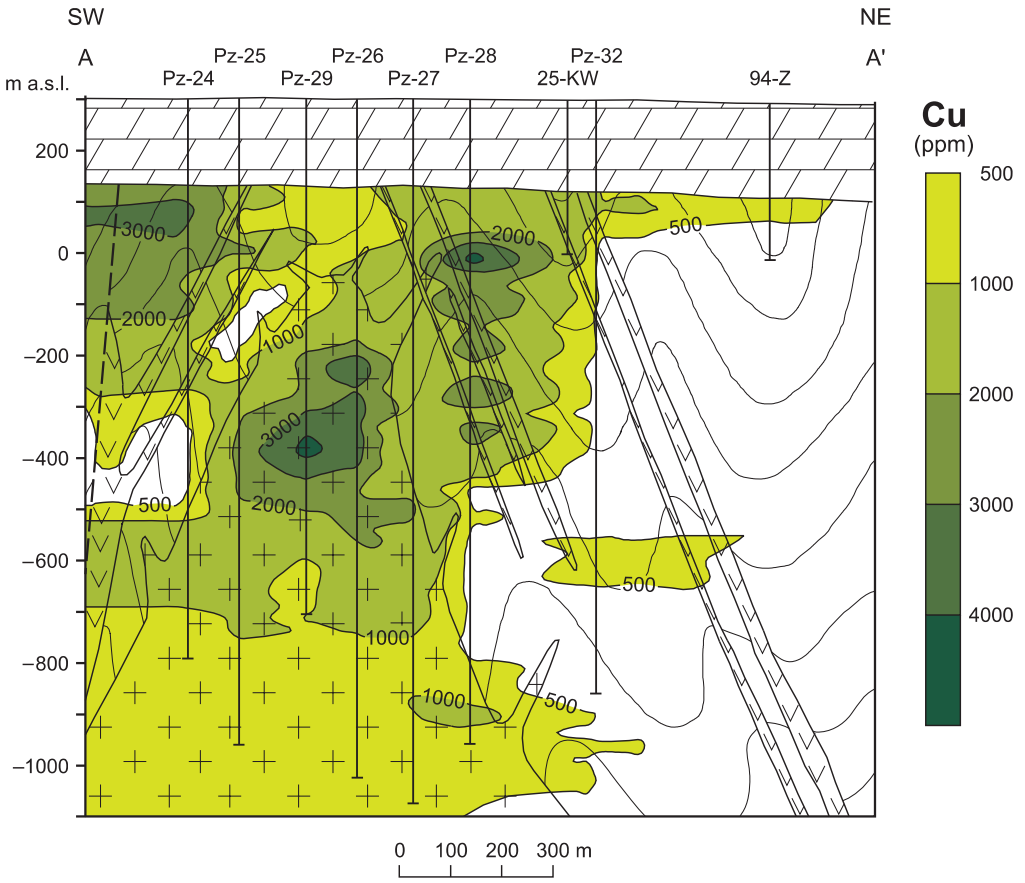

Fig. 46. Copper content on the cross-section A–A'

For explanations of geology see Figure 42

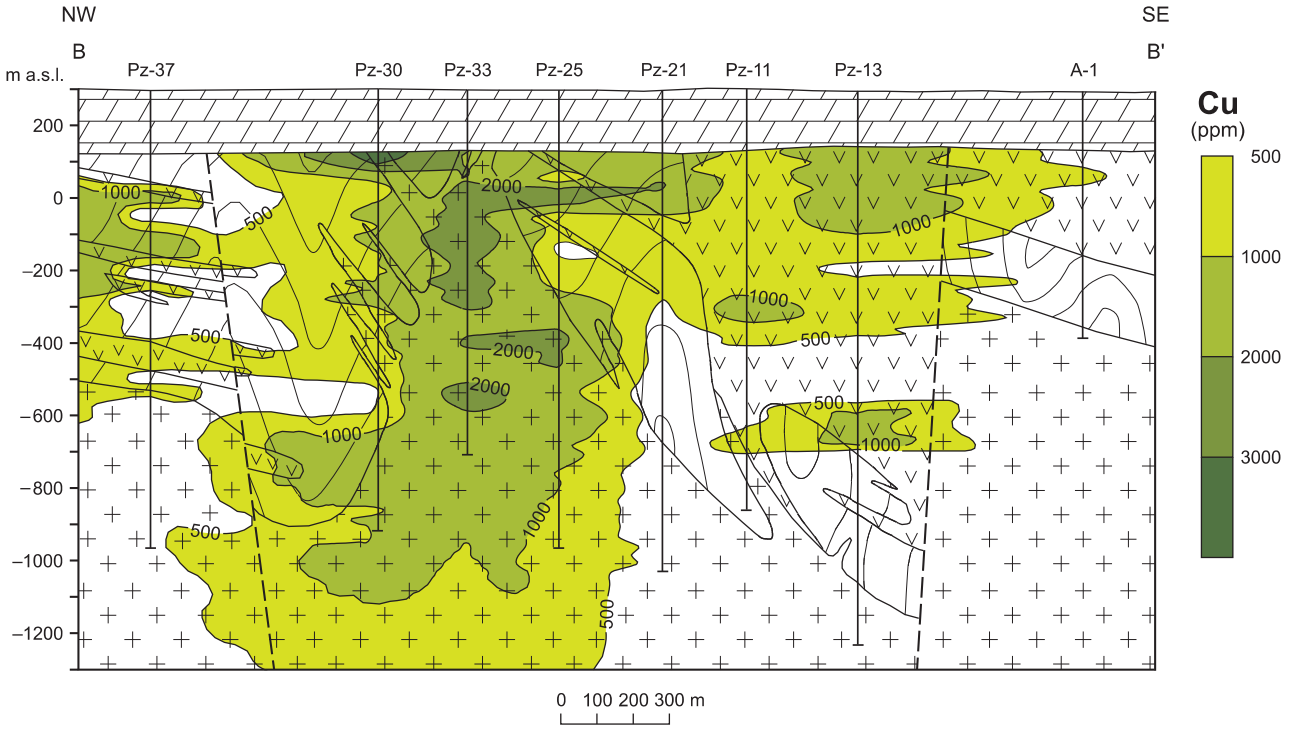

Fig. 47. Copper content on the cross-section B–B'

For explanations of geology see Figure 42

LATERAL ZONING OF THE MINERALISATION

Maps showing the thickness of "total ore" intervals (as determined in boreholes profiles) were constructed to analyse the lateral zoning of ore mineralisation in the Myszków area. Boreholes intervals of at least 10 m thick boreholes sections, having an average Mo and W concentrations greater than 0.1% and an average Cu concentrations greater than 0.4%, were used for the evaluation (Fig. 48). The thicknesses of all such intervals were calculated for each of the three elements and summed for each borehole. The resulting totals were used to construct element distribution maps. On the Cu map, the contour lines for "total ore" intervals are shown separately for the granitoid intrusion and for the host rocks.

Despite the general overlap of the mineral assemblages, containing molybdenite, scheelite, and chalcopyrite, these three minerals were generally deposited in different phases, and are, therefore, differently distributed.

The strongest Mo mineralisation was found in borehole Pz-29 and to the south-east, toward Pz-21 and Pz-22 (Fig. 48B). In contrast, the strongest W mineralisation is in the central parts of the mineralised area (Pz-25, Pz-26, and Pz-29) and continues in a nortwesterly direction toward hole Pz-31 (Fig. 48B). The wider extent of Mo mineralisation, as compared to W mineralisation, can be clearly seen on the maps (Figs. 48B, C) and cross-sections (Figs. 42–45).

Copper mineralisation has the widest distribution of the three elements (Fig. 48A). Comparing its distribution in map view (Fig. 48) and on cross-section A–A' (Fig. 46), one can see that the anomaly in the central part of the Myszków area (Pz-26 and Pz-29) is associated with the apical part of the intrusion. Other zones of strong Cu mineralisation are present in the metamorphic host rocks.

The variability of copper concentrations is very high and substantially changes almost every 100–200 m. In several places, especially in the south-western part of the Myszków area, the distribution of Cu mineralisation is still not adequately known because not enough holes were drilled in that area.

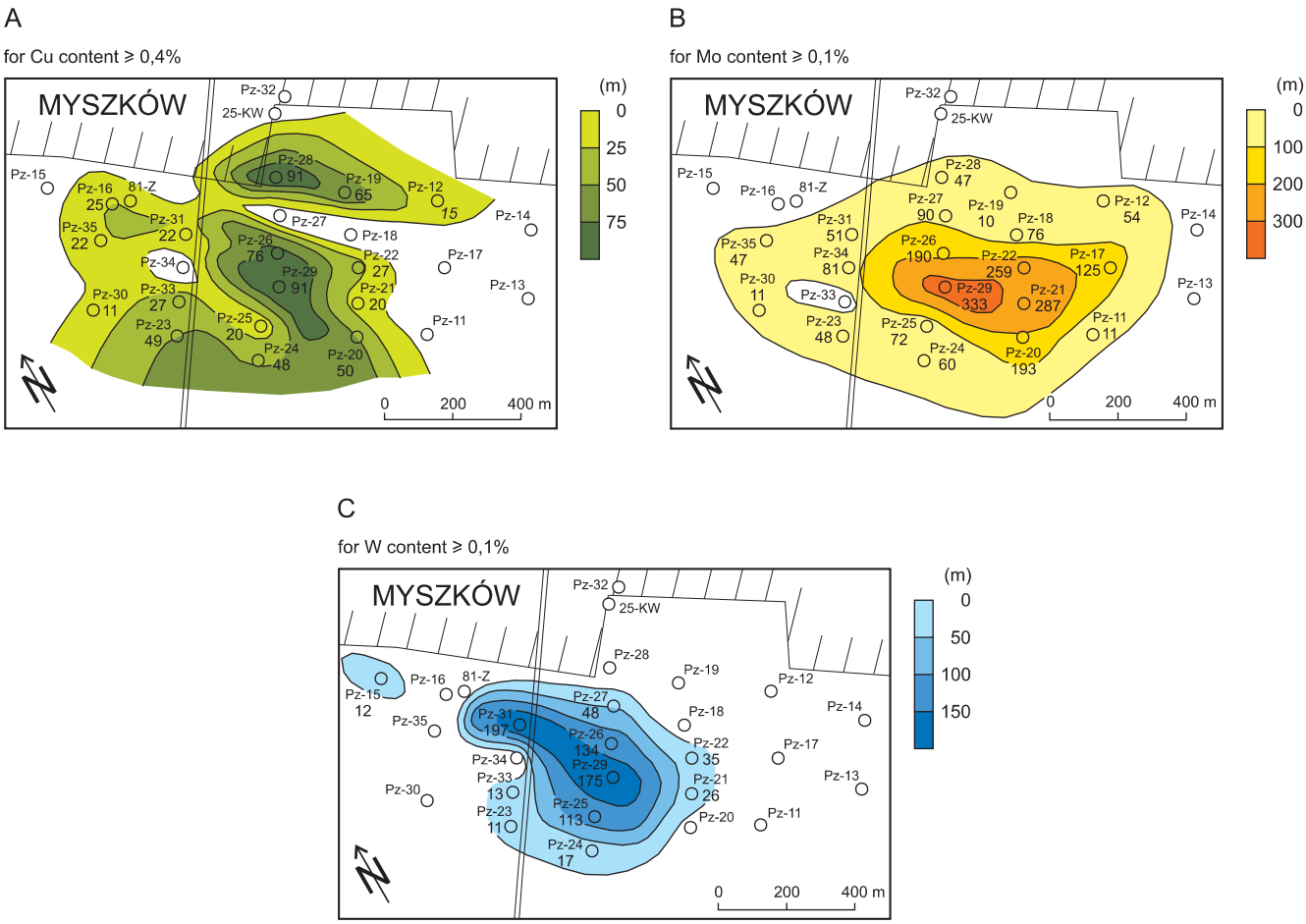

Fig. 48. Maps of the total mineralised intervals thickness of at least 10 m thick intervals

MODEL AND GENESIS OF THE MINERALISATION

All endogenetic Mo deposits can be classified as being Cu-Mo, Mo, or Mo-W types (Pokałow, 1972; Table 23). The Myszków deposit is thought to belong to the Mo-W type.

The Mo-W type of deposits is generally connected with the tectonic mobilisation of older rocks. This activity produced deep-seated fractures that separated areas of crustal rocks into tectonic blocks that were uplifted or down faulted to varying degrees. Molybdenum deposits were mainly generated in the uplifted blocks, which are also associated with the granitoid intrusions (Pavlova and Aleksandrov, 1986). These tectonically--active areas could also be interpreted as being subduction zones along active continental plates (Chaffee *et al*., 1994, 1997, 1999).

Deposits of the Mo-W type are associated with plutons composed of leucocratic granites (Pokałow, 1972), and particularly with small intrusive bodies, some of which could have developed at great distances from their primary batholith. Some Mo-W deposits develop along the endocontacts of plutons. Molybdenum-bearing plutons commonly exhibit contact metasomatic alterations zones that may include hornfelses, biotite, and feldspar minerals (Pokałow, 1972).

Hornfelses may be found as far as 100 m outward from intrusion contacts. The distance depends on the temperature and mineral content of the primary rocks. At greater distances from the intrusion, rock recrystallisation occurs as patchy textures. Biotite alteration has the widest distribution and may extend more than 1000 m from the outer edge of the intrusion. Feldspathisation occurs as numerous potassium feldspar-plagioclase-quartz-biotite veins (as much as 1.5 cm-thick) that cut the wall rocks near the intrusion in an aureole that extends as far as 300–350 m from the intrusion.

The Mo-W deposit at Myszków is located on the western edge of the Małopolska Block, close to its tectonic contact (Kraków–Lubliniec tectonic zone) with the Upper Silesian Block (Fig. 4). According to Żaba (1999), this zone was activated in two stages. The first was in the Late Silurian and the second in the Late Carboniferous to Early Permian. In contrast, Chaffee *et al*. (1994, 1997) regard this tectonic zone as a subduction zone in continentally-derived rocks.

Although it is probable that the Myszków deposit parent granitoid batholith is leucocratic, it has not as yet been penetrated by drilling. It is speculated that this batholith is the source of the large negative gravity anomaly at Kotowice (Fig. 2A). The granitoid intrusions in the Myszków–Mrzygłód, Zawiercie, Pilica and Dolina Będkowska areas may all represent small intrusive bodies, associated with this batholith.

A characteristic, though limited, zone of exocontact alteration is present near each of these intrusions. Hornfelses and biotitised host rocks have been observed in the Myszków area. The distribution of hornfelses is rather small and extends from several tens of centimetres to a few metres beyond the intrusion wall rock contact. Patches of recrystallised rocks extend much farther. No classic feldspathic alteration was observed in the Myszków area. On the other hand, biotitisation has affected rocks for a distance of as much as several hundred metres beyond the edge of the intrusion. The effects of biotitisation have also been observed in a few boreholes from the Kotowice area suggesting the presence of a granitoid intrusion at a greater depth.

Textures of the Myszków granitoids suggest that they may have crystallised at rather shallow depths. Textural features that suggest this include zoned, very often recurrent plagioclases, the presence of perthites, the characteristics of quartz grains, and the appearance of fluid inclusions.

Andalusite (Heflik *et al*., 1975) and cordierite (Banaś *et al*., unpubl. report, 1977) have been observed in the Myszków area in wall rocks near their contact with the granitoid intrusion. These minerals also suggest a shallow depth of crystallisation (2–10 km) and a contact zone temperature range of 550–700°C (Carmichael *et al*., 1974).

The chemical connection of the granitoids and associated dacitoids, and the calc-alkali characteristics of the granitoids, have been determined by chemical analyses. These rocks formed after a relatively rapid period of crystallisation, from the silica-saturated, granodioritic or dacitic magma (Juskowiak, 1971). Wieser (1957) made a similar conclusions but stated that the dacitic magma originated from tholeitic magma, which also is the parent magma for the diabases. According to Ryka (1974), the diabase-lamprophyre rocks, as well as the "porphyries" were generated from the same tholeitic magma. The resulting differences in the rocks depend on the type of host-rock contamination.

The ore mineralisation that produced the Myszków deposit was the result of a very complex process. The dominant sulphides, oxides, as well as sulphosalts, tellurides, and native Bi have been identified in many different parageneses, and in many generations of mineral deposition. These minerals have crystallised over a wide range of temperatures. This wide range is suggested by some mineral associations as well as by disintegration textures of solid solution minerals (sphalerite, cubanite, bornite, and valleriite inclusions in chalcopyrite), martitisation of magnetite, and the native Bi inclusions in the Bi minerals. The geochemical investigations of individual ore minerals did not reveal significant chemical differences within any one species, suggesting a common postmagmatic source for both the Cu-Mo-W and the skarn ores.

Differences in the composition of sulphur isotopes in the ore minerals from the main stage of Cu-Mo-W deposition, as well as from younger stages of mineralisation, might have been caused by changes in the physico-chemical environment during evolution of the hydrothermal fluids from oxides and sulphides to sulphates and (or) by the effects of contamination by host rocks incorporated into the magma.

The disseminated mineralisation and stockwork veining at Myszków are typical of most calc-alkaline porphyry Cu systems, except for the occurrence of significant concentrations of

Table 23

Mineralisation at Myszków compared with Pokałow (1972) classification of endogenic molybdenum deposits

Ore type	Geotectonic position	Magmatic complex		Type of mineralisation
		Period I	Period II	
Cu-Mo	Geoanticlinal uplifts during orogenic development of geosynclines	Large, complex plutons: monzonites, granodiorites, granites, diorites, syeniesy, gabbro etc.	Dikes and small, complex stockworks; intensive development of extrusives	Chalcopyrite-molybdenite in rocks altered through K-feldspathisation, silicification, sericitisation, and argillisation
Mo	Tectonic-magmatic activisation on platforms and in the folded zones; during the initial period, intensive development of large depressions filled with molasse type sediments	Large plutons of biotite-hornblende granites	Dikes and small, complex stockworks; intensive development of extrusives	Molybdenite in rocks altered through K-feldspathisation, silicification, sericitisation, and argillisation
W-Mo	Tectonic-magmatic activisation on platforms and in the folded zones	Plutons of leucocratic granites	Dikes of granitic, dioritic, and syenitic porphyries	Molybdenite-wolframite (scheelite) w albitic, greisenic, and, to the smaller extent, K-feldspathic rocks
Myszków	Tectonic-magmatic activisation in the contact zone of Upper Silesian and Małopolska blocks; lack of large depressions filled with molasse type sediments	The primary pluton has not been discovered (most probably, the Żarki-Pilica gravity anomaly is connected with this pluton)	Granitoid intrusion, dikes of dacites and rhyolites	Chalcopyrite, molybdenite and scheelite in magmatic rocks altered by K-feldspathisation, and in biotitised, clastic wall rocks; poorly developed sericitisation zone and absent of argillisation zone

W. As many as 11 elements (Ag, Bi, Cd, Cu, K, Mo, Pb, S, Sb, Te, and W) are clearly enriched in the area. These elements were probably added to the deposit area during at least one of the mineralisation phases. At least some of the Cu as well as Pb-Zn mineralisation, occurred in an irregular zone that is high in the system but not symmetrical with respect to the associated stock. The deposit is a low Au system and also contains only low concentrations of Hg, As, and Sb.

In plan, the deposit exhibits crude to well-defined NW–SE linear geochemical anomalies for at least 8 variables (Ag, Cu, Mo, LOI, S, Si, Te, and W). These distributions, which match geophysical patterns, may, for some variables, extend beyond the area drilled to date, especially to the north-west. The distribution of at least 9 elements (Ag, Bi, Cu, K, Mo, S, Te, W, and Zn) are still anomalous at the Palaeozoic-Triassic unconformity, suggesting that an unknown part of the original deposit has been removed.

As for the chemistry of the mineral forming fluids, the Myszków deposit is a typical example of mineralisation caused by the evolution of highly saturated chlorine brines that are enriched in metals and depleted in fluorine and carbon dioxide. The deposit is similar to the model of a low fluorine, high chlorine porphyry Mo deposit described by Theodore (in Cox and Singer, 1986; model 21b) and to the model described by Nieć (1988). The Myszków deposit could also be classified as falling somewhere between a porphyry W and a porphyry Cu deposit (Theodore and Menzie, 1984).

AGE OF THE MINERALISATION

The world's Mo deposits have been formed during a span of time that extends from the Proterozoic through the Neogene. Economic Mo stockwork ore deposits are only found in rocks of Triassic to Jurassic, and Palaeogene to Neogene ages. The previously known Palaeozoic deposits, which are mostly Permian in age, are very rare (Horton, 1978, Laznicka, 1976). The reason for their rarity may be due to deposition at rather shallow depths, where they were fairly easily eroded. Alternatively, this age of deposit may be more common than thought but the deposits are not yet exposed by erosion. Porphyry Cu deposits in other parts of Europe also vary in age, with most having formed in Cretaceous or Tertiary time (Janković, 1980).

The mineralisation at Myszków is spatially associated with a sequence of Late Precambrian to early Palaeozoic (Vendian to Early Cambrian) metasedimentary clastic rocks and a predominantly granodioritic pluton that intruded the metasedimentary rocks. These intrusive rocks are related to Variscan (Late Carboniferous) magmatism. That age of magmatism was first confirmed by the dating of biotite,

which suggested an age of 312 ±17 Ma for the pluton at Myszków (Jarmołowicz–Szulc, 1984, 1985).

In order to determine the age of the mineralisation more accurately, in early 1990's core samples that contained minerals associated with the formation of the pluton and the Myszków mineralisation, were collected. These minerals were analysed isotopically in a USGS laboratory in Denver, Colorado, using the $^{40}Ar/^{39}Ar$ dating technique (Podemski and Chaffee, unpubl. report, 1996). This technique is discussed elsewhere (Snee *et al.*, 1988). The samples collected included one of white mica (sericite), three of potassium feldspar associated with potassic alteration associated with formation of the mineral deposit, and six samples of biotite.

The results show ages varying from 305 to 290 Ma (Fig. 49). The oldest date (305 Ma) is for a sample of disturbed (partly chloritised) biotite from a diabase dike present in rocks located about 5 km west of the mineralisation. It seems unlikely that this diabase has any relationship to the formation of the mineralisation. The other biotites are interpreted as being primary biotite formed in the mineralisation-related pluton at the time of its consolidation. These biotites range from about 300 to 296 Ma, with three samples having ages of approximately 298 Ma. All of these biotite samples also yielded disturbed age spectra because of chlorite alteration.

The three samples of potassium feldspar were also from the pluton and yielded ages of approximately 292 to 290 Ma. The sample of white mica yielded an undisturbed age of 297.5 ±0.5 Ma, and thus gives the most accurate event date. A clear separation of micas and feldspar ages is apparent (Fig. 49), suggesting that formation of micas was somewhat earlier than that of the feldspars. The 298 Ma age may thus represent the time of consolidation of the pluton or the time of the earliest stage of mineralisation.

The 292 to 290 Ma range probably represents the time of most significant potassium metasomatism in the district. The presence of two apparently distinct ages (Fig. 49) is consistent with petrographic information, which shows biotite commonly present in samples of relatively unaltered plutonic rock (biotite granodiorite) as well as potassium feldspar occurring in the pluton and also in apophyses and veins in the metasedimentary wall rocks, mainly as a later-stage replacement of primary minerals or flooding in the matrix around older grains.

Most of the mineralisation-related minerals, such as chalcopyrite and molybdenite, are probably more temporally associated with this later-stage potassic alteration phase. Thus, the evidence suggests that emplacement of the pluton probably occurred about 298 Ma, followed by formation of the mineralisation between that time and about 290 Ma.

The intrusive rocks are found in a tectonic zone that is part of the main geofracture zone (the Kraków–Lubliniec zone). Tectonic activity in this zone terminated in Early Permian time (Żaba, 1999). This timing is also compatible with the Late Carboniferous age of both the intrusive activity and the mineralisation in the Myszków area.

An additional indication of the oldest possible age of the deposit was found in cores from borehole A-9, which was drilled about 4 km south-east of Myszków. The cores show pebbles of Cu mineralised porphyries and quartz as well as fragments of the Devonian and Carboniferous rocks, all of which are part of an Early Permian conglomerate. Especially interesting was the discovery of highly saline fluid inclusions in quartz from this conglomerate. These fluids are similar in composition to fluids encountered in the magmatic rocks of the Myszków area.

These observations suggest that the Cu-Mo-W mineralisation of the Myszków area was deposited no later than Early Permian time when rocks containing the mineralisation were already being eroded. The Myszków deposit as it exists today is, therefore, most probably only the deeper part of much larger, Late Carboniferous deposit.

The apparent Late Carboniferous age of the Myszków mineralisation and related mineralisation in the Myszków region has no other known analogues in Europe. The deposit thus seems to have formed at a unique time in European metallogeny.

We speculate that as much as 1.5 to 2 km of the Palaeozoic rock complex was eroded prior to Triassic time. The removal of these rocks may explain why the remaining rocks do not display more widely developed hydrothermal zoning that is typical for the upper parts of porphyry systems. Erosion may also explain the lack of the mineral zoning that is typical for porphyry-type mineralisation. The remnants of the Cu-Mo-W deposit at Myszków were buried in the Triassic.

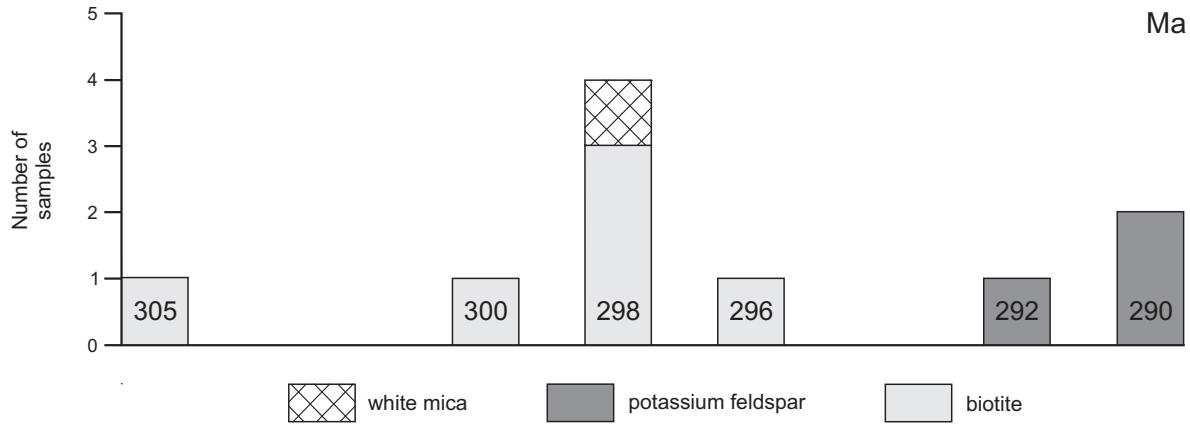

Fig. 49. Distribution of $^{40}Ar/^{39}Ar$ age dates, by mineral species

COMPARISON OF THE MYSZKÓW DEPOSIT TO OTHER PORPHYRY DEPOSITS

Comparison of the Myszków deposit to Climax-type porphyry deposits and to quartz-monzonite Mo deposits (White *et al*., 1981) reveals numerous common features. Mineralisation of the Myszków area is most similar to quartz-monzonite type Mo deposits, although there are no known monzonite rocks at Myszków (Table 24). The Myszków deposit differs, however, from the quartz-monzonite model because it has a linear shaped intrusion, lacks substantial fluorine, has a different kind of Bi mineralisation, lacks tin mineralisation, and has a fairly low Cu/Mo ratio.

The Myszków deposit also differs from porphyry Cu deposits with significant Mo concentrations found elsewhere, such as in Chile. The Mo concentrations in these porphyry Cu deposits varies between 0.01 and 0.05% and averages 0.02 %. They also contain substantial concentrations of Au and Ag (White *et al*., 1981). At Myszków, the average concentration of Mo is much higher than in typical Cu-Mo deposit and the concentrations of Au and Ag are much lower. The Myszków deposit also contains a considerably higher overall concentration level of W than do typical porphyry Cu-Mo deposit.

Many of the characteristics of the Myszków deposit are similar to those of described for the Lowell and Guilbert (1970) model for calc-alkaline-associated porphyry Cu deposits, including deposit chemistry, mineralogy, and vein morphology, tectonic setting, composition of associated plutonic rocks, fluid-inclusion compositions, and many other features.

However, for the Myszków mineralisation, several characteristics are not typical of most porphyry Cu deposits, particularly those in Europe. Mineralogically, scheelite is widespread in veins cutting the ore-related stock and is also found locally in skarn zones in the wall rocks. The literature on porphyry Cu deposits (Culver and Broughton, 1945; Hollister, 1978; Purdy, 1954) contains very few references to W minerals (principally scheelite and tungstenite); consequently, little is known about W in this deposit type. Where they have been identified in major porphyry Cu deposits, W minerals are usually found in skarn zones in the wall rocks and not in the ore-related pluton, as is the case at Myszków.

The closest analogues to the Myszków deposit may be the porphyry Cu-Mo deposits in the Cascade Mountains of the north-western United States, in the Canadian Cordillera of British Columbia and Yukon, and in Alaska that are described by Culver and Broughton (1945), Hollister (1978), and Purdy (1954). In this region of North America, scheelite and tungstenite are often mentioned as accessory minerals in many porphyry deposits. However, details concerning the abundance and distribution of W in these deposits are lacking.

No other porphyry Cu-Mo-type deposits with high concentrations of W have been reported in Europe outside of Poland. Thus, the W enrichment at Myszków also seems to be unique among deposits of this type in Europe.

Table 24

Comparison of the Myszków deposit to other Mo-porphyry deposits (the latter after White *et al*., 1981)

Characteristic elements of deposit	Climax type deposit	Quartz-monzonite type Mo deposit	the Myszków deposit
Rocks genetically connected with mineralisation	Granite porphyries	Quartz-monzonite porphyries	Granodiorite
Intrusive stages	Multistage granite intrusions	Complex intrusions: from quartz-diorites to quartz-monzonites	Intrusions composed of granodiorites, dacites, and rhyolites
Form of intrusion	Magmatic block	Magmatic block or batholith	Linear intrusion, probably connected with batholith
Type of ore body	Stockwork	Stockwork	Stockwork
Form of ore body	Reversed bowl	Reversed bowl and banded	Cone with ellipse-like basis
Average MoS_2 content	0,30–0,45%	0,10–0,20%	0,15%-0,40%
Ore body reserves	50–1000 mil. t	50–1000 mil. t	With average content = 0.25% Mo e[x] ~150 mil. t [x] Mo e = Mo + W + 0.3 Cu
MoS_2 dissemination	Rare	Rare	Rare
Age	Middle to Late Tertiary	Mesozoic and Tertiary	Late Carboniferous
Fluorine minerals	Fluorite, topaz	Fluorite	Rare fluorite
Bismuth minerals	Sulphosalts	Sulphosalts	Bismuthinite, sulphosalts, native Bi
Tungsten minerals	Wolframite (hübnerite)	Scheelite	Scheelite
Tin minerals	Cassiterite, stannine	Rare	Absent
Copper minerals	Chalcopyrite, rarely	Small amounts of chalcopyrite	Chalcopyrite
Silicification	Silica-rich core	Insignificant silicification	Insignificant silicification
Greisenisation	Greisens present	Greisens absent	Greisens absent
Cu:Mo relation in ore zone	From 1:1000 to 1:50	From 1:30 to 1:1	2:1; Cu:W:Mo = 2.7:1:14

RECOMMENDATIONS FOR FURTHER STUDIES

Widely spaced, deep drilling in the north-eastern border of the Upper Silesian Coal Basin (USCB), the area known also as Kraków–Lubliniec region, has identified many localities with Cu porphyry-type features, however, no major deposit has as yet been delineated. Our data show that the mineralised area at Myszków has not yet been completely defined by deep drilling. The criteria established for our model of the Myszków deposit should be useful in defining the lateral extent of this deposit and useful in the search for additional, similar deposits in the Kraków–Lubliniec region.

The distributions of anomalous Cu, Mo, S, W, and Te extend laterally well beyond the area of deep drilling in the Myszków area. Clearly, these elements are the best to use in exploring for porphyry-type mineralisation, both in the Myszków area and in the rest of the Kraków–Lubliniec region.

The presence of NW–SE linear parallel geochemical and geophysical anomalies near Myszków may be a pattern repeated regionally in other parts of the Kraków–Lubliniec region. This NW–SE linearity should be tested in the vicinity of other poorly defined geochemical and geophysical anomalies found elsewhere in the region.

Because the Vendian to Late Carboniferous rocks that may contain mineralisation are not exposed in most of the Kraków–Lubliniec region, additional drilling, as well as geophysical and other studies, will be necessary to evaluate the economic potential of this incompletely understood porphyry Cu province.

SUMMARY AND CONCLUSIONS

The Myszków deposit is one of several porphyry Cu-type deposits that have been identified within a poorly defined belt of Precambrian to Palaeozoic rocks in south-central Poland. This belt is nowhere exposed at the surface so that the maximum regional extent of rocks that may host porphyry deposits is unknown.

The Myszków mineralisation is in a complex of Vendian to Early Cambrian-aged metasedimentary rocks that was intruded by a stock of Late Carboniferous age. These primarily clayey to muddy to sandy wall rocks were regionally metamorphosed to produce minerals in the chloritic zone of the greenschist facies. Greenschist facies temperatures are suggested by mineral parageneses and by mineral chemistry.

The thermal and thermal–metasomatic metamorphism, which is younger than the regional metamorphism, is spatially associated with the Variscan granitoid intrusion both near wall rock direct and in more distant areas. Hornfelses, pyroxene-amphibole skarns, and metasomatites were formed during contact metamorphism. Mineral parageneses suggests an alteration temperature range of about 350–500°C, with the upper limit based on the presence of garnets (Deer *et al*., 1962).

The isotopic dating of mineralisation related feldspars and micas indicates that the age of the intrusive rocks and the mineralisation phases is Late Carboniferous, an age of porphyry--type deposit formation not known to be present elsewhere in Europe. Most porphyry Cu deposits discovered to date in Europe were formed in Cretaceous or Tertiary time. The Late Carboniferous (Variscan) age of the Myszków mineralisation may therefore be unique for European deposits of this type.

The chemistry, mineralogy, and vein morphology of the Myszków deposit are generally similar to those of the Lowell and Guilbert (1970) model for calc-alkaline-associated porphyry Cu deposits. The mineralisation at Myszków consists mainly of stockwork veins; skarn minerals are uncommon. Eight substages of mineral deposition have been identified, five of which are closely associated with formation of the Myszków porphyry Mo-W-Cu mineralisation.

The complete mineral assemblage of the Myszków deposit, which is found in all the periods and stages of mineralisation, consists of pyrite, chalcopyrite, magnetite, molybdenite, sphalerite, galena, scheelite, and rutile. More rarely bornite, hematite, pyrrhotite, marcasite, ilmenite, tungstenite, and ferberite are encountered. Bismuthinite, native Bi, chalcopyrite, cubanite, emplectite, aikinite, hessite, tetradymite, cosalite, wittichenite, tetrahedrite, tennantite, valleriite, and chalcocite appear only in trace amounts. Chalcocite, covellite, malachite, and goethite have been observed in the weathered zone.

The results of a factor analyses on the chemical data for the deposit support the concept of multiple stages of mineralisation at Myszków that has been observed in the petrographic investigations. Copper is loaded on two different factors, suggesting at least two stages of Cu mineralisation. The presence of potassic metasomatism and base-metal-related factors emphasises that additional stages of mineralisation can be documented using chemical analyses.

The abundance levels of the elements analysed for this study shows that as many as 11 elements (Ag, Bi, Cd, Cu, K, Mo, Pb, S, Sb, Te, and W) are clearly enriched in the mineralised area. In contrast, As, Hg, Au, Be, Mn, and Zn show no significant enrichment in the system. Localities with high concentrations of these latter elements are generally found in contact metasomatic zones where they were enriched by remobilization during formation of the mineral deposits.

The Myszków mineralisation is strongly enriched in Cu, Mo, and W but contains very little Au. The enrichment of Mo but not Au in this deposit is typical of many calc-alkaline-type porphyry Cu deposits whose causative pluton and ore-related elements are derived from continental rather than oceanic crust.

Guilbert and Park (1986) suggest that a "typical" calc-alkaline-type porphyry Cu deposit might contain 0.45 percent hypogene Cu and 0.015 percent Mo, giving a Cu/Mo ratio of about 30. The mean values for Cu and Mo at Myszków are 500 and 130 ppm, respectively (Table 21), giving a ratio for the Myszków mineralisation of about 4.

At Myszków the mean value for Mo is similar to the value given by Guilbert and Park (1986); however, the Cu value for Myszków is much lower than that given by these authors. Thus, even allowing for wide ranges in the overall Cu and Mo concentrations in "typical" deposits, the Myszków mineralisation does not seem to fit the "standard". The low ratio at Myszków suggests that much of any high-level, Cu-rich part of this deposit (if it ever existed) was eroded prior to deposition of the overlying Triassic rocks.

Scheelite is widespread in the ore-related stock at Myszków and is also found locally in wall rock skarn zones. In comparison to other calc-alkaline-type porphyry Cu deposits, this area contains an unusually high concentration of W, particularly in the mineralised part of the stock. Therefore, we classify the Myszków deposit as being closest to a porphyry Mo-W model.

Zoning is present in vertical section for most of the mineralisation-related elements. This zoning is spatially related: (1) to the causative pluton (especially Mo and W), (2) to contact metasomatic zones (e.g., Be, Mn, Pb, and Zn), or (3) to neither a specific lithology nor contact zones (e.g., Ag, Bi, Cu, S, and Te). A concentric, vertical aureole of elements was not found. In plan, no well-defined element zoning patterns were identified within the area of deep drilling for either level examined; however, some deposit-related elements produce wider aureoles than do others.

Pre-Triassic weathering of the Vendian to Late Carboniferous rocks at Myszków was not significant. As a result, no supergene enrichment zone is present in this area. In addition, the potassic alteration zone and the distributions of sulphide minerals and anomalies of many of the sulphide mineral-related elements (Ag, Bi, Cu, Mo, S, Te, W, and Zn) extend all the way to the erosion surface at the top of the Vendian to Late Carboniferous complex at Myszków.

Overall, the mineralisation also exhibits typical mineralogy for the deeper parts of a porphyry Cu system. Thus, it may be concluded that the upper (perhaps significant) part of this deposit was removed by rapid erosion that was followed by rapid burial of the erosion surface by a sequence of Triassic marine rocks.

However, more complete deposits of this type-deposits, which might also contain supergene enrichment zones, could be present in down-faulted blocks in other parts of the Kraków–Lubliniec region, in areas subjected to less extensive erosion.

Acknowledgments. We express our special thanks to our late colleague, **Dr. Kazimierz Piekarski**, economic geologist of the Polish Geological Institute Upper Silesian Branch, in Sosnowiec. Without his scientific enthusiasm, and sometimes even stubbornness, the Myszków Mo-W-Cu deposit would still remain undiscovered. We therefore dedicate this monograph to his memory.

We also thank all the economic geologists and other scientists investigating the Precambrian and Palaeozoic basement of the Kraków–Lubliniec area and its associated mineralisation, and especially those investigating the Myszków area, for their scientific innovation and research. Their research results are the foundation of this monograph.

We are also indebted to those scientists who have conducted supplementary investigations on the geology and ore mineralisation of the Myszków area, the results of which have been incorporated into this monograph. In particular, we thank W. Heflik, Z. Migaszewski, and O. Jeleński for their complementary petrographic investigations of the magmatic rocks, and S. Hałas and his team from the Physics Institute of the Maria Skłodowska-Curie University in Lublin, for their sulphur isotope studies of the ore minerals. D. Sikorska helped us with the illustrations and text.

Many other people assisted us as part of the Polish–American geochemical project. We especially thank L. A. Bradley, K. J. Curry, M. W. Doughten, D. L. Fey, R. J. Knight, A. H. Love, J. S. Mee, C. A. Motooka, J. M. Motooka, R. M. O'Leary, C. S. Papp, B. H. Roushey, and D. F. Siems of the USGS, and H. Bellok, B. Budzicka, A. Chabło, M. Gniadek, E. Górecka, K. Hnatyszak, A. Jaklewicz, I. Jaron, J. Kucharczyk, B. Kudłowska, E. Maciołek, W. Narkiewicz, and P. Pasławski of the Polish Geological Institute for their assistance with the analyses.

REFERENCES

AHRENS L. H., ERLANK A. J., 1978 — Bismuth, parts 83D-83M; 83O. *In*: Handbook of Geochemistry (ed. K. H. Wedepohl), v. II/5. Springer-Verlag, New York.

BADERA J., 1992 — Tektonika utworów paleozoicznych w otworze wiertniczym Mrzygłód Pz-36. [Tectonics of the Palaeozoic deposits in the Mrzygłód Pz-36 borehole; in Polish]. Arch. WNoZ UŚ., Sosnowiec.

BADERA J., 1999 — Wpływ tektoniki na rozwój mineralizacji polimetalicznej w rejonie Myszkowa. [Influence of tectonics on the polymetallic mineralisation in Myszków area; in Polish]. Arch. PIG, Sosnowiec.

BANAŚ M., MOCHNACKA K., SALAMON W., 1977 — Analiza mineralogiczno-geochemiczna okruszcowania łupków staropaleozoicznych na tle procesów metasomatycznych i charakterystyki petrograficznej skał (otwór wiertniczy Pz-5). [Mineralogic-geochemical analyses of the Old Palaeozoic shists mineralisation with regards to metasomatic processes and to petrographic characteristics of rocks (borehole Pz-5); in Polish]. Arch. PIG, Sosnowiec.

BANAŚ M., PAULO A., PIEKARSKI K., 1972 — Copper and molybdenum mineralization in the vicinity of Mrzygłód [Eng. Sum.]. *Rudy i Met. Nież.*, **1**: 3–7.

BEANE R. E., TITLEY S. R., 1984 — Medno-porfirovye mestorożdenija. C.II: Gidrotermalnye izmenenija i mineralizacija. *In*: Genezis rudnych mestorożdenij. Moskva Mir, (transl. from: Economic Geology, Seventy Fifth Anniversary, vol. 1905–1980): 278–333.

BEATY R. D., MANUEL O. K., 1973 — Tellurium in rocks. *Chemical Geology*, **12**:155–159.

BODNAR R. J., BEANE R. E., 1980 — Temporal and spatial variations in hydrothermal fluid characteristics during vein-filing in pore cover overlying deeply buried porphyry copper mineralisation at Red Mountain, Arizona. *Econ. Geol*., **75**: 876–893.

BOGACZ K., 1980 — Tectonics of the Paleozoic rocks of the Dębnik region [Eng. Sum.]. *Rocz. Pol. Tow. Geol.* **50**, 2: 183–205.

BOJKOWSKI K., BUKOWY S., 1966 — The facial zones of the Lower Carboniferous in the Silesia–Cracow Anticlinorium [Eng. Sum.]. *Acta Geol. Pol*., **16**, 2: 201–228.

BROCHWICZ-LEWIŃSKI W., POŻARYSKI W., TOMCZYK H., 1983 — Paleozoic strike-slip movements in southern Poland [Eng. Sum.]. *Prz. Geol*., **31**, 12: 651–658.

BUKOWY S., 1964a — New views on the structure of the north-eastern margin of the Upper Silesian Coal Basin [Eng. Sum.]. *Biul. Inst. Geol*., **184**: 5–34.

BUKOWY S., 1964b — Notes on the geological structure of the Paleozoic of the eastern margin of the Upper Silesian Coal Basin [Eng. Sum.]. *Biul. Inst. Geol*., **184**: 21–38.

BUKOWY S., 1982 — Problemy budowy paleozoiku regionu śląsko-krakowskiego. [Problems of the Palaeozoic structure in the Silesia–Cracow region; in Polish]. *Przew. LIV Zjazdu Pol. Tow. Geol. Sosnowiec 23–25.IX.1982*: 7–25.

BUKOWY S., 1984 — Struktury waryscyjskie regionu śląsko-krakowskiego. [Variscan structures of the Silesia-Cracow region; in Polish]. *Pr. Nauk. UŚl.,* **691**: 1–67.

BUKOWY S., 1994 — Outline of Paleozoic structure of NE margin of the Upper Silesian Coal Basin [Eng. Sum.]. *In: Przew. LXV Zjazdu Pol. Tow. Geol. Sosnowiec 22–23.IX.1994*: 14–30.

BUKOWY S., ŚLÓSARZ J., 1968 — The results of Bębło borehole [Eng. Sum.]. *Biul. Inst. Geol*., **212**: 7–34.

BUŁA Z., 1994 — Problems of stratigraphy and development of Lower Paleozoic sediments of the NE margin of the Upper Silesian Coal Basin [Eng. Sum.]. *Przew. LXV Zjazdu Pol. Tow. Geol., Sosnowiec 22–24.IX.1994*: 31–57.

BUŁA Z., 2000 — The Lower Palaeozoic of Upper Silesia and West Małopolska [Eng. Sum.]. *Pr. Państw. Inst. Geol*., **171**: 5–71.

BUŁA Z., JACHOWICZ M., 1996 — The Lower Paleozoic sediments in the Upper Silesian Block. *Geol. Quart*., **40**, 3: 299–336.

BUŁA Z., HABRYN R., KRIEGER W., KUREK S., MARKOWIAK M., PREIDL M., WOŻNIAK P., 1996 — Podsumowanie badań geologicznych wykonanych na NE obrzeżeniu Górnośląskiego Zagłębia Węglowego. [Geological studies on the NE margin of the Upper Silesian Coal Basin – a summary; in Polish]. Arch. PIG, Sosnowiec.

BUŁA Z., JACHOWICZ M., ŻABA J., 1997 — Principal characteristics of the Upper Silesian Block and Małopolska Block border zone (Southern Poland). *Geol. Mag*., **134**, 5: 669–677.

CARMICHAEL I. S., TURNER F. J., VERHOOGEN J., 1974 — Igneous petrology. McGraw-Hill, New York.

CHAFFEE M. A., EPPINGER R. G., LASOŃ K., ŚLÓSARZ J., PODEMSKI M., 1994 — The Myszków porphyry copper-molybdenum deposit, Poland: *Internat. Geol. Rev.*., **36**: 947–960.

CHAFFEE M. A., EPPINGER R. G., LASOŃ K., ŚLÓSARZ J., PODEMSKI M., 1997 — A geological alteration, and geochemical model of the Myszków porphyry Cu-Mo deposit, southern Poland. *In*: Mineral Deposits: Research and Exploration — Where do They Meet? (eds. Papunen, Heikki): 851–854. A.A. Balkema, Rotterdam.

CHAFFEE M. A., EPPINGER R. G., LASOŃ K., ŚLÓSARZ J., 1999 — Geologic information and analytical results for samples of drill core from the Myszków porphyry copper-molybdenum deposit, southern Poland: U.S. Geological Survey Open-File Report, **99-530-A**: 118 p.

CIEŚLA E., KOSOBUDZKA I., OKULUS H., 1984 — Monoklina śląsko-krakowska w naturalnych polach fizycznych Ziemi: grawitacyjnym i magnetycznym. [Silesia–Cracow Monocline in the Earth natural physical fields: gravity and magnetic ones; in Polish]. Sympozjum n.t. Badania geofizyczne przy poszukiwaniu i rozpoznawaniu złóż surowców stałych. PBG i SITG, Jabłonna k/Warszawy, 7–8 czerwca 1984: 1–33.

CLOKE P. L., KESLER S. E., 1979 — The halite trend in hydrothermal solutions. *Econ. Geol*., **74**: 1823–1831.

COX D. P., SINGER D. A., 1986 — Mineral deposit models. *U.S. Geol. Surv. Biull.*, **1693**: 73–122.

COAKLEY G. J., 1975 — Tellurium. *In*: U.S. Bureau of Mines staff, mineral facts and problems, 1975 Edition. U.S. Bureau of Mines: 1103–1108.

CULVER H. E., BROUGHTON W. A., 1945 — Tungsten resources of Washington. *State of Washington Division of Geology Bulletin*, **34**: 89 p.

DEER W. A., HOWIE R. A., ZUSSMAN J., 1962 — Rock-forming minerals. Longmans, London.

EASTOE C. J., 1978 — A fluid inclusion study of the Panguna porphyry copper deposit, Bougainville, Papua New Guinea. *Econ. Geol*., **73**: 721–748.

EKIERT F., 1957 — Geological conditions of the occurrence of magmatic rocks in Mrzygłód near Zawiercie Śląskie (Upper Silesia) [Eng. Sum.]. *Kwart. Geol*., **1**, 1: 106–112.

EKIERT F., 1971 — Geological structure of the Sub-Permian basement of the north-eastern margin of the Upper Silesian Coal Basin [Eng. Sum.]. *Pr. Inst. Geol*., **66**: 5–77.

GeoEAS, 1988 — (Geostatistical Environmental Assessment Software) User's guide. Environmental Monitoring System Laboratory, Las Vegas.

GŁADYSZ J., JACHOWICZ M., PIEKARSKI K., 1990 — Palaeozoic acritarcha from the Siewierz vicinity (northern margin of the Upper Silesian Coal Basin) [Eng. Sum.]. *Kwart. Geol*., **34**, 4: 623–630.

GUILBERT J. G., PARK C. F., Jr., 1986 — The geology of ore deposits: 985 p. W. H. Freeman and Company, New York.

HABRYN R., MARKOWIAK M., ŚLÓSARZ J., 1994 — Prospects of the discovery of a new ore body in the NW direction from the Myszków Mo-W-Cu deposit [Eng. Sum.]. *Prz. Geol*., **42**, 8: 611–614.

HARAŃCZYK C., 1982a — Mineralizacja paleozoiczna północnego i wschodniego obrzeżenia Górnośląskiego Zagłębia Węglowego. [Palaeozoic mineralisation of the Northern and Eastern margins of the Upper Silesian Coal Basin; in Polish]. *Przew. LIV Zjazdu Pol. Tow. Geol*., *Sosnowiec 23–25.IX.1982*: 38–44.

HARAŃCZYK C., 1982b — Nowe dane do poznania kaledońskiego górotworu Krakowidów. [New data to understand the Caledonian Krakowidy orogen; in Polish]. *Przew. LIV Zjazdu Pol. Tow. Geol*., *Sosnowiec 23–25.IX.1982*: 90–102.

HARAŃCZYK C., 1988 — Significance of the sutural geofracture Zawiercie–Rzeszotary for development and occurrence of Paleozoic mineralization and ore deposits of Zn-Pb [Eng. Sum.]. *Prz. Geol*., **36**, 7: 379–381.

HARAŃCZYK C., 1994a — Znaczenie sutury terranowej Zawiercie–Rzeszotary dla poznania kaledońskiego transpresyjnego górotworu krakowidów. [The importance of the Zawiercie–Rzeszotary terrane suture to understand the Caledonian transpresive Krakovidy orogene; in Polish]. *Przew. LXV Zjazdu Pol. Tow. Geol., Sosnowiec, 22–24.IX.1994*: 69–80.

HARAŃCZYK C., 1994b — Caledonian Kracovides (SW Poland) as a transpressional orogene [Eng. Sum.]. *Prz. Geol*., **11**: 893–901.

HEFLIK W., 1982 — Utwory metamorficzne z podłoża brzeżnej części Karpat obszaru Cieszyn–Rzeszotary. [Metamorphic rocks from the basement of the Carpathien marginal part, Cieszyn–Rzeszotary area; in Polish]. *Przew. LIV Zjazdu Pol. Tow. Geol*. *Sosnowiec 23–25.IX.1982*: 210–213.

HEFLIK W., 1992 — Contact metamorphic rocks from the vicinity of Myszków (Upper Silesia). *Bull. Pol. Acad. Sci*., **40**, 1: 31–42.

HEFLIK W., MORYC W., MUSZYŃSKI M., 1992 — Lamprophyres of the Silesia-Cracow Region. *Bull. Pol. Acad. Earth Sc*., **40**, 1: 23–28.

HEFLIK W., MUSZYŃSKI M., PIECZKA A., 1985 — Lamprophyres from the vicinities of Zawiercie [Eng. Sum.]. *Kwart. Geol*., **29**, 3/4: 529–542.

HEFLIK W., PIEKARSKI K., 1989 — On trachyandesite from the vicinity of Myszków, South Poland [Eng. Sum.]. *Geologia Kwart. AGH*, **15**, 4: 107–116.

HEFLIK W., PARACHONIAK W., PIEKARSKI K., RATAJCZAK T., RYSZKA J., 1975 — The petrography of the Old Palaeozoic rocks from the vicinity of Myszków (Upper Silesia) [Eng. Sum.]. *Zesz. Nauk. AGH Geologia*, **1**, 4: 35–43.

HOLLISTER V. F., 1978 — Geology of the porphyry copper deposits of the western hemisphere. New York, Society of Mining Engineers of the American Institute of Mining, Metallurgical, and Petroleum Engineers: 219 p.

HORTON D. J., 1978 — Porphyry-type copper-molybdenum mineralization belts in eastern Queensland, Australia. *Econ. Geol*., **73**: 904–921.

JACHOWICZ M., 1995 — Opracowanie stratygrafii starszego paleozoiku na NE obrzeżeniu GZW w oparciu o badania mikropaleontologiczne Acritarcha. [Report on the research on the Old Palaeozoic stratigraphy of the NE margin of the USCB, based on the micropalaeontological studies of Acritarcha; in Polish]. Arch. PIG, Sosnowiec.

JACOBS D. C., PARRY W. T., 1976 — A comparison of the geochemistry of biotite from some basin and range stocks. *Econ. Geol*., **71**: 1029–1035.

JANKOVIĆ S., 1980 — Ore-deposit types and major copper metallogenic units in Europe. *In*: European copper deposits, Proceedings of an International Symposium held at Bor, Yugoslavia, 18–22 September 1979, Belgrade (eds. S. Janković, R. H. Sillitoe). *Society for Geology Applied to Mineral Deposits Special Publication*, **1**: 9–25. UNESCO Publications.

JARMOŁOWICZ-SZULC K., 1984 — Datowania metodą K-Ar skał NE obrzeżenia Górnośląskiego Zagłębia Węglowego. [K-Ar datings of rocks from NE margin of the Upper Silesian Coal Basin; in Polish]. Sprawozdania z posiedzeń naukowych Instytutu Geologicznego. *Kwart. Geol*., **28**, 3/4: 749–750.

JARMOŁOWICZ-SZULC K., 1985 — K-Ar datings of igneous rocks from NE margin of the Upper Silesian Coal Basin [Eng. Sum.]. *Kwart. Geol*., **29**, 2: 343–354.

JURKIEWICZ H., 1975 — The geological structure of the basement of the Mezozoic in the central part of the Miechów Trough [Eng. Sum.]. *Biul. Inst. Geol*., **283**: 5–100.

JUSKOWIAK O., 1971 — Petrologia kwaśnych skał magmowych z północno-wschodniego obrzeżenia Górnośląskiego Zagłębia Węglowego. *Kwart. Geol*., **15**, 3: 705–706.

KALJUŻNYJ V. A., 1960 — Metody vyvćennja bagatofazovych vkljućen' u mineralach. Kyiv AN URSR.

KARWOWSKI Ł., 1988 — Mineral-forming fluids of the Variscan Cu-porphyry formation from the Myszków–Mrzygłód area of Cracovides [Eng. Sum.]. *Pr. Nauk. UŚl.*, **929**: 1–89.

KARWOWSKI Ł., 1989 — Badania temperaturowe metodą homogenizacji wrostków w utworach żyłowych paleozoiku z rejonu Myszkowa i Mrzygłodu. [Temperature studies, using the homogenization methods, of the inclusions in Palaeozoic veins from the Myszków and Mrzygłód regions; in Polish]. Arch. PIG, Sosnowiec.

KIERSNOWSKI H., 1991 — Lithostratigraphy of the Permian north-west of the Upper Silesia Coal Basin — a new proposal [Eng. Sum.]. *Prz. Geol*., **39**, 4: 198–203.

KOTAS A., 1982 — Zarys budowy geologicznej Górnośląskiego Zagłębia Węglowego. [Scheme of the Upper Silesian Coal Basin geological structure; in Polish]. *Przew. LIV Zjazdu Pol. Tow. Geol.*, *Sosnowiec 23–25.IX.1982*: 45–72.

KOTAS A., 1985 — Structural evolution of the Upper Silesian Coal Basin (Poland). X Cong. Int. Strat. Geol. Carb., C. R., **3**, Madrid: 459–469.

KOZŁOWSKI A., 1981 — Melt inclusions in pyroclastic quartz from Carboniferous deposits of the Holy Cross Mts., and the problem of magmatic corrosion. *Acta Geol. Pol*., **31**, 3/4: 273–284.

KOZŁOWSKI A., KARWOWSKI Ł., 1972 — Physico-chemical conditions of the drusy mineral crystallisation from Alam Kuh (Iran). *Bull. Acad. Pol. Sci., Ser. Sci. de la Terre*, **20**: 249–255.

LASOŃ K., 1990 — Opracowanie metodyki geochemicznej oceny prognoz mineralizacji polimetalicznej w północno-wschodnim obrzeżeniu GZW. [Preparation of the geochemical methodics for the assessment of the polymetallic mineralisation prospect in the NE margin of the Upper Silesian Coal Basin; in Polish]. Arch. PIG, Sosnowiec.

LASOŃ K., 1992 — Zoning of polymetallic mineralisation in the Paleozoic from the Myszków region (NE margin of the Upper Silesian Coal Basin) [Eng. Sum.]. *Arch. Miner*., **48**, 1/2: 43–59.

LAZNICKA P., 1976 — Porphyry copper and molybdenum deposits of the USSR and their plate tectonic settings. *Amer. Inst. Mining Metall. Petroleum Engineers Trans*., **82**: B14–B32.

LE MAITRE R. W., 1984 — A proposal by the IUGS Subcommission on the Systematics of igneous rocks for a chemical classification of volcanic rocks based on the total alkali-silica (TAS) diagram. *Australian J., Earth Sc*., **31**: 243–255.

LEUTWEIN F., 1978 — Tellurium. Parts 52B–52K; 52O. *In*: Handbook of Geochemistry (ed. K. H. Wedepohl), v. II/4. Springer-Verlag, New York.

LOWELL J. D., GUILBERT J. M., 1970 — Lateral and vertical alteration — mineralisation zoning in porphyry ore deposits. *Econ. Geol*., **65**: 373–406.

ŁYDKA K., 1973 — Late-Precambrian and Silurian in the Myszków area [Eng. Sum.]. *Kwart. Geol*., **17**, 4: 700–712.

MARKIEWICZ J., 1989 — Charakterystyka petrograficzna skał magmowych. Dokumentacja geologiczna otworu wiertniczego Pz-31. [Petrographic characteristics of the magmatic rocks. Geological data from the Pz-31 borehole; in Polish]. Arch. PIG, Sosnowiec.

MARKIEWICZ J., 1994 — Zróżnicowanie kwaśnych skał magmowych w strefach kontaktowych na podstawie wybranych profili otworów wiertniczych rejonu Myszkowa–Mrzygłodu. [Differentiation of the acidic magmatic rocks within the contact zones, based on the chosen boreholes profiles from Myszków–Mrzygłód region; in Polish]. *Posiedz. Nauk. PIG*, **50**, 2: 98–99.

MARKIEWICZ J., 1995 — Petrografia strefy apikalnej granitoidów mrzygłodzkich [Petrography of the Mrzygłód granitoides apical zone; in Polish]. Arch. PIG, Warszawa.

MARKIEWICZ J., 1998 — Petrography of the apical zone of the Mrzygłód granitoids [Eng. Sum.]. *Biul. PIG*, **382**: 5–29.

MARKIEWICZ J., MARKOWIAK M., 1998 — Inwentaryzacja (kolekcja skał i baza danych) paleozoicznych skał krystalicznych i piroklastycznych regionu krakowsko-częstochowskiego. [Catalogue of the Palaeozoic crystalline and pyroclastic rocks from Cracow-Częstochowa region; in Polish]. Arch. PIG, Warszawa.

MARKIEWICZ J., ŚLÓSARZ J., TRUSZEL M., 1993 — Pozycja geologiczna mineralizacji Cu-Mo-W w paleozoiku północno-wschodniego obrzeżenia GZW. [Geological position of the Cu-Mo-W mineralisation in Palaeozoic of the NE margin of the USCB; in Polish]. *Pr. Spec. Pol. Tow. Mineral*., **3**: 47–54.

MARKOWIAK M., HABRYN R., 1994 — Aktualne wyniki badań geochemicznej strefowości zmineralizowanych utworów paleozoicznych obszaru Myszkowa. [The latest results of the geochemical research on the zoning of the Palaeozoic mineralised rocks from Myszków area; in Polish]. Arch. PIG, Sosnowiec.

MASAO M., MASAO G., MITSUO H., 1965 — The geologie development of the Japanese Islands. Tsukiji Shokan Co. Ltd., Tokyo.

MORYC W., HEFLIK W., 1998 — Metamorphic rocks in the basement of the Carpathians between Bielsko-Biała and Cracow. *Geol. Quart*., **42**, 1: 1–14.

MIYASHIRO A., 1973 — Metamorphism and metamorphic belts. George Allen & Unwin Ltd., London.

NARKIEWICZ M., 1978 — Stratigraphy and facies development of the Upper Devonian in the Olkusz–Zawiercie area, Southern Poland [Eng. Sum.]. *Acta Geol. Pol*., **28**, 4: 415–470.

NARKIEWICZ M., RACKI G., 1984 — Stratigraphy of the Devonian of the Dębnik Anticline [Eng. Sum.]. *Kwart. Geol*., **28**, 3/4: 513–546.

NASH J. T., THEODORE T. G., 1971 — Ore fluids in a porphyry copper deposit at Copper Canyon, Nevada. *Econ. Geol*., **66**: 385–399.

NAUMOV V. B., MALININ S. D., 1968 — Novyj metod opredelenija davlenija po gazovo-żidkim vklućenijam. *Geochimija*, **4**: 432–441.

NEHRING-LEFELD M., MODLIŃSKI Z., SIEWNIAK-MADEJ A., 1992 — Biostratigraphy of the Old Paleozoic carbonates in the Zawiercie area (NE margin of the Upper Silesian Coal Basin). *Geol. Quart.*, **36**, 2: 171–198.

NEHRING-LEFELD M., SZYMAŃSKI B., 1998 — Ordovician stratigraphy in the Żarki-Myszków (NE margin of the Upper Silesian Coal Basin). *Geol. Quart*., **42**, 1: 29–40.

NIEĆ M., 1988 — Possibility of the ore deposits discovery within the older Paleozoic rocks, NE margin of the USCB [Eng. Sum.]. *Prz. Geol*., **36**, 7: 390–395.

NIGGLI P., 1954 — Rocks and mineral deposits. *In*: M. Freeman and Company. San Francisco.

PAJCHLOWA M., SIEWNIAK-MADEJ A., CHOROWSKA M., TRUSZEL M., SOBOŃ-PODGÓRSKA J., 1983 — Dewon. *W*: Złoża rud metali na tle budowy geologicznej NE obrzeżenia GZW. Stratygrafia. cz. 1. [Devonian. *In*: Metal ores deposits with respect to geological structure of the NE margin of the Upper Silesian Coal Basin. Stratigraphy, pt. 1; in Polish]. Arch. PIG, Sosnowiec.

PARRY W. T., 1972 — Chloride in biotite from basin and range plutons. *Econ. Geol*., **67**: 972–975.

PASZKOWSKI M., 1988 — Basen dinantu w okolicach Krakowa — próba syntezy. [Dinantian basin in the Cracow area: an attempt of a synthesis]. *Prz. Geol*., **36**: 200–207.

PAVLOVA I. G., ALEKSANDROV G. V., 1986 — Molybdenium. *In*: Kritierii prognoznoj ocienki tieritorij (ed. D. B. Rundkwist). Leningrad: 295–316.

PETTIJOHN F. J., POTTER P. E., SIEVER R., 1972 — Sand and sandstone. Springer-Verlag, Berlin–Heidelberg–New York.

PIEKARSKI K., 1970 — Projekt wierceń parametrycznych dla stworzenia podstaw do poszukiwań złóż surowców metalicznych w utworach staropaleozoicznych północno-wschodniego obrzeżenia GZW. [Parametric drillings programme, to prepare foundations for metallic deposits prospecting in the Old Paleozoic rocks of the NE margin of the Upper Silesian Coal Basin; in Polish]. Arch. PIG, Sosnowiec.

PIEKARSKI K., 1971a — Perspektywy występowania złóż miedziowo-molibdenowych w utworach staropaleozoicznych północno-wschodniego obrzeżenia GZW. [Prospects of the copper-molybdenum deposits existence in the Lower Palaeozoic formations of the NE margin of Upper Silesian Coal Basin; in Polish]. Sprawozdania z Posiedzeń Naukowych Instytutu Geologicznego. *Kwart. Geol*., **15**, 3: 710–711.

PIEKARSKI K., 1971b — Signs of mineralization in Silurian formations in the "Lubliniec" borehole [Eng. Sum]. *Rudy i Met. Nież*., **4**: 189–193.

PIEKARSKI K., 1982a — Molybdenum schists in the vicinities of Myszków [Eng. Sum.]. *Prz. Geol***. 30**, 7: 335–340.

PIEKARSKI K., 1982b — Aktualny stan badań okruszcowania paleozoiku NE obrzeżenia GZW. [The present status of the research on the Palaeozoic mineralisation in the NE margin of the USCB; in Polish]. *Przew. LIV Zjazdu Pol. Tow. Geol. Sosnowiec 23–25.IX.1982*: 26–38.

PIEKARSKI K., 1985 — Metallogenic and prognostic analysis of the Palaeozoic sequence of the NE margin of the Upper Silesian Coal Basin [Eng. Sum.]. *Rocz. Pol. Tow. Geol. (1983)*, **53**, 1–4: 207–234.

PIEKARSKI K., 1988 — New data on ore mineralization in Late Paleozoic sediments of the Myszków–Mrzygłód area, northeastern margin of the Upper Silesian Coal Basin (USCB) [Eng. Sum.]. *Prz. Geol*., **36**, 7: 381–387.

PIEKARSKI K., 1995 — Geologic setting and ore mineralisation characteristics of the Myszków area (Poland). *Geol. Quart*., **39**, 1: 31–42.

PIEKARSKI K., GAJOWIEC B., HABRYN R., KARWASIECKA M., KURBIEL H., ŁUSZCZKIEWICZ A., MARKIEWICZ J., MARKOWIAK M., SIEMIŃSKI A., STĘPNIEWSKI M., TRUSZEL M., 1993 — Dokumentacja geologiczna złoża rud molibdenowo-wolframowo-miedziowych Myszków w kategorii C_2 [Pre-feasibility study of the Myszków Mo-W-Cu ore deposit, in C_2 category; in Polish]. Arch. PIG, Sosnowiec.

PIEKARSKI K., KURBIEL H., ŚLUSARZ J., 1979 — Projekt badań geologiczno-złożowych utworów staropaleozoicznych w obszarze Poraj–Mrzygłód. [A geological-economic research programme on the Old Palaeozoic rocks from Poraj–Mrzygłód area; in Polish]. Arch. PIG, Sosnowiec.

PIEKARSKI K., MARKIEWICZ J., TRUSZEL M., 1982 — Lithological-petrographic characteristics of Ordovician strata in the Myszków–Mrzygłód area [Eng. Sum.]. *Prz. Geol*., **30**, 7: 340–347.

PIEKARSKI K., MIGASZEWSKI Z., 1993 — Old Paleozoic ore mineralization of the Myszków–Mrzygłód area (NE margin of the Upper Silesian Coal Basin). *Geol. Quart*., **37**, 3: 385–396.

PIEKARSKI K., SIEWNIAK-WITRUK A., 1978 — On the occurrence of Ordovician in the vicinities of Mrzygłód [Eng. Sum.]. *Prz. Geol*., **11**: 647–648.

PIEKARSKI K., SZYMAŃSKI B., 1982 — Stratigraphic position of the Kotowice Beds [Eng. Sum.]. *Prz. Geol*., **7**: 366–369.

PIEKARSKI K., SZYMAŃSKI B., WIELGOMAS L., 1985 — A new Ordovician stratigraphic reference point in the vicinities of Myszków [Eng. Summ.]. *Prz. Geol*., **33**, 9: 501–503.

PIEKARSKI K., WIELGOMAS L., KURBIEL H., STACHURA A., 1987 — Aneks do projektu badań geologiczno-złożowych utworów staropaleozoicznych w obszarze Poraj–Mrzygłód, obejmujący prace poszukiwawcze dla udokumentowania złoża w kat. C_2 rud molibdenu i pierwiastków towarzyszących. [An annex to the exploration programme of the Mo and associated elements ore deposit in the Old Palaeozoic rocks in Poraj–Mrzygłód area; in Polish]. Arch. PIG, Sosnowiec.

PODEMSKI M., CHAFFEE M. A., 1996 — Geochemical prospecting in areas of covered and concealed mineral deposits in Poland. Final report on the project No MOS/USGS-92-95. Polish-American Maria Skłodowska-Curie Fund II. Arch. PIG, Warszawa.

POKAŁOW W. T., 1972 — Geneticzieskije tipy i poiskowyje kritierii endogiennych miestorożdienij molibdiena. Moskwa: 3–270.

POŻARYSKI W., 1990 — The Middle Europe Caledonides — wrenching orogen composed of terranes [Eng. Sum.]. *Prz. Geol*., **38**, 1: 1–9.

POŻARYSKI W., BROCHWICZ-LEWIŃSKI W., TOMCZYK H., 1982 — On heterochroneity of the Teisseyre-Tornquist Line [Eng. Sum.]. *Prz. Geol*., **30**: 569–574.

POŻARYSKI W., GROCHOLSKI A., TOMCZYK H., KARNKOWSKI P., MORYC W., 1992 — Mapa tektoniczna Polski w epoce waryscyjskiej. [The tectonic map of Poland in the Variscan epoch]. *Prz. Geol*., **40**, 1: 643–651.

POŻARYSKI W., KOTAŃSKI Z., 1979 — The tectonic development of the Polish part of East-European Platform Forefield in the Baikalian and Caledono-Variscan Epochs [Eng. Sum.]. *Kwart. Geol*., **23**, 1: 7–20.

POŻARYSKI W., TOMCZYK H., 1968 — Assyntian orogen in Southeast Poland. *Biul. Inst. Geol*., **237**: 13–27.

PUCHELT H., 1978, — Barium, parts 56B–56O. *In*: Handbook of Geochemistry (ed. K. H. Wedepohl), v. II/4. Springer-Verlag, New York.

PURDY C. P., Jr., 1954 — Molybdenum occurrences of Washington. *State of Washington Division of Mines and Geology Report of Investigations*, **18**: 118 p.

REYNOLDS T. J., BEANE R. E., 1979 — The evolution of hydrothermal fluid characteristics through time at the Santa Rita, New Mexico; porphyry copper deposit [abstr.]. *Geol. Soc. America. Abstracts with Programs*, **11**: 502.

ROEDDER E., 1971 — Fluid inclusion studies of the porphyry-type ore deposits at Bingham, Utah Butte, Montana and Climax, Colorado. *Econ. Geol*., **66**: 98–120.

ROEDDER E., 1972 — Laboratory studies on inclusions in the minerals Ascension Island granitic blocks and their petrologic significance. *In*: Fluid Inclusion Research. Proceedings of COFFI, **5**.

DE LA ROCHE H., LETERRIER J., GRANDCLAUDE P., MARCHAL M., 1980 — A classification of volcanic and plutonic rocks using R_1R_2 - diagram and major — element analyses — its relationships with current nomenclature. *Chem. Geol*., **29**, 3/4.

RYKA W., 1971 — Przejawy metamorfizmu regionalnego w północno-wschodnim obrzeżeniu GZW. [Forms of the regional metamorphism in the NE margin of the Upper Silesian Coal Basin; in Polish]. Spraw. z Pos. Nauk. Inst. Geol. *Kwart. Geol*., **15**, 3: 706–707.

RYKA W., 1973 — Metamorphic rocks of the Caledonian basement in the vicinity of Zawiercie [Eng. Sum.]. *Kwart. Geol*., **17**, 4: 667–682.

RYKA W., 1974 — Diabase-lamprophyre association on the north-east border of the Upper Silesian Coal Basin [Eng. Sum.]. *Biul. Inst. Geol*., **278**: 35–70.

RYKA W., 1978 — Metamorphic rocks [Eng. Sum.]. *Pr. Inst. Geol*., **83**: 69–71.

RYKA W., 1987 — Klasyfikacja i nazewnictwo skał magmowych oraz materiałów piroklastycznych. [Magmatic rocks and pyroclastic material classification and nomenclature; in Polish]. *Instr. i Met. Bad. Geol*., **48**: 5–52.

RYKA W., MALISZEWSKA A., 1991 — Słownik petrograficzny. [Petrography, a dictionary; in Polish]. Wyd. Geol., Warszawa.

SALAMON W., 1989 — Studium geochemiczno-mineralogiczne głównych minerałów kruszcowych mineralizacji polimetalicznej w paleozoiku NE obrzeżenia GZW. [Geochemical-mineralogical study of the main ore minerals from polymetallic mineralisation in Palaeozoic of the north-eastern border of the Upper Silesian Coal Basin; in Polish]. Arch. PIG, Sosnowiec.

SANTOLIQUIDO P. M., EHMANN W. D., 1972 — Bismuth in stony meteorites and standard rocks. *Geochimica et Cosmochimica Acta*, **36**: 897–902.

SIEDLECKI S., 1962 — On the occurrence of Silurian in the eastern and north-eastern periphery of the Upper Silesian Coal Basin. *Bull. Acad. Pol. Sci*., **10**: 41–46.

SIEWNIAK-MADEJ A., 1994 — A review of the conodont studies of the Paleozoic deposits of the NE border of the Upper Silesia Coal Basin (SW Poland) [Eng. Sum.]. *Prz. Geol*., **42**, 8: 649–652.

SKORUPA J., 1953 — Magnetic survey in the area north-east of Krzeszowice [Eng. Sum.]. *Biul. Państw. Inst. Geol.*, **13**: 1–33.

SNEE L. W., SUTTER J. F., KELLY W. C., 1988 — Thermochronology of economic mineral deposits: Dating the stages of mineralization at Panasqueira, Portugal, by high-precision $^{40}Ar/^{39}Ar$ age spectrum techniques on muscovite. *Econ. Geol.*, **83**: 335–354.

SPRY A., 1969 — Metamorphic textures. Pergamon Press. Oxford.

SZEŁĘG E., 1997 — Warunki krystalizacji scheelitu w skałach północno-wschodniego obrzeżenia Górnośląskiego Zagłębia Węglowego — rejon Myszkowa–Mrzygłodu. [Scheelite crystallisation conditions in rocks from the NE margin of the Upper Silesian Coal Basin — Myszków–Mrzygłód area; in Polish]. Arch. WNoZ UŚ, Sosnowiec.

SZYMAŃSKI B., NEHRING-LEFELD M., 1995 — Opracowanie osadów starszego paleozoiku w podłożu NE obrzeżenia GZW. [Report on the study of the Old Palaeozoic sediments from the basement of the NE margin of the Upper Silesian Coal Basin; in Polish]. Arch. PIG, Warszawa.

SZYMAŃSKI B., TELLER L., 1998 — The Silurian stratigraphy of the Zawiercie–Żarki area (NE margin of the Upper Silesian Coal Basin). *Kwart. Geol*., **42**, 2: 183–299.

ŚLĄCZKA A., 1976 — Nowe dane o budowie podłoża Karpat na południe od Wadowic. *Rocz. Pol. Tow. Geol.*, **46**, 3: 337–350.

ŚLĄCZKA A., 1982 — Profil utworów kambru w otworach położonych na południowy wschód od Goczałkowic. [Cambrian sediments profile in the boreholes located south-east from Goczałkowice; in Polish]. *Przew. LIV Zjazdu Pol. Tow. Geol. Sosnowiec 23–25.IX.1982*: 201–205.

ŚLÓSARZ J., 1982 — Some remarks on geological setting of copper-molybdenum mineralization in the Paleozoic in the vicinities of Myszków [Eng. Sum.]. *Prz. Geol*., **30**, 7: 329–335.

ŚLÓSARZ J., 1985 — Stages and zonality of ore mineralisation in Palaeozoic rocks of the environs of Myszków [Eng. Sum.]. *Ann. Soc. Geol. Pol*., **53**, 1–4: 267–288.

ŚLÓSARZ J., 1988 — Symptoms of tungsten mineralization in Paleozoic sediments, northeastern margin of USCB [Eng. Sum.]. *Prz. Geol*., **36**, 7: 387–390.

ŚLÓSARZ, J., 1993 — The main paragenetic stages for molybdenum mineralisation in the Palaeozoic rocks of the Myszków area and their importance to the formation of the ore deposits of that area [Eng. Sum.]. *Pol. Tow. Mineral., Pr. Spec*., **3**: 123–128.

ŚLÓSARZ J., KARWOWSKI Ł., 1981 — Fizyczno-chemiczne warunki mineralizacji polimetalicznej w utworach paleozoicznych rejonu Myszkowa (NE obrzeżenie GZW). [Physico-chemical conditions of the polymetallic mineralisation in the Palaeozoic rocks in Myszków area (NE margin of the USCB); in Polish]. *In*: Procesy pomagmowe w skałach plutonicznych i wulkanicznych. Streszczenia referatów sesji naukowej, Warszawa, 16–17 października 1981: 14–15.

ŚLÓSARZ J., KARWOWSKI Ł., 1982 — Polymetallic mineralisation in Palaeozoic rocks of Myszków area, Poland (genesis and zonation). *In*: Genesis of ore deposits. *Abstracts of the 6 IAGOD Symposium, Tbilisi 1982*: 203–204.

ŚLÓSARZ J., KARWOWSKI Ł., 1983 — Physico-chemical conditions of polymetallic mineralisation in the Paleozoic formations of the Myszków region (NE border zone of the Upper Silesian Coal Basin) [Eng. Sum.]. *Arch. Mineral*., **39**, 1: 93–108.

ŚLÓSARZ J., MARKIEWICZ J., TRUSZEL M., 1995 — Uzupełniające badania petrograficzne i mineralogiczne skał paleozoicznych rej. Myszkowa. [Supplementary petrographic and mineralogical studies of the Palaeozoic rocks from Myszków area; in Polish]. Arch. PIG, Sosnowiec.

ŚLÓSARZ J., TRUSZEL M., 1997 — Skarny i metasomatyty towarzyszące mineralizacji kruszcowej, formacji porfirowej w paleozoiku w rejonie Myszkowa. [Skarns and metasomatites associated with ore mineralisation in porphyry formation from Myszków area; in Polish]. Arch. PIG, Sosnowiec.

TAYLOR S. R., 1964 — Abundance of chemical elements in the continental crust: a new table. *Geochimica et Cosmochimica Acta*, **28**: 1273–1285.

TAYLOR S. R., 1969 — Trace element chemistry of andesites and associated calc-alkaline rocks. *In*: Proceedings of the andesite conference (ed. A R. McBirney). *Oregon Department of Geology and Mineral Resources Bulletin*, **65**: 43–63.

TAYLOR S. R., McLENNAN S. M., 1995 — The geochemical evolution of the continental crust. *Reviews of Geophysics*, **33**, 2: 241–265.

THEODORE T. G., MENZIE W. D., 1984 — Fluorine-deficient porphyry molybdenum deposits in the western North America Cordillera. *Proceedings of the Sixth Quadrennial IAGOD Symposium, Tbilisi, USSR*. E. Schweizerbart'sche Verlagsbuchhandlung. Stuttgart.

TITLEY R. S., BEANE R. E., 1984 — Medno-porfirowye mestoroždenija. Č.I: Geologičeskaja pozicija, petrologija i tektogenez. *In*: Genezis rudnych mestoroždenij. Mir, Moskva (transl. from *Economic Geology Seventy-fifth Anniversary Volume 1905–1980*).

TOMCZYK H., TOMCZYKOWA E., 1983 — Sylur. W: Złoża rud metali na tle budowy geologicznej NE obrzeżenia GZW. Stratygrafia. cz. 1. [Silurian. *In*: Metal ores deposits with respect to geological structure of the NE margin of the Upper Silesian Coal Basin. Stratigraphy, pt. 1; in Polish]. Arch. PIG, Warszawa.

TRUSZEL M., 1994 — Charakterystyka petrograficzna skał metamorficznych z rejonu Myszkowa i Mrzygłodu. *Przew. LXV Zjazdu PTG*, *Sosnowiec 1994*: 187–191.

TUREKIAN K. K., WEDEPOHL K. H., 1961 — Distribution of the elements in some major units of the earth's crust. *Geological Society of America Bulletin*, **72**: 175–192.

VERNON R. H., 1976 — Metamorphic processes, reactions and microstructure development. George Allen & Unwin Ltd., London.

WEDEPOHL K. H., 1978 — Manganese. Parts **25B–25O**. *In*: Handbook of Geochemistry (ed. K. H. Wedepohl), v. II/3. Springer-Verlag, New York.

WHITE W. H., BOOKSTROM A. A., KAMILLI R. J., GANSTER M. W., SMITH R. P., RANTA D. E., STEININGER R. C., 1981 — Character and origin of Climax type molybdenum deposits. *Econ. Geol*, *75th Anniversary Volume*, Economic Geology Publishing Company: 270–316.

WIELGOMAS L., GAJEWSKI Z., CIEMNIEWSKA M., DANIEC J., DYMOWSKI W., KACPRZAK R., KERBER B., KURBIEL H., SIEMIŃSKI A., STACHURA A., SUFFCZYŃSKI S., SZATKOWSKI K., ZIĘTEK-KRUSZEWSKA A., BEDNARSKI J., KISIEL P., MOLENDZKA J., OLESIŃSKA T., PAWLIK A., 1986 — Dokumentacja geologiczna rejonu Żarki Zachód w północnej części obszaru śląsko-krakowskiego. [Geological report on the Żarki West area, northern part of the Silesia-Cracow region; in Polish]. Arch. PIG, Warszawa.

WIELGOMAS L., CIEMNIEWSKA M., DANIEC J., DYMOWSKI W., GAJEWSKI Z., KACPRZAK R., KERBER B., KURBIEL H., LISIAKIEWICZ S., SUFFCZYŃSKI S., SZATKOWSKI K., ZIĘTEK-KRUSZEWSKA A., BEDNARSKI J., KISIEL P., MOLENDZKA J., OLESIŃSKA T., PAWLIK A., 1988 — Dokumentacja geologiczno-surowcowa wyników poszukiwań złóż rud cynku i ołowiu w rejonie Winowno–Będusz. [Geological and economic-geological report on the Zn-Pb deposits prospecting results, Winowno–Będusz area; in Polish]. Arch. PIG, Warszawa.

WIESER T., 1957 — Petrographic characteristics of albitophyres, porphyries and diabases from Mrzygłód near Zawiercie [Eng. Sum.]. *Kwart. Geol*., **1**, 1: 113–126.

WILSON J. W. J., KESLER S. E., CLOKE P. L., KELLY W. C., 1980 — Fluid inclusion geochemistry of the Granisle and Bell porphyry copper deposits, British Columbia. *Econ. Geol*., **75**: 45–61.

WIMMENAUER W., 1973 — Lamprophyre, semilamprophyre und anchibasaltische Ganggesteine. *Fortschr. Miner*., **51**: 3–67.

WINKLER H. G. F., 1967 — Petrogenesis of metamorphic rocks. Springer-Verlag, New York.

WOJNAR B., 1985 — Charakterystyka tektoniczna utworów paleozoicznych. W: Dokumentacja geologiczno-wynikowa otworu wiertniczego Pz-17 Myszków. [Tectonic characteristics of the Palaeozoic rocks. *In*: Report on the geological results of the Pz-17 Myszków borehole; in Polish]. Arch. PIG, Sosnowiec.

WOJNAR B., 1989 — Charakterystyka tektoniczna utworów paleozoicznych. W: Dokumentacja geologiczno-wynikowa otworu wiertniczego Pz-31 Myszków. [Tectonic characteristics of the Palaeozoic rocks. *In*: Report on the geological results of the Pz-31 Myszków borehole; in Polish]. Arch. PIG, Sosnowiec.

ZHARIKOV V. A., 1970 — Skarns. *Internat. Geology Rev*., **12**: 541–559, 619–647, 760–775.

ZNOSKO J., 1964 — On the necessity of deeper drilling in the apical part of the Mrzygłód Batolith [Eng. Sum.]. *Kwart. Geol*., **3**, 8: 465–475.

ZNOSKO J., 1965 — Tectonic position of the Silesia-Cracow Coal Basin [Eng. Sum.]. *Biul. Inst. Geol*., **188**: 73–102.

ZNOSKO J., 1983 — Tectonics of southern part of Middle Poland (beyond the Carpathians) [Eng. Sum.]. *Kwart. Geol*., **27**, 3: 457–470.

ZNOSKO J., 1996 — The tectonic outline of the Holy Cross Mountains. *Bull. Pol. Acad. Sc.: Earth Sc*., **44**: 51–65.

ŻABA J., 1994 — Mesoscopic flower structures in the Lower Paleozoic deposits of the NE border of the Upper Silesia Coal Basin — a result of the transpresional shearing in the Kraków–Mrzygłód (Hamburg–Kraków) dislocation zone (SW Poland) [Eng. Sum.]. *Prz. Geol*., **42**: 643–648.

ŻABA J., 1995 — Tectonic activity of the Kraków–Lubliniec (Hamburg–Kraków) fault zone at the boundary of Upper Silesia and Małopolska massifs (S Poland). *Europ. Coal Conf. 95, June 26–July 1, 1995, Abstr*., *Prague*: 91.

ŻABA J., 1996a — Late Carboniferous strike slip activity at the boundary zone of Upper Silesia and Małopolska blocks (southern Poland) Eng. Sum.]. *Prz. Geol*., **44**: 173–180.

ŻABA J., 1996b — Główne etapy ewolucji strukturalnej utworów paleozoicznych w brzeżnej części bloku małopolskiego (NE obrzeżenie GZW). [The main stages of the Palaeozoic rocks structural evolution in the marginal part of the Małopolska block (NE margin of the USCB); in Polish]. *In*: Tektonika i rozwój budowy geologicznej północnej części GZW oraz strefy fałdowej Kraków–Lubliniec. Mat. Konf. Nauk., Siewierz, 08–09.11.1996. UŚ., Sosnowiec: 43–55.

ŻABA J., 1997a — Główne etapy ewolucji strukturalnej utworów paleozoicznych w brzeżnej części bloku małopolskiego (NE obrzeżenie GZW). [The main stages of the Palaeozoic rocks structural evolution in the marginal part of the Małopolska block (NE margin of the USCB); in Polish]. *Tech. Posz. Geol*., *Geosyn. Geoterm*., **1/2**: 31–42.

ŻABA J., 1997b — Ewolucja strukturalna utworów paleozoicznych NE obrzeżenia GZW (na podstawie materiałów wiertniczych). [Structural evolution of the Palaeozoic rocks in the NE margin of the USCB (based on the boreholes cores); in Polish]. *Raport końcowy z realizacji Projektu Badawczego Komitetu Badań Naukowych, nr 6 P04D 011 08*. Arch. KBN, Warszawa.

ŻABA J., 1999 — The structural evolution of lower Palaeozoic succession in the Upper Silesia Block and Małopolska Block border zone (southern Poland) [Eng. Sum.]. *Pr. Państw. Inst. Geol*., **166**: 1–162.